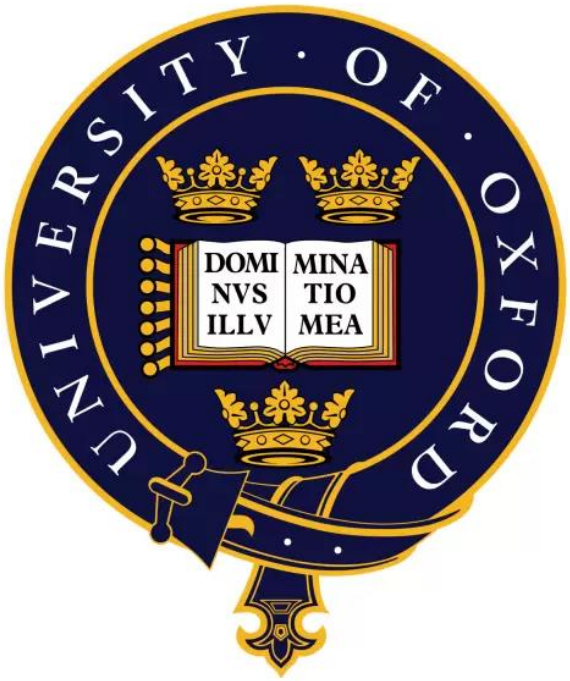
Studies Towards Novel Synthetic Methods to Access Peptidoglycans and Derivatives



A thesis submitted in fulfilment of the requirements for the degree of
MSc by Research in Pharmacology

Adrian Schembri Wismayer

Hertford College, University of Oxford

Trinity 2024

Table of Contents

Abstract ii
Acknowledgements iii
Abbreviations iv
Chapter 1 – General Introduction 1
The Bacterial Cell Wall 1
Peptidoglycan 2
Peptidoglycans and Derivatives as Medicines 4
Peptidoglycan Derivatives in Inhibiting Lipid II Translocation 5
Peptidoglycan as an Immunogen 7
Aims of this thesis 12
References 13
Chapter 2 – Efforts Towards Synthesis of Labelled Lipid II Analogues 18
Introduction 18
Results and Discussion 37
Experimental 49
References 67
Chapter 3 – Efforts Towards the Synthesis of Light Inducible Peptidoglycan Probes 72
Introduction 72
Results and Discussion 97
Experimental 107
References 121
Thesis Conclusion 125
Appendix: Exemplar NMR Spectra 126

29,500 words

Abstract

The cell wall is essential for bacterial life affording structural integrity, protection from harmful influences, and mediating exchange of substances required for survival. The peptidoglycan layer presents a key component of this structure that facilitates such function, through fortification and resistance to lysis. Peptidoglycan is a crosslinked glycopeptide polymer produced via a complex biosynthetic pathway comprising a plethora of enzymes acting on distinct chemical intermediates. Historically there has been a great interest around manipulating proteins and intermediates within this pathway for medicinal purposes, with success being found in antibiotic targeting of many of these enzymes and the use of some of these intermediates as adjuvants in vaccines. Currently bacterial resistance to antibiotics is a growing problem and there is a great need for novel medicines with diverse mechanisms of action. Peptidoglycan fragments and derivatives may prove valuable as substrates for inhibitory assays and additives to vaccines helping to combat this issue. This thesis describes work towards the synthesis of novel analogues of Lipid II (a peptidoglycan precursor) and peptidoglycan probes which can be crosslinked by light. Chapter two of this thesis describes the synthesis of a versatile intermediate which may allow for divergent synthesis of Lipid II analogues. This was carried out through a synthesis involving glycosylation of a novel *N*-Acetylmuramic acid (MurNAc/NAM) acceptor and a *N*-Acetylglucosamine (GlcNAc/NAG) donor. Chapter three of this thesis describes efforts towards accessing building blocks for assembly of peptidoglycan probes that possess light inducible crosslinking properties. This involved synthesis of a novel disaccharide bearing a high degree of orthogonal protection and efforts towards designing novel peptides for light induced radical reaction.

Acknowledgements

To begin I would like to thank my supervisors Prof. Ben Davis and Dr. Yin Dong. They have both shown me guidance, made time for me, and given me an opportunity to work in groups doing great science. The way that the groups and the Rosalind Franklin Institute have been directed has given me incredible exposure to many great researchers and ideas, which I believe have truly furthered my development as a scientist.

One particular researcher I was fortunate enough to meet was Dr. Andrew Giltrap, a former senior associate investigator at the Rosalind Franklin Institute. I would like to express my utmost gratitude to Andrew. He has personally overseen my project providing me with supervision on a day-to-day basis and has taught me virtually all the lab skills I now possess. He has also taught me additional chemistry outside of the lab and inspired a passion for organic synthesis that is seeing me pursue PhD study. Outside of acting as a mentor he has also been involved in reading drafts of my thesis even after he has left the group. I am very grateful for everything he has done for me and all his efforts have made a very difficult experience easier.

To end I would like to thank my parents and my girlfriend Sarah. My parents have provided me with financial and emotional support throughout my time at Oxford and have always encouraged me to pursue my interests. They have made many sacrifices and have put up with me in times of stress and frustration, always showing me kindness and giving me help. Finally, Sarah has been supportive of me studying away from her at Oxford and has shown me continued love and care regardless of the distance. Thank you for being so considerate when I have struggled to make time and have been greatly stressed. Thank you for the past 4.5 years!

Abbreviations

Ac – Acetyl

Ac_2O – Acetic anhydride

AcOH – Acetic acid

AgOTf – Silver triflate

Bn – Benzyl

Boc - *tert*-butyloxycarbonyl

BTFFH - Bis(tetramethylene)fluoroformamidinium hexafluorophosphate

CAN – Ceric ammonium nitrate

CDI – Carbonyl diimidazole

CDMT - 2-Chloro-4,6-dimethoxy-1,3,5-triazine

COSY – Correlation spectroscopy

DBU - 1,8-Diazabicyclo(5.4.0)undec-7-ene

DCM - Dichloromethane

DDQ - 2,3-Dichloro-5,6-dicyano-1,4-benzoquinone

DIPEA - *N*,*N*-Diisopropylethylamine

DMAP – *N*,*N* –Dimethylaminopyridine

DMF - *N*,*N*-Dimethylformamide

DMS – Dimethylsulfide

DMSO – Dimethyl sulfoxide

DMTMM - 4-(4,6-dimethoxy-1,3,5-triazin-2-yl)-4-methyl-morpholinium chloride

EDCI - 1-Ethyl-3-(3-dimethylaminopropyl)carbodiimide

ESI – Electrospray ionisation

Et – Ethyl

EtOAc – Ethyl acetate

Fm - 9-Fluorenylmethyl

Fmoc - 9-Fluorenylmethyloxycarbonyl

GlcNAc/NAG - *N*-Acetylglucosamine

HATU - *N*,*N*,*N'*,*N'*-Tetramethyl-O- (7-azabenzotriazol-1-yl)uronium hexafluorophosphate

HMBC – Heteronuclear multiple bond correlation

HMDS - Hexamethyldisilazide

HRMS – High resolution mass spectrometry

HSQC - Heteronuclear single quantum coherence

^{i}Pr – *iso*-propyl

IR – Infra-Red

LC-MS – Liquid chromatography-Mass spectrometry

Lev - Levuinoyl

LRMS – Low resolution mass spectrometry

***m*DAP** – *meso*-diaminopimelic acid

Me - Methyl

MeCN - Acetonitrile

MeOH - Methanol

MurNAc/NAM - *N*-Acetylmuramic acid

MsOH – Methanesulfonic acid

Nap - (2-naphthyl)methyl

NBD - Nitrobenzoxadiazole

NBS - *N*-Bromosuccinimide

NEt_3 - Triethylamine

NHS - *N*-Hydroxysuccinimide

NMM - *N*-methylmorpholine

NMR – Nuclear magnetic resonance

NIS - *N*-Iodosuccinimide

Oxyma - Ethyl cyanohydroxyiminoacetate

Ph – Phenyl

PMB – *p*-Methoxybenzyl

PMP – *p*-Methoxyphenyl

PSE – Phenylsulfonyl ethyl

RaNi – Raney Nickel

R_f – Retention factor

rt – Room temperature

TBAF – Tetra-n-butyl ammonium fluoride

TBDPS - *tert*-Butyldiphenylsilyl

TBHP - *tert*-Butyl hydroperoxide

TCA – Trichloro acetyl

TEOC - 2-(Trimethylsilyl)ethoxycarbonyl

TES - Triethylsilane

Tf - Triflate

TFA – Trifluoroacetic acid or Trifluoroacetyl

TfOH – Triflic acid/Trifluoromethanesulfonic acid

THF – Tetrahydrofuran

TLC – Thin layer chromatography

TMSE – Trimethylsilyl ethyl

TMSOTf – Trimethylsilyl trifluoromethanesulfonate

TOCSY – Total correlation spectroscopy

Tol – Tolyl

Troc - 2,2,2-Trichloroethoxycarbonyl

TsOH – *p*-Toluenesulfonic acid

UDP-GlcNAc – Uridine diphosphate-*N*-acetyl glucosamine

UDP-MurNAc - Uridine diphosphate-*N*-acetyl muramic acid

5–ETT – 5-Ethylthio tetrazole

Chapter 1 – General Introduction

The Bacterial Cell Wall

The cell wall represents a key feature within bacterial cells, disconnecting the interior of single cell organisms from their environments. Several functions necessary for bacterial life are contingent on the cell wall structure, examples include: Protection from harmful influences in the extracellular environment, enabling transport of substances externally or internally, providing structural solidity that guards against osmotic stress and internal turgor pressure [1]. Cell wall structures are well adapted to serve these functions such that there exists great variability across species. Nonetheless, whilst variation exists, many features are conserved and eubacteria have been classified into two distinct categories: Gram positive and Gram negative based on their cell wall compositions. These distinctions were assessed through response to a staining method developed by Christian Gram in 1884 (Fig. 1.1) [2]. It was observed that on treating cells with crystal violet and iodine gram positive cells retained a purple colour whereas gram negative cells were decolourised following a wash with ethanol or acetone; addition of a counter stain (i.e. Safranin) recoloured the gram negative species pink. These observational differences arise due to differences in thickness of the peptidoglycan layer; gram positive bacteria have a much thicker layer of peptidoglycan that retains large crystal violet iodide complexes responsible for colouring much better than the thinner peptidoglycan layer present in gram negative bacteria [3].

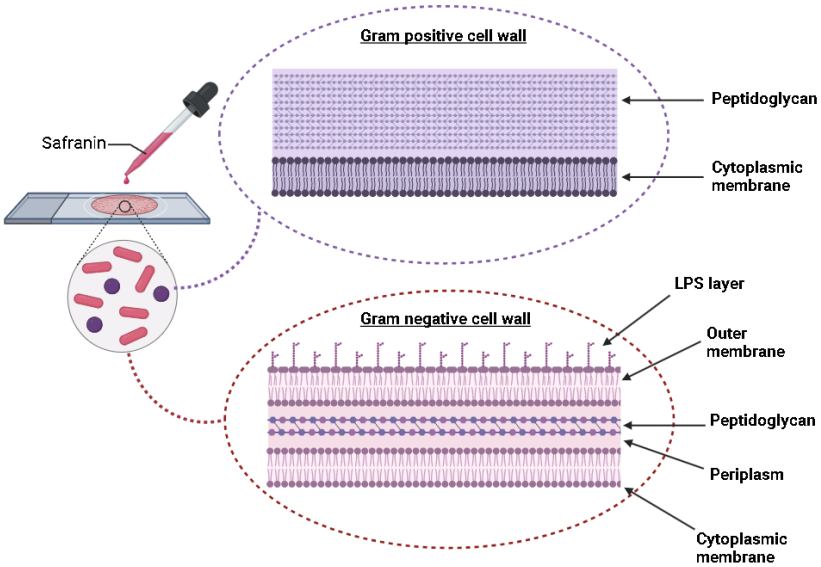


Figure 1.1 – Gram stain procedure illustrating the physiology of differentially stained cell walls

Peptidoglycan

Peptidoglycan is a glycopeptide polymer comprising alternating β(1,4) linked GlcNAc and MurNAc residues, where the MurNAc lactoyl motifs are amidated with peptide stems. The chemistry of the peptide stem differs between the classes with gram positive species typically bearing a lysine as the third residue in contrast to the *meso*-diaminopimelic acid (*m*DAP) residue found in gram negative organisms [4]. The key function of this cell wall component is the afforded increase in structural integrity and resistance to lysis [4]. This property arises due to crosslinking between the peptide stems of adjacent strands, with the nature of the residues involved in crosslinking differing among species [4].

The production of peptidoglycan requires the synthesis of monomeric subunits for integration into the expanding cell wall and the concomitant recycling of old cell wall material. These subunits are disaccharide pentapeptides consisting of a GlcNAc-MurNAc disaccharide core, and are bound to bactoprenol hydrocarbon chains at the reducing end. This phospholipid bound glycopeptide is known as Lipid II. The pyrophosphate linked lipid is essential for intermembrane transport and reactivity as a glycosyl donor [5].

Lipid II synthesis (Fig. 1.2) begins from uridine diphosphate-*N*-acetyl glucosamine (UDP-GlcNAc) where MurA facilitates the transfer of an enol pyruvate group from a phosphoenol pyruvate donor to the 3' OH of UDP-GlcNAc [6]. Reduction of this group by MurB ensues to produce the lactoyl motif, giving uridine diphosphate-*N*-acetyl muramic acid (UDP-MurNAc) [7]. Amidation at the nascent carboxyl allows for the installation of a pentapeptide sequence by an enzyme cascade, catalysed by MurC-F. The resultant structure is known as Park's nucleotide [8] and undergoes further reaction with the transfer of phospho MurNAc pentapeptide from UDP-MurNAc pentapeptide to undecaprenyl phosphate. This process is catalysed by MraY and generates the membrane associated product known as Lipid I [9]. Further reaction at the inner leaflet of the cytoplasmic membrane sees the addition of UDP-GlcNAc to the 4 OH of the Lipid I N-acetyl muramyl (MurNAc) motif. This process is catalysed by the glycosyltransferase protein, MurG [9] and produces the aforementioned Lipid II. For Lipid II to be integrated into the peptidoglycan layer it must be translocated into the outer leaflet of the cytoplasmic membrane, a process which is mediated by a flippase protein, MurJ [10]. On translocation, recognition by the N-terminal domain of Class A PBPs results in glycosylation to growing peptidoglycan chains [11], and displacement of undecaprenyl pyrophosphate, allowing its recycling [12]. Further processing by the C-terminal domains of Class A and B PBPs results in the formation of peptide crosslinks between adjacent glycan strands [11], and the formation of mature peptidoglycan.

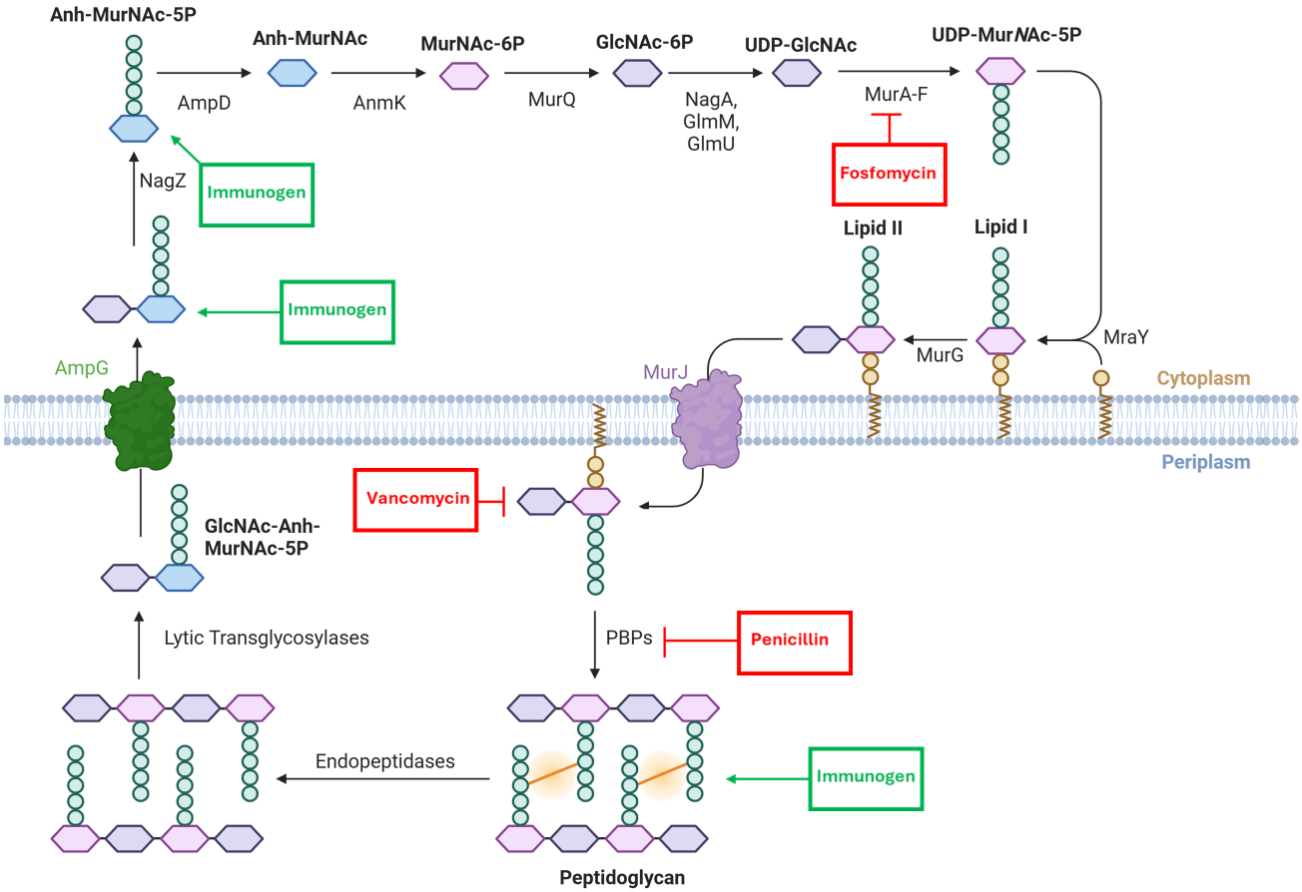


Figure 1.2 - Peptidoglycan biosynthesis and points of medicinal interest

As the cell wall is remodelled (Fig. 1.2), mature peptidoglycan is turned over, regenerating constituent material. This process begins with the cleavage of inter strand crosslinks by proteins possessing endopeptidase activity [13], as well as cleavage of the 1,4-glycosidic bonds by lytic transglycosylase enzymes [14]. The product of such processing is anhydro MurNAc-GlcNAc (Anh-MurNAc-GlcNAc) pentapeptide, due to the mechanism of cleavage by lytic transglycosylases; it is proposed that cleavage occurs via oxazolinium ring formation facilitated by a Glu residue in the active site, which can then be opened by nucleophilic attack of the neighbouring 6 OH [14]. These anhydro sugars are then internalised by the AmpG permease [15] where NagZ and AmpD activity results in hydrolysis of the glycosidic linkage and pentapeptide respectively [15], to produce Anh-MurNAc. Conversion to GlcNAc-6P proceeds through opening of the 1,6-anhydro linkage and phosphorylation by the AnmK kinase, and delactoylation by the Mur Q etherase [16]. GlcNAc-6P can then reconverted to UDP-GlcNAc via a glucosamine-1 phosphate intermediate, regenerating starting material [15, 17].

Peptidoglycans and Derivatives as Medicines

The indispensable function of peptidoglycan across bacteria has made it an attractive avenue for antibiotic therapy due to the plethora of steps and associated enzyme targets in the biosynthetic pathway. Perhaps the most famous example of successful targeting is the use of Penicillin as a suicide substrate for the penicillin binding proteins; exerting its antibiotic effect through irreversible acylation of a Ser residue in the active site crucial for activity [18]. Other medicines have been developed and clinically employed, targeting distinct stages within the pathway. Examples include: the glycopeptidic Lipid II binder vancomycin, and the MurA targeting epoxide fosfomycin (Fig. 1.2). Unfavourably, with the passing of time bacteria have evolved means of survival to circumvent killing. Such a process is referred to as antimicrobial resistance, and is underpinned by mutagenesis. The severity of this problem is amplified by the propagation of the problematic genetic sequences to other strains by horizontal gene transfer [19], and improper use of antibiotics inadvertently selecting for tolerant mutants [20]. Despite developments there is a failure to keep up with the increasing demand for new medicines, with few treatments coming through the pipeline. Only 8 of 51 newly approved antibiotics are classed as innovative, and many are structurally analogous to previous less effective treatments [21, 22]. These discoveries are incremental and to truly combat the issue, research needs to be directed into avenues of treatment with novel targets or to knocking out mechanisms of resistance. The translocation of Lipid II across the cytoplasmic membrane represents such a novel avenue of treatment, and inhibitory investigation could prove crucial in combating the antimicrobial resistance problem.

Peptidoglycan and its degradation products also play a key role in stimulating the innate immune system (Fig. 1.3) within mammals giving them potential for inclusion in vaccines. Vaccination has proved to be a greatly effective tool at preventing disease, with numerous examples concerning different antigen components being developed. In addition to the antigen, vaccines often contain adjuvants, elements which serve to stimulate and enhance the magnitude and durability of the immune response [23]. The first example of licensed adjuvants was the use of insoluble aluminium salts in 1920 that have been shown to function through enhanced antigen presentation [24] and activation of the NLRP3 inflammasome [25]. Since these earlier efforts further adjuvants have been included in live vaccines one such being Freund's adjuvant [26]. This has been investigated in complete or incomplete forms, distinguished by the presence of heat killed mycobacteria. The incomplete form has been used as an ingredient in human influenza vaccinations in the 1950s [27] however its use was severely hampered by undesired patient side effects and it is not regularly employed [28]. The minimum immunostimulatory component of Freund's adjuvant is muramyl dipeptide (MDP) an advanced peptidoglycan degradation product and functions through interactions with the NOD receptors [29]. There is a great interest around developing new adjuvants that do not display adverse effects, and alternate purified peptidoglycan structures may prove useful in this case owing to their multimodal action and unique immune effects via different receptors of the immune system.

Peptidoglycan Derivatives in Inhibiting Lipid II Translocation

The Identity of the Flippase Protein

The translocation of Lipid II across the cytoplasmic membrane had long been a topic of controversy with contrasting evidence emerging regarding the identity of the flippase. The substrate flipping was originally attributed to RodA and FtsW, proteins of the elongasome and divisome complexes respectively [30]. The evidence for this was an *in vitro* vesicular assay, where FtsW expression was correlated to flipping fluorescent analogues of Lipid II across proteoliposomes, and another protein postulated to be the flippase, MurJ, showed no activity [30]. This observation was not conclusive, and FtsW mediated flipping has not been observed *in vivo*. Additionally, new evidence that as not available at the time has highlighted several issues with the assays conducted. Biological parameters such as membrane potential [31] and ionic environment [32, 33] that have been shown to be crucial to the MurJ catalytic cycle were not properly controlled for. Furthermore, addition of a bulky fluorophore to the peptide stem may not be a tolerated modification and may disrupt recognition. Recent crystallographic data supports this assertion [34], showing that the peptide stem is held within a constrained distal site and that the nitrobenzoxadiazole (NBD) fluorophore may disrupt such binding through steric effects.

More robust studies fully support the identity of MurJ as the flippase. *Ruiz N.* conducted a reductionist bioinformatic investigation where they identified 39 candidate potential candidates from a database of 963 membrane proteins by examining conservation within model organisms bearing simple proteomes [10]. From these 39 candidates only MurJ was found to be conserved in a range of peptidoglycan producing species through BLAST searches. The study further elucidates FtsW's redundancy through identifying that peptidoglycan production is not correlated to FtsW containing genes. This work has since been supported through *in cellulo* experiments [35]. Translocation of Lipid II has been monitored using a protein toxin, ColM, administered into the periplasm of *Escherichia Coli.* ColM is capable of recognising Lipid II with hydrolase function to generate PP-MurNAc-GlcNAc pentapeptide and undecaprenol products. Metabolites were quantified with this system in the presence of wild type MurJ and an inactivated mutant. Absence of metabolites in the presence of inactive MurJ, affirmed its role in Lipid II translocation, and support FtsW's redundancy.

Other proteins have also been found to exhibit the necessary flippase activity. Amj is a structurally distinct protein that is expressed under the control of transcription factor σ^M as a consequence of the cell envelope stress response and can rescue translocation in the case of *murJ* deletion [36]. Another protein, Wzk, promiscuously transports Lipid II, such that MurJ expression is no longer a necessity [37]. These proteins have however only been identified in single strains, and as such MurJ is considered indispensable across bacteria regardless.

The Flippase Protein as an Antibiotic Target

The indispensability of MurJ to a wide range of peptidoglycan producing organisms makes it an attractive target for the development of new broad-spectrum antibiotics. Whilst the rational design of MurJ antagonists has lacked, some inhibitory compounds have been discovered, primarily as a result of screening approaches. Humimycins (Fig. 1.3) are *N*-acetylated linear heptapeptides that have been predicted as inhibitors through screens of the human microbiome [38]. Their activity has stringent structural requirements, with modifications to alcohol substitution (R^2 in Fig. 1.4) and stereochemistry resulting in loss of activity. Similarly, changes to the peptide chain are not well tolerated [39]. This implies a specific mode of binding, and it is speculated that they act as competitive inhibitors blocking Lipid II access to the central cavity (binding site) via the lateral gate from which it enters [32].

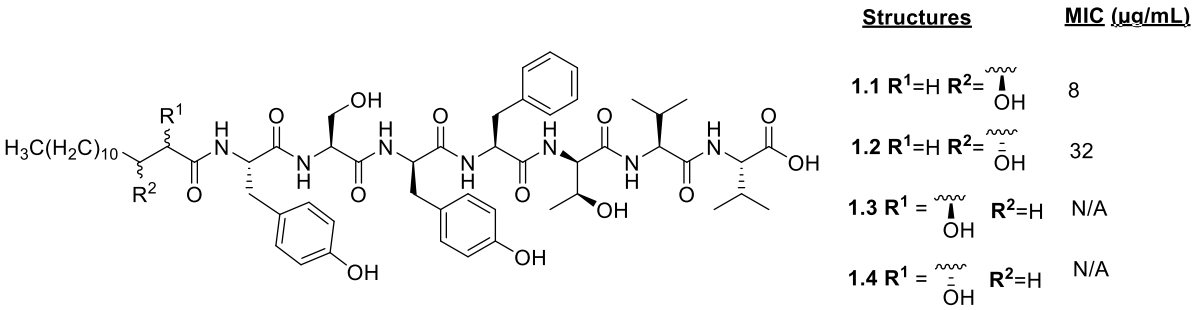


Figure 1.3 – Structure activity relationships of Humimycins

A bacteriophage protein, termed Lys^M was found to induce conformational changes in MurJ, and hence disrupt activity. The proposed mechanism of action is that binding locks the conformation of MurJ preventing transport [40]. Small molecule inhibitors have also been discovered. Two anthranilic acid derivatives were found to attenuate incorporation of radiolabelled precursors into the cell wall, as well increase their accumulation. Identification of mutated residues in resistant mutants revealed MurJ as the target [41]. At the time the structure and function of MurJ was unknown, so the binding mode could not be resolved. This has yet to be confirmed, however recent mapping of resistance points has identified the A48T mutation to be in the periplasmic domain, away from the lateral gate. As such the inhibition mode is likely non-competitive and these compounds bind allosterically [32]. Additional small molecule inhibitors DMPI and CDFI (Fig. 1.4) were discovered as MurJ antagonists during a high throughput screen assessing codrugs for potentiation of β-lactams against MRSA. Overexpression assays and site directed mutagenesis confirm MurJ as the target of these antibiotics [42]. Like the other small molecule inhibitors resistance point mutations are far from the active site and are also dispersed from one another, suggesting these molecules are allosteric inhibitors [32]. As the resistance points for the small molecule inhibitors do not overlap, MurJ likely has many druggable hotspots. This further supports its suitability as an attractive target for developing novel antibiotics and should be investigated further to identify clinically employable antagonists.

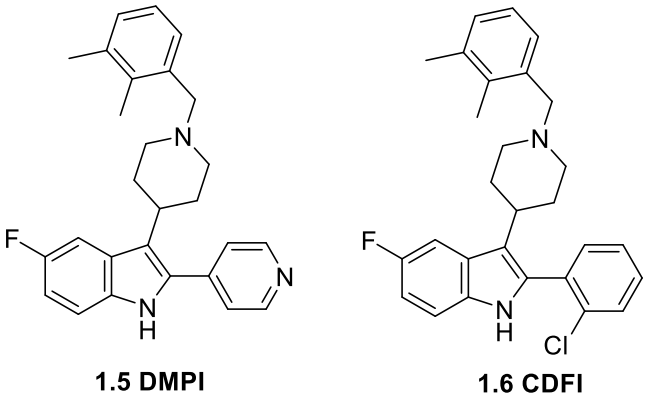


Figure 1.4 – MurJ inhibitors DMPI and CDFI

To be able to make use of the newly available crystallographic data [34, 43, 44] and proposed mechanistic data [45] for rational inhibitor design and testing, a suitable model flipping system should be established. As discussed earlier within this section attempts to recapitulate flipping activity *in vitro* with proteoliposomes have been unsuccessful. A successful model assay is of great importance to inhibitor design due to ease of testing and the ability to extract kinetic information. Synthesis of alternate substrates that possess the same reporter functionality as the previously utilised fluorophore conjugates without tolerance issues will be a key first step in developing a successful *in vitro* assay.

Peptidoglycan as an Immunogen

Recognition of Peptidoglycan by the Immune System

Peptidoglycan is a pathogen associated molecular pattern; a ligand that is sensed by the Peptidoglycan Recognition Proteins (PRPs), C-Type Lectins (CTLs), Nucleotide Oligomerisation Domain Like Proteins (NLRs) and Toll Like Receptors (TLRs) of the immune system (Fig. 1.5) [29, 46]. These proteins families possess unique structures, detection mechanism, and consequent differential immune activity. These interactions will each be summarised in turn.

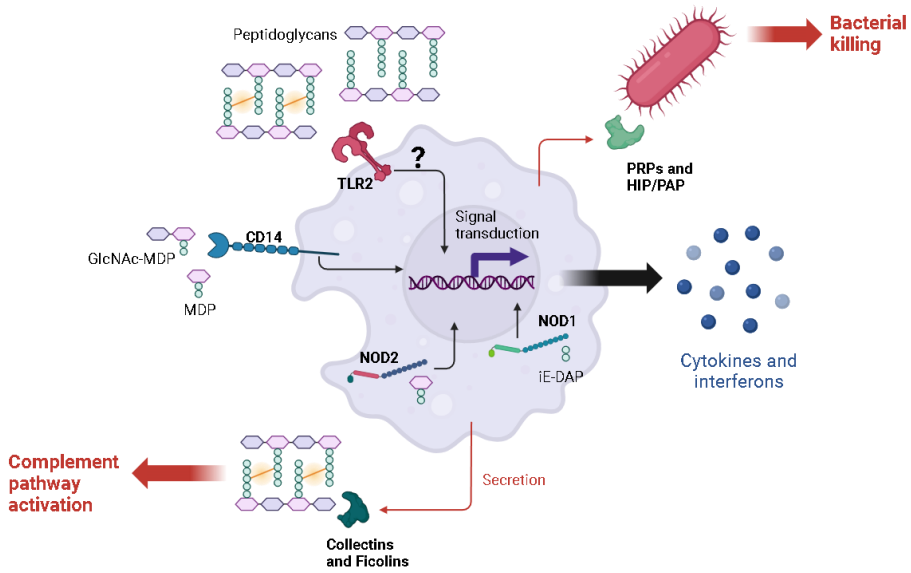


Figure 1.5 - Immune recognition mechanisms of peptidoglycan and derivatives in mammals

The PRP family contains 4 proteins (PGLYRP-1-4) that are secretory and exist, excluding PGLYRP-2, as disulfide linked dimers, a property essential for their activity [47]. PGLRYP-1, PGLRYP-3 and PGLRYP-4 function through direct binding to peptidoglycan within the cell wall, entering at the site of daughter cell separation during bacterial cell division. This binding has a bactericidal effect through activation of stress response two-component systems culminating in membrane depolarisation, production of reactive oxygen species, and termination of peptidoglycan precursor, protein, and nucleotide synthesis [48]. PGLYRP-2, is unique to the family and functions as an amidase through binding of peptidoglycan and cleavage of the lactyl-amide bond [49], breaking down the cell wall. PGLYRP-2 is also active against smaller fragments and has been shown to recognise MTP (Muramyl-L-Ala-D-*iso*-Gln-L-Lys) [49].

The CTLs are a class of secretory Ca^{2+} dependent receptors that are promiscuous for a range of sugars, including peptidoglycan, through binding at a carbohydrate recognition domain [50]. The collectins and ficolins are able to bind GlcNAc residues within peptidoglycan and initiate the lectin-complement pathway, which culminates in multiple responses including elimination of invading pathogens, promotion of inflammatory response, and clearance of apoptotic cell and necrotic cell debris, in addition to modulation of adaptive immune responses [51]. Differences exist regarding substrate specificity, with the ficolins requiring acetylation of the GlcNAc residue for recognition; class M and L ficolins display wider specificity allowing recognition of other acetylated sugar residues in addition [52]. The murine $RegIII_{\gamma}$ and Human Hepatocarcinoma-intestine-pancreas/pancreatitis-associated protein (HIP/PAP) present another class of CTL capable of binding peptidoglycan within the cell wall; acting directly as antimicrobial peptides and exerting their bactericidal effect through cell wall damage and membrane leakage [53]. The surface receptor CD14 presents a final class of CTL

that senses both insoluble and soluble peptidoglycans through a N-terminal domain. Binding ultimately activates the NF-κB transcription factor leading to cytokine and antimicrobial peptide production [54]. Recognition of substructures MDP (muramyl L-Ala-D-*iso*-Gln) and GlcNAc-MDP has been demonstrated *in vitro* [55].

The NOD receptors are members of the NLR family, and are cytosolic proteins capable of sensing peptidoglycan fragments through a characteristic C-terminal LRR domain on internalisation of cell wall components either through bacterial or host mechanisms [56]. Said fragments are bound by either the NOD1 or NOD2 proteins. The NOD1 receptors simply require iE-DAP as the minimum motif necessary for recognition [57], that is a dipeptide comprising D-*iso*-Glu and *m*DAP residues. More complex peptidoglycan degradation products such as the L-Ala-iE-DAP tripeptide and muramyl L-Ala-iE-DAP are also recognised [46]. The NOD2 receptors bind similar muramyl glycopeptides: MDP and MTP following modifications such as 6 OH phosphorylation in MDP [58]. Binding of the respective ligands triggers self-oligomerisation and interaction with receptor-interacting serine/threonine protein kinase 2 (RIPK2) [59]. This is capable of generating an immune response that culminates in the production of inflammatory cytokines and chemokines [29].

The recognition of peptidoglycans by TLRs has remained a point of controversy [29, 46, 56]. Early study proposed peptidoglycans to be TLR-2 ligands [60-62], with TLR-2 deficient macrophages showing an impaired response to cell wall extracts [61]. Later study proposed contamination with other bacterial components as an explanation; eight different highly purified peptidoglycans did not stimulate TLR-2 activation. Lesser purified commercial samples lost immunostimulatory properties on removal of lipoteichoic acids (LTAs) [63]. This has since been countered, both insoluble and soluble peptidoglycans were shown to cause TLR-2 induced TNF-α production [64]. Soluble peptidoglycans were obtained through inhibition of penicillin binding proteins and associated transpeptidation. This prevents crosslinking and leads to secretion of these fractions into the medium, preventing association with LTAs. It has been proposed that this disparity may be attributable to differences in the amino acid side chain structure and crosslinking [29].

Peptidoglycans and Fragments as Immune System Modulators

Owing to their immunostimulatory properties peptidoglycans and fragments have been investigated therapeutically as immune system modulators. These were first administered therapeutically in the form of a weakened strain of *Mycobacterium bovis* known commonly as BCG [65], and a dried, inactivated form of *Mycobacterium tuberculosis*, referred to as Freund's adjuvant [66]. Therapeutic success still sees BCG employed today as a vaccine in countries where tuberculosis infection is prominent [67]. The minimum immunostimulatory component of these medicines was found to be MDP [68], and studies following have described

the host interactions underpinning NOD receptor mediated adaptive immunity. Volunteers vaccinated with BCG presented distinct monocytes that have phenotypes advantages to clearing infection from unrelated pathogens [69]; this trained response was shown to be contingent on NOD2 expression. Peptidoglycan fragments from the endogenous microbiota have been shown to upregulate neutrophil function, with NOD1 deficient mice showing increased susceptibility to infection, consolidating its role in immune system priming [70]. BCG has also been shown to trigger immune effects through TLR2 and TLR4 receptors [71, 72], however these studies did not ascertain the identity of the TLR2 ligand responsible for observations, and is likely to be a cell wall component unrelated to peptidoglycan as discussed prior.

Issues around clinical use of peptidoglycans and fragments as adjuvants arise due to unfavourable drug-like properties. The high polarity of the glycopeptides sees them readily excreted from circulation [73]. Further issues arise surrounding undesired side effects with induction of pyrogenicity [74] and somnogenicity [75]. Design of synthetic analogues to circumvent such issues has garnered much attention, with key developments shown in Fig. 1.6. **1.7** where the *iso*-Gln residue was varied to the free acid was found to retain effectiveness as an NOD2 ligand, however did not cause fever [76]. Other modifications to the *iso*-Gln residue such as the incorporation of the butyl chain in **1.8** were also found to illicit the desired response in the absence of any side effects [77]. Acylation of the 6 OH in **1.9** and **1.10** with fatty acid chains displayed more favourable pharmacokinetics and increased potency as an NOD2 agonist, due to increased hydrophobicity [78]. Optimisation of this modification led to the design of **1.11** [79], and **1.12** [80, 81] with the introduction of hydrophobic chains to the peptide stem. Similar approaches with hydrophobic acyl groups have been applied in the design of alternative peptide NOD1 substrates with comparable results [82].

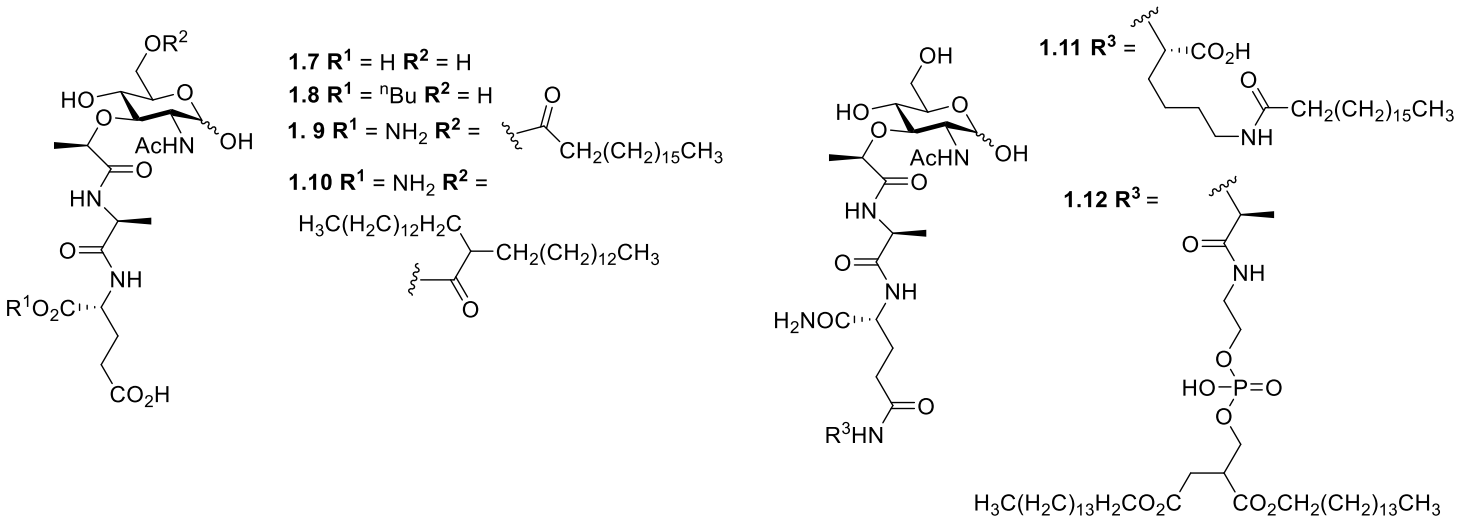


Figure 1.6 – MDP analogues bearing hydrophobic acyl groups

Substitution of the hexose ring characteristic to sugars with more hydrophobic, non-hydrolysable aromatics was explored for **1.13** and **1.14**; these structures are termed desmuramyl peptides owing to the lack of a muramyl motif (Fig. 1.7). Indole **1.13** was assessed as an NOD2 agonist in relation to **1.8** [83]. The study concluded similar agonistic activity, however the mechanism by which these drugs can permeate the cells was found to be unique, occurring by passive diffusion rather than the hPEPT1 transporter. Feruloyl derivative, **1.14**, produced the best results from reported non-carbohydrate scaffolds, displaying activity at nanomolar concentrations, potency twice that of MDP [84]. Larger oligosaccharide fragments have also been explored (Fig. 1.8). Tetrasaccharide, **1.15**, was found to be a suitable alternative to MDP with the sequence and identity of the reducing sugar affecting potency [84].

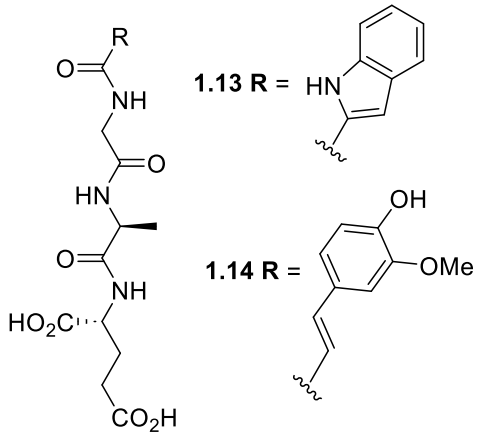


Figure 1.7 – Desmuramyl peptide analogues

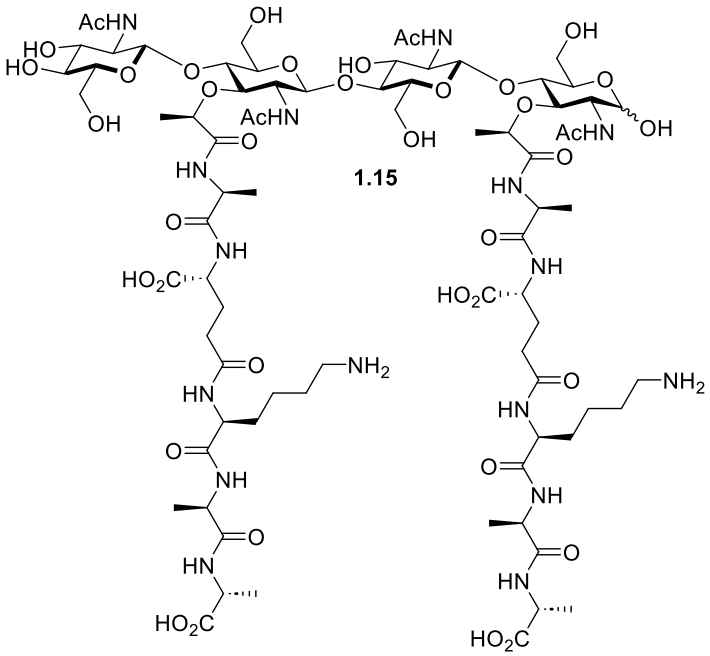


Figure 1.8 – NOD2 agonistic Peptidoglycan tetrasaccharide

Testing of these alternate NOD ligands has occurred in preclinical animal models, with protective effects being demonstrated against pathogens. Owl monkeys were successfully vaccinated against malaria, through administration of **1.9** in liposomes [85]. Vaccinal use of desmurmayl peptide, **1.14**, showed an increase in serum antibody levels, however at lower rates than MDP [84]. These compounds have not seen the clinical stage, however other similar derivatives have been tested. **1.12**, was trialled as an adjuvant for viral vaccinations, however it showed no significant benefits in comparison to MDP and greater adverse side effects [80, 81]. Testing of **1.12** continued as an anti-cancer agent, with positive results seen in murine models [86, 87], this translated to clinical success, and is currently approved for treatment of an early-stage cancer [67].

NOD agonism via peptidoglycan related compounds has demonstrated success as a strategy in immunotherapy in a range of model systems. Unfortunately, the use of many of these compounds at the clinical stage remains unsuccessful. Seeing as peptidoglycans are sensed by the host through a diverse range of proteins, future investigation should also aim to assess the suitability of these as drug targets. The TLR receptors show promise with clinical use of small molecules and biomolecules for TLR2 [88, 89] being documented. Additionally, detoxified versions of other bacterial products are clinically approved and exert their immune effects through TLR4 targeting [90]. To employ peptidoglycans as TLR2 agonists, controversy around substrate recognition will first need to be resolved. Addressing these questions will require access to a large range of pure, chemically diverse substrates. Given that these diverse chemical modifications centre around peptide stem chemistry and glycan length, design of a synthetic method with appropriate modularity will present a key first step to the inclusion of peptidoglycans in vaccines.

Aims of this thesis

The biosynthesis of peptidoglycan is a complex, multi-step process involving many proteins and biochemical intermediates. Historically there has been a great interest around manipulating proteins and intermediates from this pathway for medicinal purposes. Success has been found through developing antibiotics that inhibit key proteins within the pathway and also in the use of intermediates to protect against infection and cancer. As antibiotic resistance continues to remain a growing problem, there is a great need for new therapies that have diverse mechanisms of action. Peptidoglycan products and intermediates may prove useful as both valuable additives to microbial vaccines and substrates for the development of inhibitory assays. The aims of the work described in this thesis are to carry out synthesis of peptidoglycan products and intermediates to aid biological investigation into antibiotics and immunomodulators.

- Chapter 2 describes the successful synthesis of a versatile intermediate that may be used to access novel labelled Lipid II analogues for *in vitro* study of MurJ.
- Chapter 3 describes efforts towards the syntheses of building blocks for assembly of peptidoglycan fragments that possess light inducible crosslinking properties for use in immunological investigation.

References

(1) Seltmann, G.; Holst, O. *The Bacterial Cell Wall*; Springer Science & Business Media, 2002.
(2) Gram, C. Ueber die isolirte Farbung der Schizomyceten in Schnitt-und Trockenpraparaten. *Fortschritte der Medicin* **1884**, *2*, 185-189.
(3) Beveridge, T.; Davies, J. Cellular responses of Bacillus subtilis and Escherichia coli to the Gram stain. *Journal of Bacteriology* **1983**, *156* (2), 846-858.
(4) Vollmer, W.; Blanot, D.; De Pedro, M. A. Peptidoglycan structure and architecture. *FEMS Microbiology Reviews* **2008**, *32* (2), 149-167.
(5) El Ghachi, M.; Bouhss, A.; Blanot, D.; Mengin-Lecreulx, D. The bacA gene of Escherichia coli encodes an undecaprenyl pyrophosphate phosphatase activity. *Journal of Biological Chemistry* **2004**, *279* (29), 30106-30113.
(6) Wanke, C.; Amrhein, N. Evidence that the reaction of the UDP-N-acetylglucosamine 1-carboxyvinyltransferase proceeds through the O-phosphothioketal of pyruvic acid bound to Cys115 of the enzyme. *European Journal of Biochemistry* **1993**, *218* (3), 861-870.
(7) Benson, T. E.; Marquardt, J. L.; Marquardt, A. C.; Etzkorn, F. A.; Walsh, C. T. Overexpression, purification, and mechanistic study of UDP-N-acetylenolpyruvylglucosamine reductase. *Biochemistry* **1993**, *32* (8), 2024-2030.
(8) Chatterjee, A. N.; Park, J. T. Biosynthesis of cell wall mucopeptide by a particulate fraction from Staphylococcus aureus. *Proceedings of the National Academy of Sciences* **1964**, *51* (1), 9-16.
(9) Anderson, J. S.; Matsuhashi, M.; Haskin, M. A.; Strominger, J. L. Biosynthesis of the Peptidoglycan of Bacterial Cell Walls: II. Phospholipid carriers in the reaction sequence. *Journal of Biological Chemistry* **1967**, *242* (13), 3180-3190.
(10) Ruiz, N. Bioinformatics identification of MurJ (MviN) as the peptidoglycan lipid II flippase in Escherichia coli. *Proceedings of the National Academy of Sciences* **2008**, *105* (40), 15553-15557.
(11) Sauvage, E.; Kerff, F.; Terrak, M.; Ayala, J. A.; Charlier, P. The penicillin-binding proteins: structure and role in peptidoglycan biosynthesis. *FEMS Microbiology Reviews* **2008**, *32* (2), 234-258.
(12) Workman, S. D.; Strynadka, N. C. A slippery scaffold: synthesis and recycling of the bacterial cell wall carrier lipid. *Journal of Molecular Biology* **2020**, *432* (18), 4964-4982.
(13) Pazos, M.; Peters, K. Peptidoglycan bacterial cell walls and membranes. *Springer International Publishing Cham* **2019**, 127-168.
(14) Scheurwater, E.; Reid, C. W.; Clarke, A. J. Lytic transglycosylases: bacterial space-making autolysins. *The International Journal of Biochemistry & Cell Biology* **2008**, *40* (4), 586-591.
(15) Johnson, J. W.; Fisher, J. F.; Mobashery, S. Bacterial cell-wall recycling. *Annals of the New York Academy of Sciences* **2013**, *1277* (1), 54-75.
(16) Uehara, T.; Suefuji, K.; Valbuena, N.; Meehan, B.; Donegan, M.; Park, J. T. Recycling of the anhydro-N-acetylmuramic acid derived from cell wall murein involves a two-step conversion to N-acetylglucosamine-phosphate. *Journal of Bacteriology* **2005**, *187* (11), 3643-3649.
(17) Zhou, J.; Cai, Y.; Liu, Y.; An, H.; Deng, K.; Ashraf, M. A.; Zou, L.; Wang, J. Breaking down the cell wall: Still an attractive antibacterial strategy. *Frontiers in Microbiology* **2022**, *13*, 952633.
(18) Patrick, G. L. *An Introduction to Medicinal Chemistry*; Oxford university press, 2023.
(19) Schwarz, S.; Cloeckaert, A.; Roberts, M. C. Mechanisms and spread of bacterial resistance to antimicrobial agents. *Antimicrobial Resistance in Bacteria of Animal Origin* **2005**, 73-98.
(20) Zaman, S. B.; Hussain, M. A.; Nye, R.; Mehta, V.; Mamun, K. T.; Hossain, N. A review on antibiotic resistance: alarm bells are ringing. *Cureus* **2017**, *9* (6).
(21) Abushaheen, M. A.; Fatani, A. J.; Alosaimi, M.; Mansy, W.; George, M.; Acharya, S.; Rathod, S.; Divakar, D. D.; Jhugroo, C.; Vellappally, S. Antimicrobial resistance, mechanisms and its clinical significance. *Disease-a-Month* **2020**, *66* (6), 100971.
(22) Giurazza, R.; Mazza, M. C.; Andini, R.; Sansone, P.; Pace, M. C.; Durante-Mangoni, E. Emerging treatment options for multi-drug-resistant bacterial infections. *Life* **2021**, *11* (6), 519.

(23) Pulendran, B.; S. Arunachalam, P.; O'Hagan, D. T. Emerging concepts in the science of vaccine adjuvants. *Nature Reviews Drug Discovery* **2021**, *20* (6), 454-475.
(24) Bit, A.; Verma, N.; Tarai, S. Blood–brain barrier biomarker for neurodegenerative disorder. *Neurocognitive Perspectives of Prosocial and Positive Emotional Behaviours: Theory to application* **2021**, 3-35.
(25) Reinke, S.; Thakur, A.; Gartlan, C.; Bezbradica, J. S.; Milicic, A. Inflammasome-mediated immunogenicity of clinical and experimental vaccine adjuvants. *Vaccines* **2020**, *8* (3), 554.
(26) Facciolà, A.; Visalli, G.; Laganà, A.; Di Pietro, A. An overview of vaccine adjuvants: current evidence and future perspectives. *Vaccines* **2022**, *10* (5), 819.
(27) Salk, J. E.; Laurent, A. M. The use of adjuvants in studies on influenza immunization: I. Measurements in monkeys of the dimensions of antigenicity of virus-mineral oil emulsions. *The Journal of Experimental Medicine* **1952**, *95* (5), 429-447.
(28) Miller, L. H.; Saul, A.; Mahanty, S. Revisiting Freund's incomplete adjuvant for vaccines in the developing world. *TRENDS in Parasitology* **2005**, *21* (9), 412-414.
(29) Wolf, A. J.; Underhill, D. M. Peptidoglycan recognition by the innate immune system. *Nature Reviews Immunology* **2018**, *18* (4), 243-254.
(30) Mohammadi, T.; Van Dam, V.; Sijbrandi, R.; Vernet, T.; Zapun, A.; Bouhss, A.; Diepeveen-de Bruin, M.; Nguyen-Distèche, M.; De Kruijff, B.; Breukink, E. Identification of FtsW as a transporter of lipid-linked cell wall precursors across the membrane. *The EMBO Journal* **2011**, *30* (8), 1425-1432.
(31) Rubino, F. A.; Kumar, S.; Ruiz, N.; Walker, S.; Kahne, D. E. Membrane potential is required for MurJ function. *Journal of the American Chemical Society* **2018**, *140* (13), 4481-4484.
(32) Kuk, A. C.; Hao, A.; Lee, S.-Y. Structure and mechanism of the lipid flippase MurJ. *Annual review of Biochemistry* **2022**, *91* (1), 705-729.
(33) Kumar, S.; Mollo, A.; Rubino, F. A.; Kahne, D.; Ruiz, N. Chloride Ions Are Required for Thermosipho africanus MurJ Function. *Mbio* **2023**, *14* (1), e00089-00023.
(34) Kuk, A. C.; Mashalidis, E. H.; Lee, S.-Y. Crystal structure of the MOP flippase MurJ in an inward-facing conformation. *Nature Structural & Molecular Biology* **2017**, *24* (2), 171-176.
(35) Sham, L.-T.; Butler, E. K.; Lebar, M. D.; Kahne, D.; Bernhardt, T. G.; Ruiz, N. MurJ is the flippase of lipid-linked precursors for peptidoglycan biogenesis. *Science* **2014**, *345* (6193), 220-222.
(36) Meeske, A. J.; Sham, L.-T.; Kimsey, H.; Koo, B.-M.; Gross, C. A.; Bernhardt, T. G.; Rudner, D. Z. MurJ and a novel lipid II flippase are required for cell wall biogenesis in Bacillus subtilis. *Proceedings of the National Academy of Sciences* **2015**, *112* (20), 6437-6442.
(37) Elhenawy, W.; Davis, R. M.; Fero, J.; Salama, N. R.; Felman, M. F.; Ruiz, N. The O-antigen flippase Wzk can substitute for MurJ in peptidoglycan synthesis in Helicobacter pylori and Escherichia coli. *PLoS One* **2016**, *11* (8), e0161587.
(38) Chu, J.; Vila-Farres, X.; Inoyama, D.; Ternei, M.; Cohen, L. J.; Gordon, E. A.; Reddy, B. V. B.; Charlop-Powers, Z.; Zebroski, H. A.; Gallardo-Macias, R. Discovery of MRSA active antibiotics using primary sequence from the human microbiome. *Nature Chemical Biology* **2016**, *12* (12), 1004-1006.
(39) Chu, J.; Vila-Farres, X.; Inoyama, D.; Gallardo-Macias, R.; Jaskowski, M.; Satish, S.; Freundlich, J. S.; Brady, S. F. Human microbiome inspired antibiotics with improved β-lactam synergy against MDR Staphylococcus aureus. *ACS Infectious Diseases* **2018**, *4* (1), 33-38.
(40) Chamakura, K. R.; Sham, L.-T.; Davis, R. M.; Min, L.; Cho, H.; Ruiz, N.; Bernhardt, T. G.; Young, R. A viral protein antibiotic inhibits lipid II flippase activity. *Nature Microbiology* **2017**, *2* (11), 1480-1484.
(41) Mott, J. E.; Shaw, B. A.; Smith, J. F.; Bonin, P. D.; Romero, D. L.; Marotti, K. R.; Miller, A. A. Resistance mapping and mode of action of a novel class of antibacterial anthranilic acids: evidence for disruption of cell wall biosynthesis. *Journal of Antimicrobial Chemotherapy* **2008**, *62* (4), 720-729.
(42) Huber, J.; Donald, R. G.; Lee, S. H.; Jarantow, L. W.; Salvatore, M. J.; Meng, X.; Painter, R.; Onishi, R. H.; Occi, J.; Dorso, K. Chemical genetic identification of peptidoglycan inhibitors potentiating carbapenem activity against methicillin-resistant Staphylococcus aureus. *Chemistry & Biology* **2009**, *16* (8), 837-848.

(43) Kohga, H.; Mori, T.; Tanaka, Y.; Yoshikaie, K.; Taniguchi, K.; Fujimoto, K.; Fritz, L.; Schneider, T.; Tsukazaki, T. Crystal structure of the lipid flippase MurJ in a “squeezed” form distinct from its inward- and outward-facing forms. *Structure* **2022**, *30* (8), 1088-1097. e1083.
(44) Zheng, S.; Sham, L.-T.; Rubino, F. A.; Brock, K. P.; Robins, W. P.; Mekalanos, J. J.; Marks, D. S.; Bernhardt, T. G.; Kruse, A. C. Structure and mutagenic analysis of the lipid II flippase MurJ from Escherichia coli. *Proceedings of the National Academy of Sciences* **2018**, *115* (26), 6709-6714.
(45) Kuk, A. C.; Hao, A.; Guan, Z.; Lee, S.-Y. Visualizing conformation transitions of the Lipid II flippase MurJ. *Nature Communications* **2019**, *10* (1), 1736.
(46) Bastos, P. A.; Wheeler, R.; Boneca, I. G. Uptake, recognition and responses to peptidoglycan in the mammalian host. *FEMS Microbiology Reviews* **2021**, *45* (1), fuaa044.
(47) Lu, X.; Wang, M.; Qi, J.; Wang, H.; Li, X.; Gupta, D.; Dziarski, R. Peptidoglycan recognition proteins are a new class of human bactericidal proteins. *Journal of Biological Chemistry* **2006**, *281* (9), 5895-5907.
(48) Dziarski, R.; Kashyap, D. R.; Gupta, D. Mammalian peptidoglycan recognition proteins kill bacteria by activating two-component systems and modulate microbiome and inflammation. *Microbial Drug Resistance* **2012**, *18* (3), 280-285.
(49) Wang, Z.-M.; Li, X.; Cocklin, R. R.; Wang, M.; Wang, M.; Fukase, K.; Inamura, S.; Kusumoto, S.; Gupta, D.; Dziarski, R. Human peptidoglycan recognition protein-L is an N-acetylmuramoyl-L-alanine amidase. *Journal of Biological Chemistry* **2003**, *278* (49), 49044-49052.
(50) Hoving, J. C.; Wilson, G. J.; Brown, G. D. Signalling C-type lectin receptors, microbial recognition and immunity. *Cellular Microbiology* **2014**, *16* (2), 185-194.
(51) Lu, J.; Zhao, Z.; Li, Q.; Pang, Y. Review of the unique and dominant lectin pathway of complement activation in agnathans. *Developmental & Comparative Immunology* **2023**, *140*, 104593.
(52) Bidula, S.; Sexton, D. W.; Schelenz, S. Ficolins and the recognition of pathogenic microorganisms: an overview of the innate immune response and contribution of single nucleotide polymorphisms. *Journal of Immunology Research* **2019**, *2019* (1), 3205072.
(53) Cash, H. L.; Whitham, C. V.; Behrendt, C. L.; Hooper, L. V. Symbiotic bacteria direct expression of an intestinal bactericidal lectin. *Science* **2006**, *313* (5790), 1126-1130.
(54) Gupta, D.; Kirkland, T. N.; Viriyakosol, S.; Dziarski, R. CD14 is a cell-activating receptor for bacterial peptidoglycan. *Journal of Biological Chemistry* **1996**, *271* (38), 23310-23316.
(55) Dziarski, R.; Tapping, R. I.; Tobias, P. S. Binding of bacterial peptidoglycan to CD14. *Journal of Biological Chemistry* **1998**, *273* (15), 8680-8690.
(56) Wolf, A. J. Peptidoglycan-induced modulation of metabolic and inflammatory responses. *Immunometabolism* **2023**, *5* (2), e00024.
(57) Chamaillard, M.; Hashimoto, M.; Horie, Y.; Masumoto, J.; Qiu, S.; Saab, L.; Ogura, Y.; Kawasaki, A.; Fukase, K.; Kusumoto, S. An essential role for NOD1 in host recognition of bacterial peptidoglycan containing diaminopimelic acid. *Nature Immunology* **2003**, *4* (7), 702-707.
(58) Stafford, C. A.; Gassauer, A.-M.; de Oliveira Mann, C. C.; Tanzer, M. C.; Fessler, E.; Wefers, B.; Nagl, D.; Kuut, G.; Sulek, K.; Vasilopoulou, C. Phosphorylation of muramyl peptides by NAGK is required for NOD2 activation. *Nature* **2022**, *609* (7927), 590-596.
(59) Wagner, R. N.; Proell, M.; Kufer, T. A.; Schwarzenbacher, R. Evaluation of Nod-like receptor (NLR) effector domain interactions. *PloS one* **2009**, *4* (4), e4931.
(60) Takeda, K.; Akira, S. Toll receptors and pathogen resistance. *Cellular Microbiology* **2003**, *5* (3), 143-153.
(61) Takeuchi, O.; Hoshino, K.; Kawai, T.; Sanjo, H.; Takada, H.; Ogawa, T.; Takeda, K.; Akira, S. Differential roles of TLR2 and TLR4 in recognition of gram-negative and gram-positive bacterial cell wall components. *Immunity* **1999**, *11* (4), 443-451.
(62) Yoshimura, A.; Lien, E.; Ingalls, R. R.; Tuomanen, E.; Dziarski, R.; Golenbock, D. Cutting edge: recognition of Gram-positive bacterial cell wall components by the innate immune system occurs via Toll-like receptor 2. *The Journal of Immunology* **1999**, *163* (1), 1-5.

(63) Travassos, L. H.; Girardin, S. E.; Philpott, D. J.; Blanot, D.; Nahori, M. A.; Werts, C.; Boneca, I. G. Toll-like receptor 2-dependent bacterial sensing does not occur via peptidoglycan recognition. *EMBO Reports* **2004**, *5* (10), 1000-1006.
(64) Dziarski, R.; Gupta, D. Staphylococcus aureus peptidoglycan is a toll-like receptor 2 activator: a reevaluation. *Infection and immunity* **2005**, *73* (8), 5212-5216.
(65) Calmette, A.; Boquet, A.; Nègre, L. *L'infection bacillaire et la tuberculose chez l'homme et chez les animaux: processus d'infection et de défense, étude biologique et expérimentale, vaccination préventive*; Masson, 1928.
(66) Freund, J.; Casals, J.; Hosmer, E. P. Sensitization and antibody formation after injection of tubercle bacilli and paraffin oil. *Proceedings of the Society for Experimental Biology and Medicine* **1937**, *37* (3), 509-513.
(67) Griffin, M. E.; Hespen, C. W.; Wang, Y. C.; Hang, H. C. Translation of peptidoglycan metabolites into immunotherapeutics. *Clinical & Translational Immunology* **2019**, *8* (12), e1095.
(68) Ellouz, F.; Adam, A.; Ciorbaru, R.; Lederer, E. Minimal structural requirements for adjuvant activity of bacterial peptidoglycan derivatives. *Biochemical and Biophysical Research Communications* **1974**, *59* (4), 1317-1325.
(69) Kleinnijenhuis, J.; Quintin, J.; Preijers, F.; Joosten, L. A.; Ifrim, D. C.; Saeed, S.; Jacobs, C.; van Loenhout, J.; de Jong, D.; Stunnenberg, H. G. Bacille Calmette-Guerin induces NOD2-dependent nonspecific protection from reinfection via epigenetic reprogramming of monocytes. *Proceedings of the National Academy of Sciences* **2012**, *109* (43), 17537-17542.
(70) Clarke, T. B.; Davis, K. M.; Lysenko, E. S.; Zhou, A. Y.; Yu, Y.; Weiser, J. N. Recognition of peptidoglycan from the microbiota by Nod1 enhances systemic innate immunity. *Nature Medicine* **2010**, *16* (2), 228-231.
(71) Heldwein, K. A.; Liang, M. D.; Andresen, T. K.; Thomas, K. E.; Marty, A. M.; Cuesta, N.; Vogel, S. N.; Fenton, M. J. TLR2 and TLR4 serve distinct roles in the host immune response against Mycobacterium bovis BCG. *Journal of Leucocyte Biology* **2003**, *74* (2), 277-286.
(72) Khan, A.; Bakhru, P.; Saikolappan, S.; Das, K.; Soudani, E.; Singh, C. R.; Estrella, J. L.; Zhang, D.; Pasare, C.; Ma, Y. An autophagy-inducing and TLR-2 activating BCG vaccine induces a robust protection against tuberculosis in mice. *Npj Vaccines* **2019**, *4* (1), 34.
(73) Parant, M.; Parant, F.; Chedid, L.; Yapo, A.; Petit, J.; Lederer, E. Fate of the synthetic immunoadjuvant, muramyl dipeptide (14C-labelled) in the mouse. *International Journal of Immunopharmacology* **1979**, *1* (1), 35-41.
(74) Kotani, S.; Watanabe, Y.; Shimono, T.; Harada, K.; Shiba, T. Correlation between the immunoadjuvant activities and pyrogenicities of synthetic N-acetylmuramyl-peptides or-amino acids. *Biken Journal* **1976**, *19* (1), 9-13.
(75) Krueger, J.; Pappenheimer, J.; Karnovsky, M. Sleep-promoting effects of muramyl peptides. *Proceedings of the National Academy of Sciences* **1982**, *79* (19), 6102-6106.
(76) Lederer, E. Synthetic immunostimulants derived from the bacterial cell wall. *Journal of Medicinal Chemistry* **1980**, *23* (8), 819-825.
(77) Chedid, L.; Parant, M.; Audibert, F.; Riveau, G.; Parant, F.; Lederer, E.; Choay, J.; Lefrancier, P. Biological activity of a new synthetic muramyl peptide adjuvant devoid of pyrogenicity. *Infection and Immunity* **1982**, *35* (2), 417-424.
(78) Matsumoto, K.; Ogawa, H.; Kusama, T.; Nagase, O.; Sawaki, N.; Inage, M.; Kusumoto, S.; Shiba, T.; Azuma, I. Stimulation of nonspecific resistance to infection induced by 6-O-acyl muramyl dipeptide analogs in mice. *Infection and Immunity* **1981**, *32* (2), 748-758.
(79) Matsumoto, K.; Otani, T.; Une, T.; Osada, Y.; Ogawa, H.; Azuma, I. Stimulation of nonspecific resistance to infection induced by muramyl dipeptide analogs substituted in the gamma-carboxyl group and evaluation of N alpha-muramyl dipeptide-N epsilon-stearoyllysine. *Infection and Immunity* **1983**, *39* (3), 1029-1040.
(80) Graham, B. S.; Keefer, M. C.; McElrath, M. J.; Gorse, G. J.; Schwartz, D. H.; Weinhold, K.; Matthews, T. J.; Esterlitz, J. R.; Sinangil, F.; Fast, P. E. Safety and immunogenicity of a candidate HIV-1 vaccine in

healthy adults: recombinant glycoprotein (rgp) 120: a randomized, double-blind trial. *Annals of Internal Medicine* **1996**, *125* (4), 270-279.
(81) Keitel, W.; Couch, R.; Bond, N.; Adair, S.; Van Nest, G.; Dekker, C. Pilot evaluation of influenza virus vaccine (IVV) combined with adjuvant. *Vaccine* **1993**, *11* (9), 909-913.
(82) Kitaura, Y.; Takeno, H.; Aratani, M.; Okada, S.; Yonishi, S.; Hemmi, K.; Nakaguchi, O.; Hashimoto, M. Synsthesis and RES-stimulating activity of bacterial cell-wall peptidoglycan peptides related to FK-156. *Experientia* **1982**, *38* (9), 1101-1103.
(83) Jakopin, Z. i.; Gobec, M.; Mlinarič-Raščan, I.; Sollner Dolenc, M. Immunomodulatory properties of novel nucleotide oligomerization domain 2 (Nod2) agonistic desmuramyldipeptides. *Journal of Medicinal Chemistry* **2012**, *55* (14), 6478-6488.
(84) Gobec, M.; Tomašič, T.; Štimac, A.; Frkanec, R. a.; Trontelj, J.; Anderluh, M.; Mlinarič-Raščan, I.; Jakopin, Z. i. Discovery of nanomolar desmuramylpeptide agonists of the innate immune receptor nucleotide-binding oligomerization domain-containing protein 2 (NOD2) possessing immunostimulatory properties. *Journal of Medicinal Chemistry* **2018**, *61* (7), 2707-2724.
(85) Siddiqui, W. A.; Taylor, D. W.; Kan, S.-C.; Kramer, K.; Richmond-Crum, S. M.; Kotani, S.; Shiba, T.; Kusumoto, S. Vaccination of experimental monkeys against Plasmodium falciparum: a possible safe adjuvant. *Science* **1978**, *201* (4362), 1237-1239.
(86) Fidler, I. J. Optimization and limitations of systemic treatment of murine melanoma metastases with liposomes containing muramyl tripeptide phosphatidylethanolamine. *Cancer Immunology, Immunotherapy* **1986**, *21*, 169-173.
(87) Talmadge, J.; Lenz, B.; Klabansky, R.; Simon, R.; Riggs, C.; Guo, S.; Oldham, R.; Fidler, I. Therapy of autochthonous skin cancers in mice with intravenously injected liposomes containing muramyltripeptide. *Cancer Research* **1986**, *46* (3), 1160-1163.
(88) Kaur, A.; Baldwin, J.; Brar, D.; Salunke, D. B.; Petrovsky, N. Toll-like receptor (TLR) agonists as a driving force behind next-generation vaccine adjuvants and cancer therapeutics. *Current Opinion in Chemical Biology* **2022**, *70*, 102172.
(89) Yang, J.-X.; Tseng, J.-C.; Yu, G.-Y.; Luo, Y.; Huang, C.-Y. F.; Hong, Y.-R.; Chuang, T.-H. Recent advances in the development of toll-like receptor agonist-based vaccine adjuvants for infectious diseases. *Pharmaceutics* **2022**, *14* (2), 423.
(90) Casella, C. R.; Mitchell, T. C. Putting endotoxin to work for us: monophosphoryl lipid A as a safe and effective vaccine adjuvant. *Cellular and Molecular Life Sciences* **2008**, *65*, 3231-3240.

Chapter 2 – Efforts Towards Synthesis of Labelled Lipid II Analogues

Introduction

Interest around investigating the bacterial flippase protein, MurJ, as novel means of antibiotic therapy has led to an interest in developing suitable functional derivatives of the native substrate Lipid II. Such interest has hinged around the design of substrates for reporting activity in proteoliposomal assays (Fig. 2.1). Attempts at resolving this problem have proceeded with the synthesis of fluorophore conjugates that are likely untolerated due to steric constraints [1]. We hypothesised that radiolabelled and isosterically fluorinated analogues could prove to be suitable alternatives due to the subtlety of the chemical modification; recent crystallographic data suggests the disaccharide hydroxyls as suitable sites for such modification due to lack of interaction with specific residues and accommodation in a relatively large binding cavity [2-4]. Considering this data, a synthetic method allowing for fluorination and radiolabelling around the MurNAc 6 OH was explored.

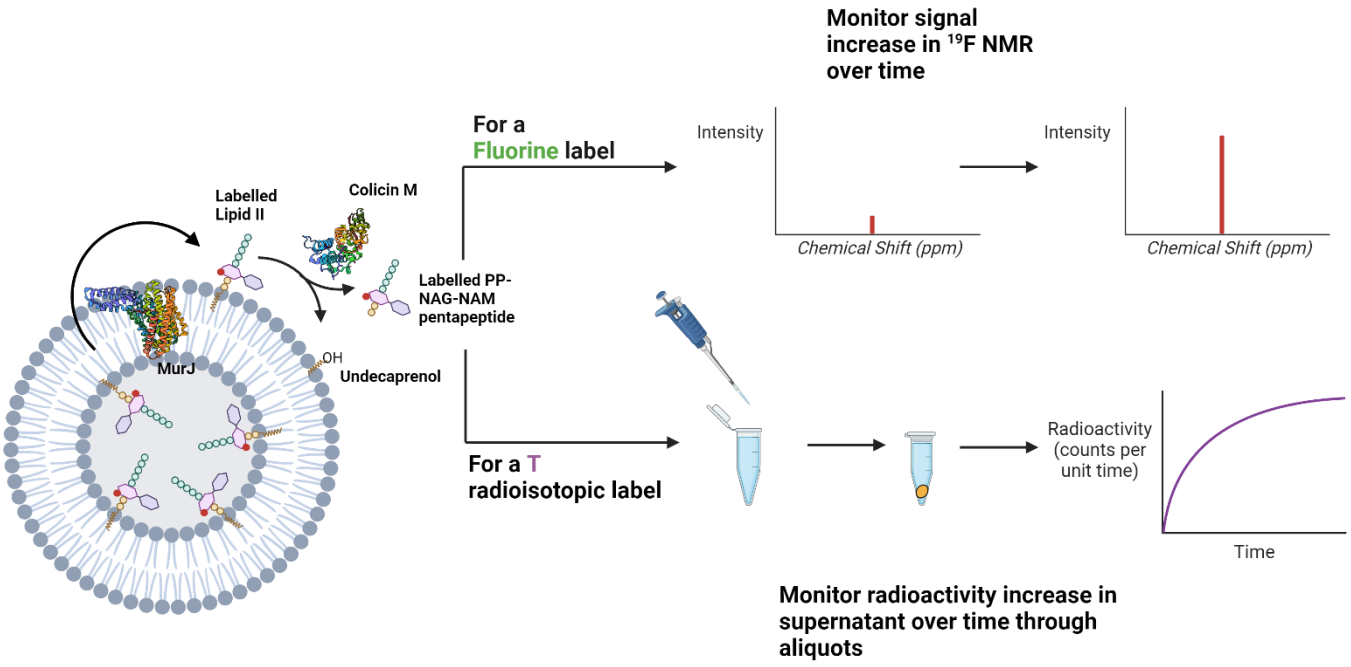


Figure 2.1 - Proposed flippase assays with labelled Lipid II

Previous Approaches to Accessing Lipid II

Chemical Synthesis

Access to Lipid II was first reported via chemical syntheses in the early 2000s (Fig. 2.2). Schwartz reported the first ever synthesis [5] beginning with **2.1**, a commonly used intermediate in the preparation of muramyl dipeptide. Amide coupling with trimethylsilyl ethyl (TMSE) protected L-Ala proceeded first, followed by acetal hydrolysis with *p*-toluenesulfonic acid (TsOH) and regioselective acetylation of the 6 OH with acetyl chloride to give glycosyl acceptor **2.4**. The regioselectivity during the acetylation is owed to the low reaction temperature strongly favouring the kinetic product; there is a lower energy barrier to acetylation at the 6 OH. The first residue of peptide stem was introduced prior to acetal hydrolysis in order to prevent undesired intramolecular lactone formation. Glycosylation with donor **2.5** yielded the β(1,4) disaccharide core, owing to the neighbouring group participation provided by the phthaloyl (Phth) group. The Phth group is able to form an oxazolinium ring from the oxocarbenium intermediate. This ring blocks axial delivery, producing the β glycoside as a result of equatorial attack [6]. The Phth group was next removed, followed by hydrogenolysis of the anomeric benzyl (Bn). The reducing sugar was reacted with *N*,*N*-diisopropyl dibenzyl phosphoramidite and tetrazole as a Brønsted acid activator to yield the phosphite which was subsequently oxidised with *meta*-chloroperoxybenzoic acid (*m*CPBA) to phosphate **2.7**. Desilylation to unmask the carboxylic acid followed by condensation with tetrapeptide **2.8** to give **2.9**. The benzylic groups on the phosphate were removed by hydrogenolysis and the free phosphate coupled to undecaprenyl phosphate with carbonyl diimidazole (CDI). Global deprotection gave Lipid II in a 0.7% overall yield.

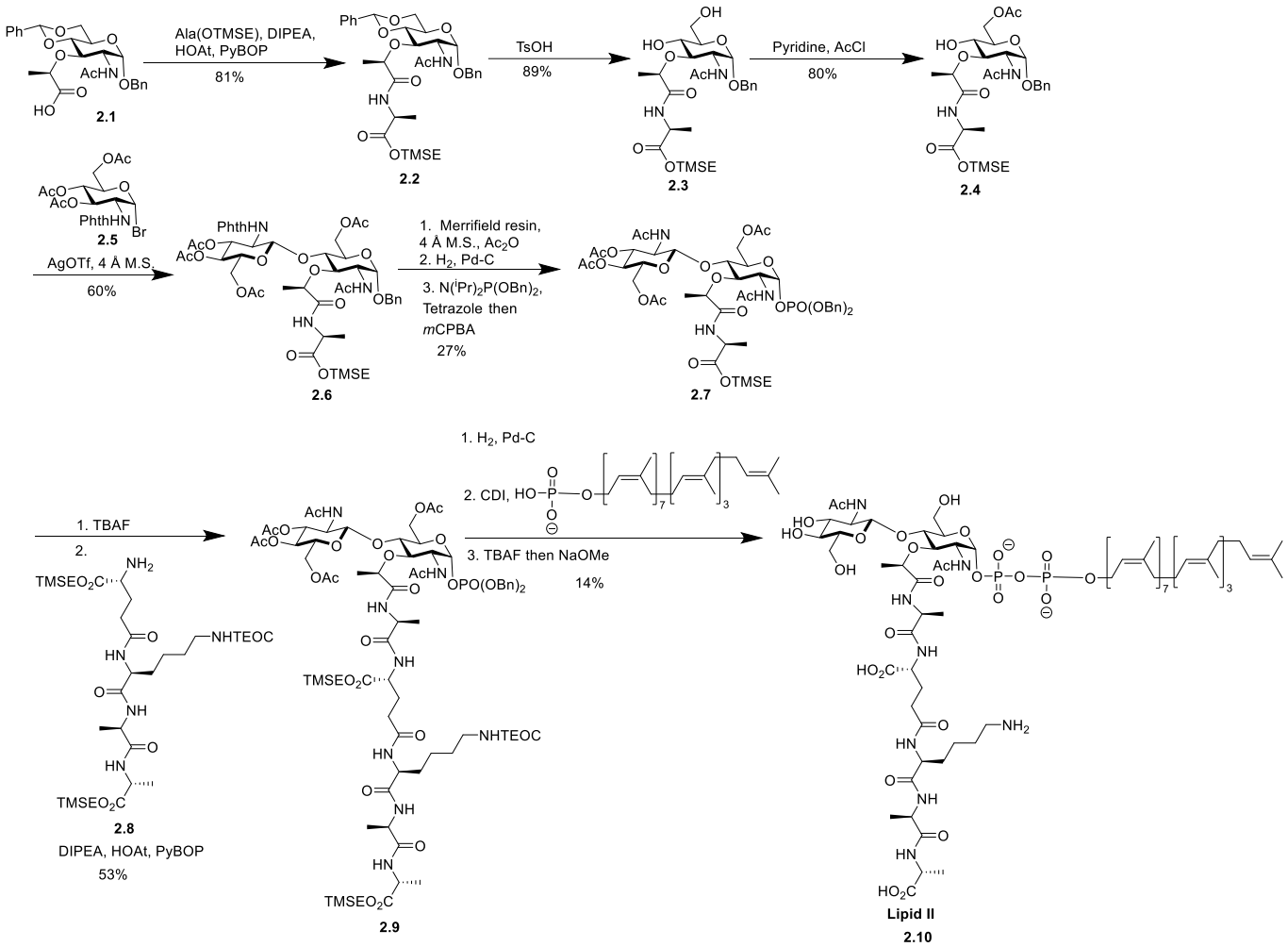


Figure 2.2 – Schwartz's synthesis of Lipid II

Shortly after, Lipid II was similarly synthesised by Van Nieuwenhze (Fig. 2.3) [7]. They accessed the disaccharide core using their previously reported methodology [8]; the core was formed through a Koenigs Knorr reaction of acceptor **2.12** with 2,2,2-trichloroethoxycarbonyl (Troc) protected glucosamine donor **2.13**. The Troc is able to participate in the same fashion as the Phth group used by Schwartz to block axial attack of the acceptor and afford the trans glycoside. Following glycosylation, regioselective 6 OBn debenzylation and acetylation was carried out with $ZnCl_2$, acetic acid (AcOH), and acetic anhydride (Ac_2O). Addition of Zn dust allowed for one pot reductive cleavage of the Troc group and acetylation. Hydrogenolysis and phosphorylation via a phosphite were carried out to give **2.16**. The phenyl sulfonyl ethyl (PSE) ester was selectively deprotected with non-nucleophilic base, allowing for condensation with a tetrapeptide **2.17** bearing base labile protecting groups to give **2.18**. The tetrapeptide was also amidated at the glutamic acid position a modification native to

biology. Deprotection of the phosphate and pyrophosphate coupling gave Lipid II after one step global deprotection with NaOMe.

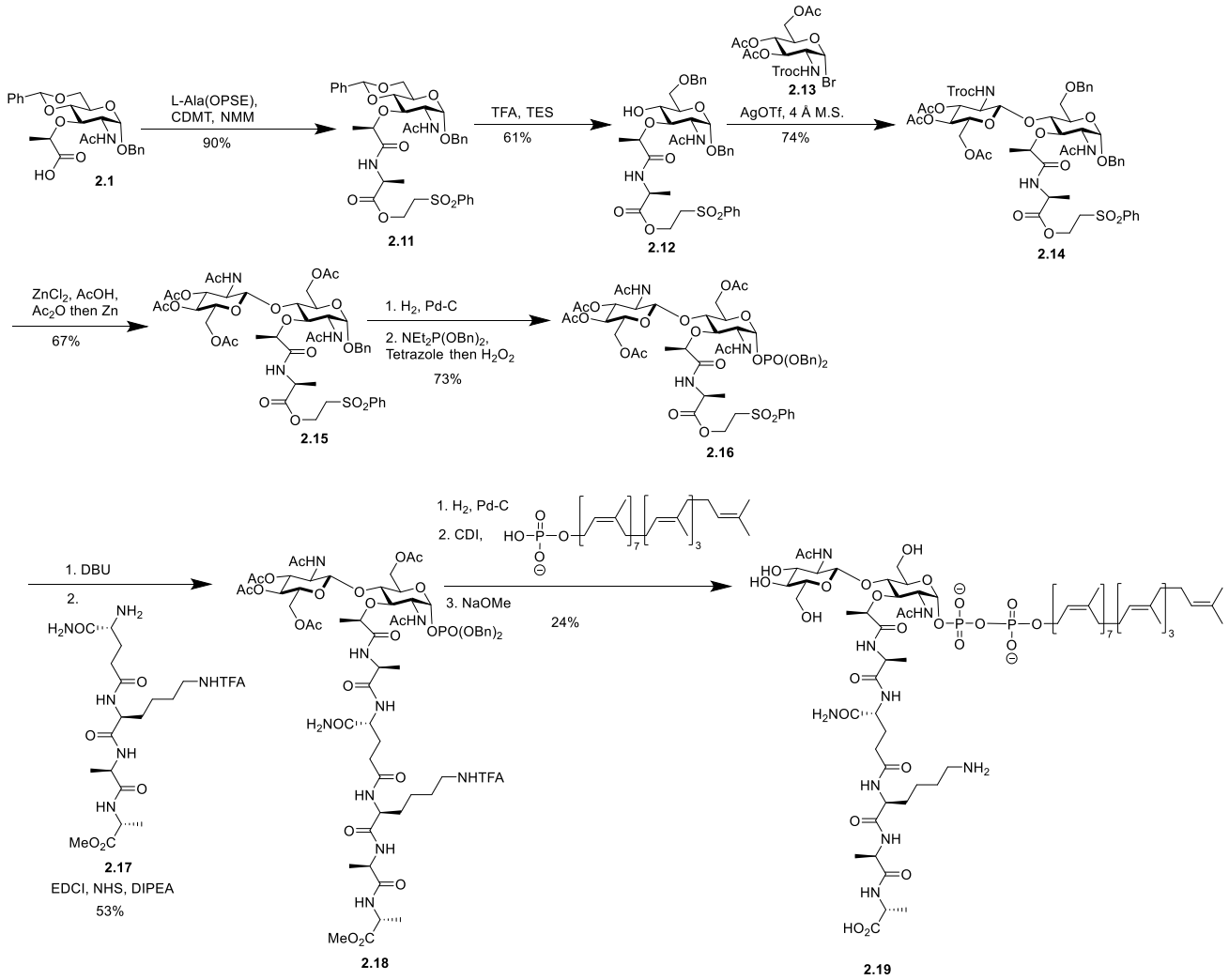


Figure 2.3 – Van Nieuwehnze's synthesis of Lipid II

Since these early efforts additional syntheses have been reported, however the sequence of assembly and adopted routes remain largely the same with the most notable deviations being in the glycosylation conditions used to construct the disaccharide core (Fig. 2.4). The recalcitrant nature of the glycosylation has seen many groups report differing conditions with optimisations of donor-acceptor pairs still being published to this date [9]. These recent findings make clear the importance of the acceptor 6 OH protecting group, the participating *N* protecting group, and show the suitability of many different donors and related promoters. This in conjunction with older findings showing the effects of differing donor protecting groups [10, 11], explain the breadth of variation reported in this step.

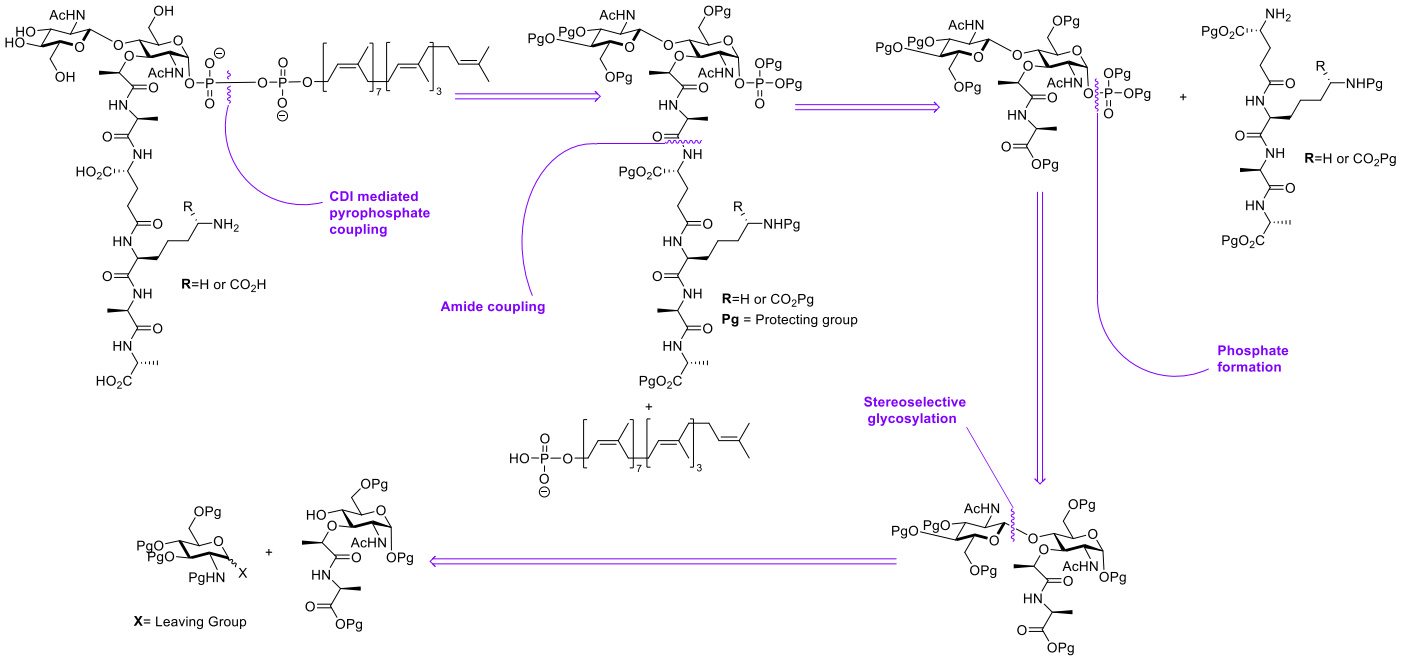


Figure 2.4 – Universal retrosynthetic approach for Lipid II synthesis

Soon after the aforementioned early efforts, use of thioglycosides was successfully reported in the synthesis of the disaccharide backbone and a nitrophenyl Lipid II analogue (Fig. 2.5) [12]. Commonly used muramyl intermediate **2.1** was protected through esterification as a PSE ester. Hydrolysis of the acetal allowed regioselective 6 OH esterification as a benzoyl ester to give acceptor **2.20**; similarly to Schwartz's synthesis, intramolecular lactone formation proved to be an undesirable side reaction during hydrolysis, so excess H_2O was added to prevent this. Successful glycosylation was carried out with peracetyl thioglycoside **2.22** using *N*-iodosuccinimide (NIS) and triflic acid (TfOH) to give the Lipid II disaccharide core in 56% yield.

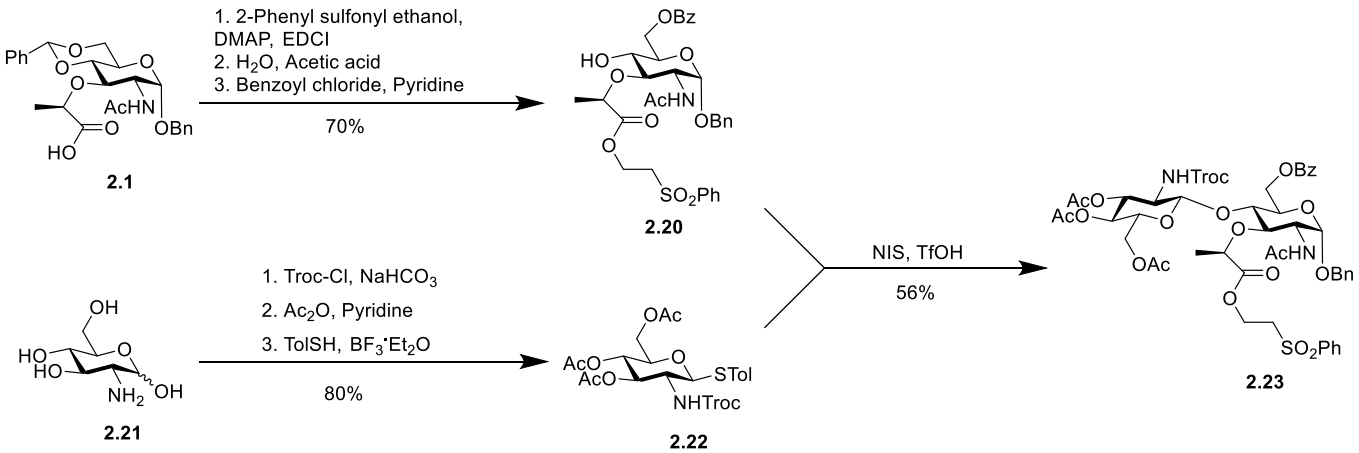


Figure 2.5 – Synthesis of the Lipid II disaccharide with thioglycosides

An optimized example of thioglycoside use in Lipid II and dimeric Lipid IV synthesis was reported by Cheng (Fig. 2.6) [13]. This work made use of their previous findings regarding relative reactivity values for one pot glycosidic couplings [11]. Incorporation of an electron withdrawing chloro ester placeholder in MurNAc motif **2.25** reduced the donor character and prevented homodimerization during glycosylation. This allowed for use of an S tolyl (Tol) functional group at the anomeric position in the acceptor, allowing either functionalisation as a phosphate for Lipid II synthesis or polymerisation to make Lipid IV. Disaccharide **2.26** was obtained in an excellent 92% yield and the ester placeholder removed reductively with $NaBH_4$. The participating phthaloyl group was removed and the free amine acetylated to give **2.27**. Lactoylation via triflate displacement ensued to generate a MurNAc-GlcNAc backbone intermediate characteristic of Lipid II syntheses. Cheng furthered the use of thioglycosides to access analogues that could serve as alternate substrates [14] or inhibitors [15, 16].

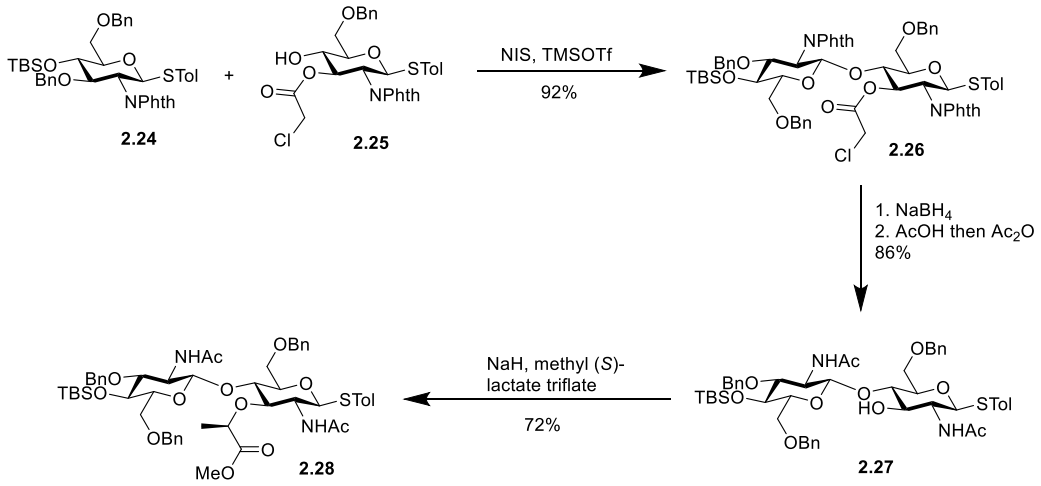


Figure 2.6 – Cheng's optimised use of thioglycosides in Lipid II synthesis

Although Schmidt reported the use of different trichloroacetamide donors developed within their group to access MurNAc-GlcNAc disaccharides and tetrasaccharides (Fig. 2.7) a decade prior to the first reports of Lipid II syntheses, applications elaborating the disaccharide into the full structure were not reported until later.

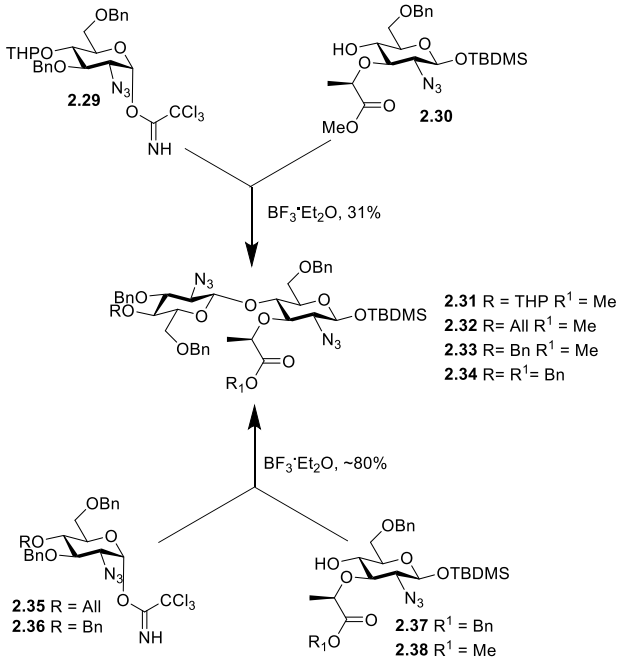


Figure 2.7 – Synthesis of the Lipid II disaccharide with trichloroacetamides

An early example is the use of trichloroacetamide donors in accessing mycobacterial Lipid II (Fig. 2.8). This substrate bears an *N*-glycol modification native to the *Mycobacterium* genus and as a result requires the glycosylation of an acceptor bearing an unusual *N* protecting group. The synthesis began with a change in the *N* substituent from acetyl to *tert*-butyloxycarbonyl (Boc). Methanolysis and transacetalisation allowed for selective exposure of the 3 OH giving **2.40**. Lactoylation via triflate displacement gave **2.41**. Base hydrolysis unmasked the carboxylic acid allowing for condensation with H-L-Ala(OTMSE) to install the first residue of the peptide stem and give **2.42**. Treatment with TsOH allowed for concomitant acetal hydrolysis and Boc removal. The more nucleophilic free amine was then acylated with acetoxy acetyl chloride followed by regioselective acetylation of the 6 OH to give acceptor **2.43**. Schmidt glycosylation with phthaloyl trichloroacetamide donor **2.44** gave disaccharide **2.45** in 50% yield.

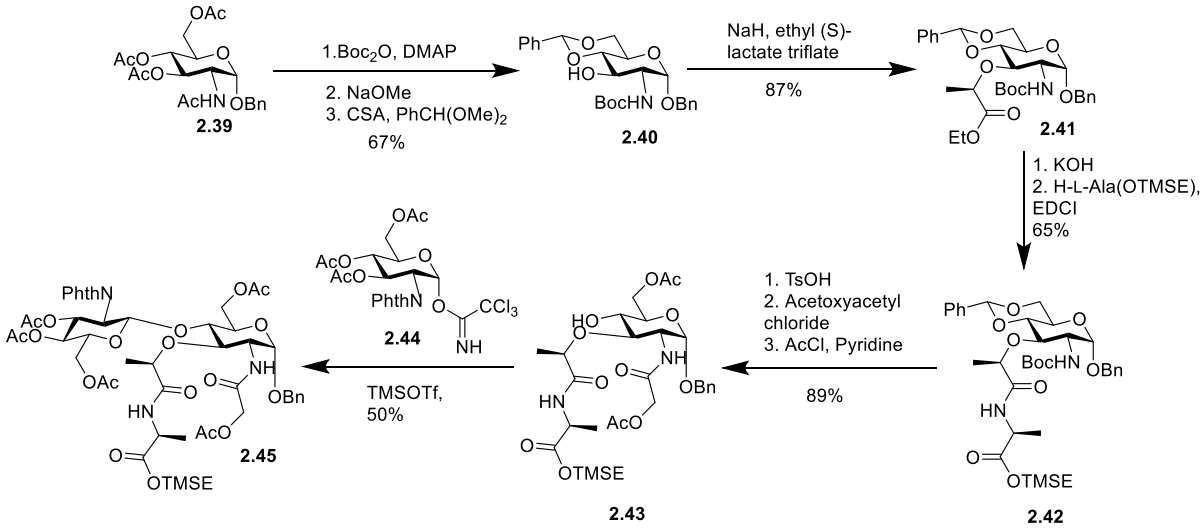


Figure 2.8 – Use of trichloroacetamides in Mycobacterial Lipid II synthesis

Optimisations involving trichloroacetamide donor use in Lipid II synthesis have used solid phase chemistry and have been reported by Kuroso (Fig. 2.9) [17]. This strategy relies on regioselective protection of the 6 OH in diol **2.46** through resin attachment with a bulky trichloroacetamide linker. Use of a resin linker with the same functionality as Schmidt donors allows for one pot addition of donor **2.47** and glycosylation, forming disaccharide **2.48** on resin in 85% yield. Liberation of **2.48** from resin could be conducted under reductive conditions with Zn, AcOH allowing for concomitant removal of the Troc group. Acetylation with Ac_2O gave disaccharide **2.15** the intermediate first reported by Van Nieuwenhze [7].

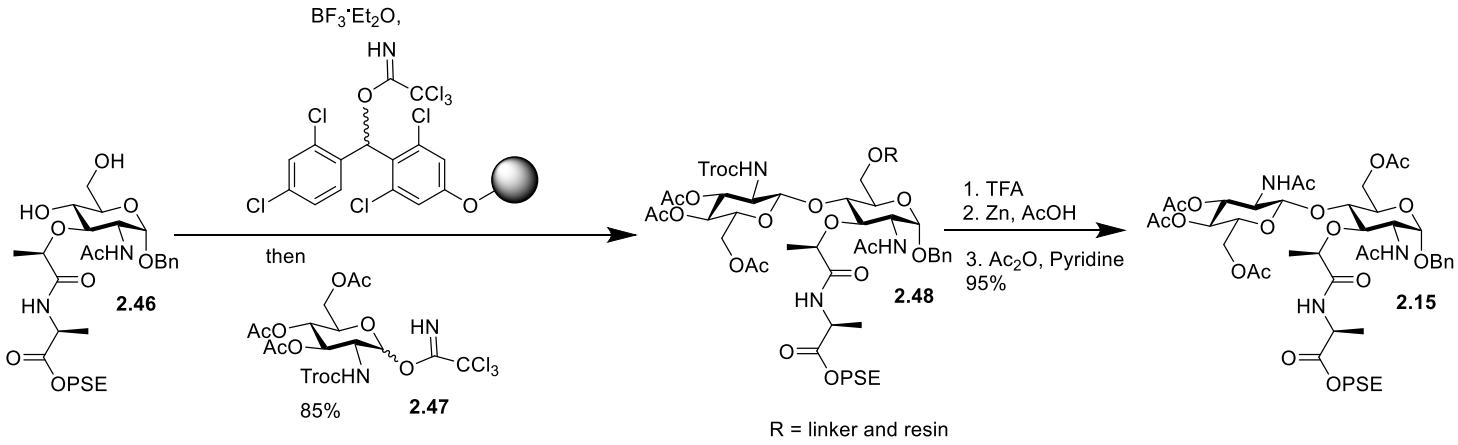


Figure 2.9 – Optimised synthesis of Lipid II with trichloroacetamides

Use of trichloroacetamide donors has remained prevalent and additional more recent examples from more canonical routes [18-22] as well as in inhibitor design [23, 24] have been reported. Outside of these alternate glycosylation strategies discussed, other methods amenable to accessing the MurNAc-GlcNAc core have been reported [25-27]. These methods have however not been used to access Lipid II and instead polymeric peptidoglycan products, because of this they are discussed in detail in chapter 3.

Until recently many of the variants and optimisations to Lipid II synthesis have focused on solution phase chemistry, however following the work of Kuroso [17], the Ichchikawa group have furthered the introduction of solid phase chemistry, assembling neryl Lipid II almost completely on resin (Fig. 2.10) [28]. The protected D-Ala-D-Ala-L-Lys-D-Glu tetrapeptide **2.50** was prepared on solid phase and amide coupled to disaccharide **2.49**. The phosphate was deprotected and pyrophosphate coupling to neryl phosphate imidazolide was achieved with a triflate salt of tetrazole; screening of different activators revealed more acidic tetrazole derivatives as more effective. This method was also used to access Lipid II precursors: Park's nucleotide and Lipid I. The group later made use of orthogonality at the L-Lys side chain to synthesise fluorophore conjugates [29]. Together these studies elucidate solid phase conditions for coupling of ubiquitous Lipid II fragments such that complete solid phase assembly may soon be possible.

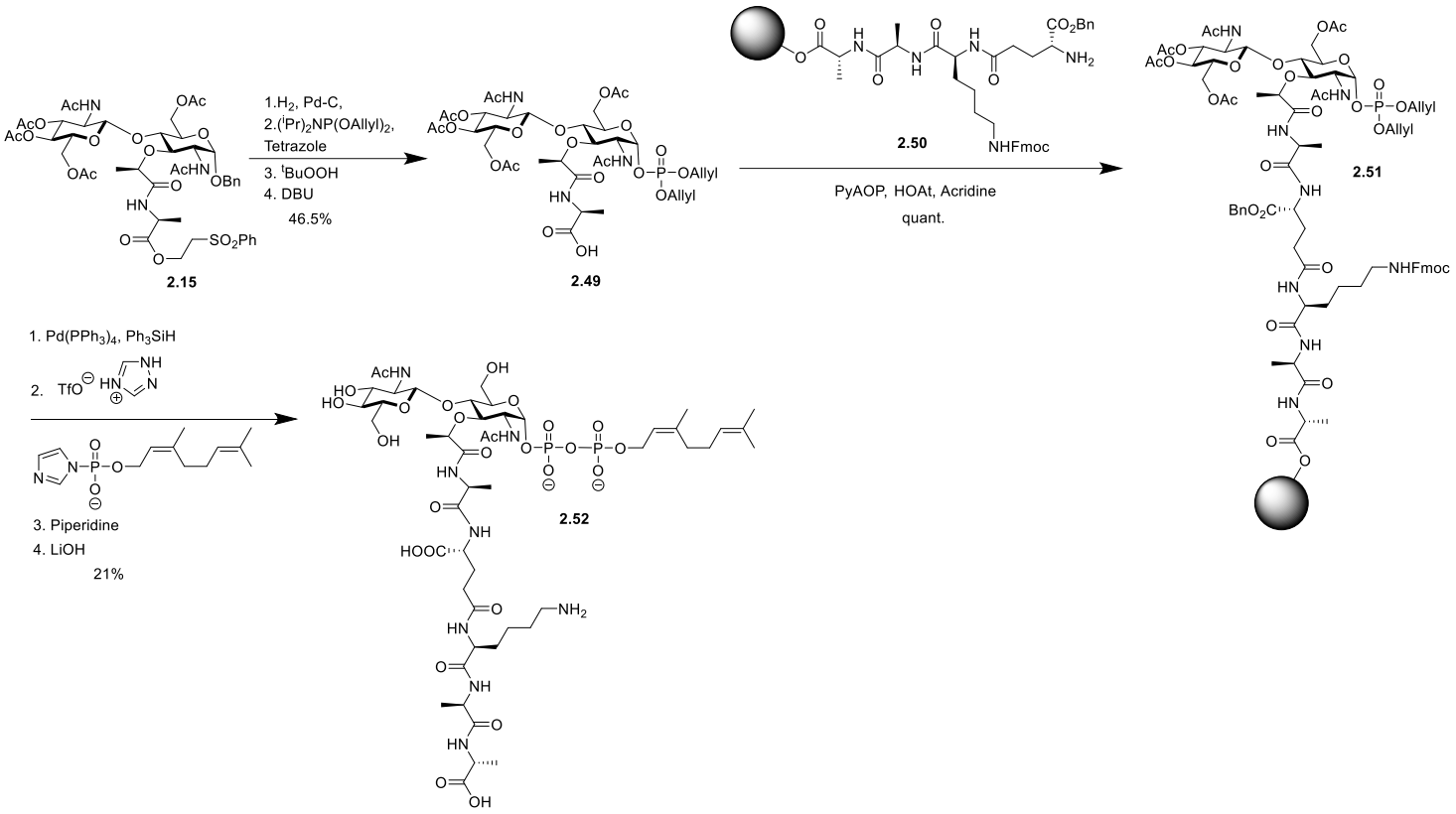


Figure 2.10 – Ichikawa's solid phase synthesis of Lipid II

Advancements in Lipid II synthesis have seen optimised solutions to assembling the notoriously challenging disaccharide core and the introduction of solid phase chemistry allowing for easier purification and expedited access. Whilst much progress has been made, careful optimisation of the glycosylation step can still be required, particularly for novel acceptor-donor pairs.

Enzymatic Synthesis

In addition to total synthetic approaches, the use of enzymes in Lipid II preparations has been explored. Chemoenzymatic syntheses were pioneered by Walker, documenting acceptance of a Lipid I analogue, **2.59**, bearing a 10 carbon citronellol chain by MurG in 1998 (Fig. 2.11) [30]. The rationale behind using the citronellol chain was the enhanced solubility and stability afforded due to the shorter hydrophobic chain and improved stability through avoiding use of an unstable allylic phosphate. Preparation of **2.56** began with esterification of the carboxyl group in commercially available, **2.1**, with trichloroethanol. Hydrogenolysis then removed the anomeric benzyl ether and undesirably the benzylidene acetal. Resultingly acid catalysed transacetalisation with benzaldehyde dimethyl acetal gave reprotected **2.54**. With the anomeric hydroxyl selectively exposed, phosphorylation was carried out via formation and

oxidation of a phosphite intermediate followed by reductive deprotection of the Troc ester to give **2.56**. Amide coupling of tetrapeptide **2.57** with the exposed carboxyl group, followed by hydrogenolytic cleavage of the benzylic phosphate and acetal bonds gave **2.58**. Phosphate exchange with protected citronellol pyrophosphate followed by treatment with tetra-n-butyl ammonium fluoride (TBAF) gave **2.59**. In addition to the silyl protecting groups in the peptide chain, the terminal methyl ester was also hydrolysed. For ease of product separation during biological assays, the lysine side chain was biotin labelled to give **2.60**. The authors were able to track MurG catalysed addition of radiolabelled UDP-GlcNAc to **2.60**, however no direct structural analysis of the product was performed.

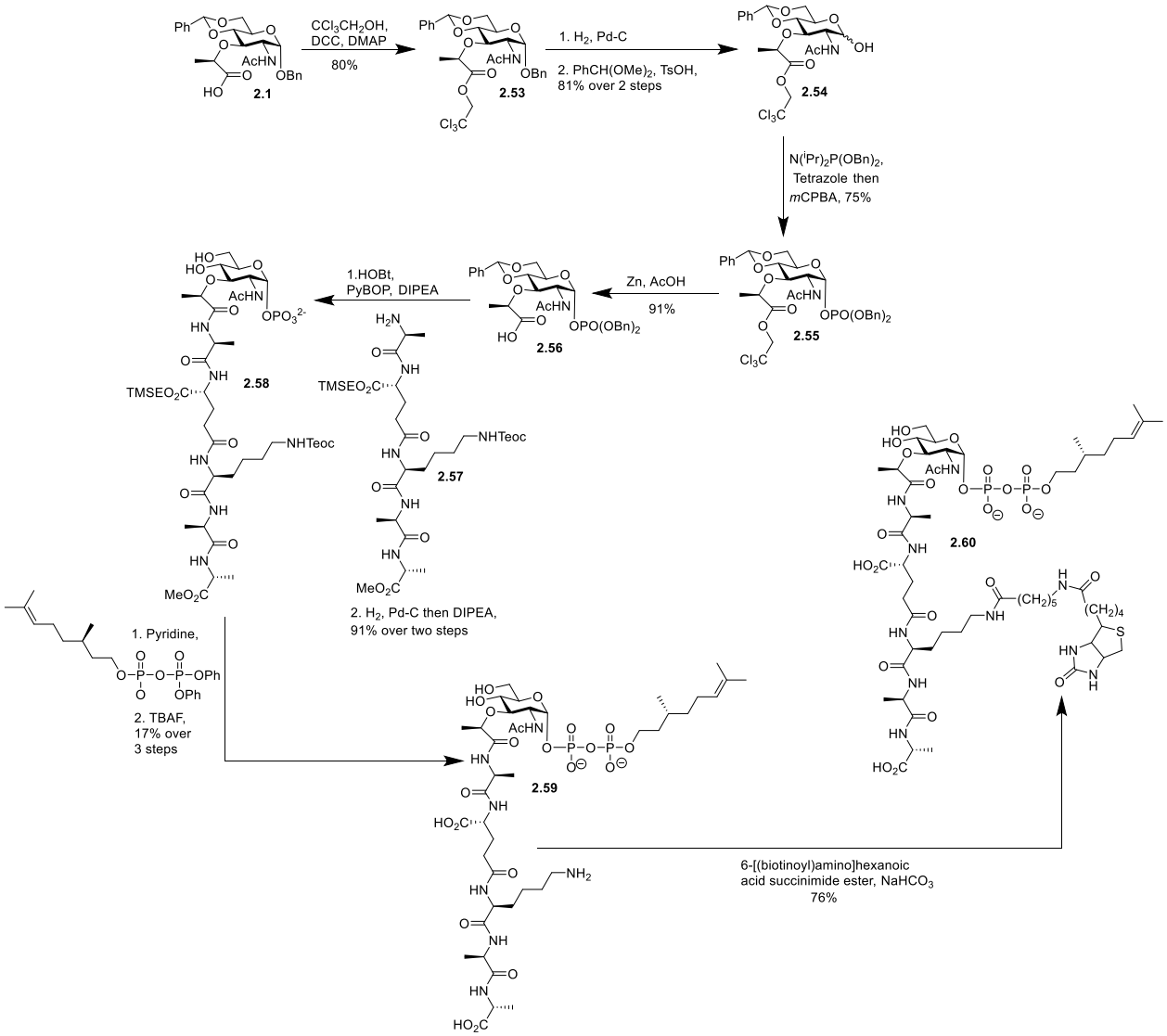


Figure 2.11 – Walker's synthesis of Biotin labelled Lipid I for MurG reaction

In 2001 Walker elaborated on this work to access authentic Lipid II and shortened chain variants bearing allylic phosphates due to the lack of recognition of citronellol by transglycosylases (Fig. 2.12) [31]. During this work Lipid II was isolated and characterised validating this chemoenzymatic approach. The incompatibility of allylic phosphates with the phosphate exchange method used to prepare **2.59** saw modifications to reaction conditions, with use of CDI mediated coupling to lipid monophosphates instead as is the case with total synthetic preparations. Additional examples using these methods have been reported [32-35] and have proved particularly valuable in accessing non-canonical Lipid II.

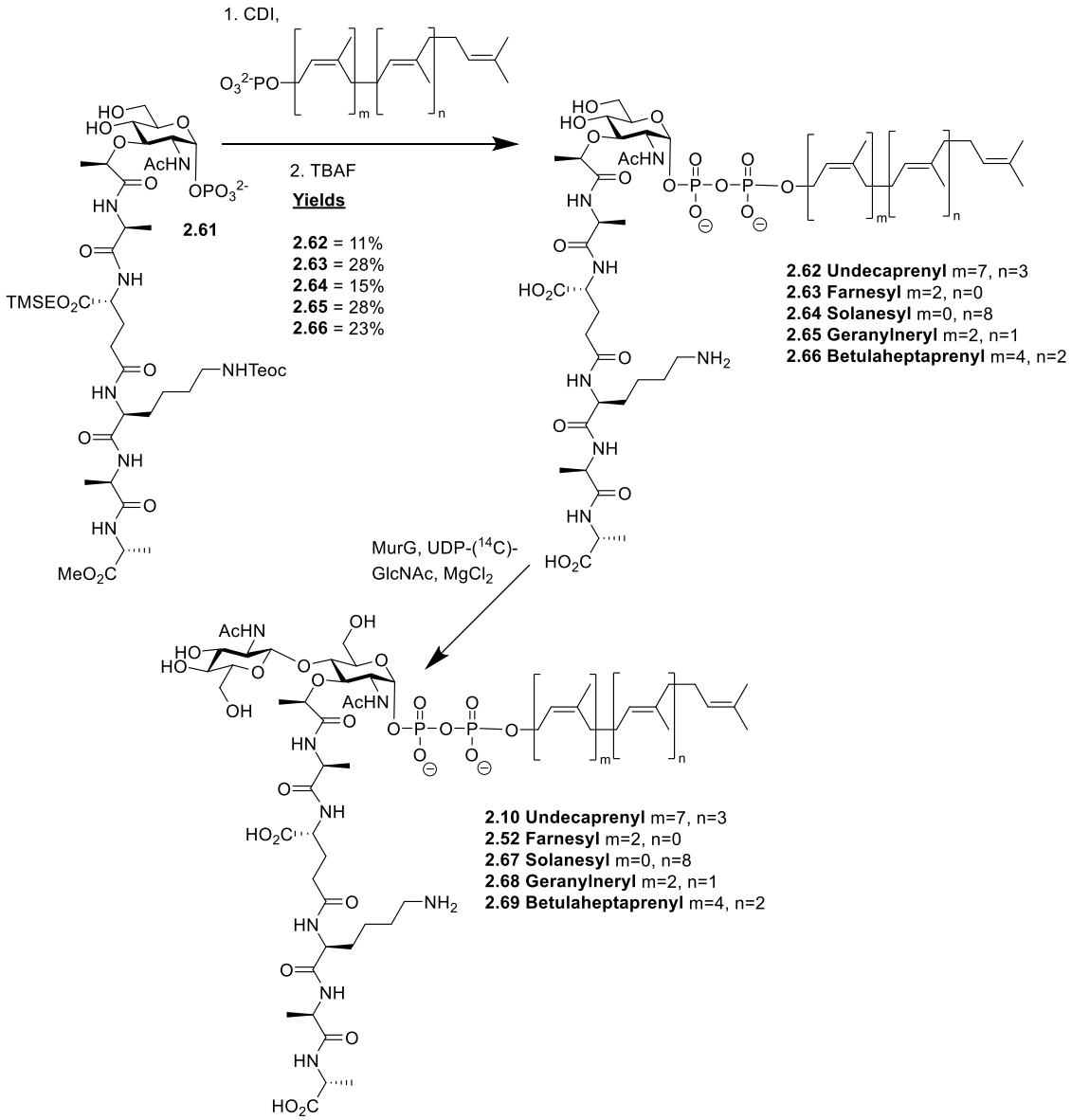


Figure 2.12 – Walker's chemoenzymatic synthesis of Lipid II with recombinant MurG

To unpick interactions between Lipid II and the known antibiotic Nisin, Walker developed an additional strategy expanding the use of enzymes in Lipid II synthesis (Fig. 2.13) [36]. This strategy relied on processing of a Park's nucleotide by the final two enzymes within the biosynthetic pathway, MraY and MurG. They showed that incubating Park's nucleotide, **2.70**, purified from *Staphylococcus simulans* with *Micrococcus flavus* membrane extracts comprising the necessary enzymes, as well as UDP-GlcNAc and polyprenyl phosphates allowed for production of Lipid II and short chain analogues. This two-enzyme strategy was further validated by Cheng during antibiotic investigation of the transglycosylase PonA [37] to access mycobacterial Lipid II (Fig. 2.14). They used synthetic Park's nucleotide, **2.71**, and conducted the enzymatic reactions in accordance with Walker's method. During this study they examined membrane extracts from other bacterial species, however optimal conversion was found with *Micrococcus flavus* validating Walker's choice. More recent work has seen this approach used as means of making Lipid II *in situ* for development of an assay suitable for high throughput [38].

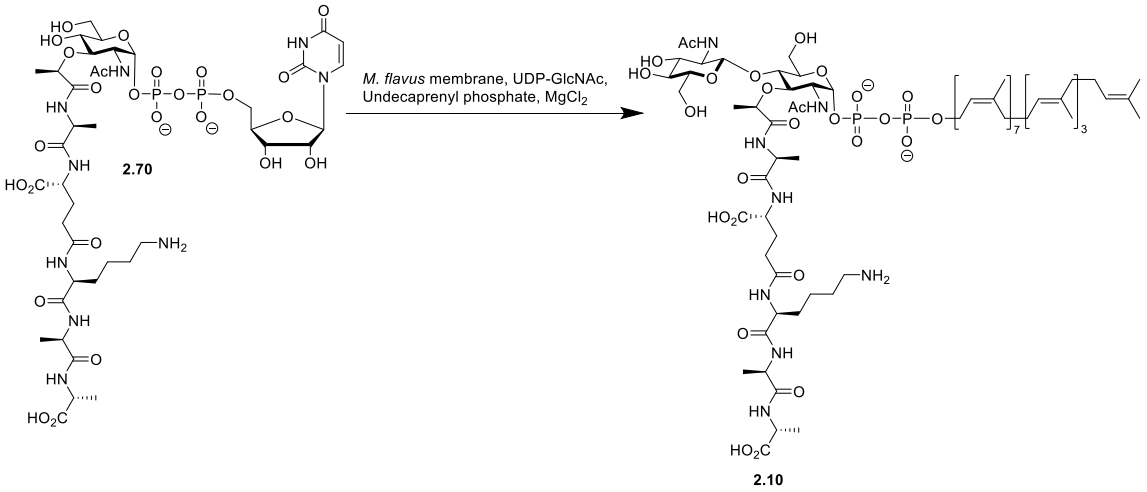


Figure 2.13 – Walker's chemoenzymatic synthesis of Lipid II with membrane extracts

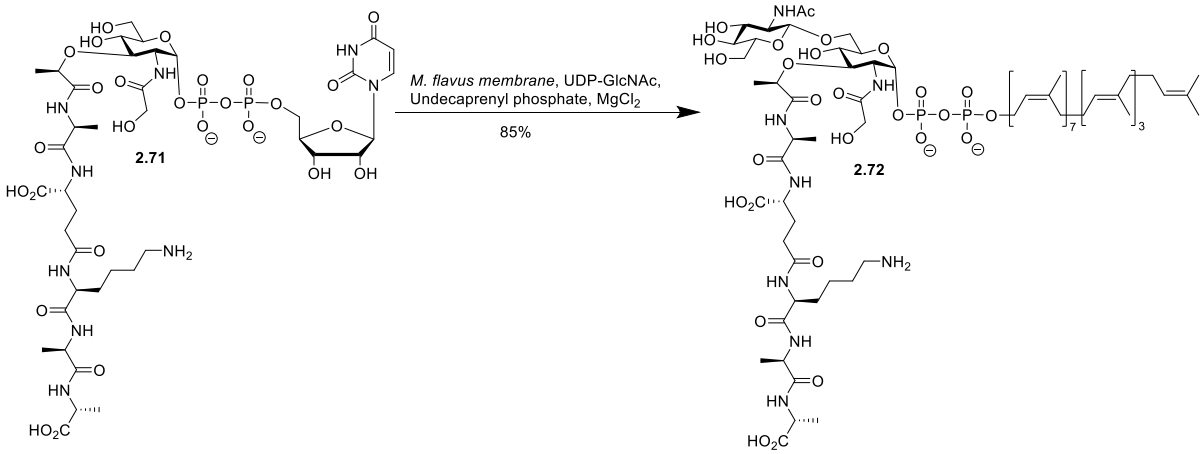


Figure 2.14 – Cheng's chemoenzymatic synthesis of Mycobacterial Lipid II with membrane extracts

Following the first reports of these one and two enzymes strategies, Cheng was able to assemble Lipid II completely enzymatically (Fig. 2.15) [39]. This strategy is the culmination of significant foundational work assessing *in vitro* recapitulation of the earlier steps within the biosynthetic pathway [40-43]. Individual expression of all the proteins from the biosynthetic pathway allowed for commencement from GlcNAc, avoiding the use of more expensive UDP-GlcNAc. The strategy prepared Park's nucleotide **2.70** from one pot with three sequential enzyme additions. First incubation with NahK and GlmU along with the necessary cosubstrates produced UDP-GlcNAc. On confirmation of product formation, MurA and MurB along with the necessary cosubstrates were added to give UDP-MurNAc. In similar fashion to before, on product formation, the MurC-F enzymes along with their necessary cosubstrates were added. Park's nucleotide, **2.70**, was then isolated in 60-80% yield. This substrate was then subjected to further reaction with MraY, MurG along with undecaprenyl phosphate and UDP-GlcNAc. Interestingly the authors were able to express an MraY chimera for use in this reaction and did not rely on the use of membrane extracts as in [36, 37]. Lipid II could then be purified from the reaction mixture in 55-70% yield. The group also demonstrated the applicability of this methodology to accessing shortened lipid chain analogues.

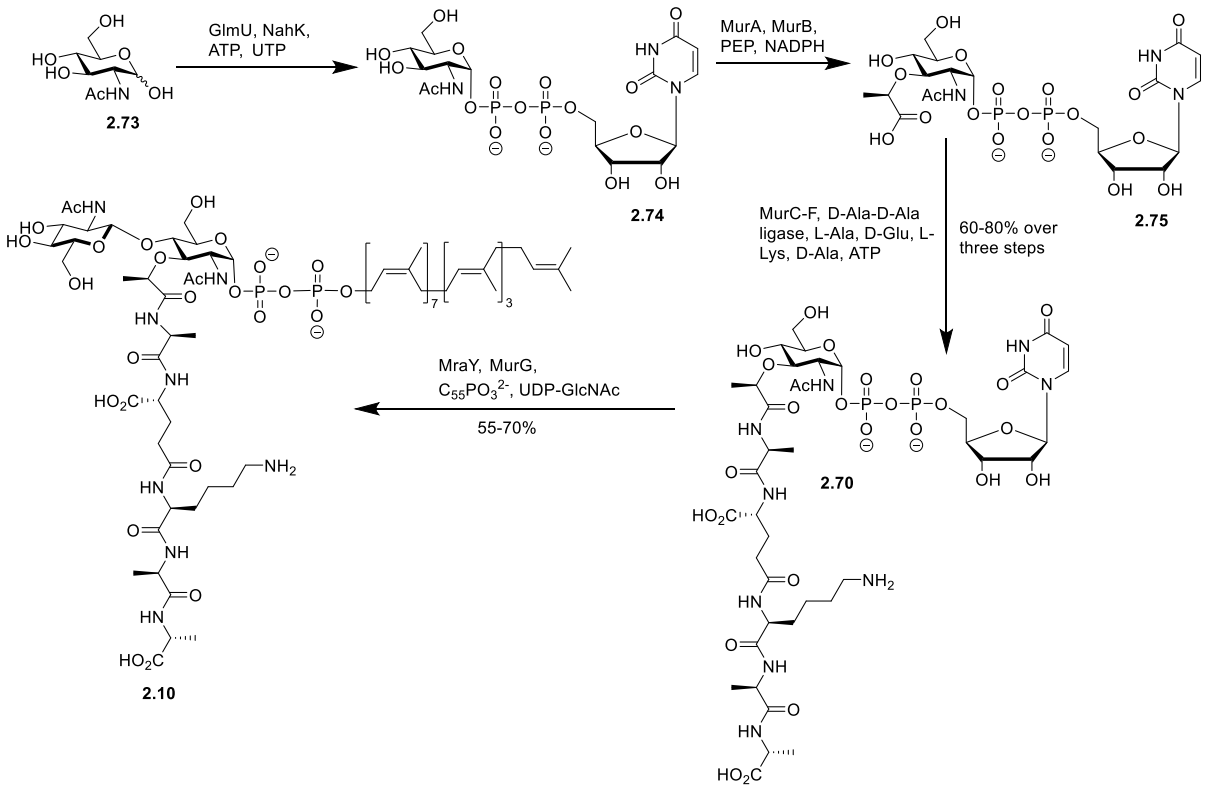


Figure 2.15 – Cheng's enzymatic synthesis of Lipid II

Advancements in enzymatic strategies have culminated in complete enzymatic preparations of Lipid II widening accessibility to groups unspecialized in chemistry. Despite this, use of the

one enzyme strategy reported by Walker has remained the most predominant. This is likely due to avoidance of laborious expression of many individual proteins, whilst retaining the advantage of bypassing a difficult glycosylation.

Radiolabelling of Lipid II

The design of biological assays to investigate protein activity often requires access to functionalised substrates to provide means of tracking substrate movement and/or processing. Evaluation of Lipid II processing enzymes as drug targets has led to a demand for such derivatives, particularly in assessing turnover by the penicillin binding proteins, known antibiotic targets possessing transglycosylase activity [44]. In many cases this demand has been met by Lipid II derivatives functionalised with fluorophores [21, 22, 36, 45], however as interest has grown surrounding another Lipid II processing protein, the flippase MurJ, these derivatives appear unsuitable [1], perhaps owing to their steric bulk [2-4]. Alongside Lipid II fluorophore conjugates, radiolabelled Lipid II has been explored for biological assays and presents an alternative substrate that may prove suitable for investigating MurJ.

Radiolabelled Lipid II was accessed in 2001 as part of a study measuring the membrane associated steps of the biosynthetic pathway (Fig. 2.16) [46]. The authors utilised Walker's 'two enzyme' strategy [36] with bacterial membrane extracts containing MraY and MurG, in conjunction with UDP-[^{3}H]-GlcNAc to incorporate a tritium label into Lipid II. A pull down-assay of peptidoglycan exposed to this reaction mixture showed radioactivity in the polysaccharide, demonstrating the utility of radiolabelled Lipid II to assay downstream enzyme function. Soon after, Mahapatra reported versatile syntheses of multiple radiolabelled products bearing ^{14}C in different positions (Fig. 2.17) [40]. The authors showed that enzymatic synthesis from UDP-MurNAc with different radioactive substrates and substrate precursors allowed for incorporation of a radiolabel in the peptide and lipid motifs as well as the GlcNAc. Since these early reports many additional preparations have been reported, with nearly all efforts similarly relying on the use of enzymes [47-50], the most common strategies utilising MurG catalysed addition of either ^{14}C or ^{3}H labelled UDP-GlcNAc donors. Chemical radiolabelling has also been reported, albeit briefly [51]. Acylation of the lysine side chain with ^{14}C acetic anhydride, gives a closely related analogue, however use of this strategy is not further reported.

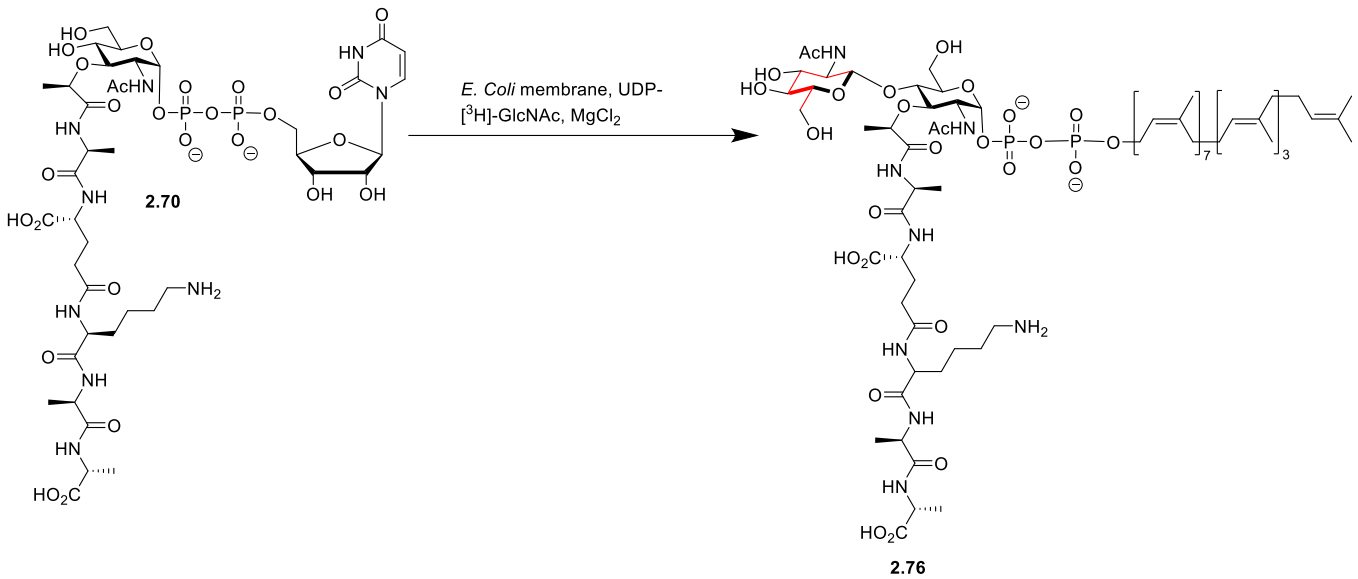


Figure 2.16 – Early report of Lipid II radiolabelling with Walker's chemoenzymatic strategy – Red colour denotes where a ^{3}H label can be found

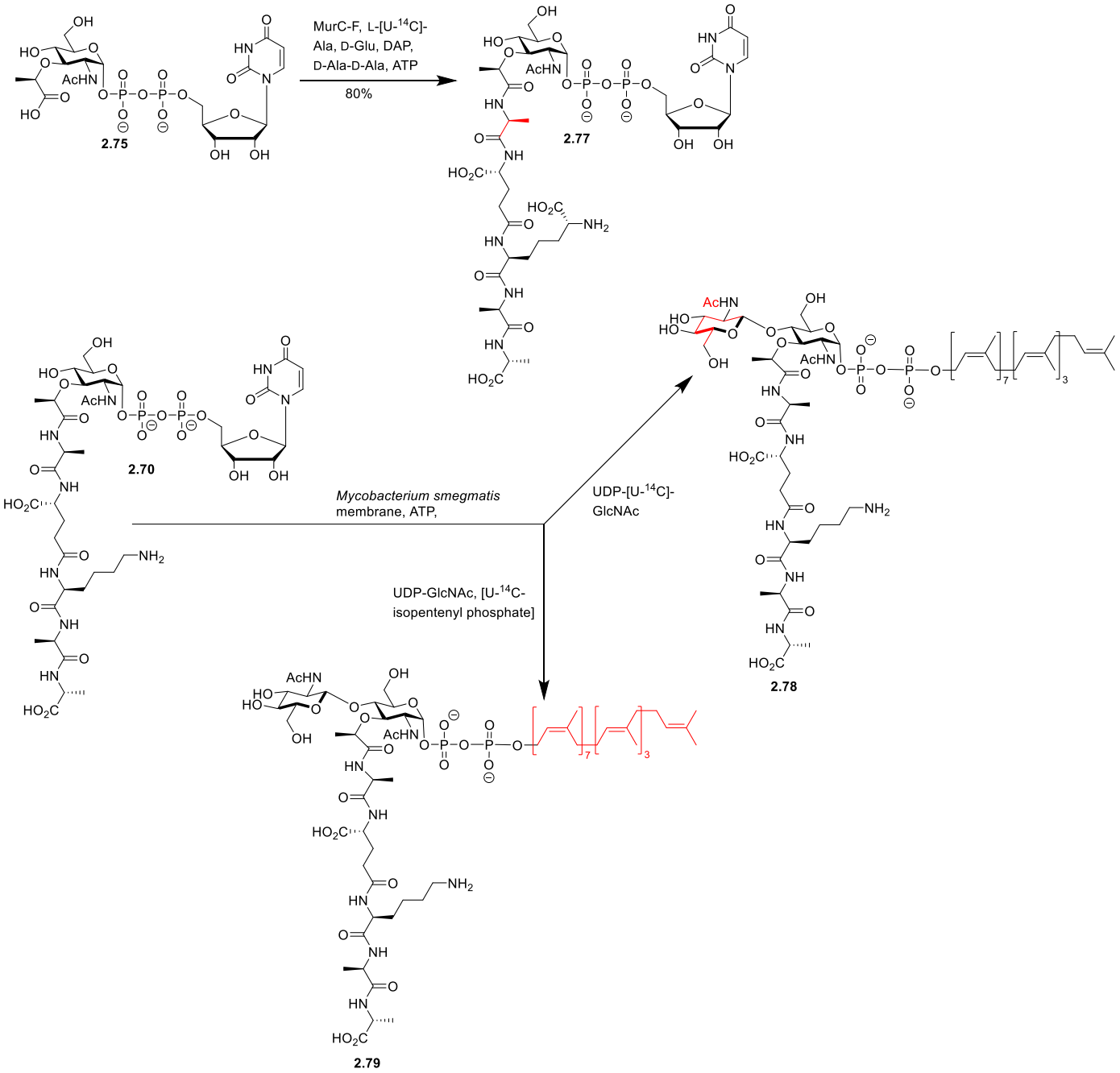


Figure 2.17 – Radiolabelling reactions from Mahapatra's synthesis of differentially radiolabelled Lipid II – Red colour denotes regions where a ^{14}C label can exist

In summary radiolabelling of Lipid II has been extensively studied and presents itself as an attractive alternative to conjugation with fluorophores due to the lack of steric imposition. Unfortunately, there are several drawbacks such as the procurement of very expensive radiolabelled substrates, safety risks associated with handling such materials, and the current reliance on chemoenzymatic methods which may not tolerate structural modifications associated with analogue design. The creation of new methodology allowing for more versatile radiolabelling strategies and synthesis of derivatives bearing new single atom labels with similar reporting capabilities would address these current issues.

A New Approach to Labelling Lipid II

Traditionally Lipid II labelling with radioisotopes has relied on the use of enzymatic methods, however these strategies may not also be amenable to accessing the fluorinated derivative required for our proposed NMR study, as MurG may not recognise fluorinated monosaccharides. Synthetic methods were consequently considered, and it was realised that incorporation of an orthogonal protecting group at the acceptor 6 OH could easily yield access to desired analogues **2.80** and **2.81** from a common intermediate (Fig. 2.18). Selective exposure of the 6 OH will allow for deoxyfluorination to ultimately yield **2.81**, whereas oxidation to the aldehyde stage and reduction with a tritide source will allow for radiolabelling to ultimately yield **2.80**. In addition to producing a candidate for probing flippase biology, demonstration of the deoxyfluorination methodology and access to fluorinated Lipid II will help address an unmet desire for accessing ^{18}F Lipid II as a radiotracer for imaging infection through PET [52]. During our synthesis we also realised that accessing such an intermediate could allow for kinetically controlled intramolecular nucleophilic substitution to give **2.82**, due to the ability of phosphates to act as leaving groups in the presence of a Lewis acid promoter [53]. Such anhydro sugars have very recently been under study as novel antibiotics and have been shown to terminate peptidoglycan elongation at high concentrations due to their lack of a reducing end [54]; a mechanism which is yet to be employed therapeutically and pertinent to the diversification of medicinal strategies required to combat antimicrobial resistance. Many syntheses rely on the preformation of the anhydro motif in monosaccharide acceptors, a strategy which is not amenable to also accessing Lipid II [54-59]. Given that these sugars act on Lipid II processing enzymes [54], concise access to both in a single route would certainly be desirable and has not been reported to the best of my knowledge.

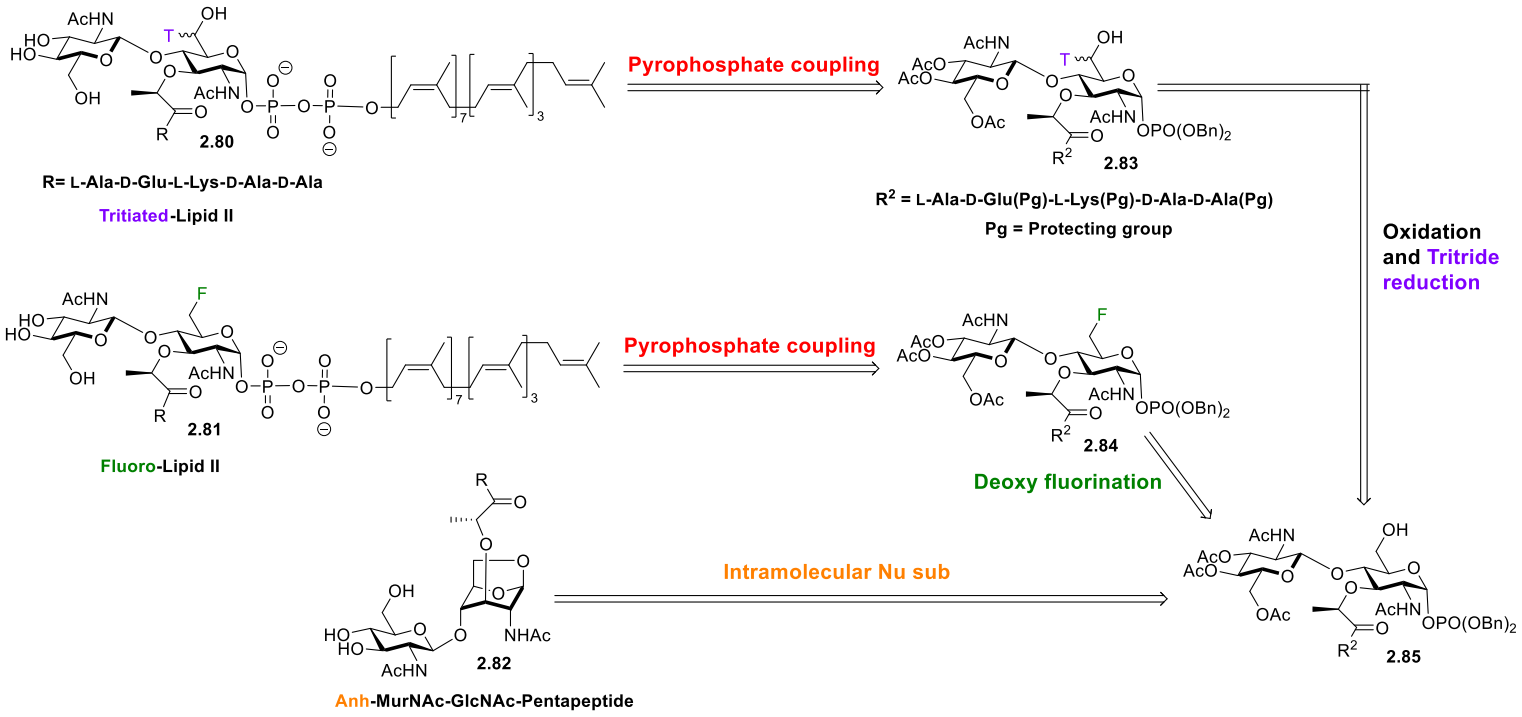


Figure 2.18 – Retrosynthesis of labelled Lipid II analogues and Anh-MurNAc-GlcNAc

Accessing **2.85** is reliant on the ability to carry an orthogonal protecting group through numerous steps, many of which employ harsh rection conditions. The acceptor 6 OH was chosen as the site for this selective protection, due to work by previous groups describing the regioselective reaction of diol intermediates [5, 12, 17] to give suitable glycosyl acceptors. In contrast to reported ester and imidate protection, a silyl ether was chosen for ease of selective deprotection with a fluoride source. A retrosynthetic scheme describing access to **2.85** from known diol intermediate **2.46** is shown below (Fig. 2.19).

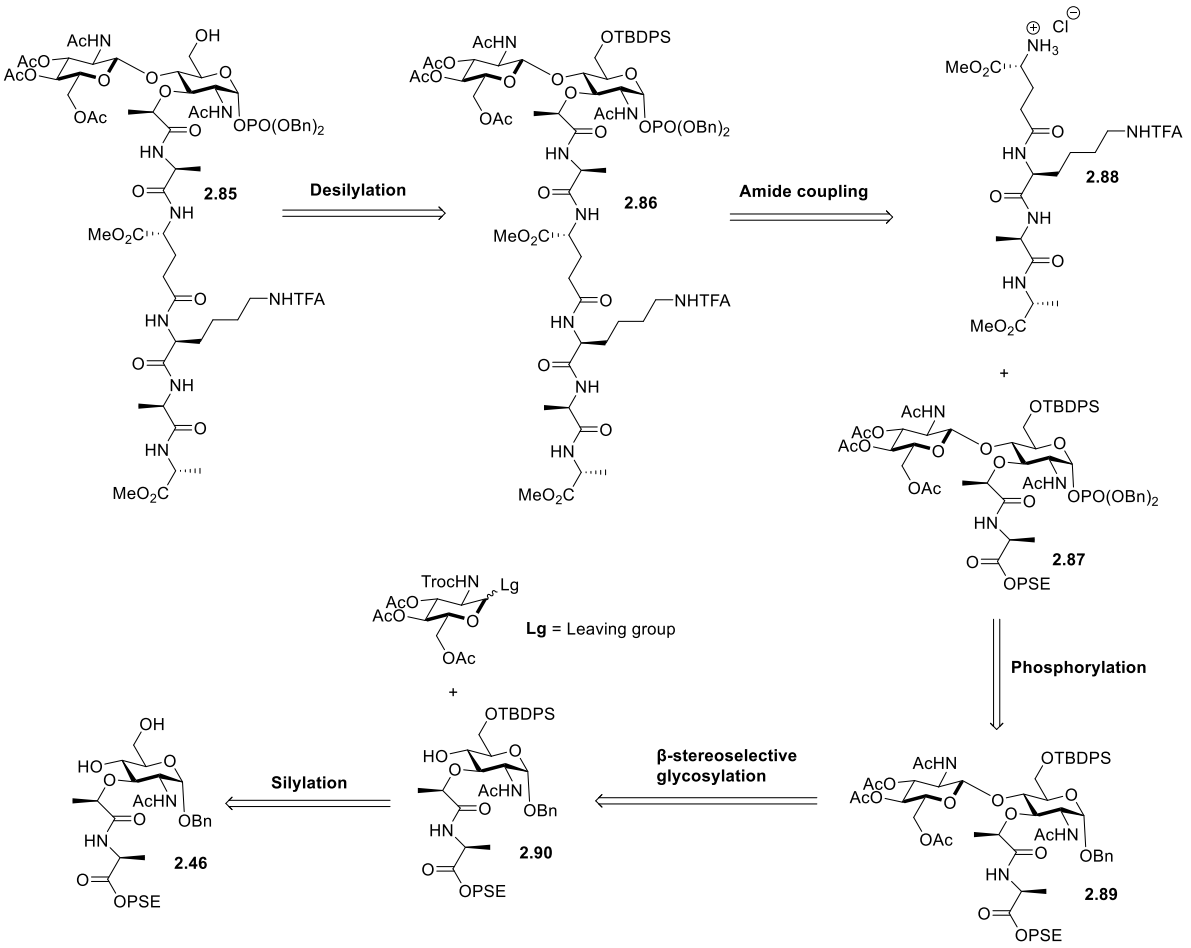


Figure 2.19 – Retrosynthesis of divergent intermediate

Results and Discussion

Access to intermediate **2.86** began with the synthesis of acceptor **2.90**. Challenges around glycosylation with donor fragments led to the preparation of differing fragments bearing unique functional groups at the anomeric centre and consequent reactivity. Investigation into glycosylation conditions enabled the production of disaccharide core **2.89**. Successful preparation of the peptide fragment **2.88** was required as part of the elaboration of the disaccharide core **2.89** into **2.86**. These processes will be discussed in more detail in the following sections.

(i) Synthesis of Glycosyl Acceptor

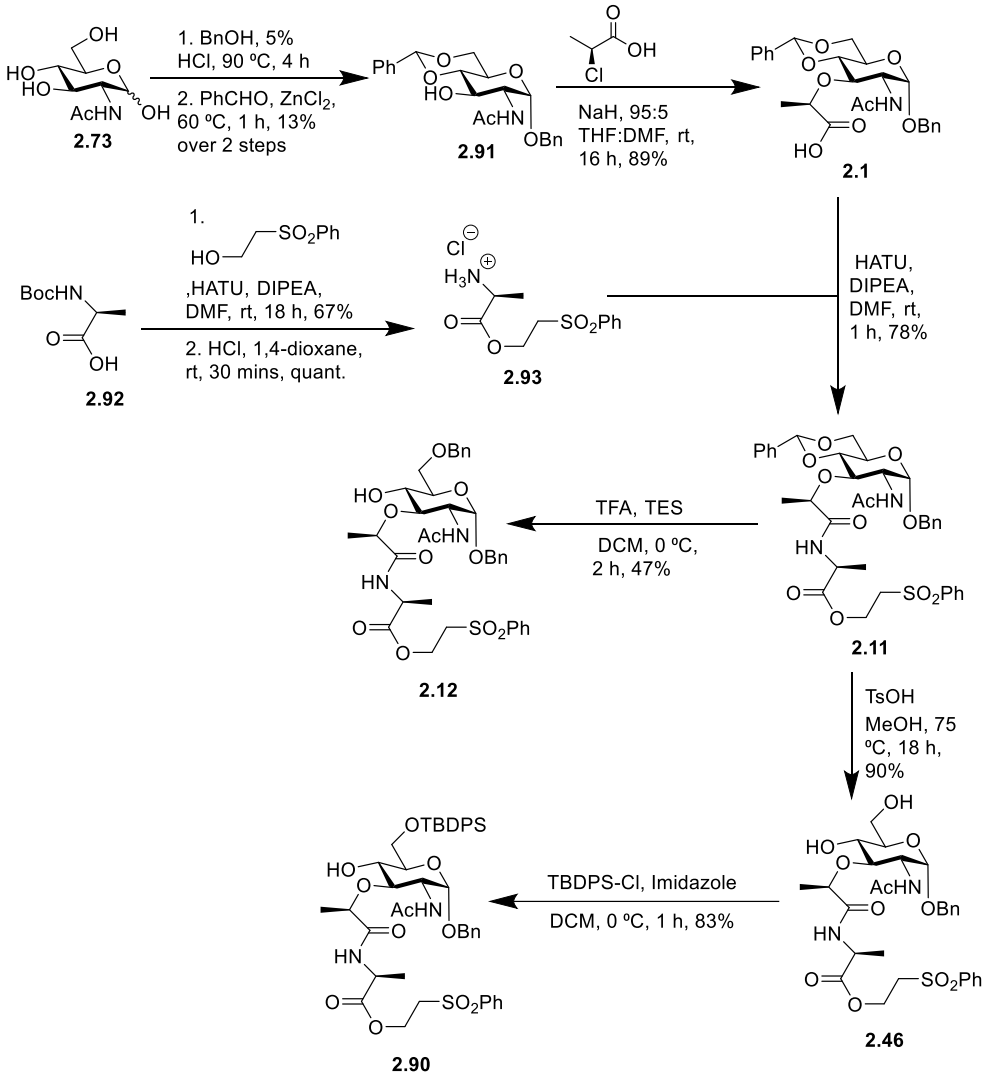


Figure 2.20 – Synthesis of glycosyl acceptor

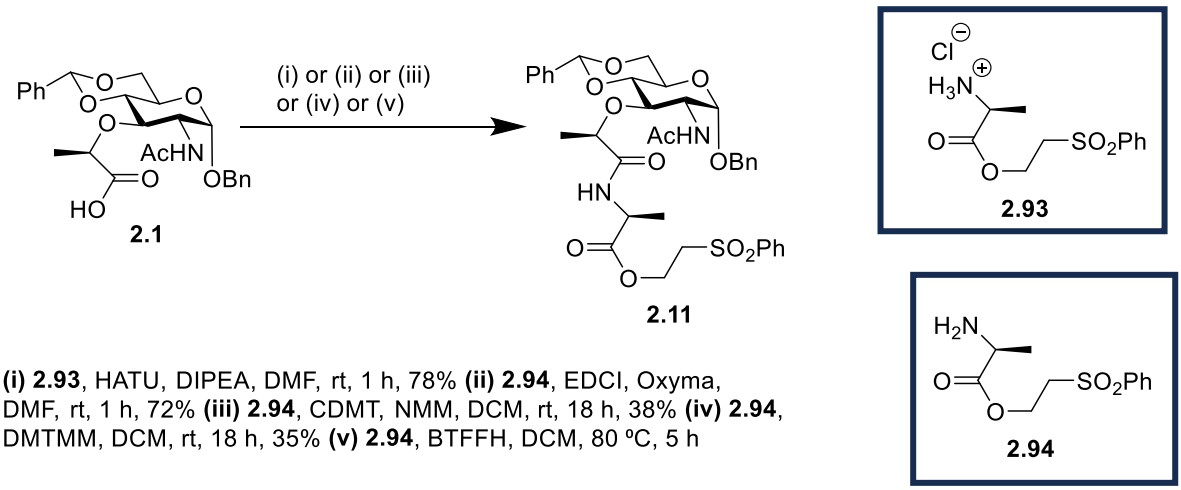
Preparation of **2.90** began with protections of GlcNAc to leave the 3 OH exposed for alkylation (Fig. 2.20). Treatment with BnOH and catalytic quantities of acid allowed for anomeric etherification, with the following Lewis acid catalysed addition to benzaldehyde protecting the 1,3-diol as a benzylidene acetal to give **2.91** in 13% yield [20]. The low yield of **2.91** may be improved through trial of different solvents for recrystallisation or alternate purification strategies.

Alkylation with (*S*)-2-chloropropionic acid proceeded with inversion of configuration to give carboxylic acid **2.1** [20]. Whilst it is known that nucleophilic substitution reactions with halogenated propionic acids may proceed with retention of configuration via intramolecular lactone formation [60, 61], the lactoylations in muramic acid synthesis have been shown to proceed with inversion [62]. This has been determined through reactions with single enantiomers of the acid to obtain both possible *R* and *S* lactoyl products, and comparison of

the relative optical rotations [62]. The optical rotation data of **2.1** was consistent with literature for the *R* lactoyl. The lactoylation to give **2.1** was first trialled in 1,4-dioxane, however poor conversion was observed, assumingly as a result of poor solubility. Additionally, attempts to purify the product by flash column chromatography resulted in loss of large amounts of material due to the affinity of the carboxylate for the silica. Change of the solvent to tetrahydrofuran (THF) with the addition of small amounts of *N*,*N*-dimethylformamide (DMF) as a co-solvent drastically improved conversion and allowed for isolation of **2.1** in 89% yield through precipitation and filtration.

Esterification of Boc-D-Ala, **2.92**, with phenyl sulfonyl ethanol using *N*,*N*,*N*′,*N*′-tetramethyl-O- (7-azabenzotriazol-1-yl)uronium hexafluorophosphate (HATU) and *N*,*N*-diisopropylethylamine (DIPEA) produced doubly protected Ala derivative **2.93** in 67% yield (Fig. 2.20). Removal of the Boc group produced problems on the large scale as the longer timescale required to remove larger amounts of trifluoroacetic acid (TFA) allowed for degradation of the product. Change of deprotection conditions to HCl in dioxane allowed for concentration under nitrogen stream and avoided the need to heat the solution in the presence of acid; under these conditions no degradation as observed. The amine salt was redissolved in DMF and neutralised with DIPEA allowing its use without further purification.

Coupling of carboxylic acid **2.1** with amine **2.94** was first trialled with 2-chloro-4,6-dimethoxy-1,3,5-triazine (CDMT) and *N*-methylmorpholine (NMM) via 4-(4,6-dimethoxy-1,3,5-triazin-2-yl)-4-methyl-morpholinium chloride (DMTMM) formation *in situ* (Fig. 2.21). This reaction produced modest levels of conversion, prompting investigation of other coupling conditions. Direct use of DMTMM did not produce additional conversion. Coupling via an acyl fluoride intermediate with bis(tetramethylene)fluoroformamidinium hexafluorophosphate (BTFFH) produced similar levels of conversion to DMTMM methods by TLC. Both HATU and DIPEA and 1-ethyl-3-(3-dimethylaminopropyl)carbodiimide (EDCI) and ethyl cyanohydroxyiminoacetate (Oxyma) produced complete conversion. HATU and DIPEA were used due to compatibility with the use of amine **2.93** as a salt, giving **2.11** at 78% yield.



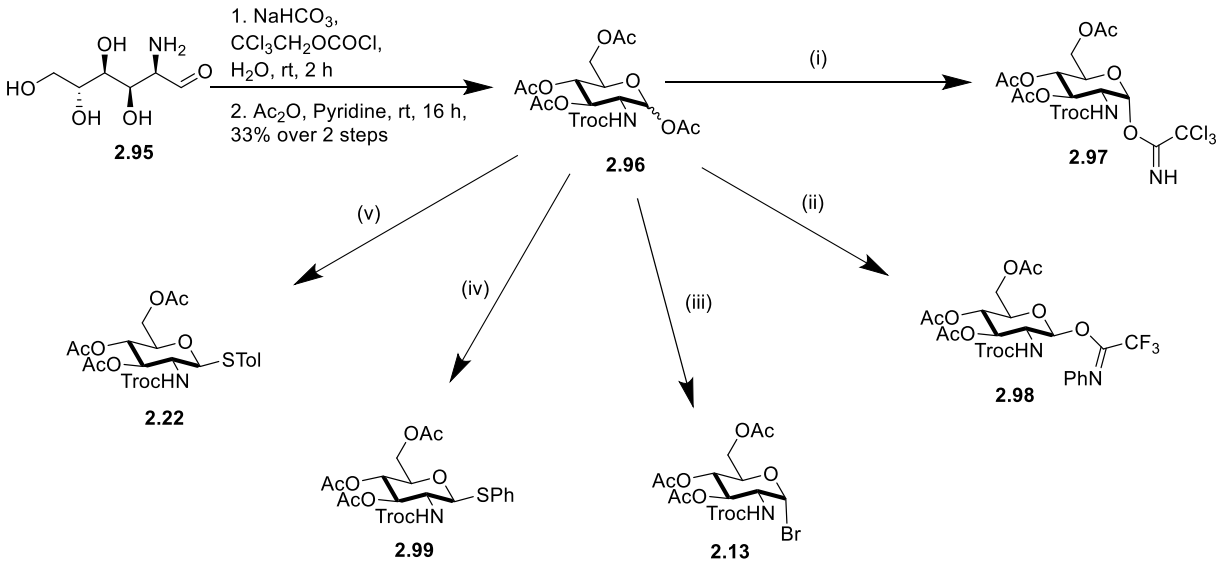
(i) 2.93, HATU, DIPEA, DMF, rt, 1 h, 78% **(ii) 2.94**, EDCI, Oxyma, DMF, rt, 1 h, 72% **(iii) 2.94**, CDMT, NMM, DCM, rt, 18 h, 38% **(iv) 2.94**, DMTMM, DCM, rt, 18 h, 35% **(v) 2.94**, BTFFH, DCM, 80 ºC, 5 h

Figure 2.21 – Screening of amide coupling conditions

The possibility of utilising benzyl derivative **2.12** as a glycosyl acceptor and installing orthogonality post glycosylation via regioselective debenzylation methods [63] was considered, however during the regioselective opening of **2.11** with TFA and triethylsilane (TES), formation of sizeable amounts of diol **2.46** was observed (Fig. 2.20). Hydrolysis is a common side reaction, particularly for bulkier, more substituted starting materials [64]. Concentrating such starting materials from toluene has been shown to reduce this effect [64], and although lesser amounts of diol **2.46** formed from the more thoroughly dried acetal **2.11**, isolated yields remained low. As such it was decided to install the orthogonality preglycosylation, utilising diol **2.46** as an intermediate. Hydrolysis catalysed by TsOH produced diol **2.46** in 90% yield and silylation with the bulky *tert*-butyldiphenylsilyl chloride (TBDPS-Cl) pleasingly gave silylated acceptor **2.90** in 83% yield.

(ii) Synthesis of Glycosyl Donors and the Disaccharide Core

The construction of the disaccharide core of Lipid II is notoriously challenging, owing to the hinderance and poor nucleophilicity of the acceptor 4 OH. It was anticipated that inclusion of the TBDPS may impose additional steric constraints and further hamper the reaction efficiency. As such extensive screening would be necessary for optimisation.

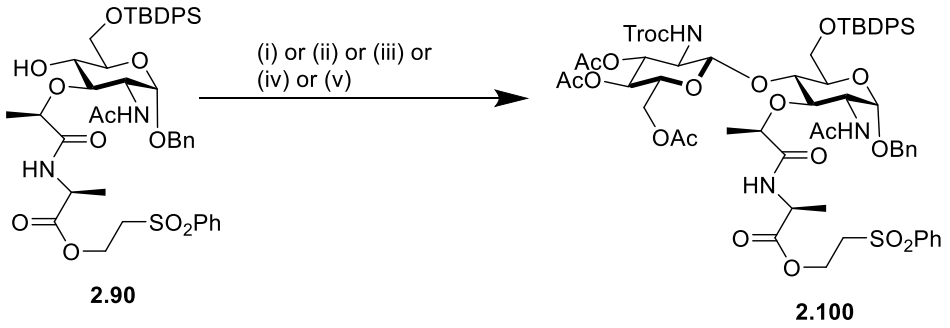


(i) 1. Hydrazine acetate, DMF, rt, 40 mins 2. Cl_3CCN, DBU, DCM, rt, 2 h, 73% over 2 steps **(ii)** 1. Hydrazine acetate, DMF, rt, 40 mins 2. $CF_3CClNPh$, DBU, DCM, rt, 2 h, 20% over 2 steps **(iii)** HBr, AcOH, DCM, rt, 1 h, 99% **(iv)** $BF_3{\cdot}Et_2O$, Thiophenol, DCM, rt, 1 h, 12% **(v)** $BF_3{\cdot}Et_2O$, TolSH, DCM, rt, 30 h, 77%

Figure 2.22 – Synthesis of donor fragments for screening

Common intermediate **2.96** that was used to access all donors was prepared through base mediated acylation of the glucosamine NH with 2,2,2-trichloroethyl chloroformate, and global acetylation with Ac_2O and Pyridine, giving 33% yield over 2 steps (Fig. 2.22). The Troc protecting group was chosen due to its pivotal role in guiding the stereochemistry in the glycosylation product.

Further reactions of **2.96** gave the desired donors (Fig. 2.22). Schmidt donors were prepared through hydrazinolysis of the anomeric acetyl followed by reaction of the nucleophilic exposed OH with an appropriate electrophilic nitrile or imine to yield **2.97** [20] and **2.98** [65] respectively. Bromo donor **2.13** [66] was prepared through acidic hydrolysis to the hemiacetal followed by nucleophilic substitution. Thioglycosides **2.99** [67] and **2.22** [11] were prepared through Lewis acid promoted nucleophilic substitution.



(i) TMSOTf, **2.97**, DCM, rt, 4 h, 19% **(ii)** TMSOTf, **2.98**, rt, 6 h, **(iii)** AgOTf, **2.13**, DCM, rt, 18 h, 15% **(iv)** NIS, TfOH, **2.99**, DCM, rt, 5 h, 63%, **(v)** NIS, TfOH, **2.22**, DCM, rt, 5 h, 70%

Figure 2.23 – Screen of glycosylation conditions to give the disaccharide core

Schmidt glycosylations with **2.97** were first examined using trimethylsilyl trifluoromethanesulfonate (TMSOTf) as a promoter (Fig. 2.23). Conversion was unsatisfactory and the similarity between the R_f of the starting material and product in a range of solvent systems led to difficulties in isolating pure material. We hypothesised that donor rearrangement [68] may limit conversion due to reattack of the leaving group outcompeting acceptor attack. The reformed *N* glycoside would be more stable and likely inert. To investigate this possibility, **2.98** was synthesised. The presence of the *N* phenyl group extends the delocalisation of electron density within the leaving group, making it a much poorer nucleophile and reattack less likely. No difference in conversion was observed by TLC or NMR, prompting further investigation of alternate conditions.

Koenigs Knorr glycosylations with **2.13** and AgOTf for Br abstraction were tested (Fig. 2.23). Complete conversion was observed by TLC, however this required vast amounts of AgOTf, up to 30 equivalents. Additionally isolated yields were low possibly due to chelation of the product by Ag^{+} resulting in loss of material during filtration. Rinsing the filtered solid with large amounts of MeOH saw slight improvements in the yield, however isolated amounts remained unsatisfactory.

Glycosylations with thioglycosides **2.99** and **2.22** using NIS and TfOH for activation produced complete conversion (Fig. 2.23). Similar to the Koenigs Knorr conditions excess equivalents of activator (1-1.2x TfOH) were needed when activation for this system should be catalytic. This may be due to the increased basicity of the NHS produced after iodine abstraction. The NHS carbonyls may preferentially accept the protons, hindering further NIS protonation and activation as an iodinating reagent. Nonetheless yields were excellent, and the key disaccharide intermediate **2.100** bearing the required orthogonal 6 OH protection was obtained in 70% yield on a 1 g scale for further steps.

(iii) Synthesis of Tetrapeptide Fragment and Undecaprenyl Phosphate

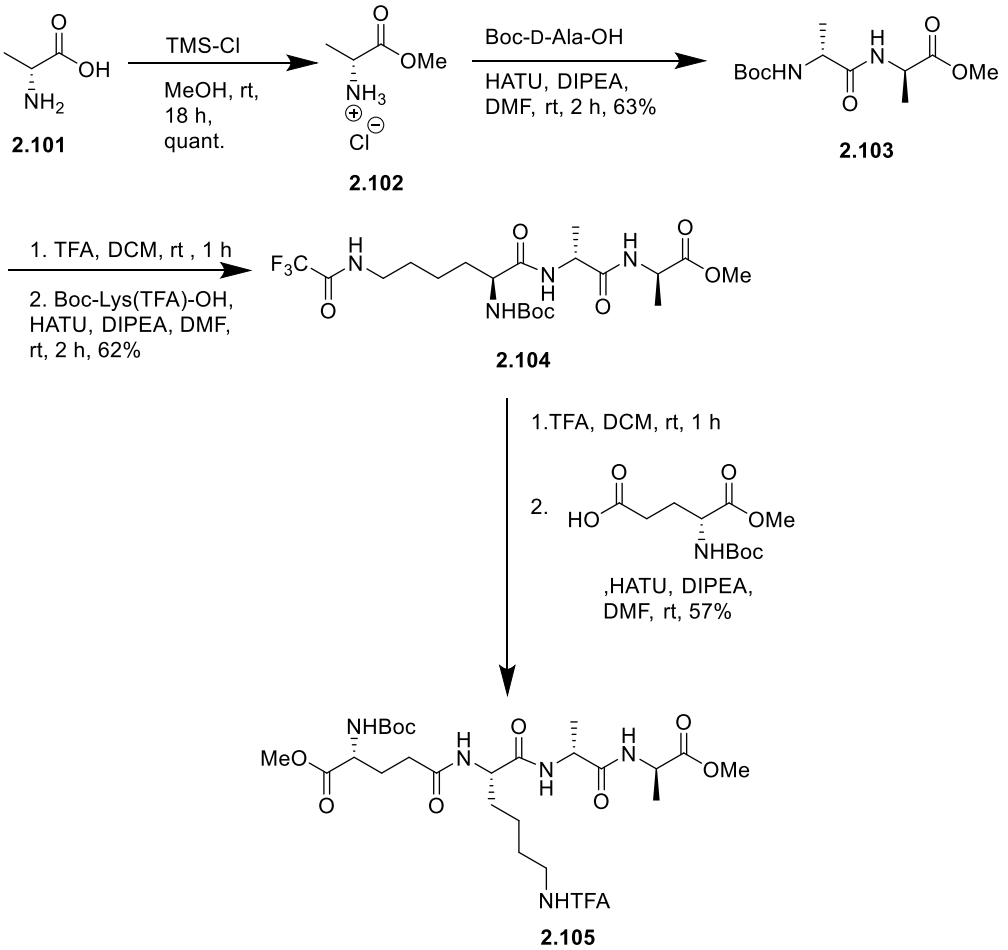


Figure 2.24 – Synthesis of tetrapeptide fragment

With disaccharide **2.100** in hand, attention was turned to accessing the peptide and phospholipid substituents of the disaccharide core. Synthesis of the tetrapeptide (Fig. 2.24) began with methylation of D-Ala, **2.101**, to give methyl ester **2.102**. This was then amide coupled to Boc-D-Ala-OH with HATU and DIPEA to give dipeptide **2.103**. Boc deprotection allowed for further coupling with HATU and DIPEA with suitably protected Boc-L-Lys(TFA)-OH. Repetition of this strategy allowed condensation with Boc-D-Glu(OH)-OMe to yield tetrapeptide **2.105**. To note is the choice of the TFA amide protecting group for the lysine side chain. This can be removed with nucleophilic base under global hydrolysis, due to enhanced electrophilic character from the trifluoro acetyl group. This allows for concomitant deprotection of all the peptide protecting groups and the acetyls in the glycan core [20].

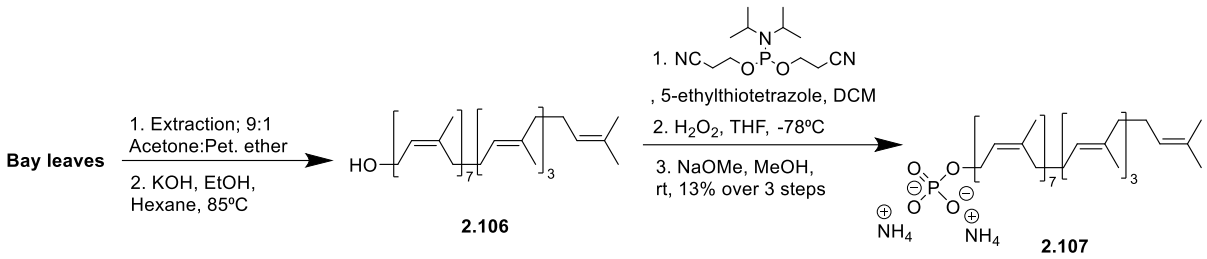


Figure 2.25 – Synthesis of undecaprenyl phospholipid fragment

Synthesis of phospholipid **2.107** began with extraction of bay leaves using 9:1 pet. ether:acetone (Fig. 2.25). Bay leaves are known to contain undecaprenyl acetate, a useful starting material for our synthesis that can be extracted through suspension in a pet. ether:acetone solvent system [69-71]. This extraction was conducted on the 300 g scale and the crude plant extract was subjected to hydrolysis conditions. Following column chromatography using a sample from another member of the group as a standard, 669 mg of undecaprenol, **2.106** was isolated. Phosphorylation of the free OH was achieved via a phosphite intermediate with bis(2-cyanoethyl)-*N, N*'-diisopropylphosphoramidite and 5-ethyl thiotetrazole (5-ETT) as a Brønsted acid activator. Oxidation to the phosphate was achieved with H_2O_2 in THF, and E1cB deprotection with NaOMe gave deprotected phosphate **2.107** in 13% yield over the 3 steps. The deprotection proceeded in a sluggish manner, requiring prolonged reaction times for full conversion; a sample quenched after 24 h indicated the presence of monoprotected phosphate by NMR.

(iv) Efforts Towards the Synthesis of Lipid II Analogues

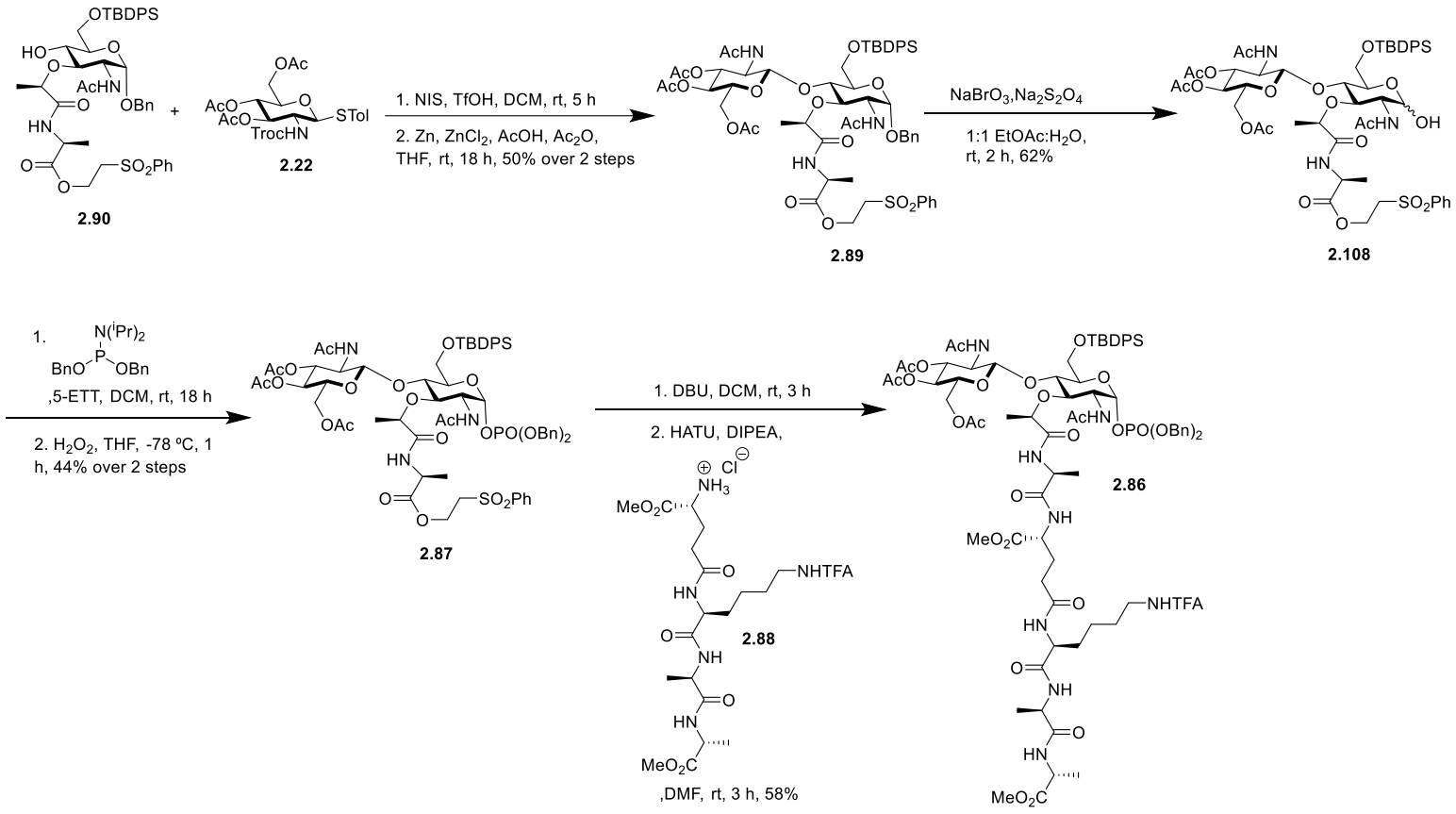
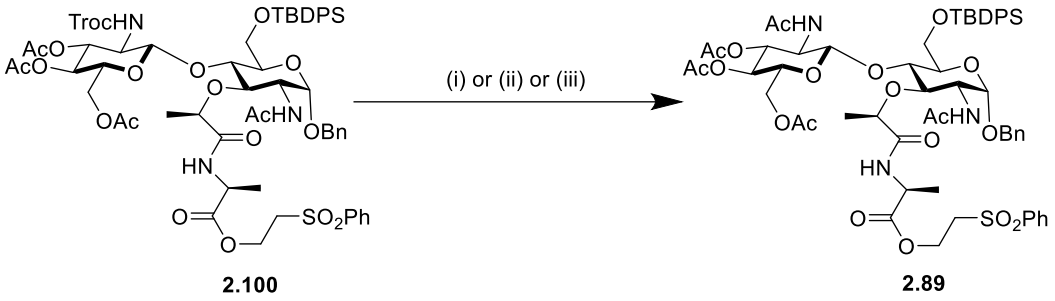


Figure 2.26 – Convergent synthesis of final intermediate

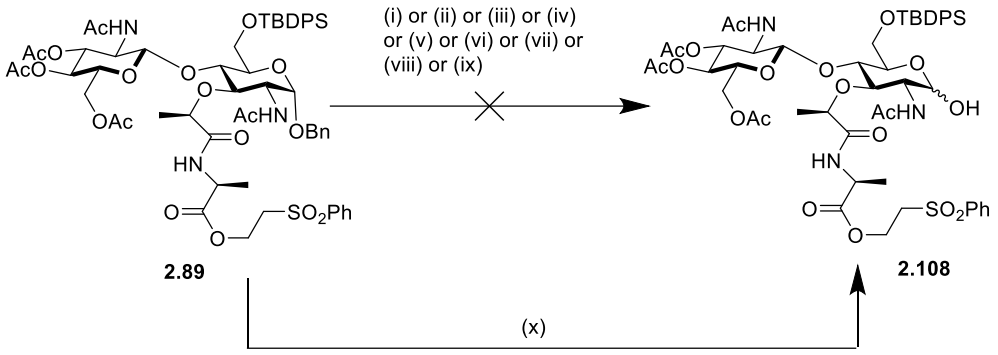
Having accessed the appropriate fragments for attachment to the glycan core, attention was turned to the convergent assembly (Fig. 2.26). The participating nature of the Troc was no longer required following glycosylation, hence it was immediately removed (Fig. 2.27). Reductive removal and different acetylation conditions were tested. A two step deprotection and acetylation with Ac_2O, pyridine and *N*,*N* –dimethylaminopyridine (DMAP) produced inferior yields likely due to chelation of the free amine with the Zn; low amounts of crude material were recovered after filtration. One pot procedures with Zn, AcOH, and Ac_2O have been reported [20] and testing produced better yields, 58%. Addition of a $ZnCl_2$ additive was observed to further promote *N*-acetylation by TLC, and produced superior yields, 72%, additionally small amounts of acceptor impurity (<5 %) that were carried through when conducting this transformation on a larger scale could be acetylated in the presence of $ZnCl_2$ making separation during purification easier.



(i) 1. Zn, AcOH, THF, rt, 3 h, 2. Ac_2O, pyridine, DMAP, rt, 18 h, 25% over 2 steps, **(ii)** Zn, AcOH, Ac_2O, THF, rt, 3 h, 58%, **(iii)** Zn, $ZnCl_2$, AcOH, Ac_2O, THF, rt, 3 h, 72%

Figure 2.27 – Screen of Troc deprotection and acetylation conditions

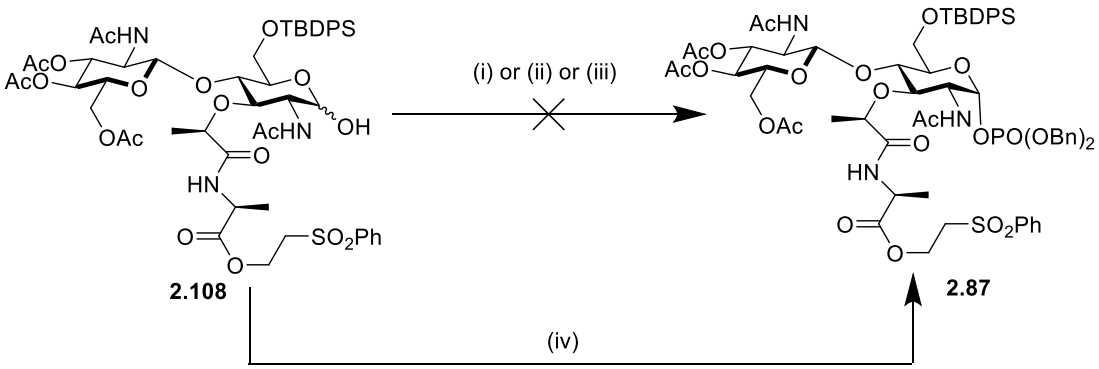
Removal of the anomeric benzyl group proved difficult (Fig. 2.28). Usually employed hydrogenolysis proved unsuccessful, even under extremely forcing conditions using elevated temperatures and pressures with more reactive catalysts such as $Pd(OH)_2$ and Raney Nickel (RaNi). This could be a result of the steric hinderance imposed by the 6 OTBDPS preventing interaction between the benzyl group and the heterogeneous catalyst. Alternate reductive debenzylation conditions were unattractive due to worries of protecting group compatibility within **2.89** (i.e. acetyls). Acidic conditions were briefly examined, 50% Methane sulfonic acid (MsOH) in Dichloromethane (DCM) produced a messy mixture (numerous spots observed by TLC) presumably due to intolerability of functional groups such as the O-acetyls and TBDPS. As such these were considered no further, and oxidative cleavage conditions were screened for efficacy. Oxidation to a benzoate was trialled due to the increased susceptibility of anomeric esters to nucleophilic deprotection methods [72]. However, oxidation with ozone produced a different product, examination of the NMR indicates loss of the PSE environments. Removal of benzyl ethers with 2,3-dichloro-5,6-dicyano-1,4-benzoquinone (DDQ) has been documented in some substrates [73-75], however different conditions trialled produced no conversion. This method is commonly used to remove more electron rich systems such as the *p*-methoxybenzyl (PMB) protecting group [76], hence this benzyl group may not be a strong enough reductant. Benzylic bromination proved to be successful at removing the anomeric benzyl group, however during Wohl Ziegler bromination concomitant glycosidic cleavage was observed. This observation may be explained through uncontrolled initiation of the reaction; too intense of a light source may have been used and off target proton abstraction may have occurred at the other ether linkage present in the starting material as a result of too high of a concentration of Br radicals. Bromination with the sodium bromate-sodium dithionite system successfully gave hemiacetal **2.108** in 62% yield; during purification 24% starting material was recovered.



(i) H_2, Pd-C, MeOH, rt, 18 h **(ii)** H_2, $Pd(OH)_2$, MeOH, 60 ºC, 60 atm, 10 mins **(iii)** RaNi, MeOH, 60 ºC, 60 atm, 10 mins, **(iv)** Et_3SiH, Pd-C, rt, 18 h, **(v)** NBS, $CaCO_3$, 2:1 Trifluorotoluene:H_2O, rt, 365 nm, 15 mins **(vi)** 1. O_3, DCM, rt, 45 mins 2. Hydrazine acetate, DMF, rt **(vii)** DDQ, wet DCM, rt, 565 nm, 18 h, **(viii)** DDQ, wet MeCN, rt, 365 nm, 18 h, **(ix)** MsOH, DCM, rt, 30 mins, **(x)** $NaBrO_3$, $Na_2S_2O_4$, 1:1 EtOAc:H_2O, rt, 2 h, 62%

Figure 2.28 – Screen of anomeric debenzylation conditions

Phosphorylation was achieved under similar conditions described for phospholipid **2.107** (Fig. 2.29). Phosphite formation with dibenzyl *N*,*N*-diisopropylphosphoramidite and 5-ETT in DCM, followed by subsequent oxidation with H_2O_2 gave **2.87** in 44% yield. This modest yield led to investigations of alternate conditions. Preferential reaction of one anomer was observed by TLC and as such, the reaction was trialled in a more polar solvent, THF, to improve the rate of mutarotation and equilibration to the more reactive anomer [77]. Unprecedently no reaction was observed. This may be rationalised as the coordinating oxygen in THF may hydrogen bond with the protonated phosphoramidite, stabilising it and reducing the propensity of diisopropylamine to act as a leaving group. Other strategies were tried with direct phosphorylation using a chlorophosphonate. This has been demonstrated previously to access glycophosphates [78], however no reaction was observed under these conditions.



(i) $PO(OBn)_2Cl$, DMAP, Et_3N, DCM, rt, 18 h **(ii)** $PO(OBn)_2Cl$, DMAP, Et_3N, Pyridine, rt, 18 h, **(iii)** 1. $(N^iPr)_2P(OBn)_2$, 5-ETT, THF, rt, 4 h 2.H_2O_2, THF, -78 ºC, **(iv)** 1. $(N^iPr)_2P(OBn)_2$, 5-ETT, DCM, rt, 4 h 2.H_2O_2, THF, -78 ºC, 2 h, 44% over 2 steps

Figure 2.29 – Screen of phosphorylation conditions

Treatment of **2.87** with 1,8-diazabicyclo(5.4.0)undec-7-ene (DBU) in DCM allowed for selective unmasking of the PSE ester (Fig. 2.30). The protons alpha to the phenyl sulfone are acidic enough such that chemo selective deprotection is possible through the use of strong non-nucleophilic base via an E1cB process. The ^{1}H and HSQC NMR spectra of the product confirmed complete loss of the PSE ester environments and as such the material was taken forward without further purification. Treatment of tetrapeptide **2.105** with HCl in dioxane allowed for removal of the Boc group to give **2.88**, and amide coupling to deprotected **2.87** with HATU and DIPEA furnished **2.86** in 58% yield.

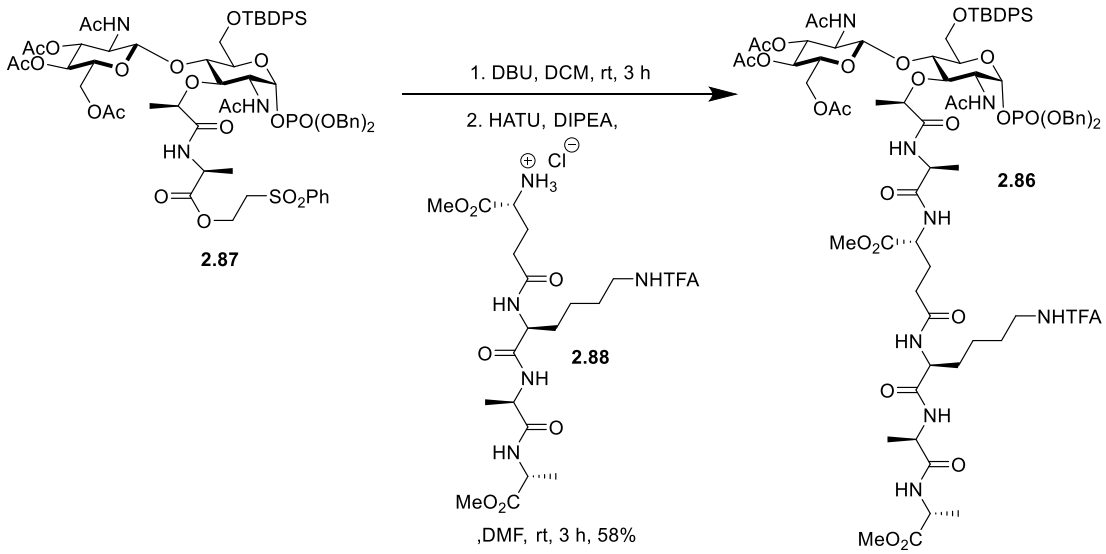


Figure 2.30 – Deprotection and amide coupling to give final intermediate

Conclusions and Future Directions

This chapter describes the synthesis of a versatile late-stage intermediate **2.7** that may be used to access novel analogues of Lipid II as well as Anh-MurNAc-GlcNAc, unfortunately due to time constraints **2.86** could not be elaborated further. In order to complete this synthesis, a novel MurNAc acceptor **2.90** was synthesised in 6.8% yield over 5 linear steps. Key steps in this synthesis involved an optimised alkylation to give lactoyl **2.1** and silylation of an underexplored diol intermediate to give acceptor **2.90**. The reactivity of this acceptor was investigated with a range of donor fragments [11, 20, 65-67] in order to produce disaccharide core **2.100** and optimal conditions were found with the use of thioglycoside species [11, 67]. With this key building block in hand, attention was turned to the required tetrapeptide and phospholipid fragments, which were prepared according to known literature procedure [20]. The convergent assembly towards intermediate **2.86** required several optimisations, most

importantly the oxidative removal of a hindered benzyl ether to give hemiacetal **2.108**. In summary the synthesis of **2.86** was achieved in 0.8% yield over 12 linear steps.

Future work should aim to investigate use of **2.86** in accessing desired biologically useful substrates (Fig. 2.31) and explore the use of labelled Lipid II analogues in developing the postulated NMR and radioactivity flippase assays. The development of such *in vitro* assays will be a crucial step in unpicking Lipid II flipping and designing inhibitors for use as next generation antibiotics.

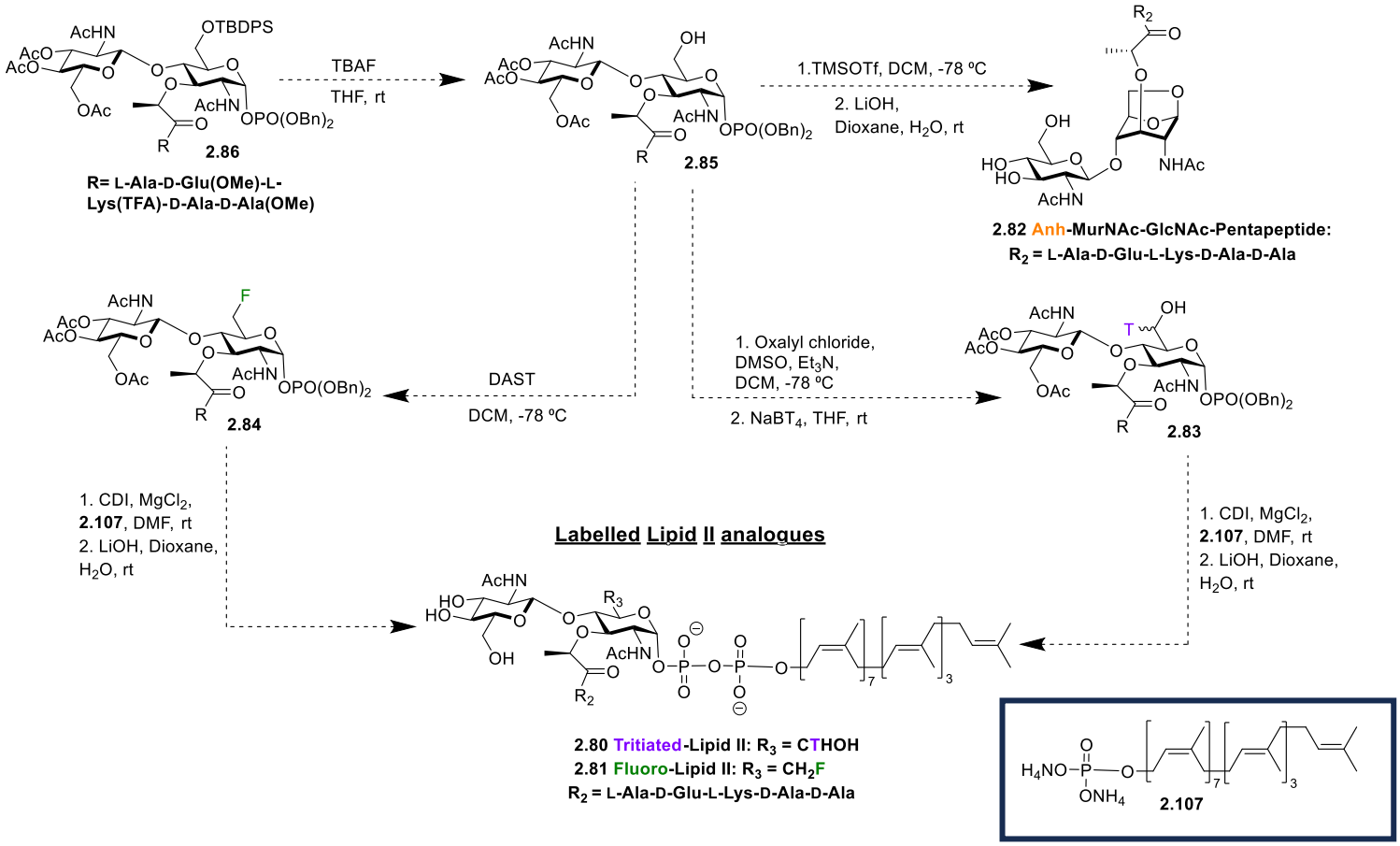
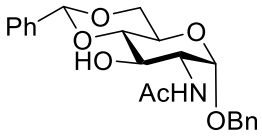


*Figure 2.31 – Proposed elaboration of disaccharide **2.86** into Labelled Lipid II analogues and Anh-MurNAc-GlcNAc*

Experimental

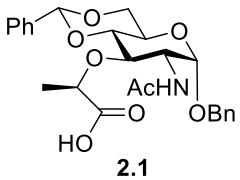
N-((2R,4aR,6S,7R,8R,8aS)-6-(benzyloxy)-8-hydroxy-2-phenylhexahydropyrano[3,2-d][1,3]dioxin-7-yl)acetamide [20]



2.91

N-acetyl-D-glucosamine (30.0 g, 136 mmol) was suspended in a mix of 300 mL benzyl alcohol and 7.5 mL 37% HCl (aq). The reaction mixture was heated to 95 °C and stirred for 4 h. The solution was poured into 500 mL Et_2O while stirring, and the resulting precipitate collected by filtration. The filtrate was repoured into stirring Et_2O until no more solid could be collected. The combined solid was washed with 1 x 100 mL Et_2O, and 2 x 50 mL Et_2O before drying under high vacuum overnight. The resulting white solid was suspended in 140 mL benzaldehyde with 38 g $ZnCl_2$ and stirred at 60°C for 1 h (The mixture became homogeneous after 10 mins). The solution was then poured into a 400 mL stirring ice water mix and the precipitate collected by filtration. The pink solid was then washed with 2 x 200 mL H_2O, 100 mL ice cold EtOH, 3 x 200 mL Et_2O. The resultant white powder was recrystallised from boiling pyridine and washed with water (2 x 100 mL). The product was then azeotroped with toluene before further drying under high vacuum overnight to yield, **2.91** (6.95g, 13%). ^{1}H NMR (DMSO-D_6, 600 MHz): δ 8.08 (d, 1H, N**H**Ac, J=8.2Hz), 7.46 (m, 2H, Ar-**H**), 7.38 (m, 7H, Ar-**H)**, 7.30 (m, 1H, Ar-**H**), 5.62 (s, 1H, PhC**H**), 4.1 (d, 1H, **H1**, J=3.7 Hz), 4.71 (d, 1H, PhC**H$_2$**, J= 12.6 Hz), 4.49 (d, 1H, PhC**H$_2$**, J= 12.6 Hz), 4.15 (dd, 1H, **H6**, J= 9.2, 4.1 Hz), 3.85 (ddd, 1H, **H2**, J=10.4,8.2,3.7Hz) 3.79-3.67 (m, 3H, **H3**, **H5**, **H6**), 3.52 (t, 1H, **H4**), 1.85 (s, 3H, **H**-Ac). ^{13}C NMR (151 MHz, DMSO) δ 169.45, 137.74, 137.71, 128.88, 128.25, 128.03, 127.64, 126.40, 100.87, 96.94, 82.11, 68.56, 68.01, 67.25, 62.87, 54.18, 22.54. LRMS (ESI) Calcd for $C_{22}H_{26}NO_6^+$ [M+H] = 400.17 found 400.08. $[\alpha]_D^{25}$ = +93 (1.1 g/100 mL, DMSO)

(R)-2-(((2R,4aR,6S,7R,8R,8aS)-7-acetamido-6-(benzyloxy)-2-phenylhexahydropyrano[3,2-d][1,3]dioxin-8-yl)oxy)propanoic acid [20]

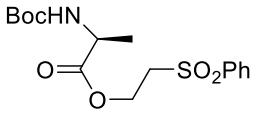


2.1

2.13 (4.63 g, 11.6 mmol)**,** was suspended in 189 ml 95:5 dry THF: DMF mix under Ar. The reaction mixture was heated under reflux to aid dissolution, before cooling back to ambient temperature once the solution was homogeneous. A 60% dispersion of NaH in mineral oil (928 mg, 23.2 mmol) was added

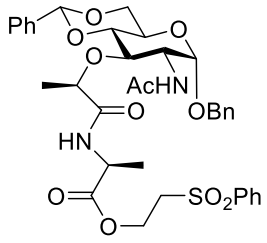
at ambient temperature and the solution left to stir for 10 mins. The mixture was then cooled to 0°C, 3.79 mL (*2S*)- chloropropionic acid (29.6 mmol) was added dropwise, and the solution stirred for 10 mins. An excess of 60% NaH in mineral oil was added (2.32 g, 58 mmol) and the mixture warmed to ambient temperature and stirred for 16 h. The reaction was quenched with the dropwise addition of 6 mL ice cold H_2O and acidified with careful addition of 1.0 M HCl at 0 °C till pH_2. The solution was then poured into 2 L stirring ice water mix and the precipitate recovered by filtration. The pinkish solid was washed with 4 x 125 mL ice cold H_2O, 2 x 125 mL petroleum ether and azetroped with 3 x 50 mL toluene, before drying under high vacuum overnight to yield **2.1** as a white solid (4.86 g, 89%). ^{1}H NMR (400 MHz, DMSO) δ 7.97 (d, *J* = 6.2 Hz, 1H, N**H**Ac), 7.59 – 7.20 (m, 10H, Ar-**H**), 5.70 (s, 1H, PhC**H**), 5.04 (d, *J* = 3.4 Hz, 1H, **H1**), 4.70 (d, *J* = 12.4 Hz, 1H, PhC**H**$_2$), 4.49 (d, *J* = 12.4 Hz, 1H, PhC**H$_2$**), 4.29 (q, *J* = 6.9 Hz, 1H, MurNAc-**H$_\alpha$**), 4.15 (dd, *J* = 9.3, 3.8 Hz, 1H, **H6**), 3.89 – 3.63 (m, 5H, **H2**, **H3**, **H4**, **H5**, **H6'**), 1.85 (s, 3H, NH**Ac**), 1.27 (d, *J* = 6.9 Hz, 3H, MurNAc-**H$_\beta$**). ^{13}C NMR (101 MHz, DMSO) δ 175.71, 169.84, 138.07 (d, *J* = 3.7 Hz), 129.27, 128.74, 128.63, 128.11 (d, *J* = 3.8 Hz), 126.30, 100.72, 97.28, 81.99, 75.54, 69.42, 68.33, 63.35, 53.96, 23.08, 19.15. LRMS (ESI) Calcd for $C_{25}H_{28}NO_8^-$ [M-H] = 470.18 found 470.30. $[\alpha]_D^{25}$ = +81 (1.0 g/100 mL, MeOH)

2-(phenylsulfonyl)ethyl (tert-butoxycarbonyl)-L-alaninate [20]



5.00 g Boc-Ala-OH (0.0265 mol) and 10.07 g mgs HATU (0.0265 mol) were dissolved in 100 mL dry DMF under Ar. The solution was cooled to 0 °C, and 9.23 mL DIPEA (0.053 mol) was added slowly. The solution was left to stir for 15 mins, after which 3.17 mL 2-(phenylsulfonyl)ethan-1-ol) (0.0265 mol) was added. The reaction was warmed to ambient temperature and left to stir for 18 h. The DMF was removed *in vacuo* and the green solid azeotroped with toluene. The solid was then redissolved in 100 mL EtOAc and washed with 100 mL 1.0M HCl; the aqueous layer was back extracted with 50 mL EtOAc. The combined organic layers were washed with 100 mL sat. $NaHCO_3$ sol.; the aqueous layer was back extracted with 50 mL EtOAc. The combined organic layers were washed with 100 mL brine, dried over anhydrous Na_2SO_4, and concentrated *in vacuo*. The solid was purified by flash column chromatography (SiO_2, 2:1 Pet. Ether:EtOAc) to yield **Boc-Ala-OPSE** as a clear oil (6.34 g, 67%). ^{1}H NMR (400 MHz, $CDCl_3$) δ 7.91 (m, 2H, Ar-**H**), 7.72 – 7.63 (m, 1H, Ar-**H**), 7.58 (m, 2H, Ar-**H**), 4.97 (d, *J* = 7.8 Hz, 1H, N**H**), 4.45 (dd, *J* = 6.8, 5.3 Hz, 2H, OC**H$_2$**), 4.04 (p, *J* = 7.4 Hz, 1H, **H$_\alpha$**), 3.47 (td, *J* = 6.1, 1.9 Hz, 2H, SC**H$_2$**), 1.41 (d, *J* = 1.6 Hz, 9H, Boc-**H**), 1.20 (dd, *J* = 7.3, 1.5 Hz, 3H, **H$_\beta$**). ^{13}C NMR (101 MHz, $CDCl_3$) δ 79.96, 58.27, 54.94, 49.03, 28.31, 18.10.

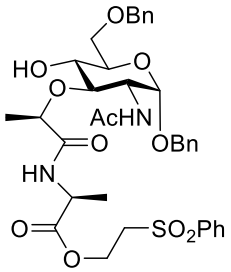
2-(phenylsulfonyl)ethyl ((R)-2-(((2R,4aR,6S,7R,8R,8aS)-7-acetamido-6-(benzyloxy)-2-phenylhexahydropyrano[3,2-d][1,3]dioxin-8-yl)oxy)propanoyl)-L-alaninate [20]



2.11

Boc-Ala-OPSE (3.37 g, 9.42 mmol) was dissolved in 24 mL 4.0 M HCl in 1,4-dioxane and stirred for 30 mins. The reaction was concentrated with a nitrogen stream and dried under high vac for 1 h. During this time **2.1** (3.00 g, 6.37 mmol) and HATU (2.42 g, 6.37 mmol) were dissolved in 35 mL dry DMF under Ar. The solution was cooled to 0 °C, and 2.22 mL DIPEA (12.73 mmol) was added slowly. The solution was stirred for 15 mins. Deprotected amine, **2.93**, was redissolved in 30 mL dry DMF under Ar and added to activated acid. The reaction was warmed to ambient temperature and left to stir for 1 h. The solution was partitioned between 200 mL EtOAc and 100 mL 1.0 M HCl. The aqueous layer was back extracted with 1 x 100 mL EtOAc, and the combined organic layers washed with 1 x 100 mL sat. $NaHCO_3$ sol. The aqueous layer was back extracted with 1 x100 mL EtOAc and the combined layers washed with 1 x 100 mL Brine, dried over anhydrous Na_2SO_4, and concentrated *in vacuo*. The resultant solid was purified via flash column chromatography (SiO_2, 80:20 DCM:EtOAc) to yield **2.11** as a white solid (3.55 g, 78%). ^{1}H NMR (601 MHz, $CDCl_3$) δ 7.95 – 7.88 (m, 2H, **Ph**SO_2), 7.69 – 7.63 (m, 1H, **Ph**SO_2), 7.56 (t, *J* = 7.8 Hz, 2H, **Ph**SO_2), 7.49 – 7.44 (m, 2H, Ar-**H**), 7.40 – 7.27 (m, 8H, Ar-**H**), 6.95 (d, *J* = 7.1 Hz, 1H, Ala1-N**H**), 6.18 (d, *J* = 8.9 Hz, 1H, N**H**Ac), 5.57 (s, 1H, O_2C**H**), 4.95 (d, *J* = 3.8 Hz, 1H, **H1**), 4.71 (d, *J* = 11.8 Hz, 1H, PhC**H₂**), 4.45 (m, 3H, PhC**H**$_2$, OC**H₂**), 4.30 (td, *J* = 9.3, 3.8 Hz, 1H, **H2**), 4.24 (dd, *J* = 10.2, 4.8 Hz, 1H, **H6**), 4.16 (p, *J* = 7.2 Hz, 1H, Ala1-**Hα**), 4.07 (q, *J* = 6.7 Hz, 1H, MurNAc-**Hα**), 3.88 (td, *J* = 9.5, 4.7 Hz, 1H, **H5**), 3.77 (t, *J* = 10.3 Hz, 1H, **H3**), 3.71 – 3.63 (m, 2H, **H4**, **H6'**), 3.49 – 3.35 (m, 2H, SC**H₂**), 1.93 (s, 3H, NH**Ac**), 1.37 (d, *J* = 6.8 Hz, 3H, MurNAc- **Hβ**), 1.29 (d, *J* = 7.2 Hz, 3H, Ala1-**Hβ**). ^{13}C NMR (101 MHz, $CDCl_3$) δ 173.30, 171.90, 139.28, 137.19, 136.85, 134.24, 129.60, 129.18 (d, *J* = 2.6 Hz), 128.81, 128.46 (d, *J* = 3.6 Hz), 128.37, 128.20, 126.08, 101.60, 97.59, 81.66, 78.55, 78.25, 70.28, 68.98, 63.30, 58.16, 55.06, 53.23, 48.13, 23.46, 19.51, 17.31. LRMS (ESI) Calcd for $C_{36}H_{43}N_2O_{11}S^+$ [M+H] = 711.25 found 711.17. $[\alpha]_D^{25}$ = +73 (0.11 g/100 mL, DCM)

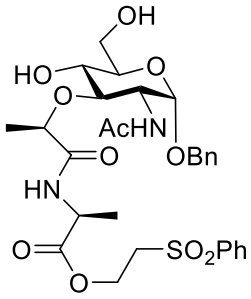
2-(phenylsulfonyl)ethyl ((R)-2-(((2S,3R,4R,5S,6R)-3-acetamido-2-(benzyloxy)-6-((benzyloxy)methyl)-5-hydroxytetrahydro-2H-pyran-4-yl)oxy)propanoyl)-L-alaninate [20]



2.12

2.11 (42 mg, 0.06 mmol) was concentrated from toluene prior to the reaction and dried under high vacuum overnight. The dry solid was then dissolved in 0.5 mL dry DCM under Ar and the solution cooled to 0 °C. 0.14 mL TES (0.9 mmol) was added, and the mix allowed to stir for 10 mins. During this time a dilute TFA stock was prepared in dry DCM under Ar. 1 mL (0.3 mmol) of the stock was added dropwise over 10 mins. The solution was stirred for 2 h. The reaction was diluted with 5 mL DCM before washing with 1 x 5 mL sat. $NaHCO_3$ sol. The aqueous layer was back extracted with 2 x 5 mL DCM. The combined organic layers were washed with 1 x 5 mL brine, dried over anhydrous Na_2SO_4, and concentrated *in vacuo*. The resulting solid was purified by flash column chromatography (SiO_2, 1:1 EtOAc:DCM) to yield **2.12** (19.6 mg, 47%). ^{1}H NMR (601 MHz, $CDCl_3$) δ 7.94 – 7.89 (m, 2H, **Ph**SO_2), 7.67 (t, *J* = 7.5 Hz, 1H, **Ph**SO_2), 7.57 (t, *J* = 7.7 Hz, 2H, **Ph**SO_2), 7.40 – 7.27 (m, 10H, Ar-**H**), 6.90 (d, *J* = 7.2 Hz, 1H, Ala-1-N**H**), 6.03 (d, *J* = 9.0 Hz, 1H, MurNAc-N**H**), 4.91 (d, *J* = 3.6 Hz, 1H, **H1**), 4.70 (d, *J* = 11.7 Hz, 1H, OC**H₂**Ph), 4.62 (d, *J* = 12.0 Hz, 1H, OC**H₂**Ph), 4.56 (d, *J* = 12.0 Hz, 1H, OC**H₂**Ph), 4.49 – 4.36 (m, 3H, OC**H₂**Ph, OC**H₂**), 4.27 – 4.19 (m, 2H, H2, Ala1-**Hα**), 4.13 (q, *J* = 6.7 Hz, 1H, MurNAc-**Hα**), 3.81 (dt, *J* = 9.3, 4.4 Hz, 1H, **H5**), 3.75 (dd, *J* = 10.2, 4.5 Hz, 1H, **H6**), 3.72 – 3.66 (m, 2H, **H3**, **H4**), 3.53 (dd, *J* = 10.5, 8.7 Hz, 1H, **H6'**), 3.41 (qdd, *J* = 14.8, 6.6, 5.4 Hz, 2H, SC**H₂**), 2.92 (bs, 1H, O**H**), 1.90 (s, 3H, NH**Ac**), 1.41 (d, *J* = 6.7 Hz, 3H, MurNAc-C**H₃**), 1.31 (d, *J* = 7.3 Hz, 3H, Ala1-**Hβ**). ^{13}C NMR (151 MHz, $CDCl_3$) δ 173.05, 172.01, 170.47, 139.26, 137.87, 137.14, 134.28, 129.63, 128.77, 128.63, 128.37, 128.22, 127.99, 127.86, 97.27, 80.65, 78.01, 73.87, 71.76, 70.51, 70.31, 70.03, 58.16, 55.09, 52.62, 48.03, 29.85, 23.55, 19.13, 17.26. HRMS (ESI) Calcd for $C_{36}H_{45}N_2O_{11}S^+$ [M+H] = 713.274 found 713.277

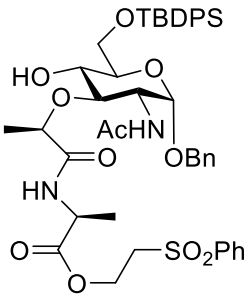
2-(phenylsulfonyl)ethyl ((R)-2-(((2S,3R,4R,5S,6R)-3-acetamido-2-(benzyloxy)-5-hydroxy-6-(hydroxymethyl)tetrahydro-2H-pyran-4-yl)oxy)propanoyl)-L-alaninate [17]



2.46

2.11 (3.55 g, 4.99 mmol) was suspended in 200 mL dry MeOH under Ar. $TsOH \cdot H_2O$ (100 mg, 0.499 mmol) was added and the suspension heated to 75 °C under reflux. The reaction was left to stir overnight during which time it became a pale-yellow solution. The solution was concentrated *in vacuo* and purified via flash column chromatography (SiO_2, 95:5 DCM:MeOH) to yield **2.46** as a white foam (2.8 g, 90%). ^{1}H NMR (400 MHz, $CDCl_3$) δ 7.95 – 7.88 (m, 2H, **Ph**SO_2), 7.73 – 7.64 (m, 1H, **Ph**SO_2), 7.64 – 7.54 (m, 2H, **Ph**SO_2), 7.43 – 7.28 (m, 5H, Ar-**H**), 6.96 (d, *J* = 7.4 Hz, 1H, Ala1-N**H**), 6.12 (d, *J* = 9.0 Hz, 1H, N**H**Ac), 4.92 (d, *J* = 3.6 Hz, 1H, **H1**), 4.70 (d, *J* = 11.7 Hz, 1H, OC**H$_2$**Ph), 4.55 – 4.36 (m, 3H, OC**H$_2$**Ph + OC**H$_2$**), 4.29 (p, *J* = 7.3 Hz, 1H, , Ala1-**H$_\alpha$**), 4.24 – 4.13 (m, 2H, **H2**, MurNAc-**H$_\alpha$**), 3.86 – 3.80 (m, 2H, **H6**, **H6'**), 3.76 – 3.64 (m, 2H, **H4**, **H5**), 3.59 (dd, *J* = 10.3, 7.8 Hz, 1H, **H3**), 3.48 – 3.31 (m, 2H, SC**H$_2$**), 1.92 (s, 3H, NH**Ac**), 1.41 (d, *J* = 6.7 Hz, 3H, MurNAc- **H$_\beta$**), 1.33 (d, *J* = 7.2 Hz, 3H, Ala1-**H$_\beta$**). ^{13}C NMR (101 MHz, $CDCl_3$) δ 173.16, 172.08, 139.22, 137.06, 134.34, 129.68, 128.80, 128.41 (d, *J* = 5.9 Hz), 128.20, 97.34, 80.18, 77.37, 71.95, 70.38, 70.12, 62.45, 58.16, 55.06, 52.72, 48.05, 23.47, 19.12, 17.25. LRMS (ESI) Calcd for $C_{29}H_{39}N_2O_{11}S^+$ [M+H] = 623.22 found 623.25. $[\alpha]_D^{25}$ = +97 (0.34 g/100 mL, MeOH)

2-(phenylsulfonyl)ethyl ((R)-2-(((2S,3R,4R,5S,6R)-3-acetamido-2-(benzyloxy)-6-(((tert-butyldiphenylsilyl)oxy)methyl)-5-hydroxytetrahydro-2H-pyran-4-yl)oxy)propanoyl)-L-alaninate

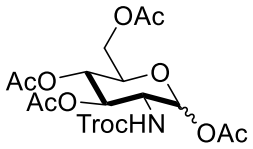


2.90

2.46 (2.8 g, 4.50 mmol) and imidazole (918 mg, 13.5 mmol) were dissolved in 60 mL dry DCM under Ar. The solution was cooled to 0 °C and 2.34 mL TBDPS-Cl added (9.00 mmol). The solution immediately

turned cloudy. The reaction was left to stir for 1 h, before dilution with 150 mL DCM. The solution was washed with 1 x 100 mL 0.01 M HCl, and the aqueous layer back extracted with 1 x 100 mL DCM. The combined organic layers were washed with 1 x 150 mL brine, dried over anhydrous Na_2SO_4, and concentrated *in vacuo*. The resultant solid was purified via flash column chromatography (SiO_2, 50:50 DCM:EtOAc) to yield **2.90** as a white foam (3.20 g, 83%). ^{1}H NMR (400 MHz, $CDCl_3$) δ 7.84 – 7.75 (m, 2H, **Ph**SO_2), 7.65 – 7.51 (m, 5H, **Ph**SO_2, Ar-**H**), 7.49 – 7.41 (m, 2H, Ar-**H**), 7.36 – 7.12 (m, 11H, Ar-**H**), 6.85 (d, *J* = 7.1 Hz, 1H, Ala1-N**H**), 6.14 (d, *J* = 8.9 Hz, 1H, N**H**Ac), 4.79 (d, *J* = 3.7 Hz, 1H, **H1**), 4.55 (d, *J* = 11.8 Hz, 1H, OC**H$_2$**Ph), 4.38 – 4.22 (m, 3H, OC**H$_2$**Ph, OC**H$_2$**), 4.16 – 4.02 (m, 3H, **H2**, MurNAc-**H$_\alpha$**, Ala1-**H$_\alpha$**), 3.82 – 3.73 (m, 2H, **H6**, **H6'**), 3.68 – 3.52 (m, 2H, **H4**, **H5**), 3.43 (dd, *J* = 10.5, 8.3 Hz, 1H, **H3**), 3.37 – 3.20 (m, 2H, SC**H$_2$**), 2.92 (bs, 1H, O**H**), 1.80 (s, 3H, NH**Ac**), 1.30 (d, *J* = 6.7 Hz, 3H, MurNAc- **H$_\beta$**), 1.19 (d, *J* = 7.2 Hz, 3H, Ala1-**H$_\beta$**), 0.96 (s, 9H, ^{t}Bu-**H**). ^{13}C NMR (101 MHz, $CDCl_3$) δ 173.18, 172.03, 170.52, 139.31, 137.14, 135.78 (d, *J* = 3.2 Hz), 134.26, 133.14, 133.03, 130.04, 129.62, 128.74, 128.33, 128.23, 127.96 (d, *J* = 1.8 Hz), 96.95, 80.95, 78.16, 77.36, 72.01, 71.49, 69.69, 64.74, 58.18, 55.11, 52.64, 48.06, 27.01, 23.58, 19.40, 19.27, 17.25, 14.35. HRMS (ESI) Calcd for $C_{45}H_{57}N_2O_{11}SSi^+$ [M+H] = 861.3447 found 861.3467. $[\alpha]_D^{25}$ = +72 (0.22 g/100 mL, DCM). IR (Transmittance): 2930, 2364, 1747, 1653, 1539, 1448, 1428, 1375, 1309, 1143, 1111, 1049, 823, 733, 701 cm^{-1}.

(3R,4R,5S,6R)-6-(acetoxymethyl)-3-(((2,2,2-trichloroethoxy)carbonyl)amino)tetrahydro-2H-pyran-2,4,5-triyl triacetate [20]

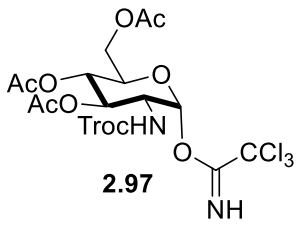


2.96

D-Glucosamine (30.0 g, 0.139 mol) and sodium bicarbonate (23.35 g, 0.278 mol) were dissolved in 360 mL H_2O and stirred for 5 mins. 23 mL 2,2,2-trichloroethoxycarbonyl chloride (0.167 mmol) was added dropwise and the reaction left to stir for 2 h. During this time a white precipitate formed. The precipitate was recovered by filtration and washed with 3 x 75 mL H_2O. The white solid was azetroped with toluene and dissolved in 200 mL dry pyridine. 100 mL acetic anhydride was added, and the reaction left to stir overnight. The solution was concentrated *in* vacuo, azetroped with toluene and redissolved in 200 mL DCM. The solution was washed with 1 x 100 mL 1.0 M HCl and the aqueous layer back extracted with 100 mL DCM. The combined organic layers were washed with 1 x 150 mL sat. $NaHCO_3$ sol., and the aqueous layer back extracted with 100 mL DCM. The combined organic layers were washed with 1 x 100 mL brine, dried over anhydrous Na_2SO_4, and concentrated *in vacuo*. The resultant yellow oil was purified via flash column chromatography (SiO_2, 60:40 pet. ether:EtOAc) to yield **2.96** (24.32 g, 33%) as a white foam. ^{1}H NMR (600 MHz, CDCl3) δ 6.23 (d, 1H, **H1**, J = 3.7 Hz), 5.31 – 5.25 (m, 1H, N**H**Troc), 5.20 (t, 1H, **H4**, J=9.8Hz), 5.12 (d, 1H, **H3** J = 9.4 Hz), 4.81 (d, Troc-C**H$_2$**, 1H, J = 12.0 Hz), 4.62 (d, 1H, Troc-C**H$_2$**, J = 12.0 Hz), 4.27 (dd, 1H, **H6**, J = 12.5, 4.1 Hz), 4.20 (ddd, J = 10.9, 9.4, 3.7 Hz, 1H, **H2**), 4.09 – 3.98(m, 2H, **H5**, **H6'**), 2.20 (s, 3H, Ac-**H**), 2.09 (s, 3H, Ac-**H**), 2.04 (s, 6H, Ac-**H**). ^{13}C NMR (101 MHz, $CDCl_3$) δ 171.41, 171.31, 170.88, 170.78 (d, *J* = 2.2 Hz), 169.49, 169.31, 168.74, 154.18, 95.35, 92.41, 90.57, 74.81, 74.62, 72.99, 72.16, 70.53, 69.87, 67.97, 67.66, 61.70, 61.61, 60.53,

55.29, 53.36, 21.18, 21.00 (d, *J* = 7.9 Hz), 20.82 (t, *J* = 3.3 Hz), 20.75 – 20.62 (m), 14.33. $[\alpha]_D^{25}$ = +64 (0.37 g/100 mL, DCM)

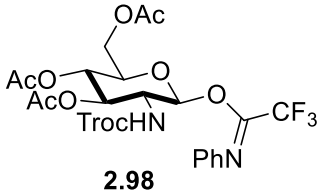
(2R,3S,4R,5R,6R)-2-(acetoxymethyl)-6-(2,2,2-trichloro-1-iminoethoxy)-5-(((2,2,2-trichloroethoxy)carbonyl)amino)tetrahydro-2H-pyran-3,4-diyl diacetate [20]



2.97

2.96 (5.0 g, 9.57 mmol) was dissolved in 45 mL dry DMF under Ar. Hydrazine acetate (326 mg, 3.54 mmol) was added and the reaction was left to stir for 40 min. At this point an additional 720 mg hydrazine acetate was added (7.82 mmol). The reaction was left to stir for a further 20 min, before dilution with 200 mL EtOAc. The solution was washed with 1 x 200 mL H_2O, and the aqueous layer back extracted with 100 mL EtOAc. The combined organic layers were washed with 1 x 140 mL sat. $NaHCO_3$ sol., and the aqueous layer back extracted with 100 mL EtOAc. The combined organic layers were washed with 1 x 100 mL brine, dried over anhydrous Na_2SO_4, and concentrated *in vacuo*. The resultant white foam was dissolved in 45 mL dry DCM under Ar and 9.57 mL trichloroacetonitrile (95.7 mmol) was added. DBU (0.29 mL, 1.91 mmol) was added slowly and the reaction left to stir for 2 h. The reaction was concentrated *in vacuo*, and the orange oil purified via flash column chromatography (97:3 $CHCl_3$:acetone) to yield **2.97** (4.36 g, 73%). ^{1}H NMR (601 MHz, $CDCl_3$) δ 8.80 (s, 1H, acetamide-N**H**), 6.42 (d, *J* = 3.6 Hz, 1H, **H1**), 5.35 (dd, *J* = 10.9, 9.5 Hz, 1H, **H3**), 5.25 (t, *J* = 9.9 Hz, 1H, **H4**), 5.20 (d, *J* = 9.2 Hz, 1H, N**H**Troc), 4.77 – 4.67 (m, 2H, Troc-C**H₂**), 4.28 (ddd, *J* = 12.1, 9.5, 3.9 Hz, 2H, **H2**, **H6**), 4.17 – 4.09 (m, 2H, **H5**, **H6'**), 2.08 (s, 3H, Ac-**H**), 2.06 (s, 6H, Ac-**H**). ^{13}C NMR (151 MHz, $CDCl_3$) δ 171.16, 170.59, 169.27, 160.40, 154.13, 95.22, 94.54, 90.65, 74.66, 70.27, 67.36, 61.38, 53.89, 20.69, 20.59. $[\alpha]_D^{25}$ = +77 (0.31 g/100 mL, DCM).

(2R,3S,4R,5R,6S)-2-(acetoxymethyl)-5-(((2,2,2-trichloroethoxy)carbonyl)amino)-6-((E)-2,2,2-trifluoro-1-(phenylimino)ethoxy)tetrahydro-2H-pyran-3,4-diyl diacetate [65]

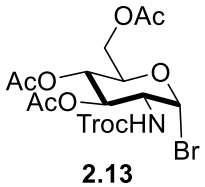


2.98

2.96 (100 mg, 0.191 mmol) was dissolved in 1 mL dry DMF under Ar. Hydrazine acetate (6.5 mg, 0.071 mmol) was added and the solution stirred at ambient temperature for 1 hr. A further 11 mg Hydrazine

acetate (0.191 mmol) was added, and the solution stirred for 1 hr at ambient temperature. The reaction was diluted with 5 mL EtOAc, washed with 1 x 5 mL water, 1 x 4 mL sat. $NaHCO_3$ sol., and 1 x 4 mL water. The combined aqueous layers were back extracted with 1 x 5 mL EtOAc. The combined organic layers were washed with 1 x 5 mL brine, dried over anhydrous Na_2SO_4, and concentrated *in vacuo*. The white solid was dissolved in 2 mL dry DCM under Ar and 0.3 mL 2,2,2-trifluoro-N-phenylacetimidoyl chloride (2.09 mmol) was added. Following this, 5.3 µl DBU (0.0382 mmol) was added, and the reaction left to stir. After 1 h an additional 5.3 µl DBU (0.0382 mmol) was added, then a further 21.2 µl (0.1528 mmol) after 2h. The mixture was concentrated *in vacuo* and purified via flash column chromatography (SiO_2, 97:3 $CHCl_3$:acetone) to yield **2.98** (25.2 mg, 20%). ^{1}H NMR (400 MHz, $CDCl_3$) δ 7.37 – 7.27 (m, 2H, Ar-**H**), 7.17 – 7.08 (m, 1H, Ar-**H**), 6.82 (d, *J* = 7.7 Hz, 2H, Ar-**H**), 5.92 (bs, 1H, **H1**), 5.39 (d, *J* = 9.0 Hz, 1H, N**H**Troc), 5.31 (t, *J* = 9.8 Hz, 1H, **H3**), 5.13 (t, *J* = 9.5 Hz, 1H, **H4**), 4.83 – 4.69 (m, 2H, Troc-C**H$_2$**), 4.28 (dd, *J* = 12.4, 4.7 Hz, 1H, **H6**), 4.19 – 4.09 (m, 1H, **H6'**), 3.99 (bs, 1H, **H2**), 3.78 (bs, 1H, **H5**), 2.08 (s, 3H, Ac-**H**), 2.05 (s, 3H, Ac-**H**), 2.02 (s, 3H, Ac-**H**). ^{13}C NMR (101 MHz, $CDCl_3$) δ 170.82, 170.75, 169.48, 154.04, 143.06, 129.00, 124.82, 119.32, 94.76, 74.73, 72.99, 71.70, 68.10, 61.76, 55.41, 20.82, 20.72, 20.70. ^{19}F NMR (376 MHz, $CDCl_3$) δ -65.63, -75.69.

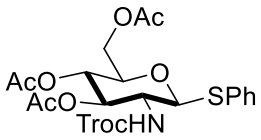
(2R,3S,4R,5R,6R)-2-(acetoxymethyl)-6-bromo-5-(((2,2,2-trichloroethoxy)carbonyl)amino)tetrahydro-2H-pyran-3,4-diyl diacetate [66]



2.13

2.96 (2.21 g, 4.23 mmol) was dissolved in 50 mL dry DCM and cooled to 0 °C. 33% HBr in AcOH (5 mL) was added and the reaction left to stir for 1 h, after which it was warmed to ambient temperature. After 1 hr the reaction was diluted with 100 mL dry DCM, and washed with 1 x 50 mL H_2O, 2 x 50 mL sat. $NaHCO_3$ sol., 1x 50 mL brine. The organic layer was dried over anhydrous Na_2SO_4 and concentrated *in vacuo* to yield **2.13** (2.28 g, 99%) as a white foam. ^{1}H NMR (400 MHz, $CDCl_3$) δ 6.52 (d, *J* = 3.7 Hz, 1H, **H1**), 5.39 – 5.31 (m, 2H, N**H**Troc, **H3**), 5.24 (t, *J* = 9.8 Hz, 1H, **H4**), 4.81 (d, *J* = 12.1 Hz, 1H, Troc-C**H$_2$**), 4.66 (d, *J* = 12.0 Hz, 1H, Troc-C**H$_2$**), 4.33 (dd, *J* = 12.6, 4.0 Hz, 1H, **H6**), 4.26 (ddd, *J* = 10.2, 4.2, 2.0 Hz, 1H, H), 4.13 (m, 2H, **H2**, **H6'**), 2.11 (s, 3H Ac-**H**), 2.06 (s, 3H, Ac-**H**), 2.04 (s, 3H, Ac-**H**). ^{13}C NMR (101 MHz, $CDCl_3$) δ 171.17, 170.67, 169.36, 154.12, 95.25, 91.06, 74.89, 72.84, 70.83, 66.90, 61.08, 20.81, 20.74, 20.68. $[\alpha]_D^{25}$ = +120 (0.5 g/100 mL, DCM).

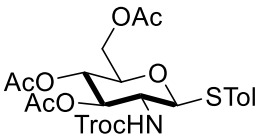
(2R,3S,4R,5R,6S)-2-(acetoxymethyl)-6-(phenylthio)-5-(((2,2,2-trichloroethoxy)carbonyl)amino)tetrahydro-2H-pyran-3,4-diyl diacetate [67]



2.99

2.96 (11.5 g, 22.0 mmol) was dissolved in 100 mL dry DCM under Ar. Thiophenol (4.49 mL, 44.0 mmol) was added and the solution cooled to 0 °C. BF_3**.**Et_2O (8.15 mL, 66.0 mmol) was added, and the reaction warmed to ambient temperature. After 1 h the reaction was diluted with 100 mL DCM, washed with 1 x 100 mL sat. $NaHCO_3$ sol., and 1 x 100 mL brine. The organic layer was dried over anhydrous Na_2SO_4 and concentrated *in vacuo*. Purification via flash column chromatography (SiO_2, 90:10 DCM:EtOAc) yielded **2.99** (1.46 g, 12%) as a waxy white solid. ^{1}H NMR (400 MHz, $CDCl_3$) δ 7.55 – 7.48 (m, 2H, S**Ph**), 7.37 – 7.28 (m, 3H, S**Ph**), 5.28 (dd, *J* = 11.2, 8.6 Hz, 2H, N**H**Troc, **H3**), 5.03 (t, *J* = 9.7 Hz, 1H, **H4**), 4.87 (d, *J* = 10.4 Hz, 1H, **H1**), 4.79 (d, *J* = 12.0 Hz, 1H, TrocC**H₂**), 4.72 (d, *J* = 12.0 Hz, 1H, TrocC**H₂**), 4.23 (dd, *J* = 12.3, 5.3 Hz, 1H, **H6**), 4.20 – 4.14 (m, 1H, **H6'**), 3.77 – 3.63 (m, 2H, **H2**, **H5**), 2.08 (s, 3H, Ac-**H**), 2.01 (s, 6H, Ac-**H**). ^{13}C NMR (101 MHz, $CDCl_3$) δ 133.12, 129.13, 128.50, 86.74, 75.98, 74.69, 73.28, 68.63, 62.45, 55.25, 21.19, 20.88, 20.74 (d, *J* = 3.3 Hz).

(2R,3S,4R,5R,6S)-2-(acetoxymethyl)-6-(p-tolylthio)-5-(((2,2,2-trichloroethoxy)carbonyl)amino)tetrahydro-2H-pyran-3,4-diyl diacetate [11]

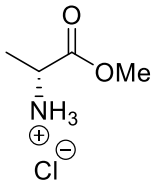


2.22

2.96 (19.32 g, 36.96 mmol) was dissolved in 100 mL dry DCM under Ar. p-thiocresol (9.18 g, 73.92 mmol) was added and the solution cooled to 0 °C. BF_3**.**Et_2O (13.68 mL, 110.88 mmol) was added, and the reaction warmed to ambient temperature. After 24 h the reaction was diluted with 100 mL DCM, washed with 1 x 100 mL sat. $NaHCO_3$ sol., and 1 x 100 mL brine. The organic layer was dried over anhydrous Na_2SO_4 and concentrated *in vacuo*. Purification via flash column chromatography (SiO_2, 85:15 toluene:EtOAc) yielded **2.22** (16.6 g, 77%) as a white solid. ^{1}H NMR (601 MHz, $CDCl_3$) δ 7.34 (d,

J = 8.1 Hz, 2H), 7.05 (d, *J* = 7.9 Hz, 2H), 5.26 (d, *J* = 9.1 Hz, 1H), 5.21 (t, *J* = 9.8 Hz, 1H), 4.94 (t, *J* = 9.7 Hz, 1H), 4.73 (d, *J* = 11.2 Hz, 2H), 4.66 (d, *J* = 12.1 Hz, 1H), 4.15 (dd, *J* = 12.3, 5.2 Hz, 1H), 4.10 (dd, *J* = 12.2, 2.4 Hz, 1H), 3.67 – 3.55 (m, 2H), 2.28 (s, 4H), 2.02 (s, 4H), 1.94 (s, 4H), 1.93 (s, 4H).

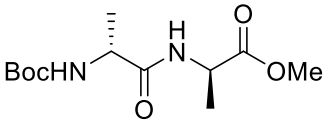
(R)-1-methoxy-1-oxopropan-2-aminium chloride [20]



2.102

D-Alanine (1.0 g, 11.2 mmol) was dissolved in 25 mL MeOH and TMS-Cl (5.66 mL, 44.9 mmol) was added dropwise. The solution was left to stir at ambient temperature for 18h and concentrated under vacuum to yield H-D-Ala-OMe**.**HCl, **2.102** (1.56 g, 100% yield). ^{1}H NMR (600 MHz, MeOD) δ 4.02 (q, 1H, J = 7.2 Hz, **H**$_{\alpha}$), 3.75 (s, 3H, **H**-CO_2Me), 1.46 (d, 3H, J = 7.2 Hz, **H**$_{\beta}$). ^{13}C NMR (101 MHz, DMSO) δ 170.35, 52.74, 47.77, 15.64.

methyl (tert-butoxycarbonyl)-D-alanyl-D-alaninate [20]

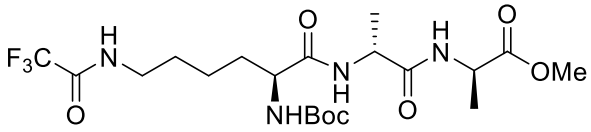


2.103

2.102 (1.56 g, 11.2 mmol), Boc-D-Ala-OH (1.37 g, 7.2 mmol), and HATU (2.75 g, 7.2 mmol) were dissolved in 20 mL dry DMF under Ar. The solution was cooled to 0 °C. and DIPEA (3.78 mL, 21.7 mmol) was added slowly. The reaction mix was warmed to ambient temperature and left to stir for 2 h. The solution was poured into 100 mL stirring H_2O and extracted with 3 x 70 mL EtOAc. The combined layers were washed with 3 x 250 mL H_2O, followed by 150 mL brine. The organic extract was dried over anhydrous Na_2SO_4 and concentrated *in vacuo* to yield **2.103** (1.25 g, 63%) as a white solid. ^{1}H NMR (400 MHz, $CDCl_3$) δ 6.66 (d, *J* = 7.1 Hz, 1H, Ala5-N**H**), 5.03 (m, 1H, Ala4-N**H**), 4.56 (p, *J* = 7.2 Hz, 1H, Ala5-**H**$_{\alpha}$), 4.17 (s, 1H, Ala4- **H**$_{\alpha}$), 3.74 (s, 3H, Ala5-O**Me**), 1.44 (s, 9H, NH**Boc**), 1.40 (d, *J* = 7.1 Hz, 3H,

Ala5-**H$_\beta$**), 1.35 (d, *J* = 7.1 Hz, 3H, Ala4-**H$_\beta$**) . ^{13}C NMR (101 MHz, $CDCl_3$) δ 173.32, 172.31, 52.60, 50.13, 48.14, 28.42, 18.44 (d, *J* = 10.3 Hz).

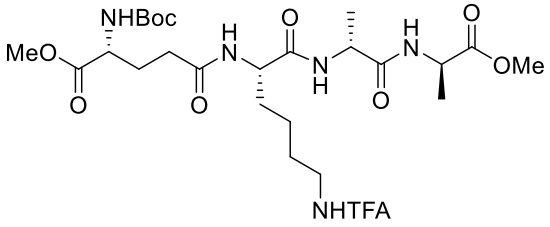
methyl ((S)-2-((tert-butoxycarbonyl)amino)-5-(2,2,2-trifluoroacetamido)pentanoyl)-D-alanyl-D-alaninate [20]



2.104

2.103 (100 mg, 0.365 mmol) was dissolved in 1 mL dry DCM under Ar and cooled to 0°C. 1 mL TFA was added slowly. The reaction was warmed to ambient temperature and stirred for 1 h. The reaction was concentrated *in vacuo*, azetroped with toluene and dried under high vacuum for 1 h. During this time, Boc-Lys-TFA-OH (150 mg, 0.438 mmol) and HATU (148 mg, 0.389 mmol) were dissolved in 1 mL dry DMF under Ar and cooled to 0°C. DIPEA (0.35 mL, 2.02 mmol) was added slowly, and the reaction stirred for 15 mins. Deprotected **2.103** was dissolved in 1 mL dry DMF under Ar and added to the preactivated acid. The reaction was then warmed to ambient temperature and left to stir for 2 h. The DMF was co-evaporated with toluene and the resulting oil redissolved in 20 mL EtOAc. The solution was washed with 1 x 20 mL 1.0M HCl, 1 x 20 mL sat. $NaHCO_3$ sol., and 1 x 20 mL brine. Following this the extract was dried over anhydrous Na_2SO_4 and concentrated *in vacuo*. **2.104** (113 mg, 64%) was obtained after purification via flash column chromatography (100:0 EtOAc). ^{1}H NMR (601 MHz, DMSO) δ 9.38 (m, 1H, Lys3-N**H**TFA), 8.20 (d, *J* = 7.1 Hz, 1H, Ala4-N**H**), 8.00 (d, *J* = 7.9 Hz, 1H, Ala5-N**H**), 6.92 (d, *J* = 7.5 Hz, 1H, Lys3-N**H**Boc), 4.29 (m, 7.2 Hz, 2H, Lys3-**H$_\alpha$**, Ala4-**H$_\alpha$**), 3.86 (q, *J* = 7.5 Hz, 1H, Ala5-**H$_\alpha$**), 3.60 (s, 3H, Ala5-O**Me**), 3.15 (q, *J* = 6.5 Hz, 2H, Lys3-**H$_\varepsilon$**), 1.61 – 1.39 (m, 4H, Lys-**H$_\beta$**,Lys-**H$_\delta$**), 1.37 (s, 9H, NH**Boc**), 1.30 (d, *J* = 7.3 Hz, 3H, Ala4-**H$_\beta$**), 1.28-1.21(m, 2H, Lys-**H$_\gamma$**), 1.18 (d, *J* = 7.0 Hz, 3H, Ala5-**H$_\beta$**). ^{13}C NMR (101 MHz, DMSO) δ 172.77, 171.98, 171.71, 156.29, 155.93, 155.46, 78.13, 54.26, 51.84, 47.49 (d, *J* = 8.1 Hz), 31.27, 28.13, 27.90, 22.66, 18.14, 16.75.

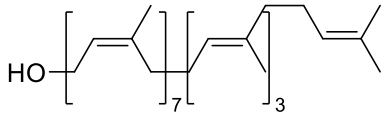
methyl N2-(tert-butoxycarbonyl)-N5-((S)-1-(((R)-1-(((R)-1-methoxy-1-oxopropan-2-yl)amino)-1-oxopropan-2-yl)amino)-1-oxo-6-(2,2,2-trifluoroacetamido)hexan-2-yl)-D-glutaminate [20]



2.105

2.104 (500 mg, 1.00 mmol) was dissolved in 5 mL dry DCM under Ar and cooled to 0 °C. TFA (5 mL) was added slowly and the solution warmed to ambient temperature. After 1 hr the reaction was concentrated, azetroped with toluene, and dried on high vac for 1 hr. During this time Boc-D-Glu(OMe)-OH (261 mg, 1.00 mmol) and HATU (380 mg, 1.00 mmol) were dissolved in 5 mL dry DMF under Ar and cooled to 0 °C. DIPEA (0.35 mL, 2.00 mmol) was added slowly and the reaction left to stir for 15 mins. At this point a solution of deprotected **2.104** in 5 mL dry DMF was added, and the reaction warmed to ambient temperature. The reaction was left to stir overnight, at which point it was concentrated *in vacuo*. The solid was redissolved in 20 mL EtOAc and washed with 1 x 20 mL 0.5M HCl, 1 x 20 mL sat. $NaHCO_3$ sol., and 1 x 20 mL brine. The organic layer was dried over anhydrous Na_2SO_4 and concentrated *in vacuo*. Purification via flash column chromatography (SiO_2, 95:5 DCM:MeOH) gave **2.105** (378.6 mgs, 59%) as a white solid. ^{1}H NMR (400 MHz, DMSO) δ 9.37 (t, *J* = 5.7 Hz, 1H, N**H**TFA), 8.18 (dd, *J* = 11.6, 7.5 Hz, 2H, Ala4-N**H** + Ala5N**H**), 7.99 (d, *J* = 7.4 Hz, 1H, Lys3-N**H**), 7.23 (d, *J* = 7.7 Hz, 1H, Glu2-N**H**), 4.24 (tt, *J* = 21.4, 7.2 Hz, 3H, Ala4-$\mathbf{H_\alpha}$ + Ala5-$\mathbf{H_\alpha}$ + Lys3-$\mathbf{H_\alpha}$), 3.94 (td, *J* = 8.6, 5.5 Hz, 1H, Glu2-$\mathbf{H_\alpha}$), 3.62 (s, 3H, **H**-OMe), 3.59 (s, 3H, **H**-OMe), 3.15 (q, *J* = 6.7 Hz, 2H, Lys3-$\mathbf{H_\varepsilon}$), 2.26 – 2.12 (m, 2H, Glu-$\mathbf{H_\gamma}$), 1.88 (tq, *J* = 8.7, 5.3 Hz, 1H, Glu-$\mathbf{H_\beta}$), 1.80 – 1.66 (m, 1H, Glu-$\mathbf{H_\beta}$'), 1.65 – 1.40 (m, 4H, , Lys3-$\mathbf{H_\beta}$ + Lys3-$\mathbf{H_\delta}$), 1.37 (s, 9H, N**H**Boc), 1.29 (d, *J* = 7.3 Hz, 3H, Ala5-$\mathbf{H_\beta}$), 1.24 (q, *J* = 7.5 Hz, 2H, , Lys3-$\mathbf{H_\gamma}$), 1.19 (d, *J* = 7.1 Hz, 3H, Ala4-$\mathbf{H_\beta}$). ^{13}C NMR (101 MHz, DMSO) δ 172.85 (d, *J* = 3.1 Hz), 172.02, 171.55, 171.32, 156.29, 155.93, 155.46, 117.40, 114.54, 78.23, 53.16, 52.63, 51.79, 51.70, 47.54, 39.03, 31.42, 28.15, 27.91, 26.71, 22.49, 17.98, 16.75. $[\alpha]_D^{25}$ = -3.64 (0.11 g/100 mL, MeOH). HRMS (ESI) Calc'd for $C_{21}H_{35}F_3N_5O_8^+$ [M+H-Boc] = 542.2333 found 542.2479.

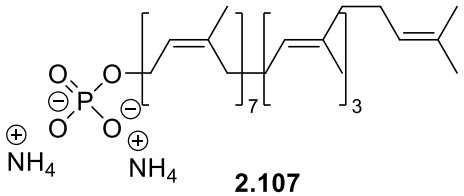
Undecaprenol [20]



2.106

Ground bay leaves (300g, *Laurus nobilis*) were suspended in a 9:1 mixture of acetone: pet. ether (4 L) and stirred for 4 days. The resulting green suspension was filtered over celite and concentrated under vacuum. The solid was resuspended in 260 mL n-hexane, 1.3 L EtOH, 175 mL 15% KOH in water and heated under reflux for 1 h. The resulting solution was cooled to ambient temperature and partitioned between 250 mL ether and 250 mL H_2O. The aqueous layer was back extracted with 3 x 250 mL ether. The combined ether extracts were dried over anhydrous $Na_2SO_4$and concentrated *in vacuo*. The crude extract was purified by flash column chromatography (SiO_2, 95:5 Pet. ether: EtOAc) to yield **2.106** (669 mg) as a yellow oil. ^{1}H NMR ($CDCl_3$, 600 MHz): δ 5.40-5.35 (1H, C**H**CH_2OH), 5.09-5.01 (10H, m), 4.10 (2H, d, J= 7.2 Hz, C**H$_2$**OH), 2.05-1.85 (40H, m), 1.68 (3H, s), 1.62-1.59 (21H, m), 1.58-1.56 (12H, m)

Undecaprenyl phosphate [20]

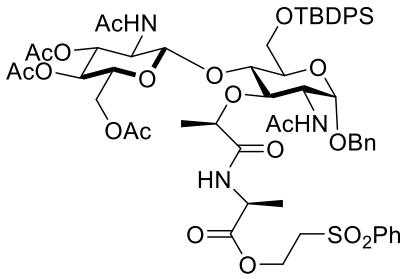


2.107

2.106 (400 mg, 0.56 mmol) and 5-ethylthiotetrazole (323 mg, 2.47 mmol) were suspended in dry 11 mL DCM under Ar. The suspension was stirred vigorously and bis(2-cyanoethyl)-*N, N*'-diisopropylphosphoramidite (0.42 mL, 1.60 mmol) was added. The reaction was stirred at ambient temperature for 3 h. The solution was diluted with 50 mL DCM and washed with 1 x 30 mL sat. $NaHCO_3$, 1 x 30 mL H_2O, and 1 x 30 mL brine. The organic extract was dried over anhydrous Na_2SO_4 and concentrated *in vacuo*. The solid was dissolved in 13 mL THF and cooled to -78 °C. 1.05 mL 30% H_2O_2 solution was added dropwise via syringe to the stirring solution. Following this addition, the solution was warmed to ambient temperature and left to stir for 2 h. The reaction mix was then quenched through dropwise addition of2.8 mL ice-cold sodium sulfite at 0°C and was left to stir for 5 mins. The resulting solution was extracted with 1 x 45 mL EtOAc, and the organic layer washed with 1 x 30 mL sat. $NaHCO_3$, 1 x 30 mL H_2O, and 1 x 30 mL brine, dried over anhydrous Na_2SO_4, and concentrated *in vacuo*. The solid was dissolved in 10 mL dry MeOH under Ar and 0.4 mL of 25% NaOMe in methanol solution was added via syringe. The reaction was stirred at ambient temperature for 48 h. The reaction mix was diluted by 10 mL of a 1:1 mix of chloroform: methanol and concentrated *in vacuo*. The resulting yellow oil was purified by flash column chromatography (SiO_2, 90:10 $CHCl_3$:MeOH to 80:20:2:0.1 $CHCl_3$:MeOH:H_2O:NH_4OH) to yield **2.107** (60 mg, 13%), as a white foam. Aggregation

prevented acquisition of good NMR spectra. LRMS (ESI) Calcd for $C_{55}H_{90}O_4P^-$ [M-H] = 845.6 found 845.9.

(2R,3S,4R,5R,6S)-5-acetamido-6-(((2R,3S,4R,5R,6S)-5-acetamido-6-(benzyloxy)-2-(((tert-butyldiphenylsilyl)oxy)methyl)-4-(((R)-1-oxo-1-(((S)-1-oxo-1-(2-(phenylsulfonyl)ethoxy)propan-2-yl)amino)propan-2-yl)oxy)tetrahydro-2H-pyran-3-yl)oxy)-2-(acetoxymethyl)tetrahydro-2H-pyran-3,4-diyl diacetate

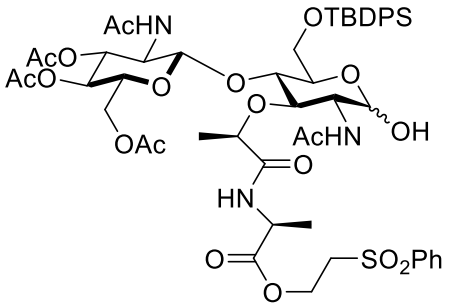


2.89

Prior to the reaction 3 Å Molecular Sieves were activated at 350 ^oC overnight. These were added to a rigorously flame dried flask under Ar. To this flask a solution of **2.90** (1.0 g, 1.16 mmol) and NIS (1.05 g, 4.65 mmol) in 15 mL dry DCM was added. **2.22** (2.16 g, 4.65 mmol) was added and the solution cooled to -10 ^oC. TfOH (0.13 mL, 1.45 mmol) was added, the reaction warmed to ambient temperature and left to stir for 5 h. The reaction was diluted with 20 mL DCM and filtered. The red filtrate was washed with 1 x 15 mL sat. $NaHCO_3$ sol., and 1 x 15 mL sat NaS_2O_3 sol. The NaS_2O_3 layer was back extracted with 20 mL DCM, the combined organic layers washed with 1 x 15 mL brine, dried over anhydrous Na_2SO_4, and concentrated *in vacuo*. The solid was partially purified via flash column chromatography (SiO_2, 50:50 DCM:EtOAc) to yield 1.2 gs crude solid. A portion of the crude solid (872 mgs), 1.72 g Zn, 898.2 mg $ZnCl_2$ was dissolved in 10 mL dry THF under Ar. AcOH (6.5 mL) and Ac_2O (15 mL) were added. The reaction was left to stir overnight and filtered over celite. The celite was rinsed thoroughly with 50 mL EtOAc. The solution was washed 1 x 20 mL sat. $NaHCO_3$ sol. and the aqueous layer back extracted 1 x 20 mL EtOAc. The combined organic layers were washed 1 x 20 mL brine, dried over anhydrous Na_2SO_4, and concentrated *in vacuo*. Purification via flash column chromatography (SiO_2, gradient 90:10 DCM:acetone to 80:20 DCM:acetone) to yield **2.89** (454 mgs, 50%). ^1H NMR (601 MHz, $CDCl_3$) δ 7.88 (d, *J* = 7.8 Hz, 2H, Ar-**H**), 7.77 (dd, *J* = 6.6, 2.9 Hz, 2H, Ar-**H**), 7.73 – 7.68 (m, 2H, Ar-**H**), 7.65 (t, *J* = 7.5 Hz, 1H, Ar-**H**), 7.58 – 7.52 (m, 5H, Ar-**H**), 7.49 (d, *J* = 7.2 Hz, 1H, Ar-**H**), 7.46 (t, *J* = 7.3 Hz, 2H, Ar-**H**), 7.30 – 7.20 (m, 5H, Ar-**H**), 7.10 (dd, *J* = 11.4, 6.9 Hz, 2H, GlcNAc-N**H** + Ala-N**H**), 5.22 (d, *J* = 3.6 Hz, 1H, **H1**), 5.02 (t, *J* = 9.7 Hz, 1H, GlcNAc-**H4**), 4.78 (t, *J* = 10.0 Hz, 1H, GlcNAc-**H3**), 4.62 (d, *J* = 9.7 Hz, 1H, MurNAc-N**H**), 4.58 (d, *J* = 12.2 Hz, 1H, OC**H₂**Ph), 4.48 (d, *J* = 12.2 Hz, 1H, OC**H₂**Ph), 4.41 (d, *J* = 8.5 Hz, 1H, GlcNAc-**H1**), 4.40 – 4.30 (m, 3H, OC**H₂** + MurNAc-**Hα**), 4.30 – 4.25 (m, 1H, GlcNAc-**H6**), 4.22 (q, *J* = 7.3 Hz, 1H, Ala-**Hα**), 4.06 (t, *J* = 9.4 Hz, 1H, MurNAc-**H4**), 4.03 – 3.94 (m, 3H, MurNAc-**H2** + GlcNAc-**H2** + GlcNAc-**H6'**), 3.77 (d, *J* = 11.0 Hz, 1H, MurNAc-**H6**), 3.50 (t, *J* = 10.5 Hz, 3H, MurNAc-**H3**, MurNAc-**H5**, MurNAc-**H6'**), 3.41 – 3.33 (m, 3H, SC**H₂** + GlcNAc-**H5**), 2.04 (s, 3H, Ac-**H**), 2.01 (s, 3H, Ac-**H**), 2.00 (s, 3H, Ac-**H**), 1.96 (s, 3H, Ac-**H**), 1.59 (s, 3H, GlcNAc-NH**Ac**), 1.36 (d, *J* = 6.7 Hz, 3H, MurNAc-**Hβ**), 1.31 – 1.23 (d, *J* = 7.3 Hz, 3H, Ala-**Hβ**), 1.12 (s, 9H, ^{t}Bu-**H**). ^{13}C NMR (151 MHz, $CDCl_3$) δ 174.43, 171.94, 171.00, 170.89, 170.77, 169.49, 165.83, 139.28, 137.74, 136.18, 135.82, 133.91, 132.24, 130.58, 130.26, 129.56, 128.23, 128.05, 127.91, 113.87, 100.09, 96.98, 76.30, 75.39, 72.80, 71.60,

71.50, 70.20, 68.15, 61.60 (d, *J* = 2.7 Hz), 60.55, 58.22, 54.92, 54.21, 54.09, 48.02, 29.84, 27.15, 23.37, 23.11, 20.78 (d, *J* = 4.4 Hz), 19.42, 18.91, 17.38, 14.34. HRMS (ESI) Calcd for $C_{59}H_{76}N_3O_{19}SSi^+$ [M+H] = 1190.46 found 1190.49. $[\alpha]_D^{25}$ = +18.6 (0.28 g/100 mL, DCM). IR (Transmittance): 2932, 2349, 2245, 2190, 2060, 2033, 1965, 1747, 1671, 1519, 1449, 1428, 1372, 1323, 1274, 1231, 1146, 1113, 1088, 871, 823, 803, 748 cm^{-1}.

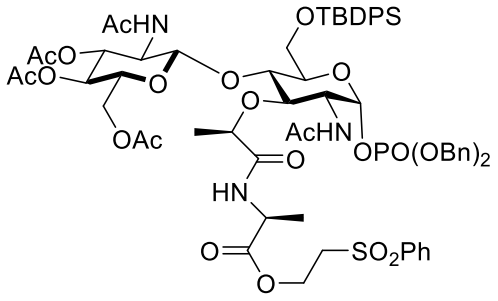
(2R,3S,4R,5R,6S)-5-acetamido-6-(((2R,3S,4R,5R)-5-acetamido-2-(((tert-butyldiphenylsilyl)oxy)methyl)-6-hydroxy-4-(((R)-1-oxo-1-(((S)-1-oxo-1-(2-(phenylsulfonyl)ethoxy)propan-2-yl)amino)propan-2-yl)oxy)tetrahydro-2H-pyran-3-yl)oxy)-2-(acetoxymethyl)tetrahydro-2H-pyran-3,4-diyl diacetate



2.108

2.89 (230.5 mg, 0.194 mmol) was dissolved in 5 mL EtOAc and vigorously stirred. A solution of $NaBrO_3$ (1.5 mL, 1.74 mmol) water was added, followed by the slow addition of a solution of $Na_2S_2O_4$ in water (1.5 mL, 1.94 mmol) over 5 mins. As $Na_2S_2O_4$ was added the mixture turned yellow. The suspension was left to stir for 2 hrs. The reaction was diluted with 10 mL EtOAc, washed with 1 x 7 mL sat. $NaHCO_3$ sol. And washed with 1 x 7 mL brine. The organic layer was dried over anhydrous Na_2SO_4 and concentrated *in vacuo*. Purification via flash column chromatography (SiO_2, gradient 80:20 EtOAc:pet. ether to 100:0 EtOAc: pet. ether to 96:4 EtOAc:MeOH) yielded **2.108** as a white solid (118.7 mg, 62%). ^{1}H NMR (400 MHz, $CDCl_3$) δ 7.93 (ddt, *J* = 7.1, 3.5, 1.4 Hz, 2H), 7.83 – 7.74 (m, 2H), 7.69 (ddt, *J* = 10.2, 4.2, 2.3 Hz, 3H), 7.64 – 7.51 (m, 4H), 7.51 – 7.41 (m, 3H), 5.64 (d, *J* = 3.4 Hz, 1H), 5.04 (td, *J* = 9.6, 3.8 Hz, 1H), 4.81 – 4.64 (m, 2H), 4.55 (q, *J* = 6.6 Hz, 1H), 4.46 (ddd, *J* = 7.1, 5.1, 2.0 Hz, 2H), 4.40 – 4.26 (m, 3H), 4.24 – 4.08 (m, 1H), 4.09 – 3.94 (m, 2H), 3.93 – 3.79 (m, 1H), 3.80 – 3.60 (m, 1H), 3.62 – 3.44 (m, 3H), 3.38 (ddd, *J* = 10.1, 4.0, 2.2 Hz, 1H), 3.33 – 3.16 (m, 1H), 2.06 (q, *J* = 1.8 Hz, 5H), 2.04 (d, *J* = 2.3 Hz, 2H), 2.02 (d, *J* = 3.2 Hz, 3H), 1.98 (s, 2H), 1.66 (s, 2H), 1.41 – 1.31 (m, 6H).

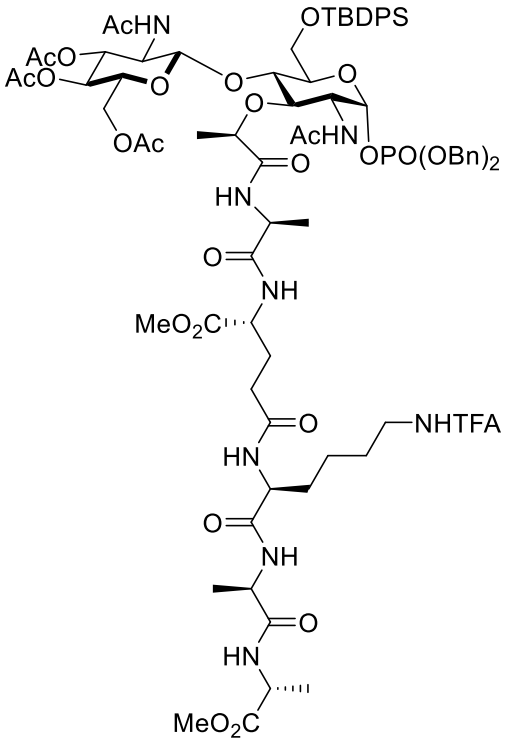
(2R,3S,4R,5R,6S)-5-acetamido-6-(((2R,3S,4R,5R,6R)-5-acetamido-6-((bis(benzyloxy)phosphoryl)oxy)-2-(((tert-butyldiphenylsilyl)oxy)methyl)-4-(((R)-1-oxo-1-(((S)-1-oxo-1-(2-(phenylsulfonyl)ethoxy)propan-2-yl)amino)propan-2-yl)oxy)tetrahydro-2H-pyran-3-yl)oxy)-2-(acetoxymethyl)tetrahydro-2H-pyran-3,4-diyl diacetate



2.87

2.108 (10 mg, 0.0091 mmol) was dissolved in 0.5 mL dry DCM under Ar and added to a vigorously stirred solution of dibenzyl *N*,*N*-diisopropylphosphoramidite (9.7 µl, 0.027 mmol) and 5-ETT (5.33mg, 0.041 mmol) in 0.5 mL dry DCM under Ar. The reaction was left to stir for 4 hrs after which time it was diluted with 10 mL DCM, washed with 1 x 10 mL sat. $NaHCO_3$ sol. And washed with 1 x 10 mL H_2O. The organic layer was dried over anhydrous Na_2SO_4, concentrated *in vacuo,* and dried on high vac. overnight. The solid was redissolved in 1.5 mL THF and cooled to -78 °C. 30% H_2O_2 solution (1.5 mL) was added dropwise, the reaction warmed to ambient temperature and stirred for 3 hrs. The reaction was quenched with sat. ice cold sodium sulfite and diluted with 10 mL EtOAc. The organic layer was washed with 1 x 7 mL sat. $NaHCO_3$ sol., 1 x 7 mL brine, dried over anhydrous Na_2SO_4 and concentrated *in vacuo.* Purification via flash column chromatography (SiO_2, gradient 85:15 DCM:acetone to 70:30 DCM:acetone) yielded **2.87** (4.0 mg, 26%). ^{1}H NMR (400 MHz, $CDCl_3$) δ 7.89 – 7.86 (m, 2H, Ar-**H**), 7.73 (dd, *J* = 6.9, 2.6 Hz, 2H, Ar-**H**), 7.66 – 7.58 (m, 3H, Ar-**H**), 7.58 – 7.49 (m, 5H, Ar-**H**), 7.49 – 7.35 (m, 4H, Ar-**H** + MurNAc-N**H**), 7.29 (s, 5H, Ar-**H**), 7.25 – 7.20 (m, 5H, Ar-**H**), 7.11 (d, *J* = 7.7 Hz, 1H, Ala1-N**H**), 6.09 (dd, *J* = 5.3, 3.2 Hz, 1H, MurNAc-**H1**), 5.06 – 4.91 (m, 5H, POBn-C**H₂** + GlcNAc-**H4**), 4.76 (dd, *J* = 10.8, 9.3 Hz, 1H, GlcNAc-**H3**), 4.59 (d, *J* = 9.7 Hz, 1H, GlcNAc-N**H**), 4.49 (q, *J* = 6.7 Hz, 1H, MurNAc-**Hα**), 4.40 – 4.25 (m, 5H, OC**H₂** + Ala1-**Hα** + GlcNAc-H1 + GlcNAc-**H6**), 4.16 (t, *J* = 9.6 Hz, 1H, MurNAc-**H4**), 4.03 – 3.89 (m, 3H, MurNAc-**H2** + GlcNAc-**H2** + GlcNAc-**H6'**), 3.77 – 3.66 (m, 2H, MurNAc-**H5** + MurNAc-**H6**), 3.52 (dd, *J* = 10.9, 9.2 Hz, 1H, MurNAc-**H3**), 3.43 – 3.31 (m, 4H, SC**H₂** + GlcNAc-**H5** + MurNAc-**H6'**), 2.04 (s, 3H, Ac-**H**), 2.02 (s, 3H, Ac-**H**), 1.99 (s, 3H, Ac-**H**), 1.85 (s, 3H, Ac-**H**), 1.60 (s, 3H, GlcNAc-NH**Ac**), 1.37 (d, *J* = 6.7 Hz, 3H, MurNAc-**Hβ**), 1.30 (d, *J* = 7.2 Hz, 3H, Ala-**Hβ**), 1.10 (s, 9H, ^{t}Bu-**H**). ^{13}C NMR (101 MHz, $CDCl_3$) δ 174.71, 171.75, 171.31, 170.94, 170.70, 170.27, 169.52, 139.29, 136.10, 135.86, 135.84, 134.14, 133.68, 132.00, 130.62, 130.33, 129.54, 128.78, 128.69, 128.58, 128.47, 128.28, 128.11, 128.01, 127.97, 99.83, 74.67, 74.43, 73.24, 72.59, 71.66, 69.61, 69.55, 69.43, 69. 36, 68.21, 61.60, 61.07, 58.36, 54.97, 54.26, 48.08, 29.84, 27.13, 23.14, 23.08, 20.80, 20.75, 19.39, 18.97, 17.38. ^{31}P NMR (162 MHz, $CDCl_3$) δ -2.87. $[\alpha]_D^{25}$ = (g/100 mL, MeOH). HRMS (ESI) Calcd for $C_{66}H_{83}N_3O_{22}PSSi^+$ [M+H] = 1360.4691 found 1360.4700. IR (Transmittance) 3320, 2925, 1752, 1665, 1540, 1449, 1429, 1374, 1321, 1308, 1234, 1145, 1113, 1087, 1044, 919, 878. 824, 791, 740, 704, 604, cm^{-1}

(2R,3S,4R,5R,6S)-5-acetamido-6-(((2R,3S,4R,5R,6R)-5-acetamido-6-((bis(benzyloxy)phosphoryl)oxy)-2-(((tert-butyldiphenylsilyl)oxy)methyl)-4-(((4R,7R,15R,18S,21R)-15-(methoxycarbonyl)-4,7,18-trimethyl-3,6,9,12,17,20-hexaoxo-10-(4-(2,2,2-trifluoroacetamido)butyl)-2-oxa-5,8,11,16,19-pentaazadocosan-21-yl)oxy)tetrahydro-2H-pyran-3-yl)oxy)-2-(acetoxymethyl)tetrahydro-2H-pyran-3,4-diyl diacetate



2.86

2.87 (10.0 mg, 0.00735 mmol) was dissolved in 0.4 mL dry DCM under Ar. DBU (1.1 µl, 0.00735 mmol) was added and the reaction left to stir for 2 hrs. After this time DBU (1.1 µl, 0.00735 mmol) was added and the solution left to stir for 1hr. The reaction was diluted with 15 mL DCM and washed with 7 mL 1.0M HCl and 7 mL sat. $NaHCO_3$ sol. Both aqueous layers were back extracted with 1 x 7 mL DCM. The combined organic layers were dried over anhydrous Na_2SO_4, concentrated *in vacuo*, and dried on high vac. overnight. The resultant solid and HATU (2.79 mg, 0.00735 mmol) were dissolved in 1.0 mL dry DMF under Ar. The solution was cooled to 0 ^oC and DIPEA (1.92 µl, 0.011 mmol) was added dropwise. The reaction was left to stir for 45 mins, during this time **2.105** (7.06 mg, 0.011 mmol) was dissolved in 4.0M HCl in dioxane (1.0 mL) under Ar and left to stir for 30 mins. The reaction was concentrated under nitrogen stream and the solid redissolved in 1.0 mL dry DCM under Ar. The solution was pre-neutralised with DIPEA (2.56 µl, 0.0147 mmol) and added to the activated acid. The reaction was warmed to ambient temperature and left to stir for 2 h. The solution was concentrated *in vacuo*, redissolved in 10 mL EtOAc, washed with 1 x 5 mL 1.0M HCl, 1 x 5 mL sat. $NaHCO_3$ sol. Both aqueous layers were back extracted with 1 x 5 mL EtOAc. The combined organic layers were washed with 1 x 10 mL brine, dried over anhydrous Na_2SO_4 and concentrated *in vacuo*. Purification via flash column chromatography (SiO_2, gradient 97:3 DCM:MeOH to 95:5 DCM:MeOH) yielded **2.86** (7.4 mg, 58%). ^1H NMR (601 MHz, $CDCl_3$) δ 7.73 (dd, *J* = 6.3, 2.4 Hz, 3H, Ar-**H** + 2xN**H**), 7.66 – 7.51 (m, 5H, Ar-**H**), 7.43 (dq, *J* = 30.3, 7.5 Hz, 4H, Ar-**H**), 7.31 (d, *J* = 11.7 Hz, 6H, Ar-**H**), 7.24 – 7.07 (m, 7H, Ar-**H** + 2xN**H** + N**H**TFA + Glu-N**H**), 5.79 (d, *J* = 4.5 Hz, 1H, MurNAc-**H1**), 5.12 – 4.98 (m, 4H, POBn-C**H₂**), 4.94 (t, *J* = 9.6 Hz, 1H,

GlcNAc-**H4**), 4.67 (t, *J* = 10.1 Hz, 1H, GlcNAc-**H3**), 4.61 – 4.21 (m, 11H, MurNAc-**H2** + GlcNAc-**H1** + GlcNAc-**H6** + MurNAc-$\mathbf{H_\alpha}$ + Ala1-$\mathbf{H_\alpha}$ + Glu2-$\mathbf{H_\alpha}$ + Lys3-$\mathbf{H_\alpha}$ + Ala4-$\mathbf{H_\alpha}$ + Ala5-$\mathbf{H_\alpha}$ + GlcNAc-N**H** + MurNAc-N**H**), 4.14 (t, *J* = 9.5 Hz, 1H, MurNAc-**H4**), 4.02 (d, *J* = 12.2 Hz, 1H, GlcNAc-**H6**), 3.94 (t, *J* = 9.2 Hz, 1H, GlcNAc-**H2**), 3.81 – 3.60 (m, 8H, MurNAc-**H5** + MurNAc-**H6** + Glu-CO_2Me-**H** + Ala-CO_2Me-**H**), 3.54 (t, *J* = 10.0 Hz, 1H, MurNAc-**H3**), 3.42 – 3.21 (m, 5H, GlcNAc-**H5** + MurNAc-**H3** + MurNAc-**H6** + Lys3-$\mathbf{H_\varepsilon}$), 2.04 (d, *J* = 4.5 Hz, 6H, OAc-**H**), 2.00 – 1.98 (m, 3H, OAc-**H**), 1.85 – 1.78 (m, 2H, Lys3-$\mathbf{H_\delta}$), 1.64 (ddt, *J* = 34.8, 14.4, 7.2 Hz, 2H, Lys3-$\mathbf{H_\gamma}$), 1.54 – 1.45 (m, 2H, Lys3-$\mathbf{H_\beta}$), 1.45 – 1.33 (m, 12H, + MurNAc-$\mathbf{H_\beta}$ + Ala1-$\mathbf{H_\beta}$ + Ala4-$\mathbf{H_\beta}$ + Ala5-$\mathbf{H_\beta}$), 1.25 (s, 4H, Glu2-$\mathbf{H_\beta}$ + Glu2-$\mathbf{H_\gamma}$), 1.12 (s, 9H, TBDPS-^{t}Bu-**H**). ^{13}C NMR (151 MHz, $CDCl_3$) δ 171.80, 170.54, 169.51, 135.96, 135.71, 133.42, 131.63, 130.67, 130.30, 128.90 – 128.33 (m), 128.06, 127.84, 99.88, 72.68 (d, *J* = 17.5 Hz), 71.45, 69.48, 68.10, 61.46, 60.50, 53.81, 53.46, 52.41 (d, *J* = 12.2 Hz), 51.90, 50.92, 49.01, 48.10, 39.19, 31.95, 31.68, 29.70 (d, *J* = 6.7 Hz), 28.35, 27.01, 22.92, 22.78, 22.72, 22.59, 20.66 (d, *J* = 4.6 Hz), 20.54, 19.39, 19.20, 17.88, 17.59, 14.15. $[\alpha]_D^{25}$ = + 16.00 (0.1 g/100 mL, MeOH). HRMS (ESI) Calc'd for $C_{79}H_{107}F_3N_8O_{27}PSi^+$ [M+H] = 1715.6700 found 1715.6708. IR (Transmittance) 3409, 3197, 2367, 2186, 1752, 1656, 1557, 1373, 1218, 1164, 1114, 1057, 1033, 1012, 956, 736, 703, 602 cm^{-1}

References

(1) Mohammadi, T.; Van Dam, V.; Sijbrandi, R.; Vernet, T.; Zapun, A.; Bouhss, A.; Diepeveen-de Bruin, M.; Nguyen-Distèche, M.; De Kruijff, B.; Breukink, E. Identification of FtsW as a transporter of lipid-linked cell wall precursors across the membrane. *The EMBO Journal* **2011**, *30* (8), 1425-1432.
(2) Kuk, A. C.; Mashalidis, E. H.; Lee, S.-Y. Crystal structure of the MOP flippase MurJ in an inward-facing conformation. *Nature Structural & Molecular Biology* **2017**, *24* (2), 171-176.
(3) Zheng, S.; Sham, L.-T.; Rubino, F. A.; Brock, K. P.; Robins, W. P.; Mekalanos, J. J.; Marks, D. S.; Bernhardt, T. G.; Kruse, A. C. Structure and mutagenic analysis of the lipid II flippase MurJ from Escherichia coli. *Proceedings of the National Academy of Sciences* **2018**, *115* (26), 6709-6714.
(4) Kuk, A. C.; Hao, A.; Lee, S.-Y. Structure and mechanism of the lipid flippase MurJ. *Annual Review of Biochemistry* **2022**, *91* (1), 705-729.
(5) Schwartz, B.; Markwalder, J. A.; Wang, Y. Lipid II: Total Synthesis of the Bacterial Cell Wall Precursor and Utilization as a Substrate for Glycosyltransfer and Transpeptidation by Penicillin Binding Protein (PBP) 1b of Eschericia c oli. *Journal of the American Chemical Society* **2001**, *123* (47), 11638-11643.
(6) Enugala, R.; Carvalho, L. C.; Dias Pires, M. J.; Marques, M. M. B. Stereoselective Glycosylation of Glucosamine: The Role of the N-Protecting Group. *Chemistry–An Asian Journal* **2012**, *7* (11), 2482-2501.
(7) VanNieuwenhze, M. S.; Mauldin, S. C.; Zia-Ebrahimi, M.; Winger, B. E.; Hornback, W. J.; Saha, S. L.; Aikins, J. A.; Blaszczak, L. C. The first total synthesis of lipid II: the final monomeric intermediate in bacterial cell wall biosynthesis. *Journal of the American Chemical Society* **2002**, *124* (14), 3656-3660.
(8) Saha, S. L.; Van Nieuwenhze, M. S.; Hornback, W. J.; Aikins, J. A.; Blaszczak, L. C. Synthesis of an orthogonally protected precursor to the glycan repeating unit of the bacterial cell wall. *Organic Letters* **2001**, *3* (22), 3575-3577.
(9) Karak, M.; Cloonan, C. R.; Baker, B. R.; Cochrane, R. V.; Cochrane, S. A. Optimizations of lipid II synthesis: an essential glycolipid precursor in bacterial cell wall synthesis and a validated antibiotic target. *Beilstein Journal of Organic Chemistry* **2024**, *20* (1), 220-227.
(10) Termin, A.; Schmidt, R. R. Glycosylimidates, 54. Synthesis of the GlcNAcβ (1→ 4) MurNAcβ (1→ 4) GlcNAcβ (1→ 4) MurNAc tetrasaccharide of bacterial peptidoglycan. *Liebigs Annalen der Chemie* **1992**, *1992* (5), 527-533.
(11) Zhang, Z.; Ollmann, I. R.; Ye, X.-S.; Wischnat, R.; Baasov, T.; Wong, C.-H. Programmable one-pot oligosaccharide synthesis. *Journal of the American Chemical Society* **1999**, *121* (4), 734-753.
(12) Liu, H.; Wong, C.-H. Characterization of a transglycosylase domain of Streptococcus pneumoniae PBP1b. *Bioorganic & Medicinal Chemistry* **2006**, *14* (21), 7187-7195.
(13) Shih, H.-W.; Chen, K.-T.; Cheng, T.-J. R.; Wong, C.-H.; Cheng, W.-C. A new synthetic approach toward bacterial transglycosylase substrates, Lipid II and Lipid IV. *Organic Letters* **2011**, *13* (17), 4600-4603.
(14) Shih, H. W.; Chang, Y. F.; Li, W. J.; Meng, F. C.; Huang, C. Y.; Ma, C.; Cheng, T. J. R.; Wong, C. H.; Cheng, W. C. Effect of the peptide moiety of lipid II on bacterial transglycosylase. *Angewandte Chemie International Edition* **2012**, *40* (51), 10123-10126.
(15) Wang, X.; Krasnova, L.; Wu, K. B.; Wu, W.-S.; Cheng, T.-J.; Wong, C.-H. Towards new antibiotics targeting bacterial transglycosylase: Synthesis of a Lipid II analog as stable transition-state mimic inhibitor. *Bioorganic & Medicinal Chemistry Letters* **2018**, *28* (16), 2708-2712.
(16) Chen, K.-T.; Lin, C.-K.; Guo, C.-W.; Chang, Y.-F.; Hu, C.-M.; Lin, H.-H.; Lai, Y.; Cheng, T.-J. R.; Cheng, W.-C. Effect of the lipid II sugar moiety on bacterial transglycosylase: the 4-hydroxy epimer of lipid II is a TGase inhibitor. *Chemical Communications* **2017**, *53* (4), 771-774.
(17) Mitachi, K.; Mohan, P.; Siricilla, S.; Kurosu, M. One-Pot Protection-Glycosylation Reactions for Synthesis of Lipid II Analogues. *Chemistry–A European Journal* **2014**, *20* (16), 4554-4558.

(18) Bakhtiary, A.; Cochrane, S. A.; Mercier, P.; McKay, R. T.; Miskolzie, M.; Sit, C. S.; Vederas, J. C. Insights into the mechanism of action of the two-peptide lantibiotic lacticin 3147. *Journal of the American Chemical Society* **2017**, *139* (49), 17803-17810.
(19) Cochrane, S. A.; Findlay, B.; Bakhtiary, A.; Acedo, J. Z.; Rodriguez-Lopez, E. M.; Mercier, P.; Vederas, J. C. Antimicrobial lipopeptide tridecaptin A1 selectively binds to Gram-negative lipid II. *Proceedings of the National Academy of Sciences* **2016**, *113* (41), 11561-11566.
(20) Dong, Y. Y.; Wang, H.; Pike, A. C.; Cochrane, S. A.; Hamedzadeh, S.; Wyszyński, F. J.; Bushell, S. R.; Royer, S. F.; Widdick, D. A.; Sajid, A. Structures of DPAGT1 explain glycosylation disease mechanisms and advance TB antibiotic design. *Cell* **2018**, *175* (4), 1045-1058. e1016.
(21) Huang, S.-H.; Wu, W.-S.; Huang, L.-Y.; Huang, W.-F.; Fu, W.-C.; Chen, P.-T.; Fang, J.-M.; Cheng, W.-C.; Cheng, T.-J. R.; Wong, C.-H. New continuous fluorometric assay for bacterial transglycosylase using Forster resonance energy transfer. *Journal of the American Chemical Society* **2013**, *135* (45), 17078-17089.
(22) Liu, C.-Y.; Guo, C.-W.; Chang, Y.-F.; Wang, J.-T.; Shih, H.-W.; Hsu, Y.-F.; Chen, C.-W.; Chen, S.-K.; Wang, Y.-C.; Cheng, T.-J. R. Synthesis and evaluation of a new fluorescent transglycosylase substrate: lipid II-based molecule possessing a dansyl-C20 polyprenyl moiety. *Organic Letters* **2010**, *12* (7), 1608-1611.
(23) Dumbre, S.; Derouaux, A.; Lescrinier, E.; Piette, A.; Joris, B.; Terrak, M.; Herdewijn, P. Synthesis of modified peptidoglycan precursor analogues for the inhibition of glycosyltransferase. *Journal of the American Chemical Society* **2012**, *134* (22), 9343-9351.
(24) Lin, C. K.; Chen, K. T.; Hu, C. M.; Yun, W. Y.; Cheng, W. C. Synthesis of 1-C-Glycoside-Linked Lipid II Analogues Toward Bacterial Transglycosylase Inhibition. *Chemistry–A European Journal* **2015**, *21* (20), 7511-7519.
(25) Ding, H.; Lyu, J.; Zhang, X.-L.; Xiao, X.; Liu, X.-W. Efficient and versatile formation of glycosidic bonds via catalytic strain-release glycosylation with glycosyl ortho− 2, 2-dimethoxycarbonylcyclopropylbenzoate donors. *Nature Communications* **2023**, *14* (1), 4010.
(26) Zhang, Y.; Fechter, E. J.; Wang, T.-S. A.; Barrett, D.; Walker, S.; Kahne, D. E. Synthesis of heptaprenyl− Lipid IV to analyze peptidoglycan glycosyltransferases. *Journal of the American Chemical Society* **2007**, *129* (11), 3080-3081.
(27) Gampe, C. M.; Tsukamoto, H.; Wang, T.-S. A.; Walker, S.; Kahne, D. Modular synthesis of diphospholipid oligosaccharide fragments of the bacterial cell wall and their use to study the mechanism of moenomycin and other antibiotics. *Tetrahedron* **2011**, *67* (51), 9771-9778.
(28) Katsuyama, A.; Sato, K.; Yakushiji, F.; Matsumaru, T.; Ichikawa, S. Solid-phase modular synthesis of park nucleotide and lipids I and II analogues. *Chemical and Pharmaceutical Bulletin* **2018**, *66* (1), 84-95.
(29) Katsuyama, A.; Yakushiji, F.; Ichikawa, S. Solid-phase synthesis of fluorescent analogues of Park's nucleotide, lipid I and lipid II. *Tetrahedron Letters* **2021**, *73*, 153101.
(30) Men, H.; Park, P.; Ge, M.; Walker, S. Substrate synthesis and activity assay for MurG. *Journal of the American Chemical Society* **1998**, *120* (10), 2484-2485.
(31) Ye, X.-Y.; Lo, M.-C.; Brunner, L.; Walker, D.; Kahne, D.; Walker, S. Better substrates for bacterial transglycosylases. *Journal of the American Chemical Society* **2001**, *123* (13), 3155-3156.
(32) Lebar, M. D.; May, J. M.; Meeske, A. J.; Leiman, S. A.; Lupoli, T. J.; Tsukamoto, H.; Losick, R.; Rudner, D. Z.; Walker, S.; Kahne, D. Reconstitution of peptidoglycan cross-linking leads to improved fluorescent probes of cell wall synthesis. *Journal of the American Chemical Society* **2014**, *136* (31), 10874-10877.
(33) Wingen, L. M.; Rausch, M.; Schneider, T.; Menche, D. Modular Total Synthesis of Farnesyl Analogues of Cell Wall Precursors Lipid I and II Containing the Staphylococcus aureus Pentaglycine Bridge Modification. *The Journal of Organic Chemistry* **2020**, *85* (15), 10206-10215.
(34) Wingen, L. M.; Braun, C.; Rausch, M.; Gross, H.; Schneider, T.; Menche, D. Versatile synthesis of pathogen specific bacterial cell wall building blocks. *Rsc Advances* **2022**, *12* (24), 15046-15069.

(35) Lebar, M. D.; Lupoli, T. J.; Tsukamoto, H.; May, J. M.; Walker, S.; Kahne, D. Forming cross-linked peptidoglycan from synthetic gram-negative Lipid II. *Journal of the American Chemical Society* **2013**, *135* (12), 4632-4635.
(36) Breukink, E.; van Heusden, H. E.; Vollmerhaus, P. J.; Swiezewska, E.; Brunner, L.; Walker, S.; Heck, A. J.; de Kruijff, B. Lipid II is an intrinsic component of the pore induced by nisin in bacterial membranes. *Journal of Biological Chemistry* **2003**, *278* (22), 19898-19903.
(37) Chen, K. T.; Kuan, Y. C.; Fu, W. C.; Liang, P. H.; Cheng, T. J. R.; Wong, C. H.; Cheng, W. C. Rapid Preparation of Mycobacterium N-Glycolyl Lipid I and Lipid II Derivatives: A Biocatalytic Approach. *Chemistry–A European Journal* **2013**, *19* (3), 834-838.
(38) Mitachi, K.; Yun, H. G.; Gillman, C. D.; Skorupinska-Tudek, K.; Swiezewska, E.; Clemons Jr, W. M.; Kurosu, M. Substrate tolerance of bacterial glycosyltransferase MurG: Novel fluorescence-based assays. *ACS Infectious Diseases* **2019**, *6* (6), 1501-1516.
(39) Huang, L. Y.; Huang, S. H.; Chang, Y. C.; Cheng, W. C.; Cheng, T. J. R.; Wong, C. H. Enzymatic synthesis of lipid II and analogues. *Angewandte Chemie* **2014**, *126* (31), 8198-8203.
(40) Mahapatra, S.; Yagi, T.; Belisle, J. T.; Espinosa, B. J.; Hill, P. J.; McNeil, M. R.; Brennan, P. J.; Crick, D. C. Mycobacterial lipid II is composed of a complex mixture of modified muramyl and peptide moieties linked to decaprenyl phosphate. *Journal of Bacteriology* **2005**, *187* (8), 2747-2757.
(41) Mahapatra, S.; Crick, D. C.; Brennan, P. J. Comparison of the UDP-N-acetylmuramate: L-alanine ligase enzymes from Mycobacterium tuberculosis and Mycobacterium leprae. *Journal of Bacteriology* **2000**, *182* (23), 6827-6830.
(42) Reddy, S. G.; Waddell, S. T.; Kuo, D. W.; Wong, K. K.; Pompliano, D. L. Preparative enzymatic synthesis and characterization of the cytoplasmic intermediates of murein biosynthesis. *Journal of the American Chemical Society* **1999**, *121* (6), 1175-1178.
(43) Yagi, T.; Mahapatra, S.; Mikušová, K. n.; Crick, D. C.; Brennan, P. J. Polymerization of mycobacterial arabinogalactan and ligation to peptidoglycan. *Journal of Biological Chemistry* **2003**, *278* (29), 26497-26504.
(44) Patrick, G. L. *An Introduction to Medicinal Chemistry*; Oxford university press, 2023.
(45) Auger, G.; van Heijenoort, J.; Mengin-Lecreulx, D.; Blanot, D. A MurG assay which utilises a synthetic analogue of lipid I. *FEMS Microbiology Letters* **2003**, *219* (1), 115-119.
(46) Chandrakala, B.; Elias, B. C.; Mehra, U.; Umapathy, N.; Dwarakanath, P.; Balganesh, T.; deSousa, S. M. Novel scintillation proximity assay for measuring membrane-associated steps of peptidoglycan biosynthesis in Escherichia coli. *Antimicrobial Agents and Chemotherapy* **2001**, *45* (3), 768-775.
(47) Ramachandran, V.; Chandrakala, B.; Kumar, V. P.; Usha, V.; Solapure, S. M.; de Sousa, S. M. Screen for inhibitors of the coupled transglycosylase-transpeptidase of peptidoglycan biosynthesis in Escherichia coli. *Antimicrobial Agents and Chemotherapy* **2006**, *50* (4), 1425-1432.
(48) Perlstein, D. L.; Zhang, Y.; Wang, T.-S.; Kahne, D. E.; Walker, S. The direction of glycan chain elongation by peptidoglycan glycosyltransferases. *Journal of the American Chemical Society* **2007**, *129* (42), 12674-12675.
(49) Wiedemann, I.; Böttiger, T.; Bonelli, R. R.; Schneider, T.; Sahl, H.-G.; Martínez, B. Lipid II-based antimicrobial activity of the lantibiotic plantaricin C. *Applied and Environmental Microbiology* **2006**, *72* (4), 2809-2814.
(50) Schaefer, K.; Matano, L. M.; Qiao, Y.; Kahne, D.; Walker, S. In vitro reconstitution demonstrates the cell wall ligase activity of LCP proteins. *Nature Chemical Biology* **2017**, *13* (4), 396-401.
(51) Barrett, D.; Wang, T.-S. A.; Yuan, Y.; Zhang, Y.; Kahne, D.; Walker, S. Analysis of glycan polymers produced by peptidoglycan glycosyltransferases. *Journal of Biological Chemistry* **2007**, *282* (44), 31964-31971.
(52) Koatale, P. C.; Welling, M. M.; Ndlovu, H.; Kgatle, M.; Mdanda, S.; Mdlophane, A.; Okem, A.; Takyi-Williams, J.; Sathekge, M. M.; Ebenhan, T. Insights into Peptidoglycan-Targeting Radiotracers for Imaging Bacterial Infections: Updates, Challenges, and Future Perspectives. *ACS Infectious Diseases* **2024**, *10* (2), 270-286.

(53) Plante, O. J.; Andrade, R. B.; Seeberger, P. H. Synthesis and use of glycosyl phosphates as glycosyl donors. *Organic Letters* **1999**, *1* (2), 211-214.
(54) Zhang, X.-L.; Báti, G.; Li, C.; Guo, A.; Yeo, C.; Ding, H.; Pal, K. B.; Xu, Y.; Qiao, Y.; Liu, X.-W. GlcNAc-1, 6-anhydro-MurNAc moiety affords unusual glycosyl acceptor that terminates peptidoglycan elongation. *Journal of the American Chemical Society* **2024**, *146* (11), 7400-7407.
(55) Hesek, D.; Lee, M.; Zhang, W.; Noll, B. C.; Mobashery, S. Total synthesis of N-acetylglucosamine-1, 6-anhydro-N-acetylmuramylpentapeptide and evaluation of its turnover by AmpD from Escherichia coli. *Journal of the American Chemical Society* **2009**, *131* (14), 5187-5193.
(56) Kawasaki, A.; Karasudani, Y.; Otsuka, Y.; Hasegawa, M.; Inohara, N.; Fujimoto, Y.; Fukase, K. Synthesis of diaminopimelic acid containing peptidoglycan fragments and tracheal cytotoxin (TCT) and investigation of their biological functions. *Chemistry–A European Journal* **2008**, *14* (33), 10318-10330.
(57) Lee, M.; Hesek, D.; Dik, D. A.; Fishovitz, J.; Lastochkin, E.; Boggess, B.; Fisher, J. F.; Mobashery, S. From genome to proteome to elucidation of reactions for all eleven known lytic transglycosylases from Pseudomonas aeruginosa. *Angewandte Chemie International Edition* **2017**, *56* (10), 2735-2739.
(58) Paulsen, H.; Himpkamp, P.; Peters, T. Bausteine von Oligosacchariden, LXIX. Synthese von 1, 6-Anhydromuramylpeptiden. *Liebigs Annalen der Chemie* **1986**, *1986* (4), 664-674.
(59) Wang, Q.; Matsuo, Y.; Pradipta, A. R.; Inohara, N.; Fujimoto, Y.; Fukase, K. Synthesis of characteristic Mycobacterium peptidoglycan (PGN) fragments utilizing with chemoenzymatic preparation of meso-diaminopimelic acid (DAP), and their modulation of innate immune responses. *Organic & Biomolecular Chemistry* **2016**, *14* (3), 1013-1023.
(60) Brewster, P.; Hiron, F.; Hughes, E.; Ingold, C.; Rao, P. Configuration of carbohydrates, hydroxy-acids and amino-acids: configurations of amino-compounds and the steric course of deamination. *Nature* **1950**, *166* (4213), 179-180.
(61) Cowdrey, W.; Hughes, E.; Ingold, C.; Masterman, S.; Scott, A. 257. Reaction kinetics and the Walden inversion. Part VI. Relation of steric orientation to mechanism in substitutions involving halogen atoms and simple or substituted hydroxyl groups. *Journal of the Chemical Society (Resumed)* **1937**, 1252-1271.
(62) Matsushima, Y.; Park, J. T. Stereospecific Synthesis of 2-Amino-3-O-(D-1'-carboxyethyl)-2-deoxy-D-glucose (Muramic Acid) and Related Compounds1, 2. *The Journal of Organic Chemistry* **1962**, *27* (10), 3581-3583.
(63) Wang, T.; Demchenko, A. V. Synthesis of carbohydrate building blocks via regioselective uniform protection/deprotection strategies. *Organic & Biomolecular Chemistry* **2019**, *17* (20), 4934-4950.
(64) DeNinno, M. P.; Etienne, J. B.; Duplantier, K. C. A method for the selective reduction of carbohydrate 4, 6-O-benzylidene acetals. *Tetrahedron Letters* **1995**, *36* (5), 669-672.
(65) Walczewska, A.; Grzywacz, D.; Bednarczyk, D.; Dawgul, M.; Nowacki, A.; Kamysz, W.; Liberek, B.; Myszka, H. N-Alkyl derivatives of diosgenyl 2-amino-2-deoxy-β-D-glucopyranoside; synthesis and antimicrobial activity. *Beilstein Journal of Organic Chemistry* **2015**, *11* (1), 869-874.
(66) Boullanger, P.; Jouineau, M.; Bouammali, B.; Lafont, D.; Descotes, G. The use of N-alkoxycarbonyl derivatives of 2-amino-2-deoxy-D-glucose as donors in glycosylation reactions. *Carbohydrate Research* **1990**, *202*, 151-164.
(67) Takaku, H.; Ishida, H.-k.; Fujita, M.; Inazu, T.; Ishida, H.; Kiso, M. A Chemical Synthesis of GlcNAcβ (1→ 4) GlcUA-UDP to Elucidate the Catalytic Mechanism of Hyaluronic Acid Synthases (HAS). *Synlett* **2007**, *2007* (05), 0818-0820.
(68) van de Vrande, K. N.; Filippov, D. V.; Codée, J. D. Formation of Glycosyl Trichloroacetamides from Trichloroacetimidate Donors Occurs through an Intermolecular Aglycon Transfer Reaction. *Organic Letters* **2023**, *25* (33), 6128-6132.
(69) Cochrane, R. V.; Alexander, F. M.; Boland, C.; Fetics, S. K.; Caffrey, M.; Cochrane, S. A. From plant to probe: semi-synthesis of labelled undecaprenol analogues allows rapid access to probes for antibiotic targets. *Chemical Communications* **2020**, *56* (61), 8603-8606.
(70) Khidyrova, N.; Shakhidoyatov, K. M. Plant polyprenols and their biological activity. *Chemistry of natural compounds* **2002**, *38*, 107-121.

(71) Swiezewska, E.; Sasak, W.; Mankowski, T.; Jankowski, W.; Vogtman, T.; Krajewska, I.; Hertel, J.; Skoczylas, E.; Chojnacki, T. The search for plant polyprenols. *Acta Biochimica Polonica* **1994**, *41* (3).
(72) Ghosh, B.; Kulkarni, S. S. Common protection–deprotection strategies in carbohydrate synthesis. *Synthetic Strategies in Carbohydrate Chemistry*, Elsevier, 2024; pp 273-295.
(73) Baek, S.; Jo, H.; Kim, H.; Kim, H.; Kim, S.; Kim, D. Highly stereoselective and efficient total synthesis of (+)-laurencin. *Organic Letters* **2005**, *7* (1), 75-77.
(74) Ikemoto, N.; Schreiber, S. L. Total synthesis of (-)-hikizimycin employing the strategy of two-directional chain synthesis. *Journal of the American Chemical Society* **1992**, *114* (7), 2524-2536.
(75) Ochiai, M.; Ito, T.; Takahashi, H.; Nakanishi, A.; Toyonari, M.; Sueda, T.; Goto, S.; Shiro, M. Hypervalent (tert-butylperoxy) iodanes generate iodine-centered radicals at room temperature in solution: Oxidation and deprotection of benzyl and allyl ethers, and evidence for generation of α-oxy carbon radicals. *Journal of the American Chemical Society* **1996**, *118* (33), 7716-7730.
(76) Kim, H. M.; Kim, I. J.; Danishefsky, S. J. Total syntheses of tumor-related antigens N3: probing the feasibility limits of the glycal assembly method. *Journal of the American Chemical Society* **2001**, *123* (1), 35-48.
(77) Rudd, T.; Skidmore, M. A.; Yates, E. A. Surface-Based Studies of Heparin/Heparan Sulfate-Protein Interactions: Considerations for Surface Immobilisation of HS/Heparin Saccharides and Monitoring Their Interactions with Binding Proteins. *Chemistry and Biology of Heparin and Heparan Sulfate*, Elsevier, 2005; pp 345-366.
(78) Liu, C.; Mariano, P. S. An improved method for the large scale preparation of α, α'-trehalose-6-phosphate. *Tetrahedron Letters* **2015**, *56* (23), 3008-3010.

Chapter 3 – Efforts Towards the Synthesis of Light Inducible Peptidoglycan Probes

Introduction

Peptidoglycans are proposed to be immunogenic through recognition by the TLR2 like receptors of the human innate immune system with crosslinking properties possibly being a contributing factor to recognition [1]. The advent of new stereoretentive radical chemistry within our group [2] has led to our interest in its application in the production of light inducible peptidoglycan probes. Peptidoglycan degradation products are under investigation for use as immune system adjuvants due to immunostimulatory properties resulting from recognition by another class of immune receptors, NOD2 [3]. We recognise that this chemistry offers potential to generate such medicines with the extended benefit of spatial and temporal control over their action (Fig. 3.1).

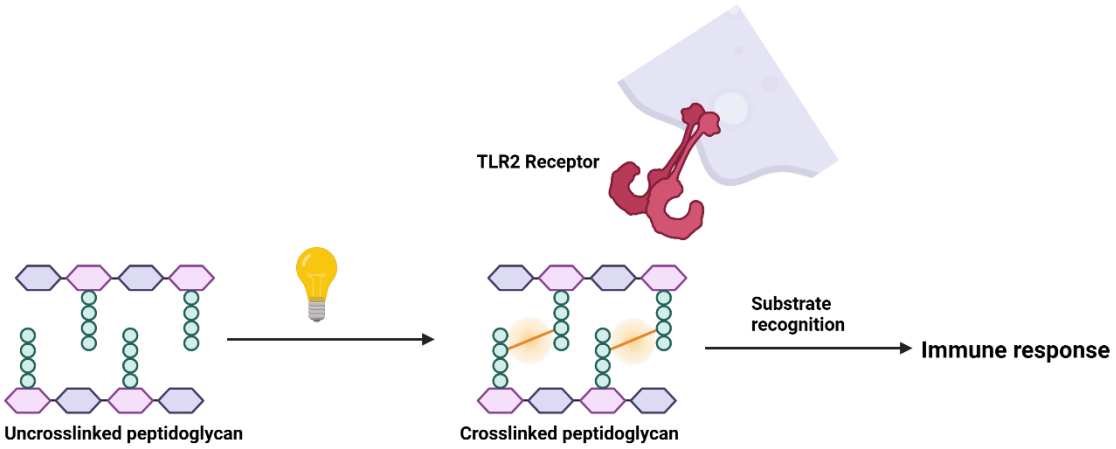


Figure 3.1 – Light inducible crosslinking of peptidoglycan substrates for TLR2 recognition

Previous Approaches to Accessing Peptidoglycan Fragments

Access to peptidoglycan products has seen variation around assembly of the oligosaccharide backbone, with groups reporting synthesis of fragments from different building blocks. Differences in building blocks typically arise regarding the size i.e. monosaccharide vs disaccharide, as well as the nature of functionalisation for glycosylation, as was discussed for Lipid II syntheses in chapter 2. Additionally, like Lipid II synthesis the introduction of solid phase methodology has been reported recently and has provided an alternative to more classical solution phase approaches. The following sections will discuss important developments in solution phase and solid phase methodology separately, as well as their applications to access desirable crosslinked structures.

Solution Phase Strategies

Bottom-Up Synthesis

Access to the oligomeric backbone of peptidoglycan was reported by Schmidt in 1992 [4] (Fig. 3.2), making use of the groups trichloroacetamide donors. The group condensed monosaccharide building blocks into disaccharides. Similar condensation allowed for easy access to tetrasaccharides in just two glycosylation steps. The monosaccharide blocks were equipped with the azide at C2 due to anchimeric assistance providing the desired β stereochemistry [5]. Donor **3.1** was equipped with the 4-OAllyl protecting group such that orthogonal reductive cleavage could be carried out following glycosylation to **3.4** to give acceptor **3.6.** Acceptor **3.2** was equipped with an anomeric silyl ether which could be orthogonally unmasked with fluoride following glycosylation with donor **3.3** and converted into a glycosyl imidate donor **3.7** through base mediated nucleophilic addition to trichloroacetonitrile. Disaccharide acceptor **3.6** and donor **3.7** could be reacted under the same glycosylation conditions to yield protected tetramer **3.8**. Desilylation and catalytic hydrogenation in the presence of acetic acid allowed for global unmasking bar the lactate giving **3.9**.

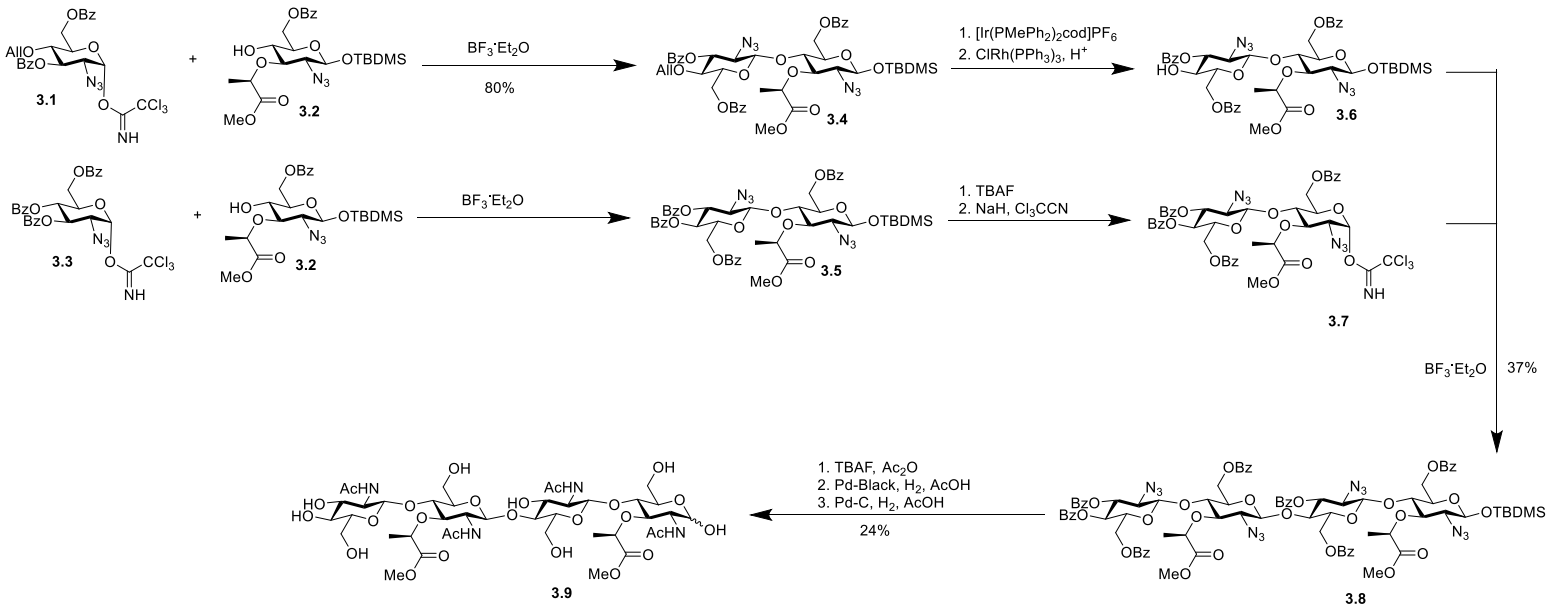


Figure 3.2 – Schmidt's synthesis of a tetrasaccharide fragment

Following Schmidt's work, Fukase synthesised the first glycopeptide fragments bearing peptide stems containing two of the four/five residues native to biology [6]; the minimum requirement for immunogenicity [1] (Fig. 3.3-3.5). This work utilised a similar method of assembly to Schmidt where monosaccharide blocks were condensed into disaccharides for

further condensation into tetrasaccharides. These tetrasaccharides were further utilised as parent compounds for octasaccharide fragments. The notable improvement to Schmidt's strategy was the conversion of a single parent fragment into both donor and acceptor moieties through the use of orthogonal protection at the reducing and non-reducing ends. The group began by preparing both donor and acceptor monosaccharides from glucosamine. Troc protection, anomeric allylic etherification and benzylidene acetal formation gave intermediate **3.12**. Mildly acidic benzylation followed by conversion of the allyl ether to a trichloroacetamide gave donor **3.14**. Intermediate **3.11** was prepared through allylation of the anomeric position and formation of the allylic carbamate from the amino group. The 4 and 6 OH were protected as a benzylidene acetal allowing for alkylation at the 3 OH with the appropriate lactate. The allyloxycarbonyl (Alloc) group was then removed allowing for installation of the participating Troc. Regioselective acetal opening at the 4 OH gave acceptor **3.13**. Schmidt glycosylation with donor **3.14** produced the consequent disaccharide **3.15** which was used to yield donor and acceptor sugars for accessing larger fragments. Regioselective acetal opening at the 4 OH gave the acceptor **3.16**, and deallylation and conversion to a trichloroacetamide gave the donor **3.17**. Glycosylation of these compounds gave tetrasaccharide fragments. This procedure was reiterated to yield octamers (Fig. 3.4). Unmasking of the lactoyls through base hydrolysis allowed for incorporation of the immunogenic peptide stem, L-Ala-D-*iso*-Glu (Fig. 3.5). Further work expanded on this strategy, incorporating the full pentapeptide stem native to many gram-positive organisms [7, 8]. Use of this methodology has since been documented, namely in the design of immunological probes [9-12]. Refinements to this method have seen the pre-opening of the benzylidene acetal and capping of the 4 OH with 9-fluorenylmethyloxycarbonyl (Fmoc) [13]. This is able to be selectively unmasked with base, still allowing for selective conversion to an acceptor motif without the need to carry a sensitive acetal through acidic glycosylation conditions.

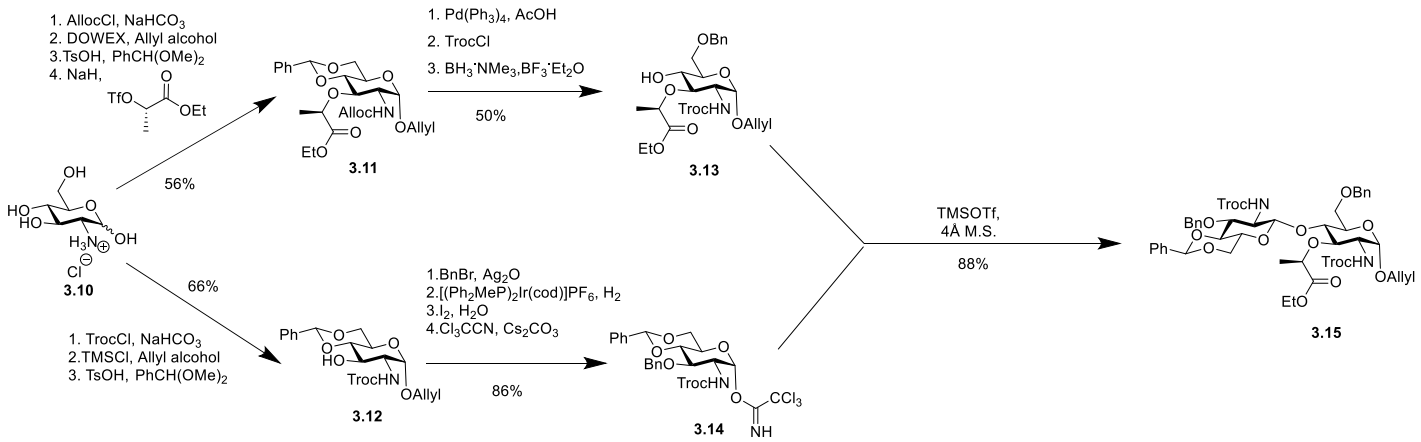


Figure 3.3 – Fukase's synthesis of disaccharide building blocks

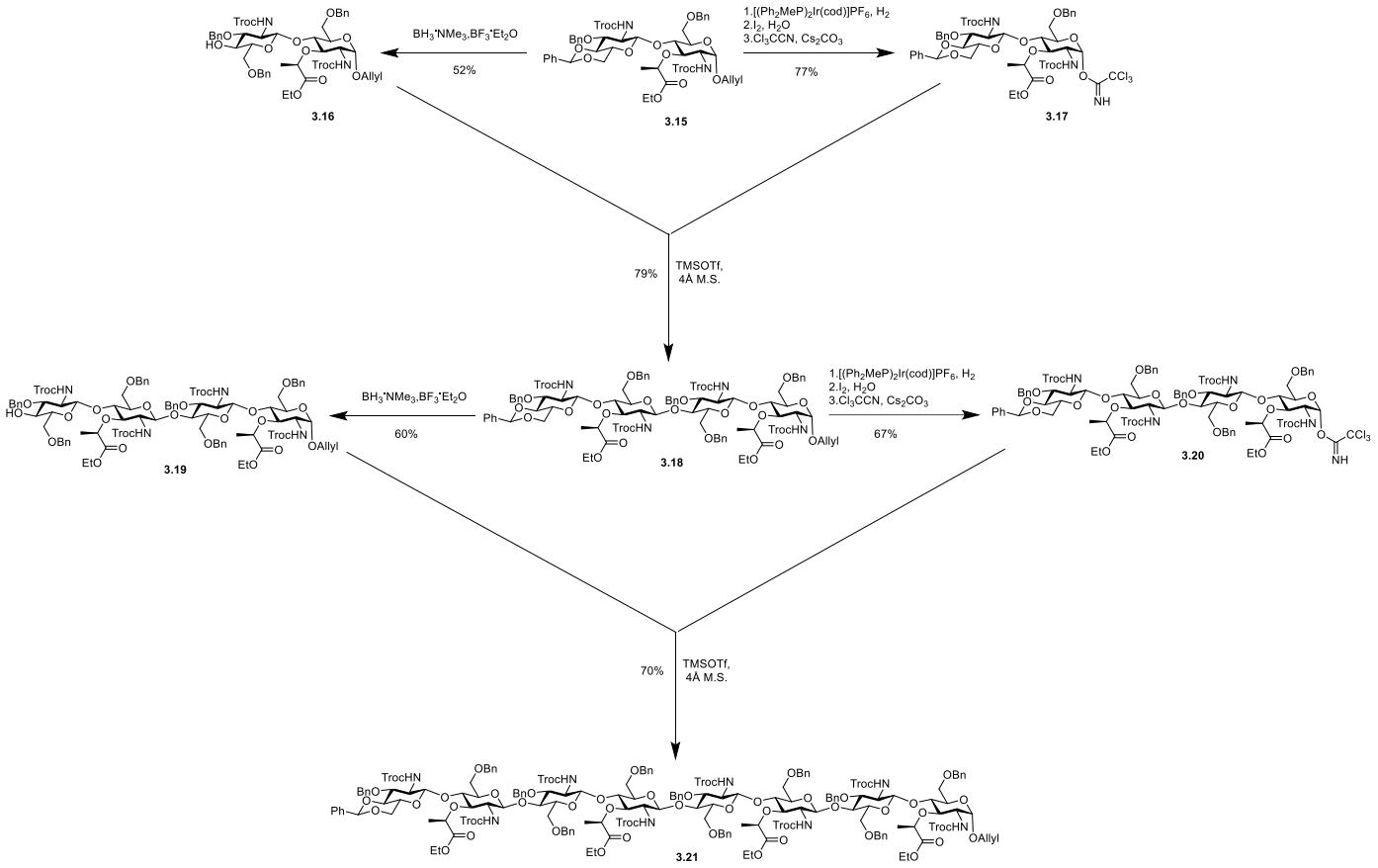


Figure 3.4 – Fukase's elaboration into tetrasaccharides and octasaccharides

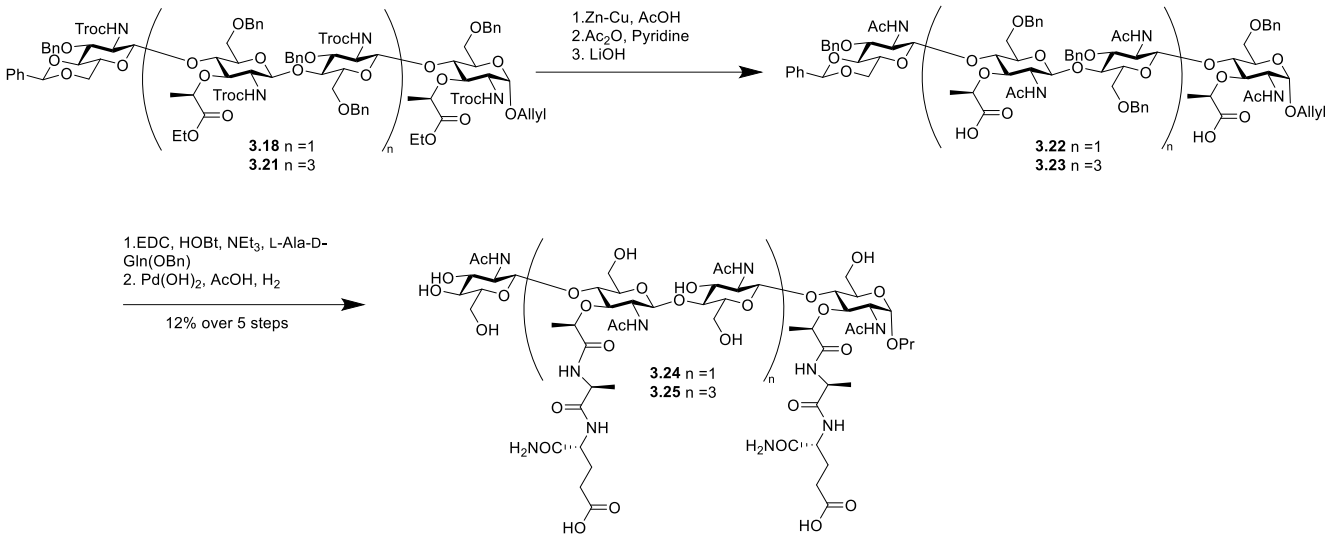


Figure 3.5 – Fukase's elaboration into glycopeptides

Kahne later reported synthesis of glycopeptide fragments during their synthesis of Lipid IV also utilising an improved version of Schmidt's original assembly method [14] (Fig. 3.6). Polymerisation relies on the use of sulfoxide donors developed in their group [15] that can be activated by Triflic anhydride and 2,6-Di-tert-butyl-4-methylpyridine selectively in the presence of thioglycosides. This allows for functionalisation of the acceptor motif as a thioglycoside, such that the glycosylation product can be oxidised at the reducing end to act as a donor if required. This ablates the need for an anomeric protecting group and consequent removal prior to functionlisation as a donor, as in the case of Fukase's methodology [6]. *N*-tetrachlorophthalimido (TCP) 6-*O*-benzyl thiophenylglucoside, **3.30**, was utilised as an acceptor. Use of TCP as the 2 - amino protecting group in all sugars allows for stereochemical control of glycoside formation [5]. This bulky protecting group also reduces reactivity of the neighbouring 3 OH as a nucleophile allowing for the use of 3 OH unprotected acceptors. Common donor precursor **3.27** was prepared through 3,6 OH benzylation mediated by dibutylstannylene acetal formation. Oxidation to a sulfoxide with *m*CPBA gave donor **3.29**, whereas silylation at the 4 OH and oxidation to the sulfoxide gave **3.28**. Triflic anhydride promoted glycosylation using donors **3.28** and **3.29** gave disaccharides **3.31** and **3.33** respectively. Oxidation of **3.31** allowed conversion to a donor, and glycosylation with **3.33** gave tetrasaccharide **3.34**. Removal of the TCP groups allowed for lactoylation at the now unhindered 3 OHs and later amidation to the peptide stem. The Cheng group refined this strategy further during their synthesis of Lipid IV through tuning reactivity of a GlcNAc-MurNAc thioglycoside donor-acceptor pair [16] in accordance with their previous work on relative reactivity values during glycosylations [17] (Fig. 3.7). Incorporation of an electron withdrawing ester placeholder in the MurNAc motif **3.39** reduced the donor character and prevented homodimerization during glycosylation. This circumvented the need for donor oxidation to the sulfoxide and selective activation.

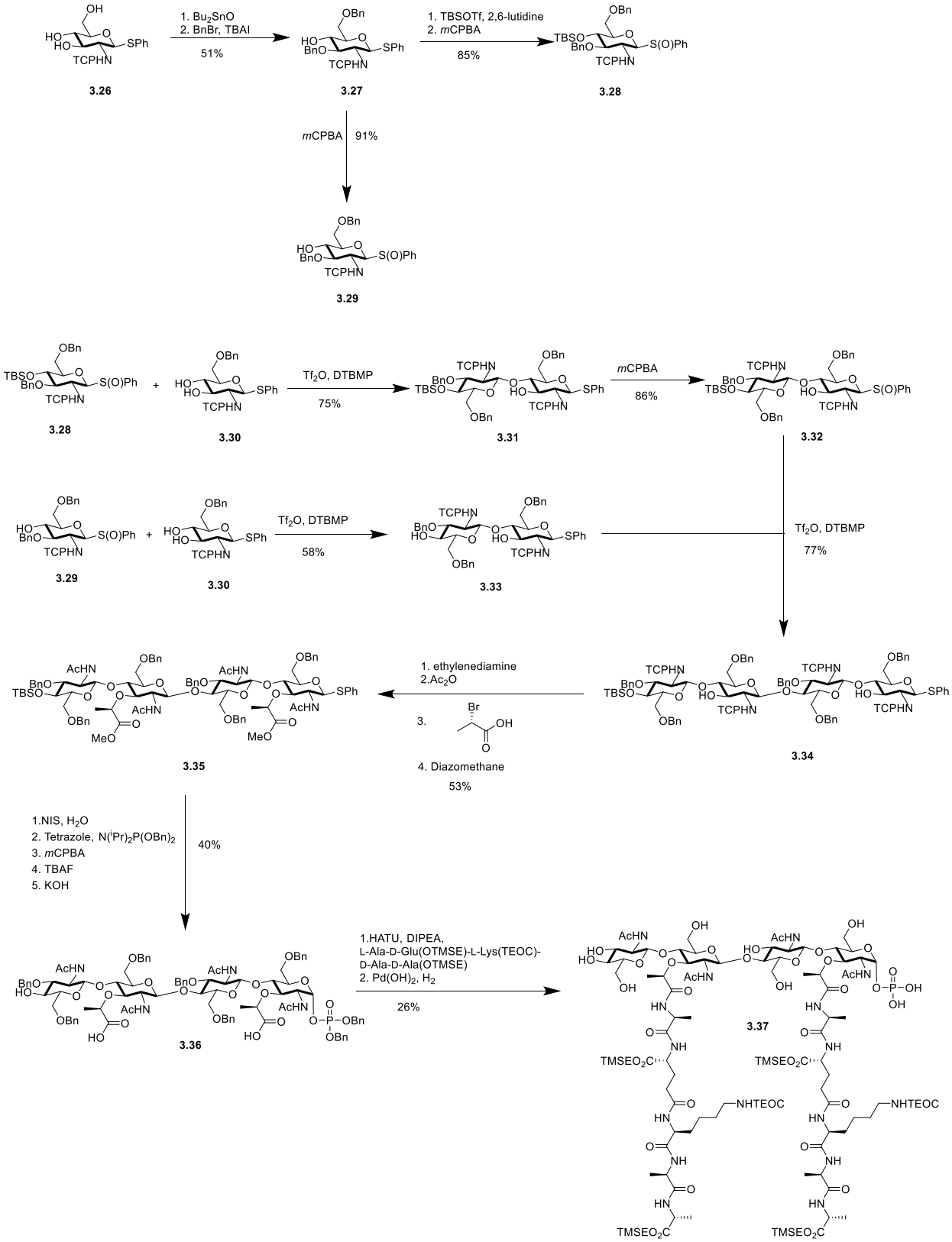


Figure 3.6 – Khane's synthesis of a glycopeptide fragment during Lipid IV synthesis

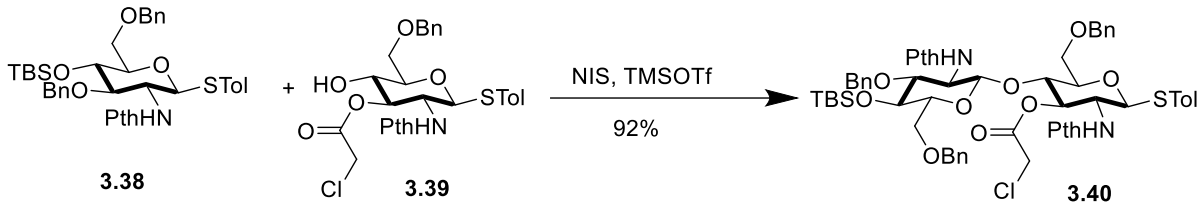


Figure 3.7 – Cheng's refined glycosylation strategy

After Fukase's first report, another synthesis was reported by the Mobashery group using a different assembly method where tetramers are synthesised through sole propagation of monosaccharide blocks [18] (Fig. 3.8 + 3.9). Both of the starting acceptor and donor monosaccharides were made from a common intermediate **3.44**. Stannylene acetal mediated 3,6 benzylation of **3.44** gave acceptor **3.45**. Benzylidene acetal formation and acetylation allowed for 4,6 and 3 OH protection respectively to give intermediate **3.47**. The anomeric silyl ether could then be unmasked for functionalisation as a trichloroacetamide to yield donor **3.49**. Glycosylation of **3.45** and **3.49** with TfOH as a promoter gave disaccharide **3.50**. Similarly to Fukase's approach orthogonal protection at both the reducing (silyl ether) and non-reducing ends (acetal) allowed for selective elongation. Disaccharides could be converted to donors via desilylation and functionalisation with trichloroacetonitrile or acceptors through regioselective acetal opening. Conversion to donor **3.51** allowed reaction with acceptor **3.52** to produce trisaccharide **3.53**. Conversion to an acceptor allowed reaction with donor **3.54** to produce the desired tetramer intermediate. Deprotection of the dimethylmaleoyl (DMM) and acetyl groups allowed for lactoylation at the exposed 3 OHs, and subsequent amide coupling with an appropriate pentapeptide gave desired glycopeptide **3.57** after global hydrogenolysis. The group have since reported additional work using this strategy to access more complex peptidoglycan fragments such as octasaccharides [19], fragments containing *m*DAP [20] and anhydro MurNAc residues [21]. Very recently another group has adopted a similar assembly strategy utilising monosaccharides with silyl ether protection, and lactoylation post glycosylation, however they report the use of a novel donor class that was activated under much milder conditions [22].

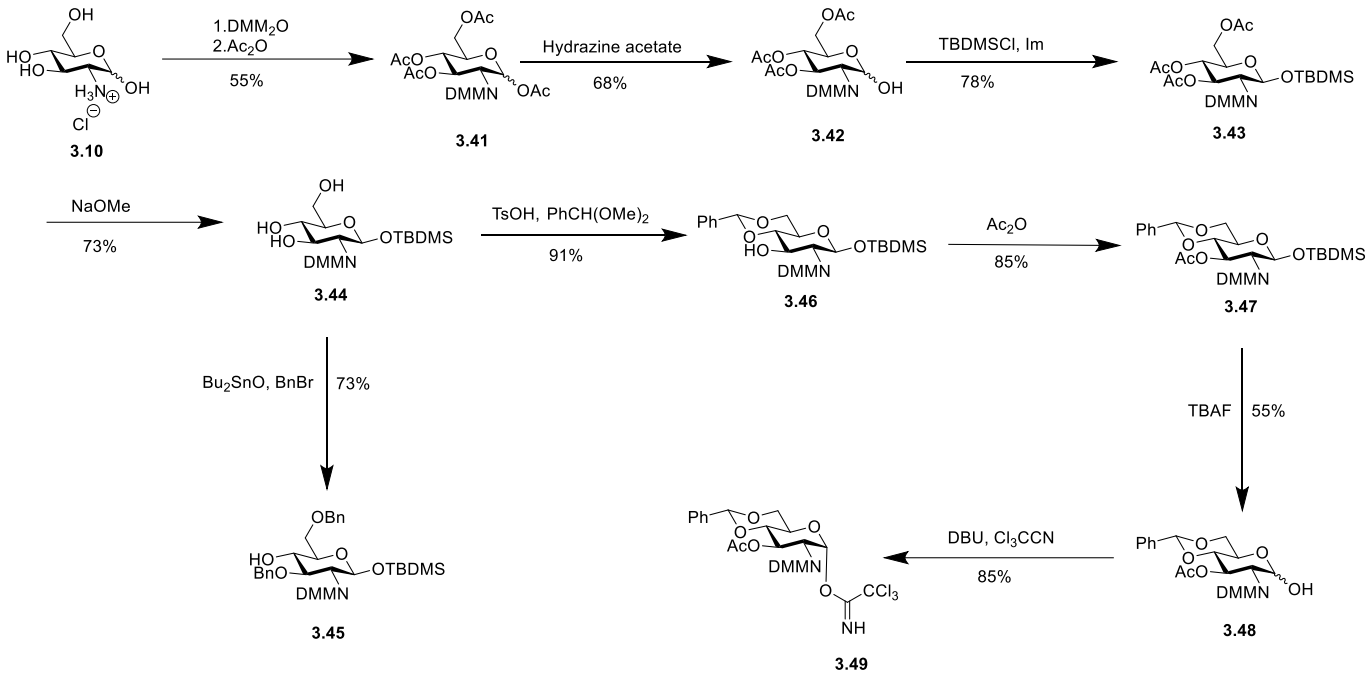


Figure 3.8 – Mobashery's synthesis of monosaccharide building blocks

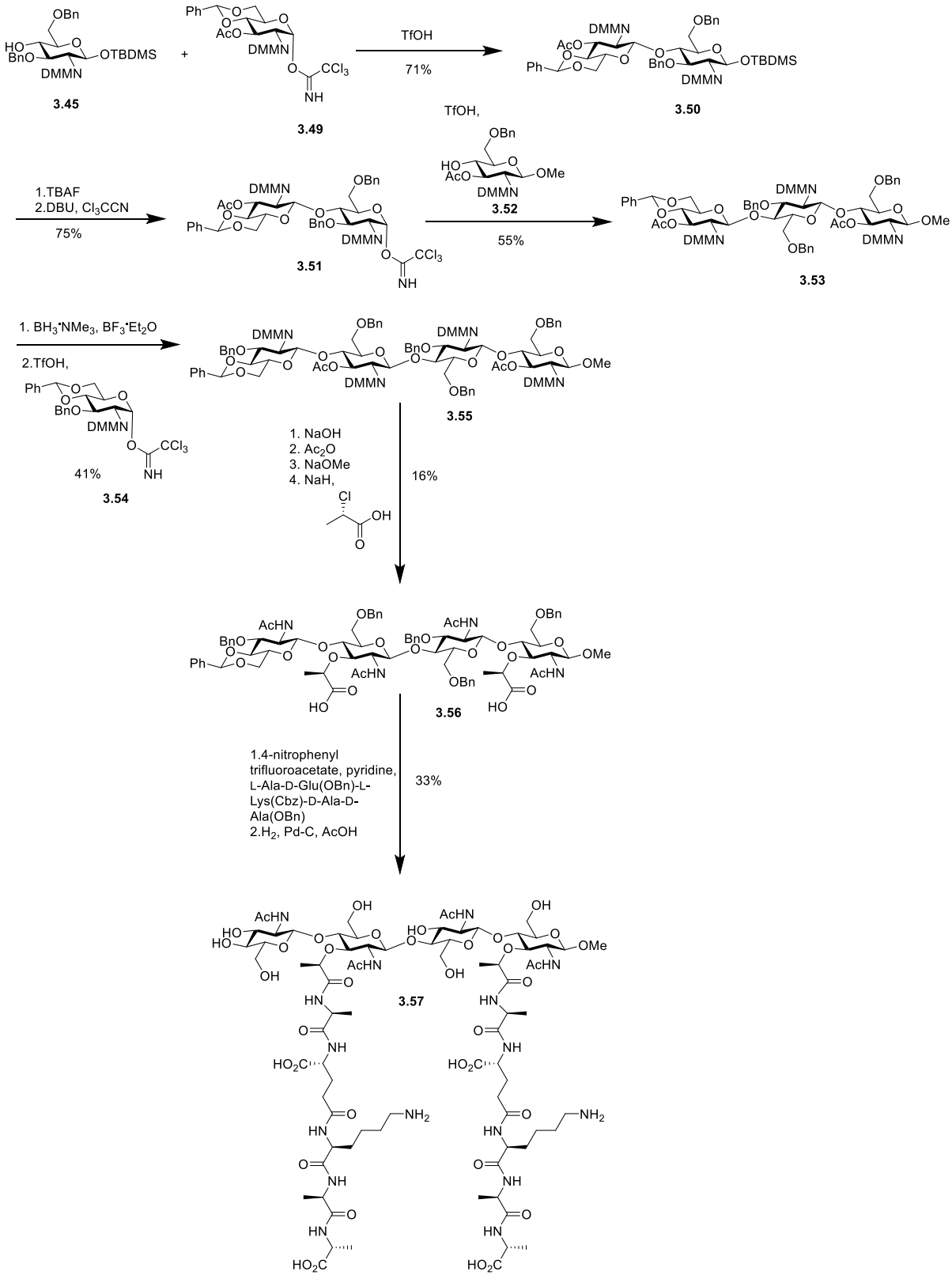


Figure 3.9 – Mobashery's synthesis of tetrasaccharide fragment

Top-Down Synthesis

More recently, researchers have sought to access peptidoglycans by fragmenting and transforming chemically similar polymers from natural sources in a top-down approach. These methods utilise Chitin and Chitosan, polymers comprising repeating GlcNAc and Glucosamine residues respectively joined by a β(1,4) glycosidic bond. Using these as starting materials offers the advantage of having the glycosidic linkage preinstalled and removes some of the complexity associated with other preparations, as well as making accessing much larger fragments easily possible. Synthesis of a NAG-NAM disaccharide from per acetylated Chitobiose **3.58**, a disaccharide unit obtained from Chitin [23], was reported by Marques in 2018 [24] (Fig. 3.10). The sequence began with a transacylation to the TFA amide to overcome the low solubility of Chitobiose. Anomeric deprotection with Hydrazine followed by silyl ether formation was trialled, however the silyl ether was found to be labile to downstream base hydrolysis conditions, as such differential protection as a thioglycoside was explored to give **3.60**. Methanolysis of the acetyls exposed the hydroxyls and treatment with the orthoester protected the 1,2-diol to give ketal **3.61**. Primary hydroxyls were capped with *tert*-butyldimethylsilyl chloride (TBDMS-Cl) allowing for lactoylation at the unexposed 3 OH via triflate displacement to give **3.63**. Whilst the authors did not further progress this structure into a larger glycan, they reported synthesis of large peptidoglycan polymers from Chitosan, with a degree of polymerisation up to 1800 a year later in 2019 [25] (Fig. 3.11). Large Chitosan polymers (degree of polymerisations = 398 and 1800) were reacted with phthalic anhydride to protect the amino groups. CDI mediated esterification with a dicarboxylic acid molecular clamp ensued to give **3.66**. The molecular clamp leads to regio discrimination between the hydroxyls in the polymer, due to the differences in sterics imposed by the linker. This allowed for alternating introduction of the lactoyl at the 3 OH after silylation of the 6 OHs with TBDMS-Cl. Successful formation of the NAM moieties was followed by deprotection; hydrazinolysis allowed for concomitant removal of the phthaloyl group and ester linker. *N*-Acetylation with Ac_2O and desilylation with TBAF afforded the peptidoglycan fragments **3.69**. This method provided simplistic and economical means to access sizeable peptidoglycan fragments, however the lack of homogeneity limits their utility as substrates in biochemical research.

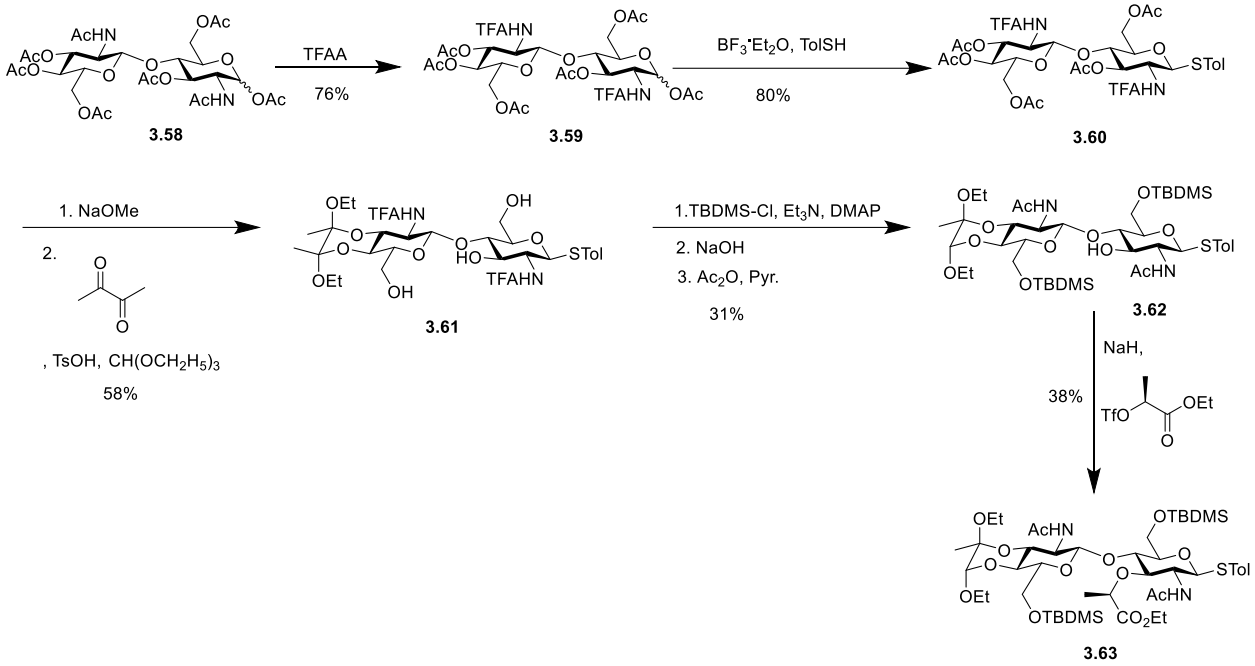


Figure 3.10 – Marques' synthesis of a NAG-NAM disaccharide from Chitobiose

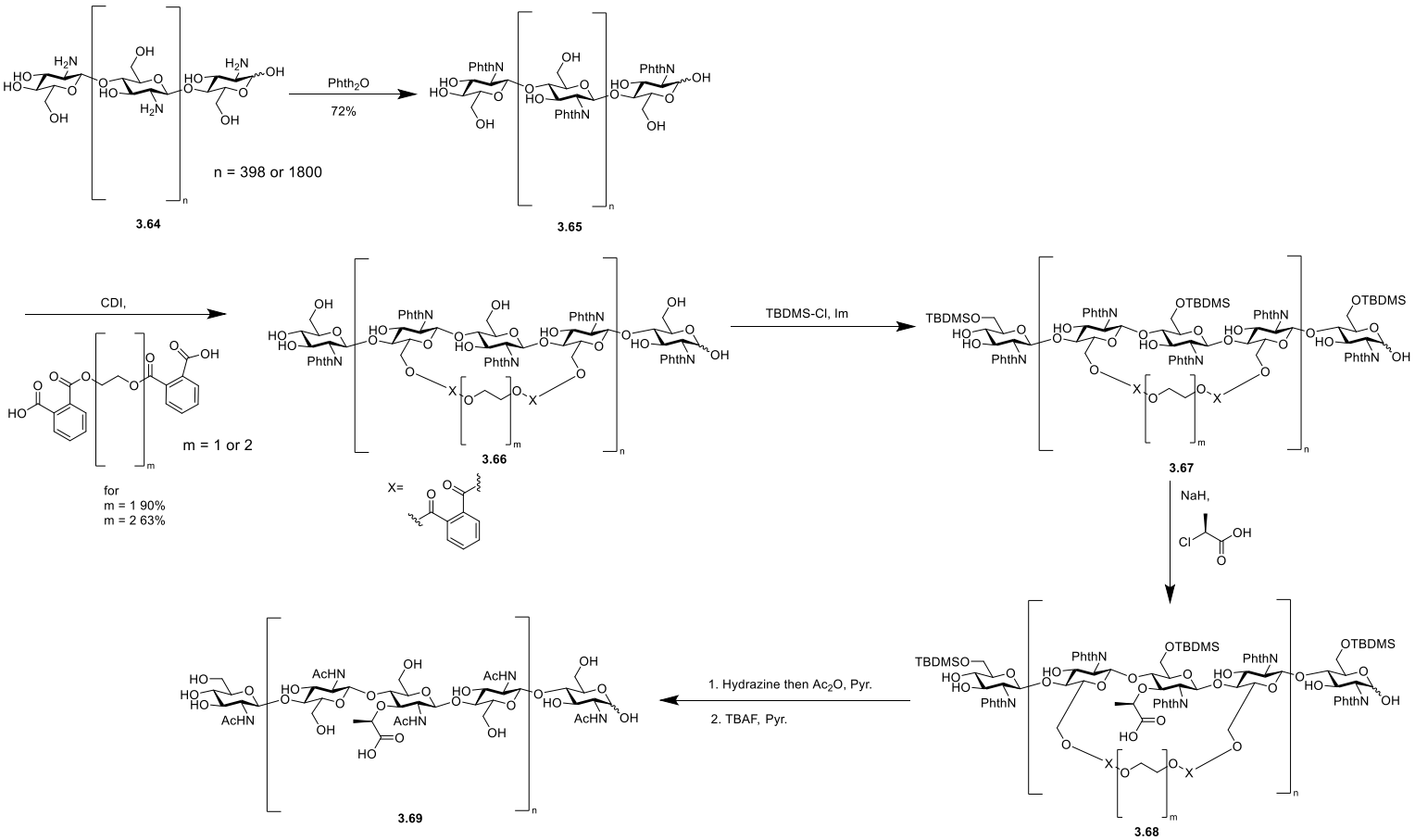


Figure 3.11 – Marques' synthesis of peptidoglycan from Chitosan

Developments in solution phase methods have seen reports of a variety of assembly methods such that building blocks of varying sizes and fewer protecting groups can be used. Additionally, options to access the required building blocks has evolved from early reports that mandated bottom-up syntheses from simple sugars to top-down approaches from large biopolymers. This presents a less complex and more economical route to access desired structures; however additional study is still needed to expand the use of these into accessing homogeneous glycans.

Solid Phase Strategies

Resin Attachment via the Peptide

First efforts towards applying solid phase chemistry to the synthesis of peptidoglycans looked at coupling of MurNAc and MurNAc-GlcNAc structures to a resin bound tripeptide [26] (Fig. 3.12). GlcNAc, **3.70**, was protected through anomeric allylation and acetal formation to give **3.72**. Nucleophilic substitution gave lactate **3.72**. Oxidation to a carboxylic acid, allowed for coupling to an amine bearing a long chain (phospholipid mimic), and base hydrolysis unmasked the lactoyls giving **3.74**. The tripeptide was grown off a tritylchloro linker before amide coupling with the MurNAc lactoyl of **3.74**. The structure could then be concomitantly cleaved off resin and deprotected with TFA to give **3.75**. The applicability of this early study to preparation of biologically useful compounds is severely limited; no glycosylation reactions were performed on the resin bound substrate. The value of the work lies in the study of resin attachment. Optimal amide coupling conditions were screened and loading was not attenuated by increasing building block size. This suggested adjoining via peptide side chain chemistry to be a viable strategy. This method has since been reproduced as means of synthesising muramyl peptides [27, 28] and attaching peptidoglycans to resin for NMR study [29].

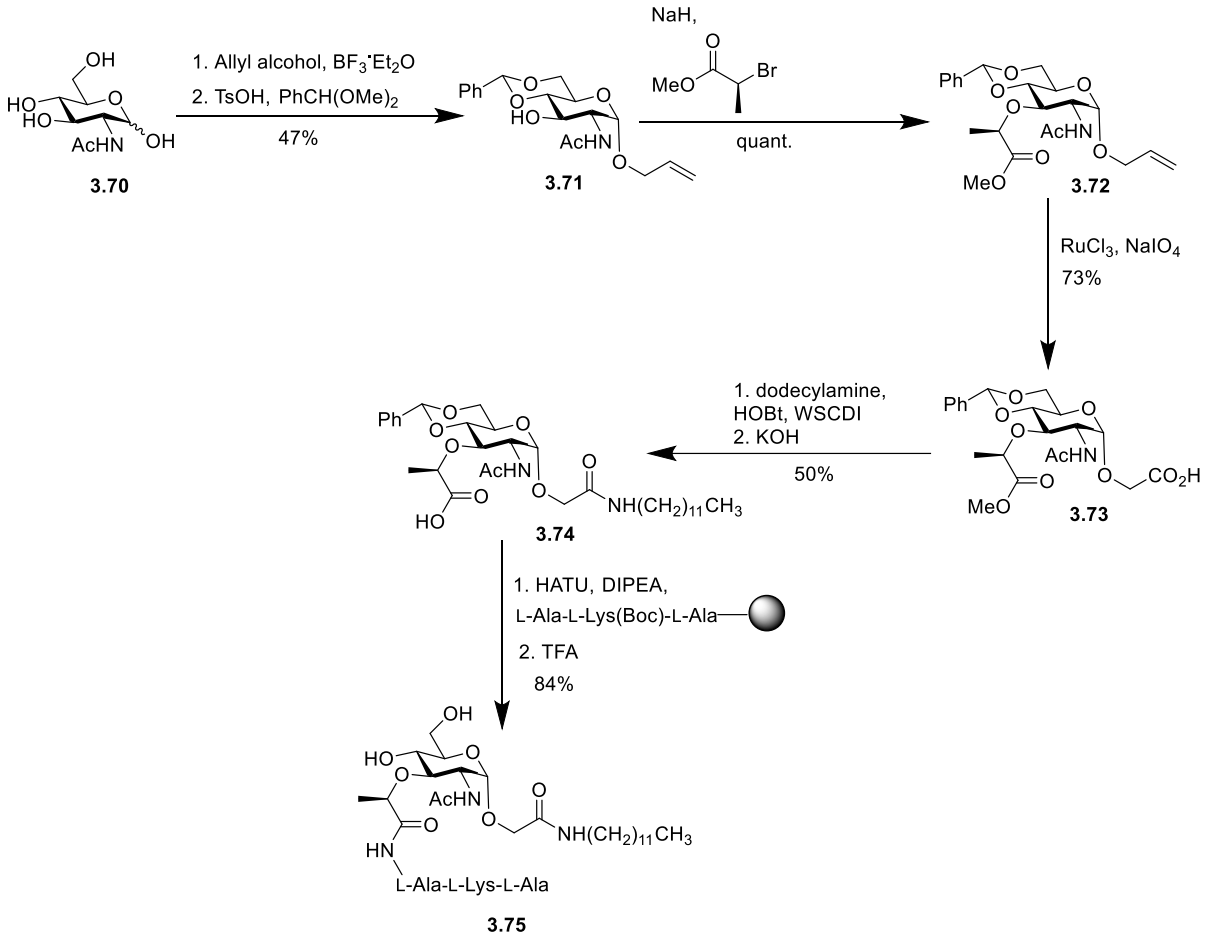


Figure 3.12 – Assembly of MurNAc tripeptide substrate on resin

Resin Attachment via the Sugar

To date few groups have assembled oligomeric peptidoglycan fragments on resin. The first report came from the Fukase group in 2014 [30] (Fig. 3.13), where tetrasaccharide dipeptides were prepared from disaccharide building blocks, **3.76**, bearing a 4-OFmoc protecting group at the non-reducing end. Loading of the building block was achieved through reaction of the *N*-phenyl trifluoroacetamide donor moiety with a benzyl alcohol Wang linker and TMSOTf as a promoter. After sites on unreacted resin were capped with acetyl groups, polymerisation to the tetrasaccharide, **3.78**, was achieved through triethylamine (Et_3N) deprotection of the 4-Fmoc of the resin bound disaccharide and subsequent TMSOTf catalysed glycosylation with additional building block, **3.76**. Exposure of the carboxyl groups allowed for amide coupling with L-Ala-D-*iso*-Glu to make glycopeptide **3.79** after resin cleavage. The linker was chosen as product can be liberated under acidic conditions, allowing the use of base labile protecting groups. Liberation from resin with 50% TFA in DCM led to an undesired dehydration reaction of the product to yield a 1,6-anhydrosugar. Addition of THF and water supresses this side reaction, allowing resin cleavage in good yields, and isolation of the desired glycopeptide. Fukase's methodology was notably different from the prior reports of solid phase chemistry

as resin attachment was achieved at the reducing end of the sugar in contrast to via the peptide chain. This allowed the glycosylation steps to be conducted on solid phase without modifying the route, a desirable improvement for accessing larger structures.

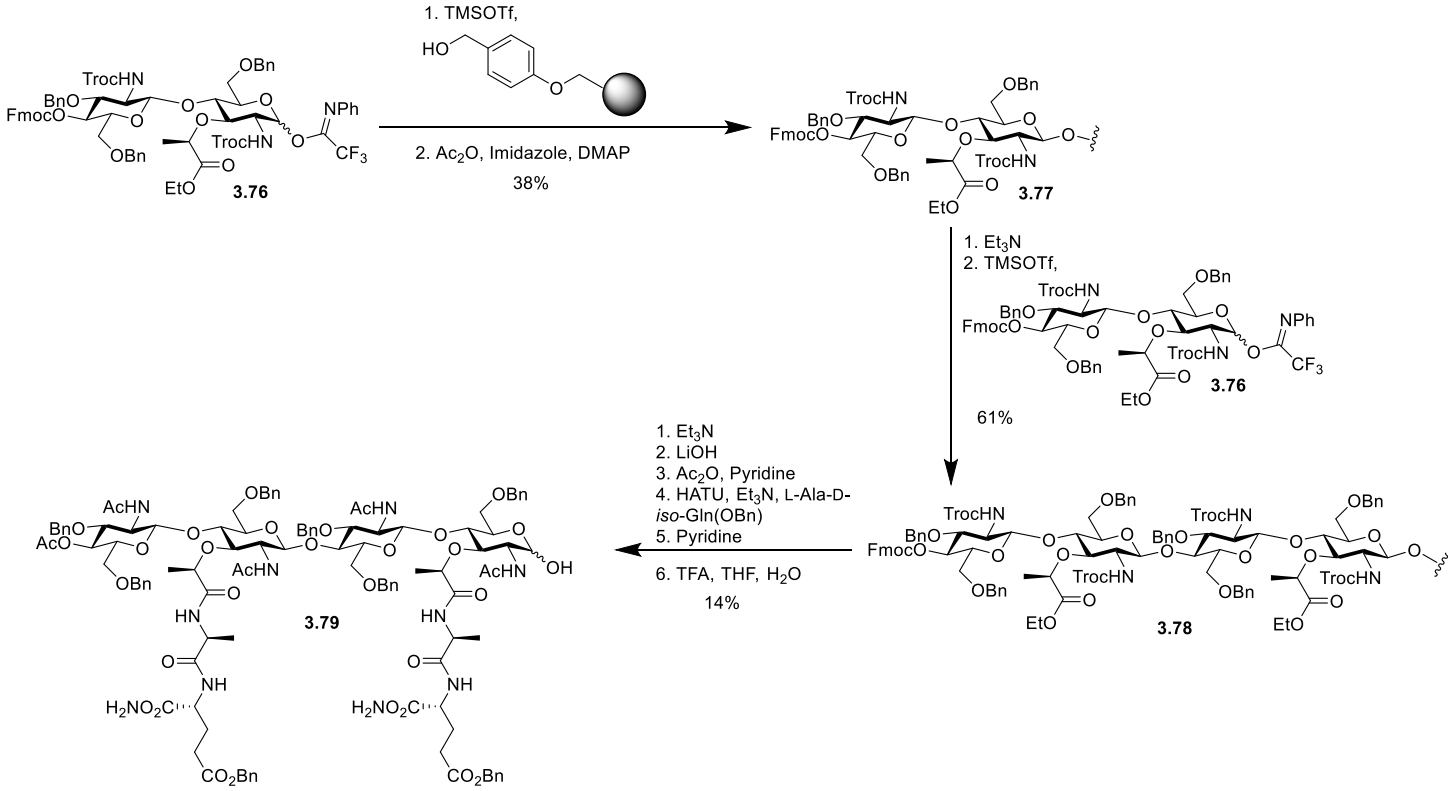


Figure 3.13 – Fukase's synthesis of tetrasaccharide fragments on resin

Following Fukase's work, Seeberger reported synthesis of fragments as large as hexamers from monosaccharide building blocks [31] (Fig. 3.14 + 3.15). This work utilised the same resin attachment strategy grafting the sugar to the resin, and the same Fmoc protecting strategy for elongation. In addition to using monosaccharide building blocks, differences from Fukase's work arise in the choice of donor functionality. Thioglycosides were first trialled, however poor observed reactivity spurred conversion to phosphates; glycosyl donors developed previously by the group [32]. The synthesis began with preparation of divergent intermediate **3.82** (Fig. 3.14). This started with acylation of the free amine in glucosamine, **3.10**, with trichloro acetyl chloride, and acetylation of the hydroxyls with Ac_2O and pyridine. Nucleophilic substitution with ethane thiol gave thioglycoside **3.81**, and methanolysis followed by transacetalisation with benzaldehyde dimethyl acetal gave the required divergent intermediate, **3.82**. At this point the GlcNAc building block was prepared through reductive benzylation of the 3 OH with benzaldehyde and regioselective opening of the acetal to give **3.87**, whereas the MurNAc building block, **3.83**, was prepared through base mediated lactoylation with (–)-ethyl (*S*)-2-trifluromethanesulfonyl propionate. As was done

to access **3.87**, the acetal in **3.83** was next opened regioselectively, however borane was used, as Brønsted acid openings led to undesired cyclisation with the lactate. With the 4 OH exposed, both products **3.84** and **3.87** were treated with FmocCl and pyridine to give the required carbonates, **3.85** and **3.88**, and nucleophilic substitution with dibutyl phosphate gave building blocks **3.86** and **3.89**. Building blocks were loaded onto resin through TMSOTf promoted reaction of the phosphate donor group with a hydroxyl on a photocleavable linker (Fig. 3.15). Unreacted hydroxyls on the resin were acetylated and the 4-Fmoc was unmasked with piperidine. Glycosylation with the next alternating building block ensued, and the cycle was repeated for varying iterations to yield glycan backbones as large as hexamers after resin cleavage with 365 nm light and deprotection.

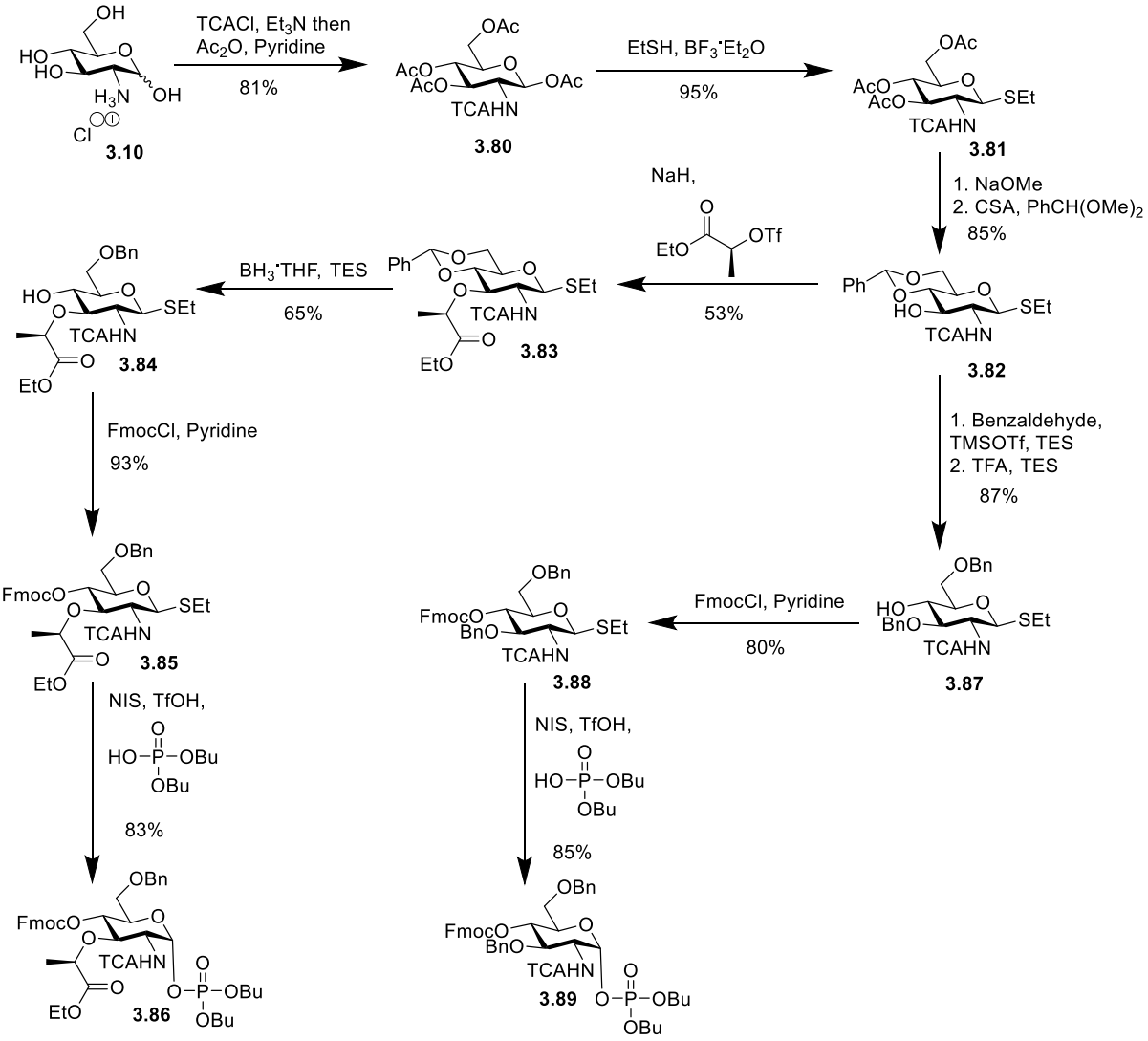


Figure 3.14 – Seeberger's synthesis of building blocks for accessing peptidoglycan fragments

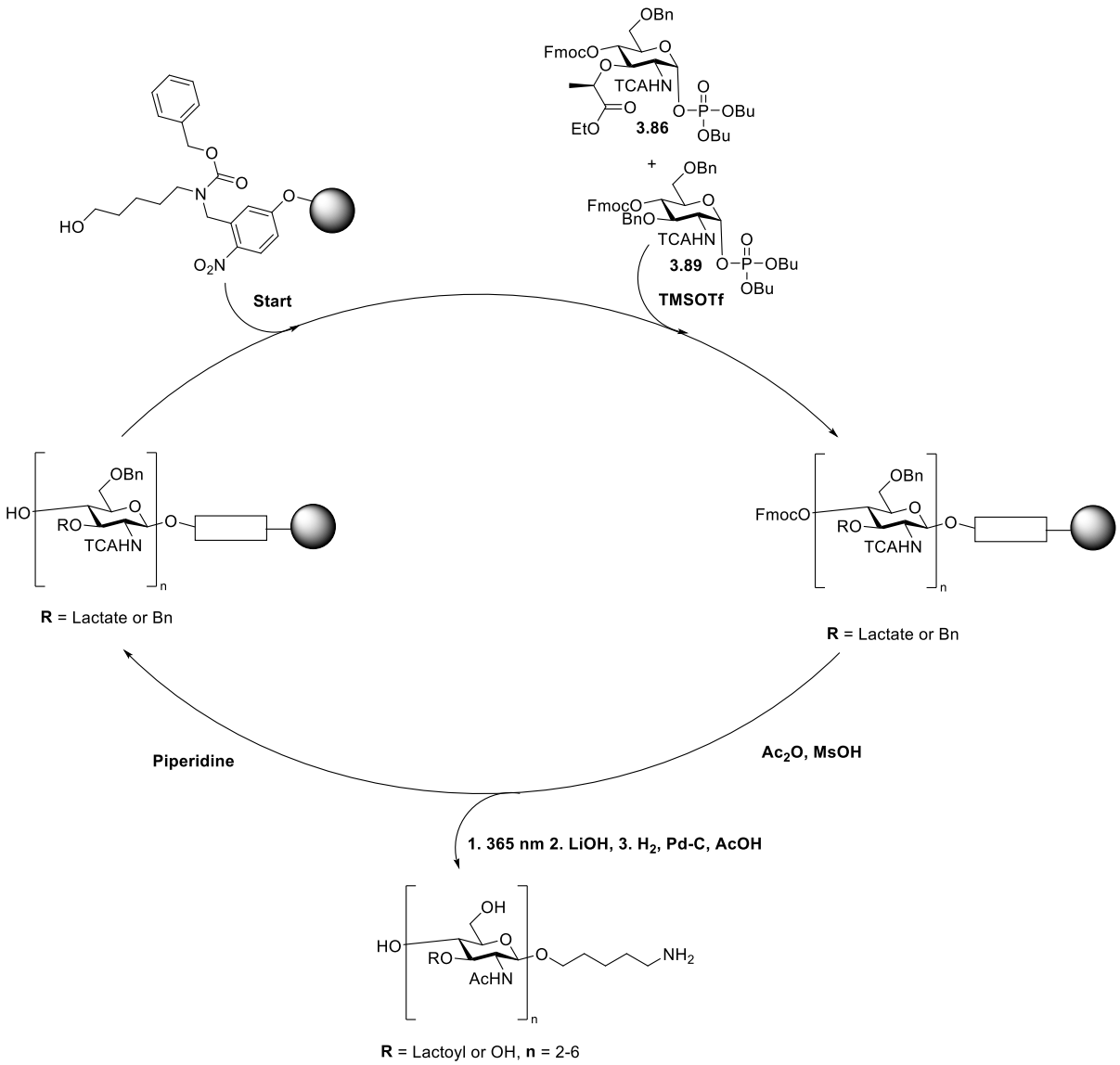


Figure 3.15 – Seeberger's synthesis of peptidoglycan fragments on resin

The development of solid phase syntheses of peptidoglycan fragments has seen optimisations regarding resin attachment, liberation conditions and building block design such that larger oligosaccharides can easily be accessed from simple monosaccharides.

Synthesis of Crosslinked Peptidoglycans

Existing strategies have been further employed to access crosslinked structures for biological study. An early report of access to the crosslinked disaccharides of peptidoglycan was reported by Fukase in 2009 [33] (Fig. 3.16 + 3.17). The group used a preformed crosslinked heptapeptide, **3.94**, and a disaccharide **3.15**, which had been used in their initial synthesis of the linear peptidoglycan backbone [6]. The first step in the synthesis of the heptapeptide **3.94**

was coupling of the side chain of Fmoc protected lysine, **3.90** with the C terminus of Boc protected Alanine (Fig. 3.16). These would be the terminal residue of each linear chain such that making this amide bond establishes a 4-3 crosslink common to biology [34]. The choice of *N* protecting groups allows for selective unmasking of either *N* termini with either acid or base allowing for selective chain elongation. The Alanine chain was first elongated following Boc deprotection with the addition of a Boc protected lysine residue. Preprepared dipeptides were then added to each chain. The lysine chain was first Fmoc deprotected with piperidine before amide coupling to Fmoc-L-Ala-D-*iso*-Gln to make the full three residue linear chain. Boc deprotection and coupling to Boc-L-Ala-D-*iso*-Gln ensued to give the full four residue linear chain and orthogonally protected heptapeptide **3.94**. With both disaccharide and peptide in hand, the carboxyl group of the MurNAc motif was exposed through base hydrolysis and amide coupled with L-Ala of the four-residue chain after Boc deprotection giving **3.96** (Fig. 3.17). The Fmoc at the other *N* termini could be removed with piperidine and amide coupled with another unit of disaccharide **3.95**, to give the desired crosslinked structure, **3.97**, after global hydrogenolysis.

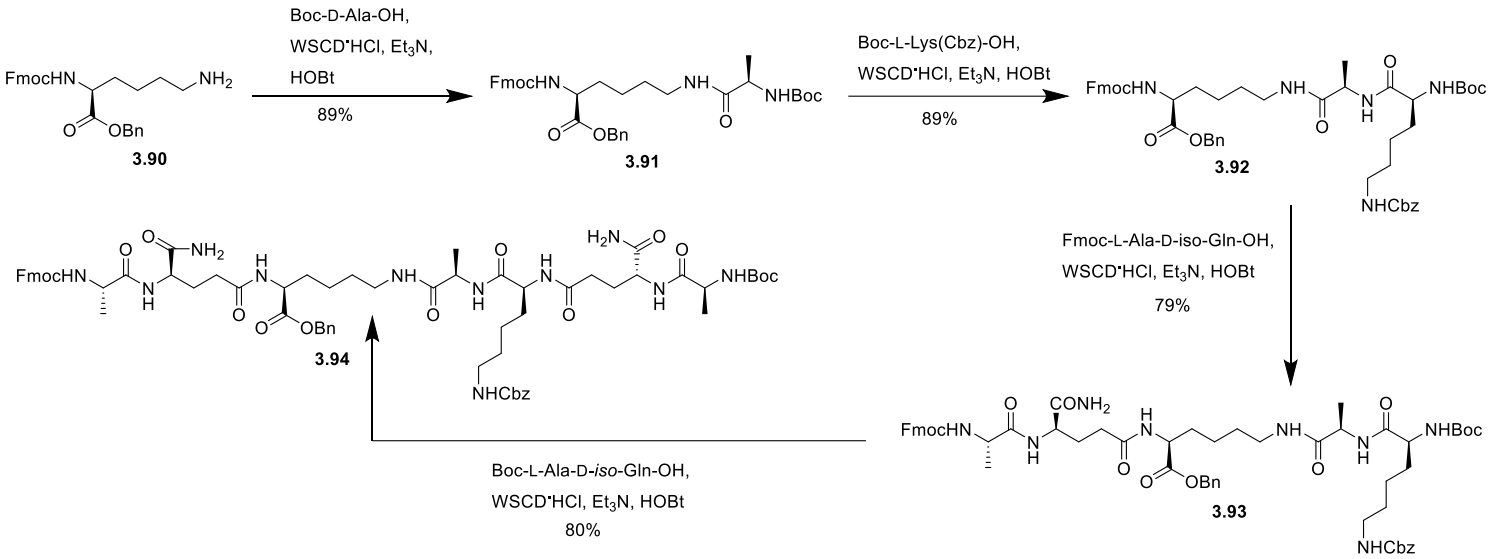


Figure 3.16 – Fukase's synthesis of crosslinked heptapeptide

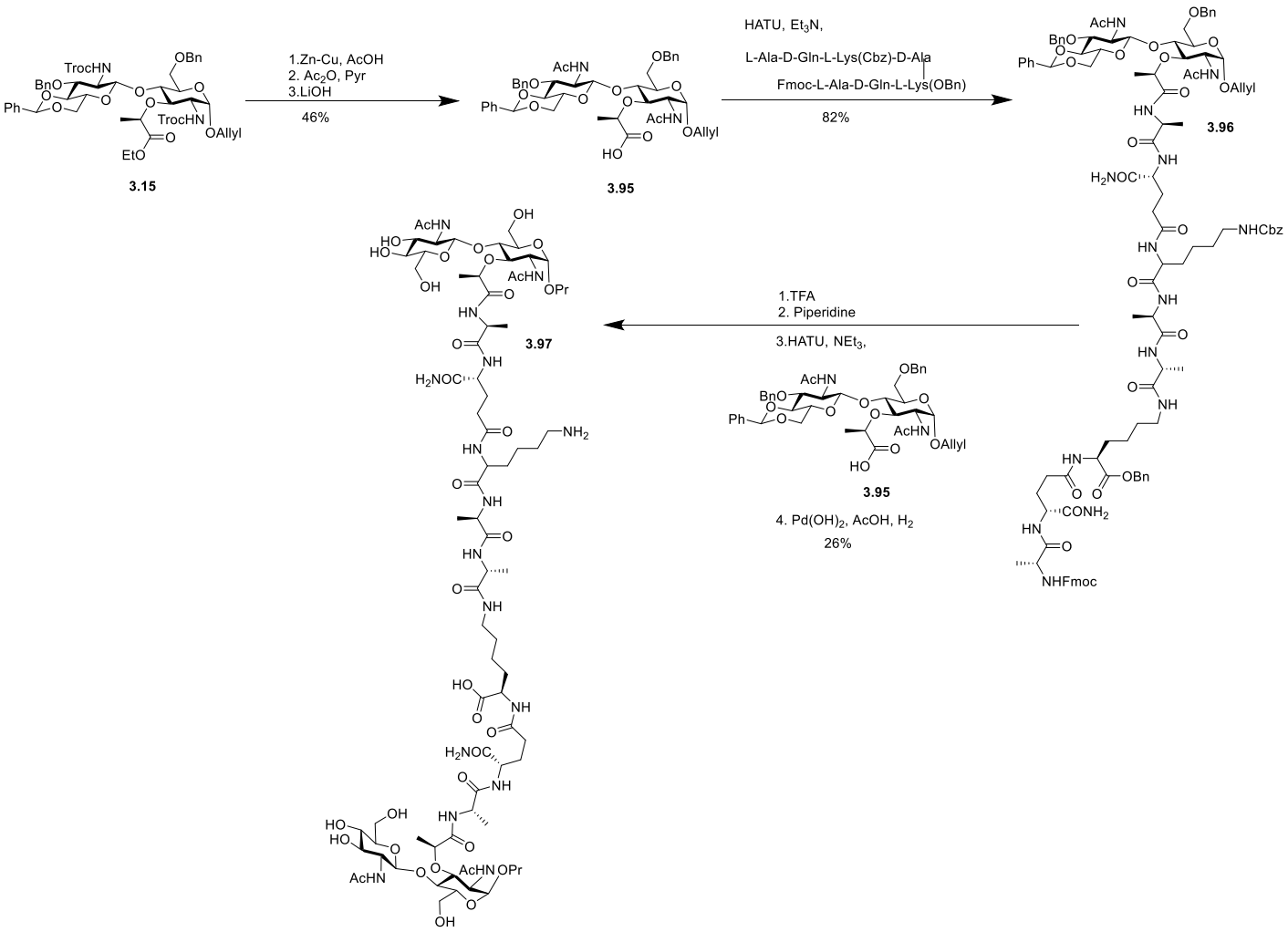


Figure 3.17 – Fukase's synthesis of crosslinked peptidoglycan fragments

The next report of crosslinking of peptidoglycan fragments came in 2015 from Mobashery [35] (Fig. 3.18 + 3.19), where the same overarching strategy was used of preforming a crosslinked heptapeptide for amide coupling to sugar lactoyls. This method was used to access anhydro sugars cross linked with an *m*DAP heptapeptide. The synthesis of an *m*DAP containing heptapeptide presented a much greater synthetic challenge and began with maksed *m*DAP **3.98**, where one of the amino acid groups was doubly protected at the C and N termini as an acetonide and azide respectively (Fig. 3.18). The free carboxyl was coupled with L-Ala-OPSE to give dipeptide **3.99**, and the acetonide hydrolysed. The free diol was then oxidised to a carboxylic acid and protected as a benzoate. The PSE ester was unmasked with DBU, and amide coupled to **3.102**, which was accessed from Staudinger reduction of azide **3.101**. This azide was similarly produced from the starting acetonide **3.98**, however the amide coupling step with L-Ala was substituted for benzoate protection. The produced tripeptide **3.103**, defines the 4-3 crosslink and at this point treatment with TFA was able to expose both the NBoc protected amines for coupling to a dipeptide comprising protected L-Ala-D-Glu to give

desired heptapeptide **3.104**. Further TFA treatment deprotected the nascent L-Ala C termini for coupling with lactoyls in anhydro sugar **3.105** (Fig. 3.19). Global hydrogenolysis of the amide coupled product gave the desired crosslinked structure, **3.106**.

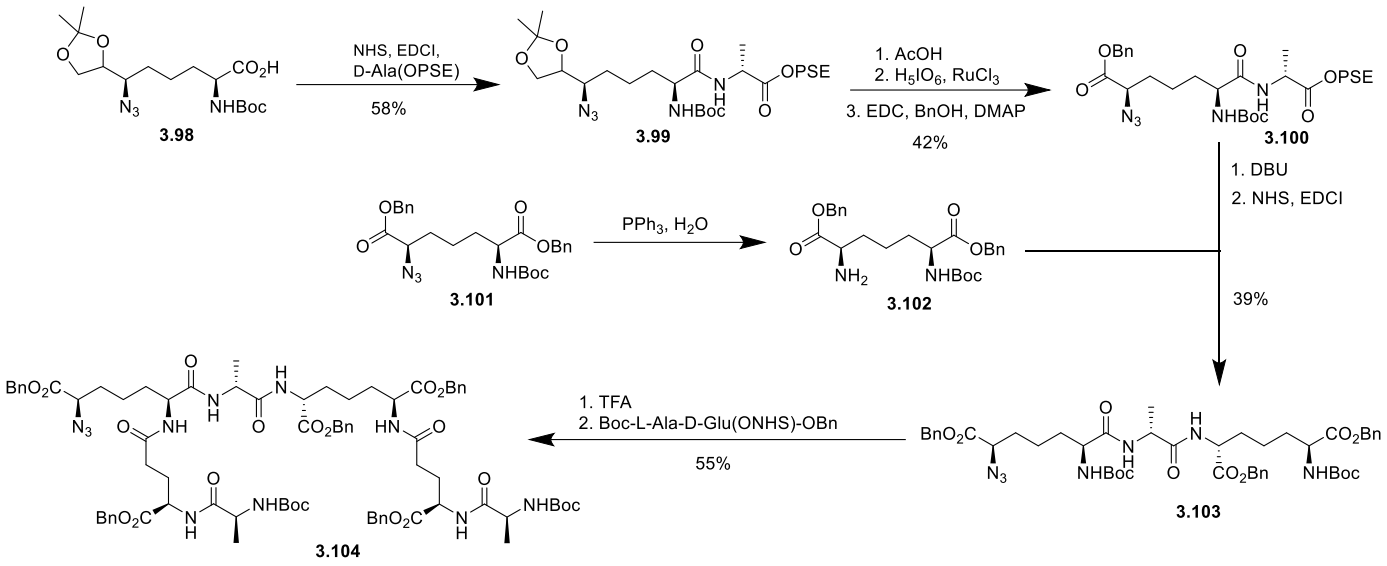


Figure 3.18 – Mobashery synthesis of crosslinked mDAP heptapeptide

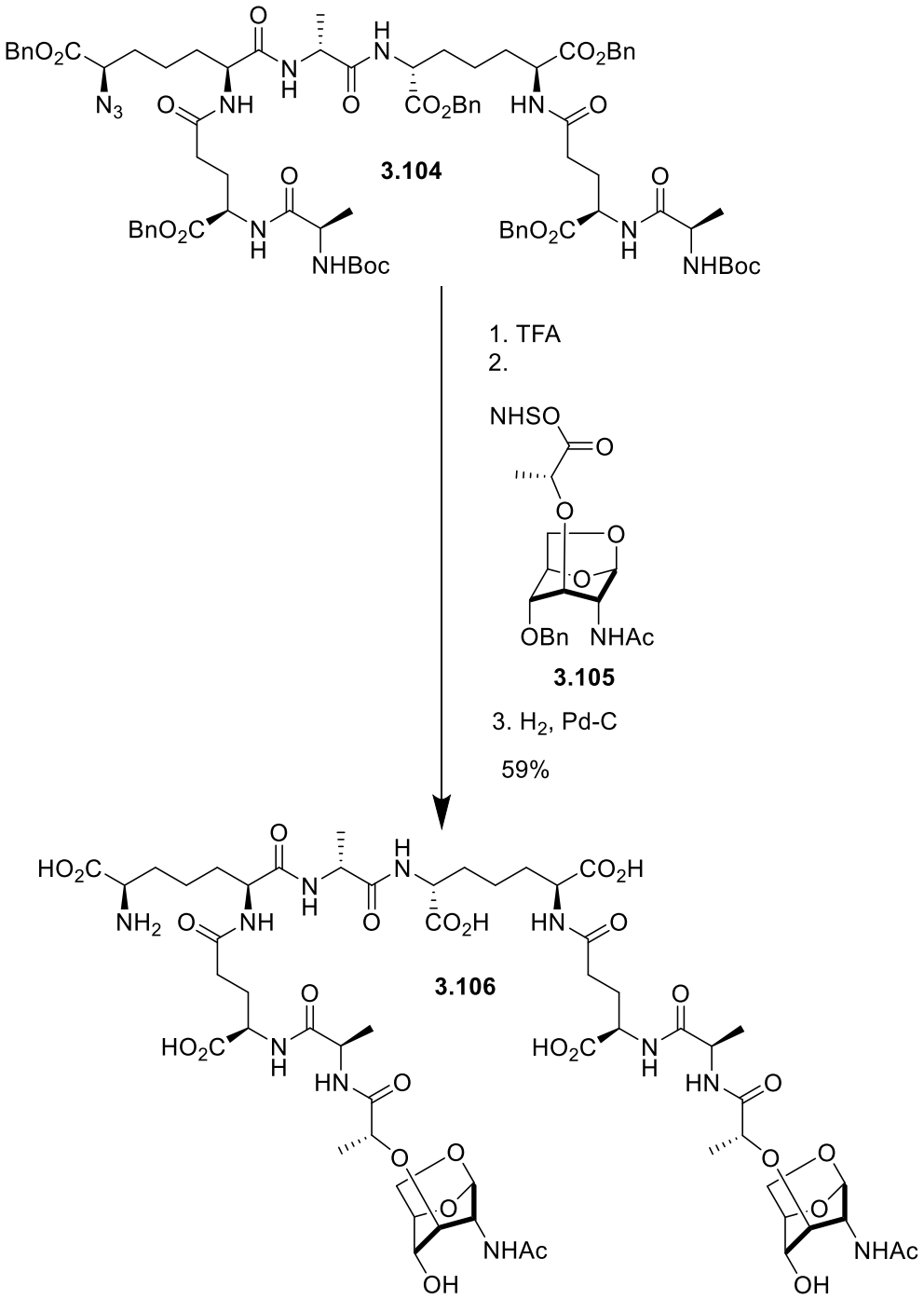


Figure 3.19 – Mobashery's synthesis of crosslinked anhydro MurNAc monosaccharides

Most recently, Grimes reported the synthesis of both 3-3 and 4-3 crosslinked fragments [36] (Fig. 3.20), both relevant biological structures [34]. Like the previous reports the same peptide preformation strategy was utilised, however owing to solubility problems in solution, solid phase syntheses were used. Synthesis of a 3-3 crosslinked structure began with dimerisation of Lysine derivatives to form the Lys-Lys crosslink in dipeptide **3.108**. Owing to the symmetry in the desired structure concomitant Fmoc deprotection and elongation could be utilised. Removal of the Fmoc groups with piperidine allowed amide coupling to Fmoc protected D-

iso-Gln and Fmoc protected L-Ala sequentially to give hexapeptide **3.109**. On synthesis of the desired hexapeptide Fmoc deprotection allowed for amide coupling to MurNAc derivative **3.110**, and global deprotection gave the desired final product **3.111**.

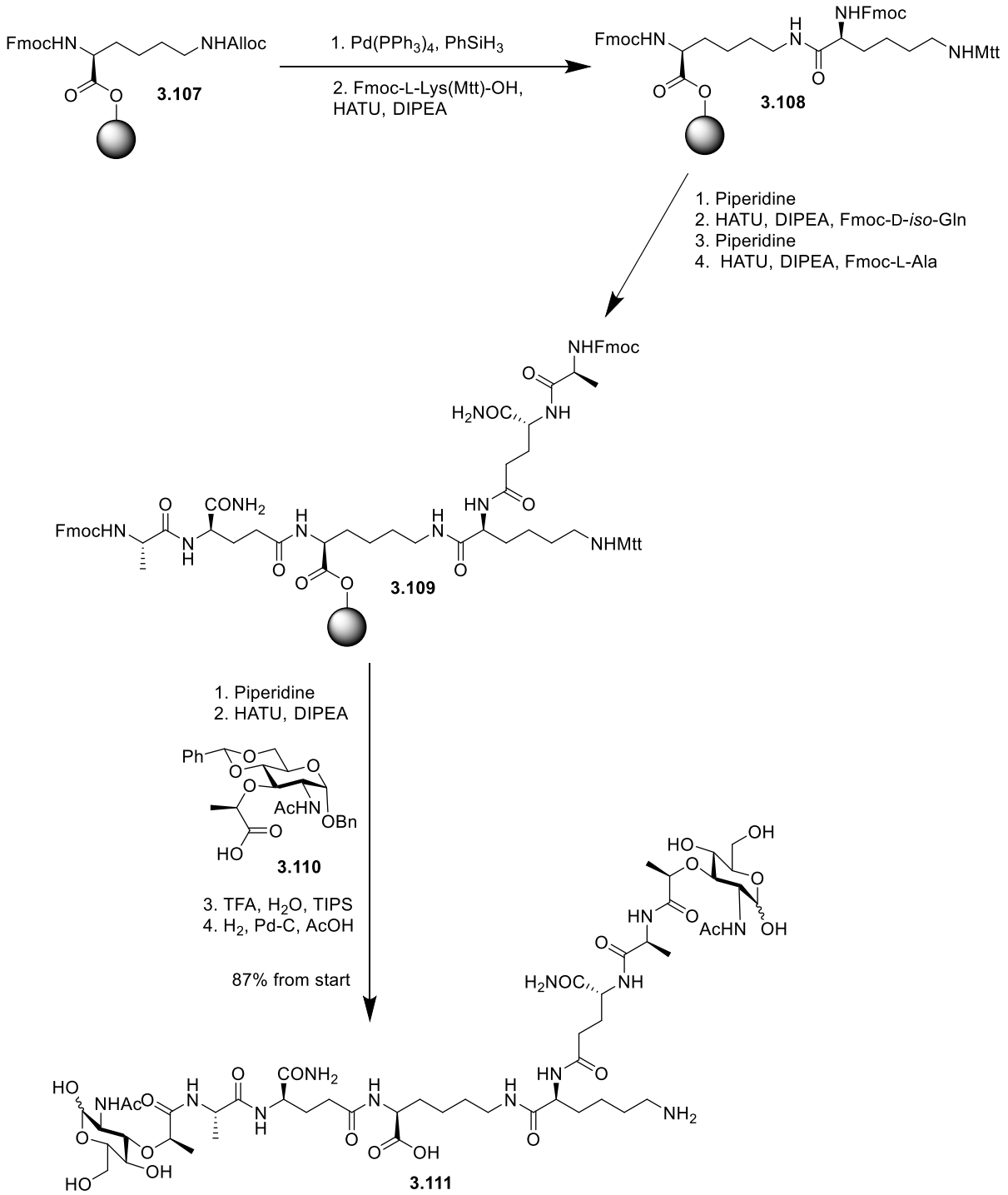


Figure 3.20 – Grimes' synthesis of crosslinked MurNAc monosaccharides on resin

Different strategies for accessing crosslinked peptidoglycan motifs have been reported such that desired substrates for biology are now accessible, however many limitations still remain unresolved. Firstly, all methods rely on the use of precrosslinked peptides and are not amenable to *in situ* crosslinking that may be of interest to biological study. Additionally, no reports document elongation of the disaccharide motif to access crosslinked oligomers, a property which could also be desirable for biological investigation.

A New Approach to Accessing Crosslinked Peptidoglycan Fragments

This chapter describes synthetic efforts towards accessing building blocks for the solid phase synthesis of crosslinked and procrosslinked peptidoglycans. A retrosynthetic strategy for assembling a crosslinked fragment **3.112** on resin is detailed below (Fig. 3.21). The inter fragment C-C bond can be formed through light inducible radical chemistry. Our group has shown that the electron deficient tetrafluoropyridyl group in **3.113** can undergo reduction either through SET or formation of a donor acceptor complex with a suitable reductant [2]. Use of a thiolate species as a reductant result in donor acceptor SET to generate a radical anion intermediate and a thiyl radical [37]. Formation of the radical anion intermediate results in homolysis of an Sp^3 C-S bond to generate a β centred alkyl radical on the glycopeptide backbone. This is then able to react with the SOMOphilic allyl glycine motif in **3.114** to crosslink disaccharide fragments. Such radical donor functionality can be incorporated into resin bound **3.113** through arylation of a free thiol following deprotection. This must be achievable through selective unmasking and as such an appropriate orthogonal protecting group must be selected. The 9-fluorenylmethyl (Fm) protecting group is removable with non-nucleophilic base via deprotonation of the acidic proton in the fluorenyl ring system. No other protecting groups chosen in the structure are susceptible to such phenomenon allowing for selective exposure. We chose to attach the radical donor fragment to resin over the acceptor as the process of deprotection and arylation should be easier to carry out on solid phase due to ease of purification. Both fragments **3.114** and **3.115** can be similarly disconnected via amide coupling into constituent glycopeptides **3.116** and **3.118** and peptides **3.117** and **3.119**.

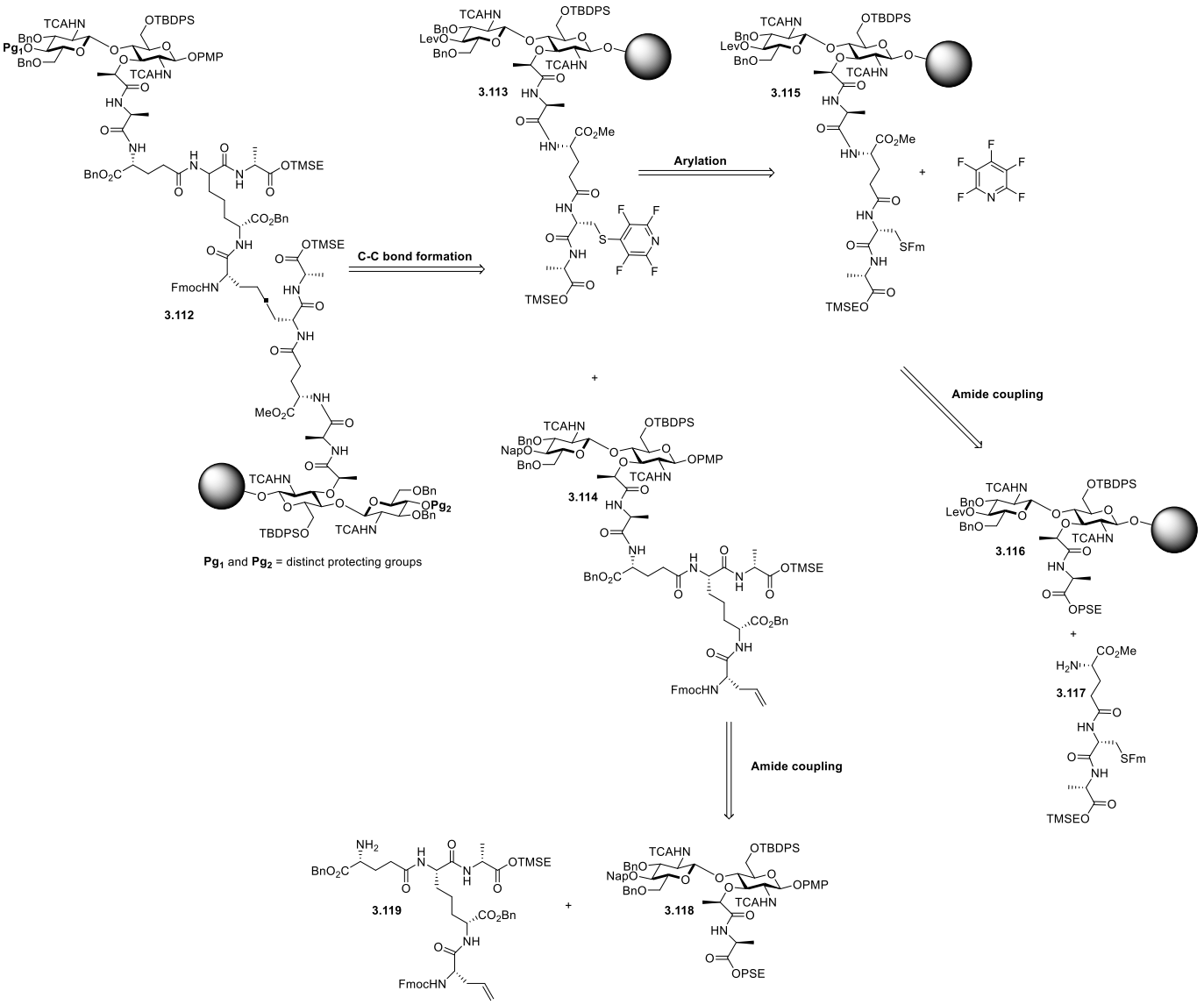


Figure 3.21 – Retrosynthesis for a crosslinked peptidoglycan fragment

Further disconnections of glycopeptide fragments are shown below (Fig. 3.22). Resin attachment to produce **3.116** is achievable through glycosylation between a suitable leaving group at the reducing end of the disaccharide and a free hydroxyl on the resin linker, as has been previously reported [30, 31]. Literature suggests the reaction to be superior with phosphate donors on resin [31], however thioglycosides may be preferable due to easier access [38]. Both disaccharides **3.121** and **3.118** are accessible from the stereoselective glycosylation of the same acceptor **3.122** with differential donors **3.123** and **3.124**.

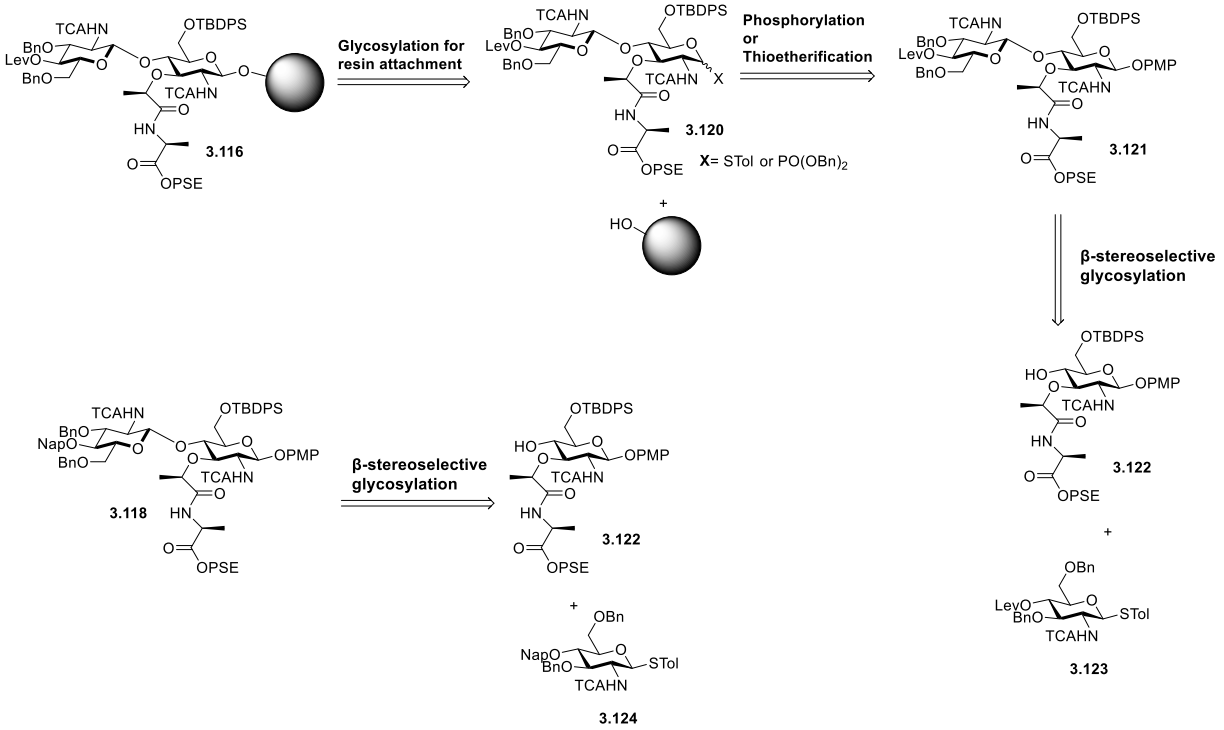


Figure 3.22 – Retrosynthesis of building blocks required to access crosslinked peptidoglycan fragments

Concise access to the required peptide fragments was envisioned as detailed below (Fig. 3.23). Assembly of tripeptide **3.117** could simply proceed through solution phase synthesis with Boc protected amino acids. Removal of the Fm protecting group and arylation could be used for conversion to a radical donor species, **3.127**. Suitable reaction with allyl glycine derivative **3.128** would generate the *m*DAP motif present in **3.119**. This means of accessing the *m*DAP motif provides two key advantages: It allows for verification of the intended crosslinking reaction in a simpler model system prior to any resin work, it is also arguably simpler than any alternate means of making *m*DAP; many preparations exist [39-41] however the only approach bearing such simplicity is the olefin cross metathesis between allyl glycine and rarer vinyl glycine followed by reduction [42]. Transformation of **3.125** to **3.119** could then proceed through attachment of an allyl glycine handle, **3.126**, to install SOMOphilic character.

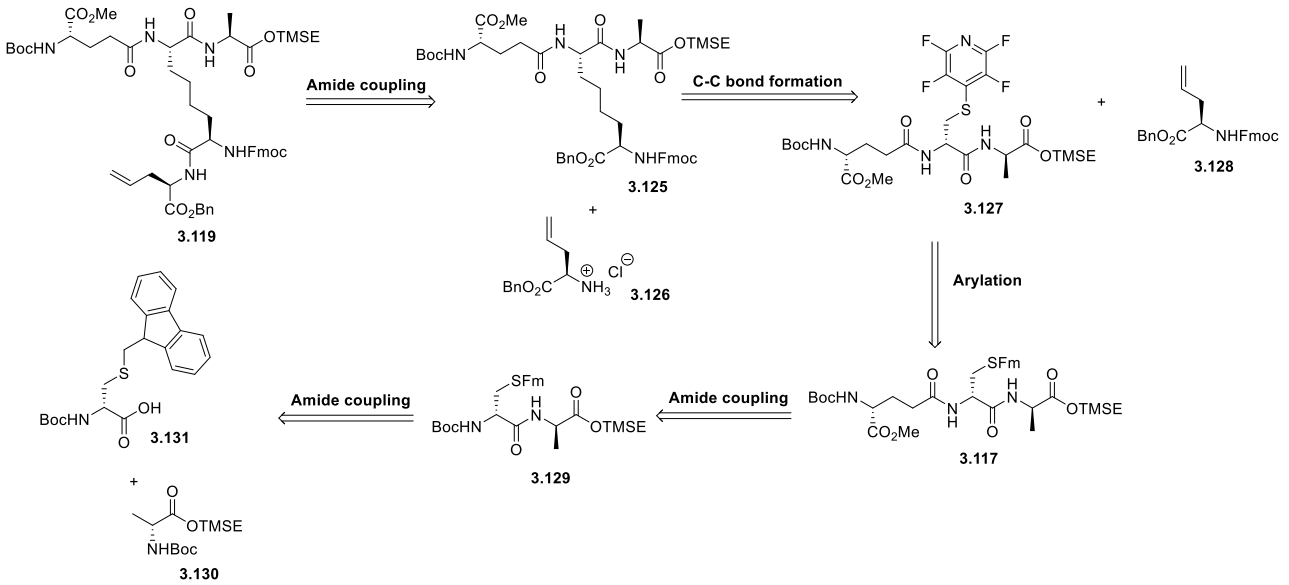


Figure 3.23 – Retrosynthesis of radical donor and acceptor peptides

To access oligomeric substrates that may possess the aforementioned tuneable specificity, on resin elongation can be conducted as shown below (Fig. 3.24). The levuinoyl (Lev) and (2-naphthyl)methyl (Nap) protecting group pair were chosen due to their orthogonality with one another and documented extended orthogonality with the *p*-methoxyphenyl (PMP) at the reducing end of the non-resin bound glycan [43]. To achieve this an additional donor, bearing orthogonal ONap protection at the non-reducing end must be prepared. Such a building block can easily be accessed from **3.118** (Fig. 3.24).

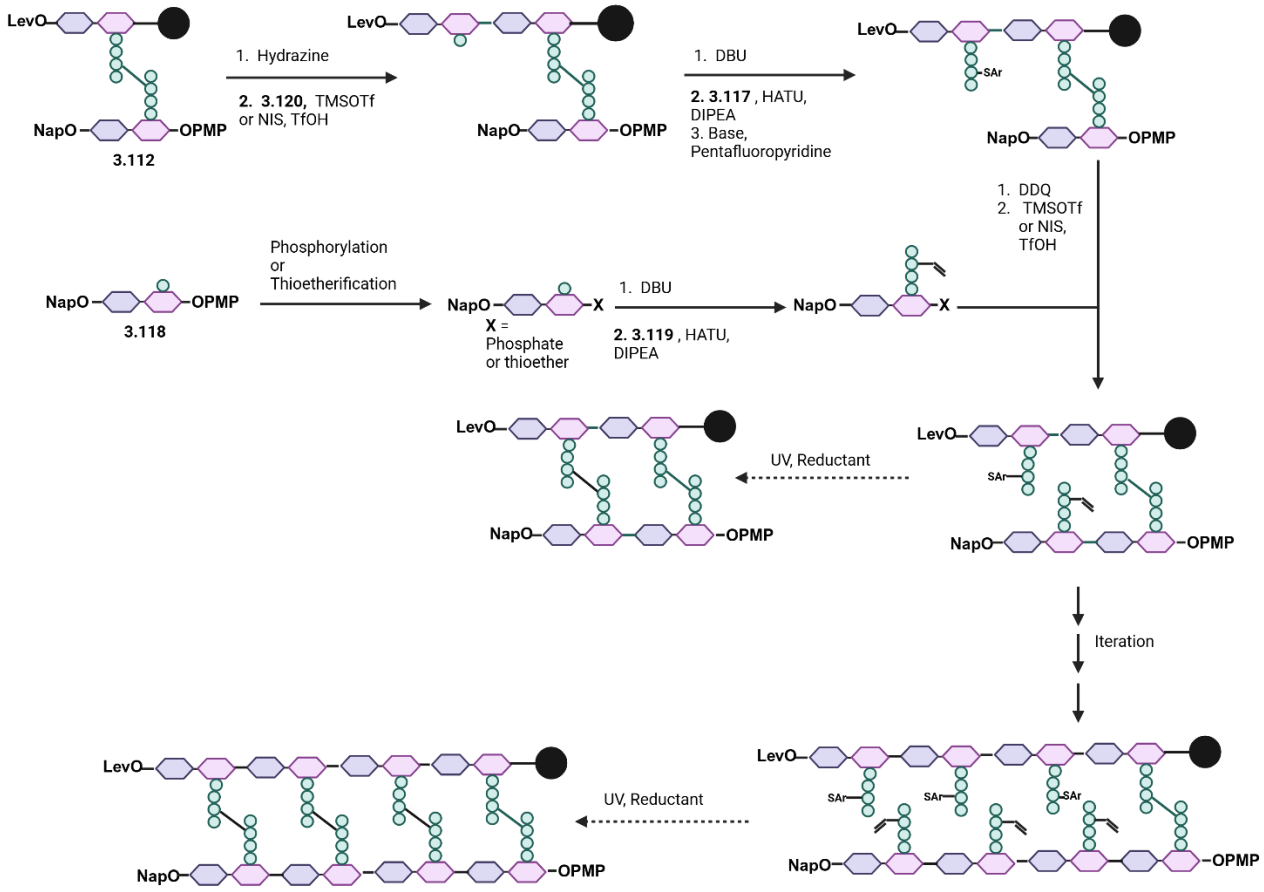


Figure 3.24 – Strategy for Glycan elongation on resin

Results and Discussion

Access to crosslinked structure **3.112** requires the synthesis of disaccharide building blocks **3.116** and **3.118** to assemble the glycan backbone, as well as peptides **3.117** and **3.119** bearing appropriate functionality such that crosslinking may be induced through radical reaction between the desired side chains. Efforts began with synthesis of a universal glycosyl acceptor fragment amenable to accessing both disaccharide building blocks **3.116** and **3.118**, followed by divergent synthesis of donor fragments **3.123** and **3.124** for combination with the glycosyl acceptor. Successful glycosylation with **3.123** gave disaccharide intermediate **3.121**. Access to the required peptides was explored via a universal route; new methodology was also employed to investigate synthesis of related peptides that may enhance reactivity. These processes are discussed in more detail in the following sections.

(i) Synthesis of Glycosyl Acceptor

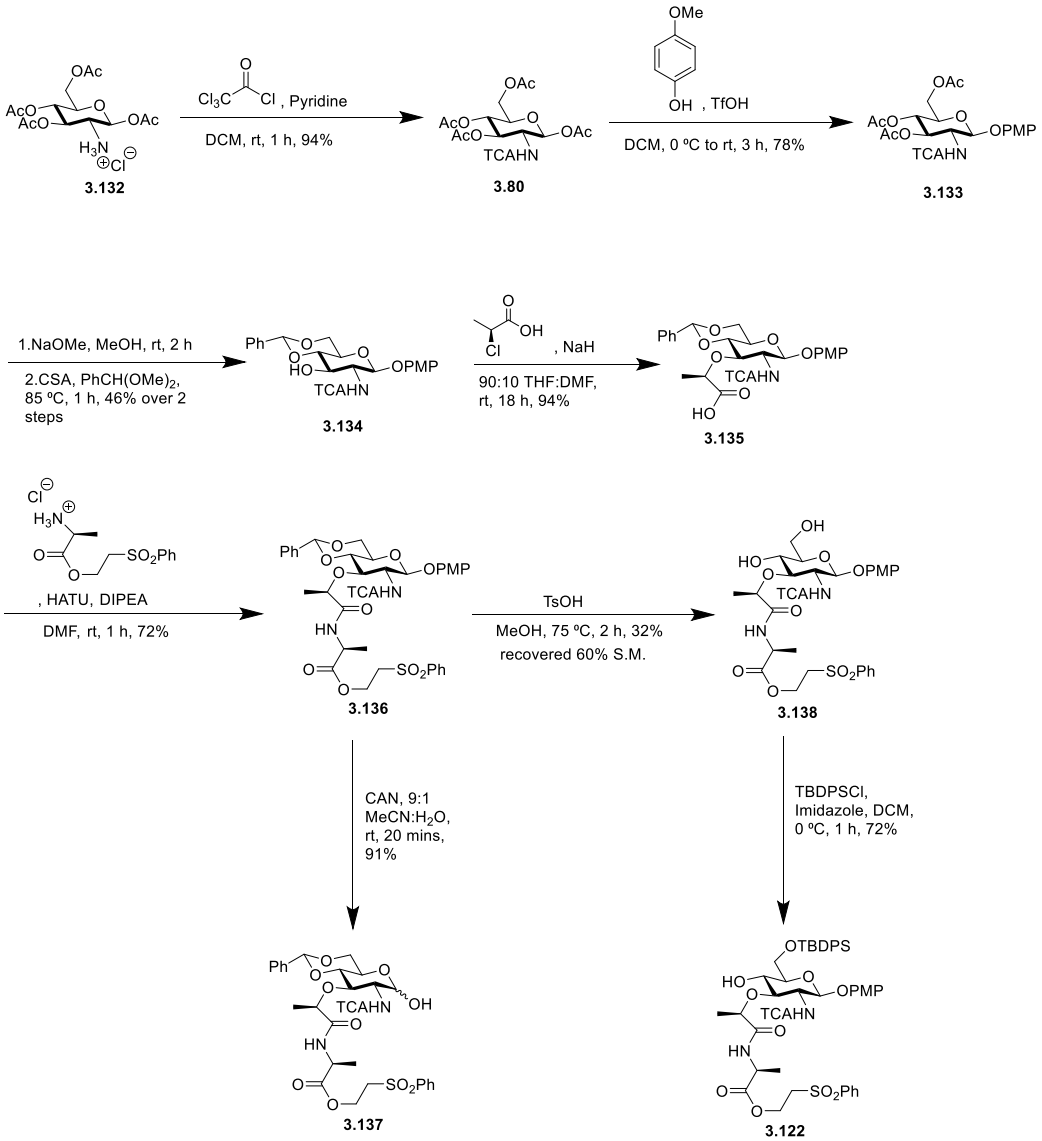


Figure 3.25 – Synthesis of universal glycosyl acceptor

Preparation of glycosyl acceptor **3.122** (Fig. 3.25) began with the installation of TCA as the amino protecting group through acylation of **3.132** with trichloroacetyl (TCA) chloride affording **3.80** in near quantative yield. Similarly to the Troc protecting group utilised in the synthesis of donors in chapter 2, TCA is capable of preventing axial nucleophilic attack through neighbouring group participation, providing β stereoselectivity [5]. Treatment with catalytic acid allowed for nucleophilic substitution with 4-OMe Phenol to generate the PMP glycoside **3.133** as a tough to separate mixture of anomers. On small scale both anomers were isolated to provide isolated yields in the ratio of 1:16 α:β; only the β anomer was taken forwards. PMP was chosen due to the possibility of direct conversion to a donor post glycosylation, with direct thioetherification having been reported [38]. Whilst it is possible to directly carry

thioglycosides through glycosylations using conditions that activate the desired GlcNAc donor selectively i.e. activation of sulfoxides with Triflic anhydride [15], it was thought that it would be sensical to construct the NAG-NAM disaccharide using sulfides due to observed success with a similar acceptor in chapter 2. Methanolysis and transacetalisation gave **3.134** in 46% yield, selectively exposing the 3 OH for alkylation. Whilst conversion was near quantative, purification proved tricky due to the low solubility of the partially protected sugar and modest amounts of **3.134** were isolated as pure. Lactoylation ensued to generate the MurNAc structure **3.135** in an excellent 94% yield. Similarly to the lactoylation discussed in chapter 2, the reaction efficiency was greatly aided by adding small amounts of DMF as a co-solvent to improve solubility. To the lactoyl, was coupled the PSE protected L-Ala chloride salt to give **3.136**. Amide coupling was achieved with HATU and DIPEA in a 72% yield. Whilst it may be possible to convert the PMP to a thioether directly as in [38], this work has not been reproduced on more complex substrates bearing rarer protecting groups. In the incident that this reaction would not work, alternate conditions to install donor functionality would have to be employed. To prepare for this possibility the removal of the PMP group was tested with widely reported oxidative cleavage conditions [44]. Treatment of **3.136** with ceric ammonium nitrate (CAN) in wet MeCN furnished the hemiacetal **3.137** in 91% yield as a mixture of anomers, 4:1 α:β. Limited amounts of material prevented full assignment of the β anomer by NMR, however the ratio was able to be determined through integration of the anomeric H peaks. Acid catalysed acetal hydrolysis gave diol **3.138** in a 30% yield. Sluggish removal of methanol prior to purification allowed for reversal of the reaction and regeneration of starting material. This starting material was recovered in 60% yield giving only 30% product. The 6 OH was then selectively capped as a silyl ether with TBDPS-Cl and imidazole to give acceptor **3.122** in 72% yield.

(ii) Divergent Synthesis of Glycosyl Donors

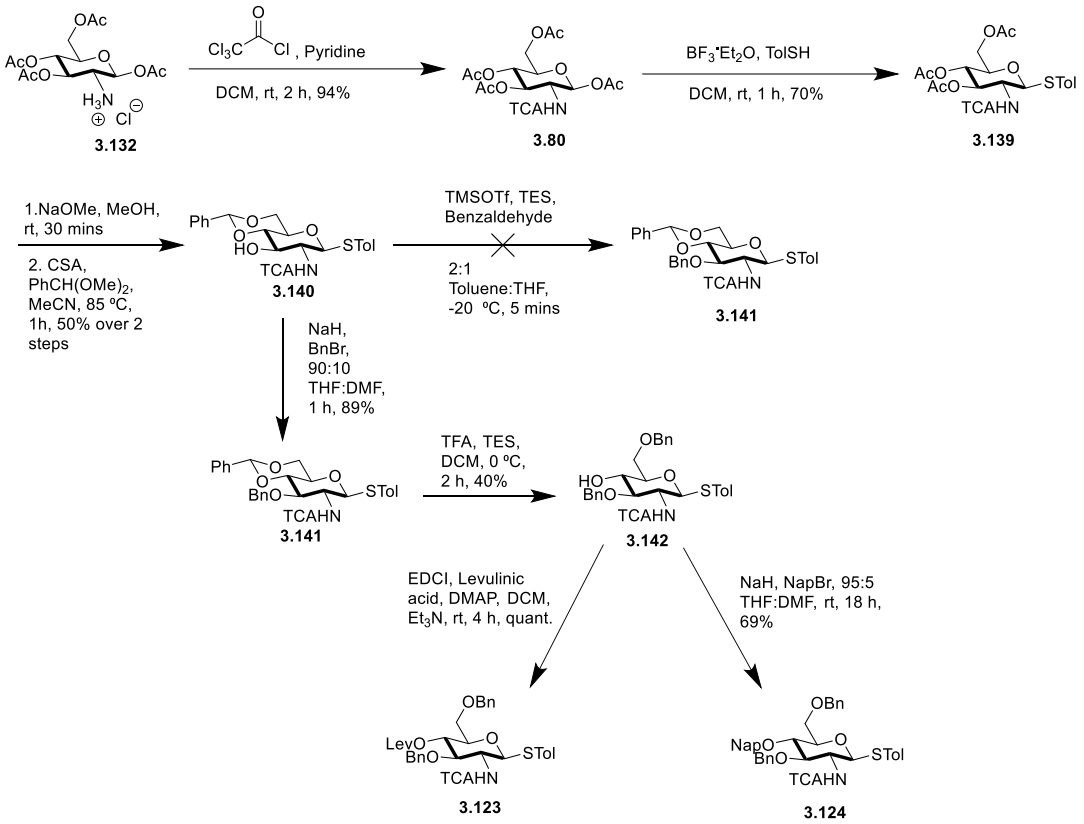


Figure 3.26 – Divergent synthesis of donor fragments

With acceptor **3.122** in hand, attention was turned to the synthesis of the GlcNAc donor fragments (Fig. 3.26). Known intermediate **3.142** has previously been used to access 4-OFmoc protected donors [31]. It was hypothesised that **3.142** could be used divergently to yield both desired donors. Thioglycoside **3.139** was prepared from Lewis acid promoted nucleophilic substitution of **3.80** with 4-methyl benzene thiol to afford **3.139** in 70% yield. Methanolysis and acetal formation gave **3.140**. As occurred with preparation of the acceptor, conversion was quantative, however isolation proved challenging. At first, it was attempted to use material that was 90% pure for reductive benzylation. The hope was that the impurities from the previous step would be inert under these conditions and that the benzylated product would be more soluble and easier to purify. Unfortunately, the reaction produced a messy mixture (numerous products observed by TLC) on addition of TMSOTf and as a result the starting material was recolumned to yield 50% of pure **3.140**. Benzylation was successfully achieved under basic conditions through the use of NaH and benzyl bromide, giving **3.141** in 89% yield. Regioselective acetal opening with TFA and TES was utilised to give the free 4 OH product, **3.142**. As was observed in chapter 2 significant amounts of the respective diol (22%) was generated as a side product. Donor **3.123** was prepared through esterification with

levulinic acid, EDCI and DMAP. The reaction required either near stoichiometric quantities of DMAP or an Et_3N additive to reach completion. The other donor **3.124** was successfully accessed through alkylation with NapBr and NaH in a 69% yield.

(iii) Efforts Towards Accessing SOMOphilic Amino Acids

An allyl glycine acceptor **3.144** was accessed through protection as a benzoate ester (Fig. 3.27). The transformation was achieved through use of K_2CO_3 as a base and benzyl bromide as a benzylating agent. Use of the allyl glycine derivative as a radical acceptor produced worries due to presumed poor reactivity with nucleophilic alkyl radicals. It was sought to access **3.146**, as the carbonyl should stabilise the alpha centred radical generated in the product and lower the energy of the transition state, hence improving the reactivity. Synthesis of this compound has been reported prior; however, the authors utilise a diazo β keto ester starting material subjected to Rh catalysed NH insertion chemistry [45]. Such an approach is less attractive due to the inconvenience of accessing the reactants. It was thought that it might be possible to synthesise **3.146** directly from **3.144** through allylic oxidation methods. Riley oxidation is a widely employed strategy to access allylic alcohols [46], which can be further oxidised to α, β unsaturated carbonyls with MnO_2 [47]. As such the reaction was attempted using sub stoichiometric quantities of SeO_2 with *tert*-Butyl hydroperoxide (TBHP) as a co-oxidant. The reaction produced no conversion by TLC.

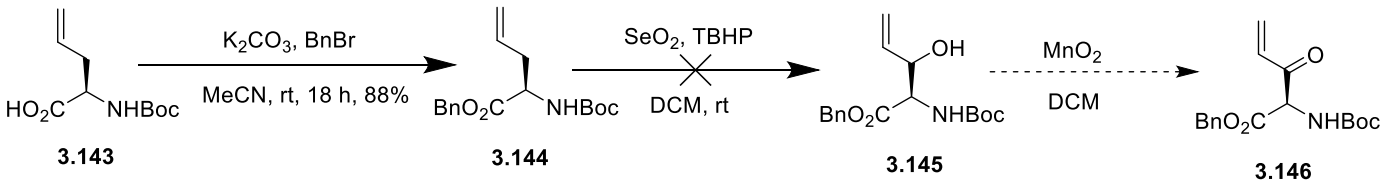


Figure 3.27 – Synthesis of protected radical acceptor amino acids

Similar to the above, introduction of vinylic substituents should improve the rate of reactions through lowering the energy of associated transition states. It was sought to access a range of derivatives (Fig. 3.28) that met this condition. The fluorinated analogue was chosen due to close resemblance of the native structure. The phenyl analogue was chosen due to easy commercial accessibility of the bromo styrene coupling partner making it an ideal model reaction. The phosphonate and sulfone derivatives were chosen based on our groups previous work documenting use of similar phosphonates and sulfones as radical acceptors [2]. The fluorinated and phenyl derivatives have previously been accessed [48, 49], however the syntheses are either laborious or require uncommon reagents and conditions. Additionally, preparation of the phosphonate and sulfone compounds have not been reported to the best of my knowledge. It was thought it might be possible to access all the desired targets from a universal approach.

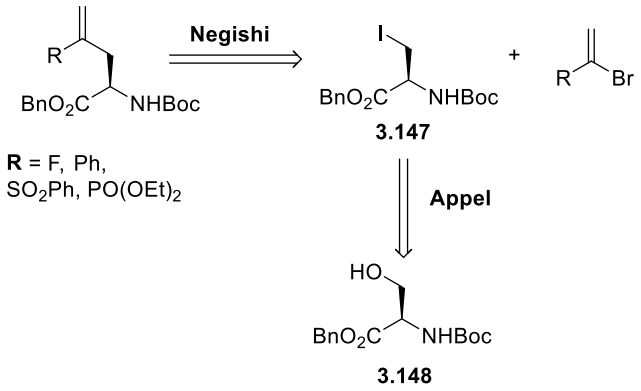


Figure 3.28 – Retrosynthesis of alternate SOMOphilic amino acids

The Negishi coupling is a renowned C-C bond forming reaction that makes use of a Pd(0) species to couple an alkyl iodide or bromide with either aryl or vinylic iodides, bromides or triflates via an organozinc intermediate [50]. The Negishi coupling has been applied to amino acids bearing an appropriate halide side chain, nominally in the synthesis of tryptophan analogues [51]. **3.147** was accessed through an Appel reaction in accordance with previously published procedure (Fig. 3.29) [52]. **3.147** was then treated with excess Zn and catalytic iodine as means of Zn activation under anhydrous conditions. Modest conversion to the organozinc species was observed by TLC at which point bis(dibenzylideneacetone)palladium(0) ($Pd(dba)_2$) precatalyst, Tri(o-tolyl)phosphine ($P(o\text{-}tol)_3$) ligand and bromostyrene coupling partner were added and the reaction heated to 50 °C. The Pd(0) complex was chosen on the basis that tolyl ligands improve oxidative addition into Sp^2 alkyl halide bonds relative to $Pd(Ph_3)_4$ [53]. The reaction was unsuccessful with isolated products not corresponding to the desired structure, additionally examination of the crude HMBC did not show desired correlation between possible beta CH_2's and olefinic and aromatic carbons. Further work should aim to improve formation of the organozinc intermediate through alternate activation procedures and trial different catalysts.

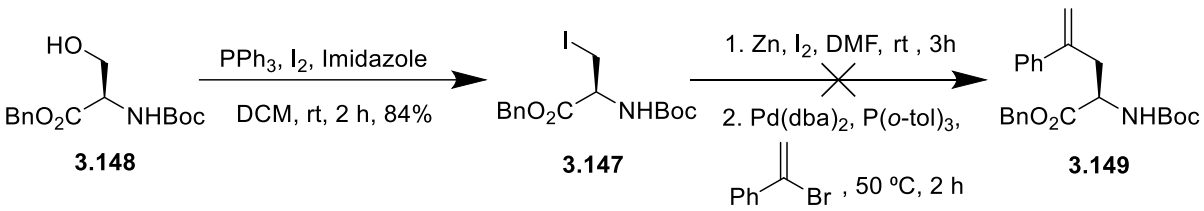


Figure 3.29 – Attempted synthesis of amino acid bearing vinylic phenyl substituent

(iv) Efforts Towards the Synthesis of Tripeptide Radical Donor

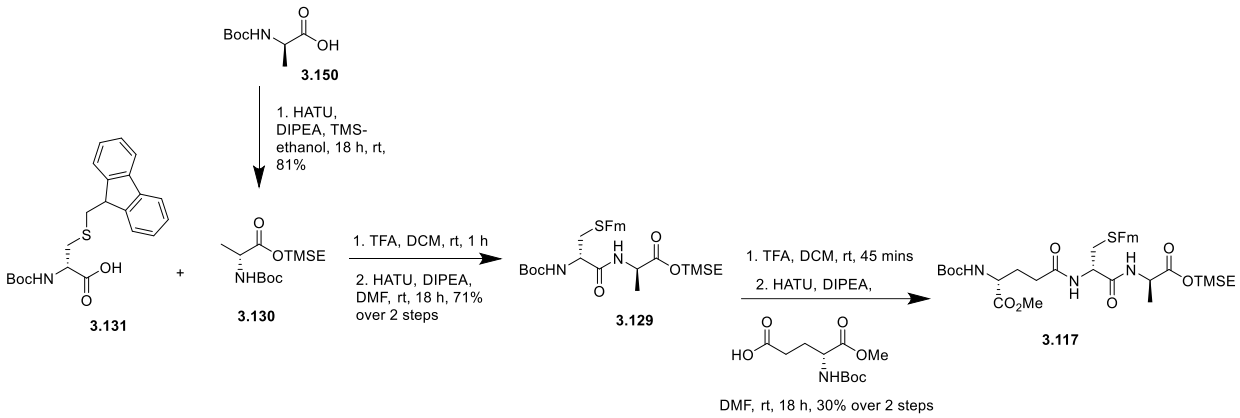
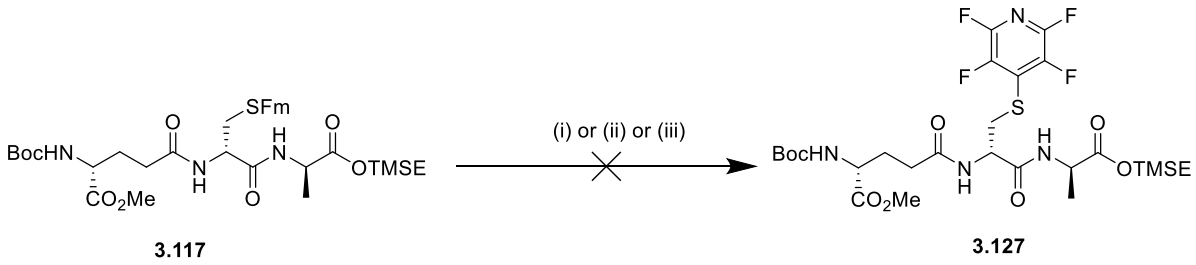


Figure 3.30 – Synthesis of precursor to radical donor tripeptide

The synthesis of tripeptide **3.117** began with protection of the carboxyl group of Boc-D-Ala-OH as a TMSE ester (Fig. 3.30). Esterification with HATU, DIPEA and trimethylsilyl (TMS) ethanol afforded **3.130** in 81% yield. Use of 20% TFA in DCM allowed chemo selective removal of the Boc protecting group; the TMSE ester has been noted to be labile under more acidic conditions [54]. The deprotected amine was then coupled to Boc-L-Cys(Fm)-OH with HATU and DIPEA in 71% yield. The dipeptide was further elongated to form tripeptide **3.117** in 30% yield through the aforementioned Boc deprotection and amide coupling approach using Boc-D-Glu(OH)-OMe.



(i) 4-Me Piperidine, Pentafluoropyridine, MeCN, rt, 1 h **(ii)** DIPEA, Pentafluoropyridine, 1:1 MeCN:DMF , rt, 18 h **(iii)** DBU, Pentafluoropyridine, 1:1 MeCN:DMF , -20 ºC, 10 mins

Figure 3.31 – Attempted one pot Fm deprotection and Arylation reactions

It was aimed to establish one pot deprotection and arylation conditions in solution prior to on resin reaction (Fig. 3.31). One pot deprotection and treatment with electrophiles has been reported by other groups in the cases of intramolecular Michael addition [55] and 2-(trimethylsilyl)ethoxycarbonyl (TEOC) thiocarbamate formation [56]. Piperidine is commonly used as base to remove the thioether [57], as such testing of conditions began with treatment with 4-Me piperidine and pentafluoropyridine in MeCN. The reaction did not produce the

desired product, however Fm removal was successful. The identity of the product has not yet been determined (Fig. 3.32). ^{19}F NMR indicates 3 environments in a 1:1:1 ratio suggesting a second substitution on the ring has taken place. The ^{1}H NMR shows additional environments that would suggest 4-Me piperidine as the nucleophile in the second substitution, however neither the mass of the desired product or possible disubstituted product were detectable by HRMS. Assuming the product of the reaction is a result of additional substitution, more poorly nucleophilic bases were trialled to circumvent such an issue. Use of DIPEA resulted in negligible conversion and use of DBU produced no reaction due to arylation of the DBU (Fig. 3.32) even at low temperature (-20 °C). The identity of the arylated product was confirmed through ^{1}H NMR and HRMS and likely proceeds through iminium formation and consequent hydration. This observation further supports the idea that nucleophilic addition to the electron deficient ring is a problem in such one pot reactions. Further attempts should aim to trial more hindered bases such as a 2,6- ditert butyl piperidine derivative or hexamethyldisilazide (HMDS).

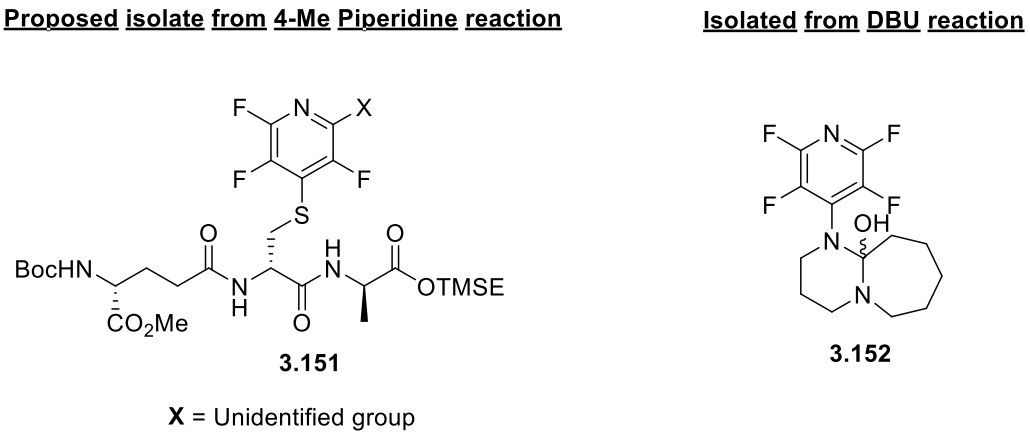


Figure 3.32 – Products from one pot Fm deprotection and arylation reactions

(v) Efforts Towards Synthesis of Disaccharide Blocks for Accessing Peptidoglycan Fragments

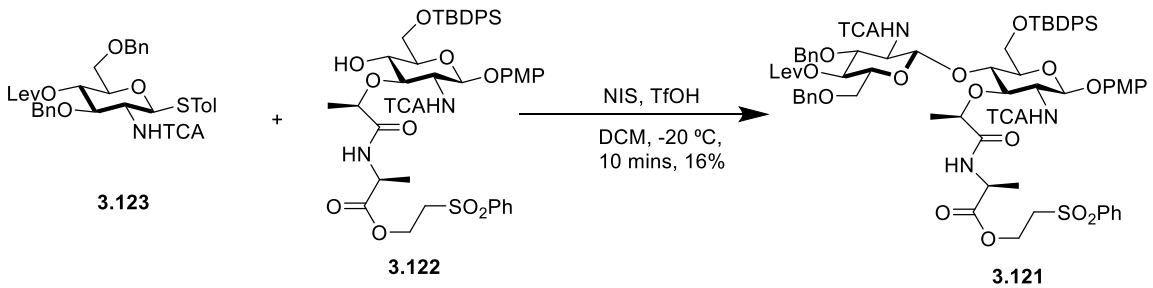


Figure 3.33 – Synthesis of disaccharide intermediate

With the required monosaccharide fragments in hand, glycosylation of donor **3.123** with acceptor **3.122** furnished the desired disaccharide **3.121** in 16% isolated yield (Fig. 3.33). The reaction proceeds vigorously relative to the other NAG-NAM fragment synthesised in chapter 2. This difference can be attributed to donor electronics with only one electron withdrawing group being present in **3.123** relative to the triacetyl donors used in chapter 2 (Fig. 3.34). The presence of fewer electron withdrawing groups results in a weaker disarming effect and destabilisation of the positively charged intermediates and greater electrophilic character [58].

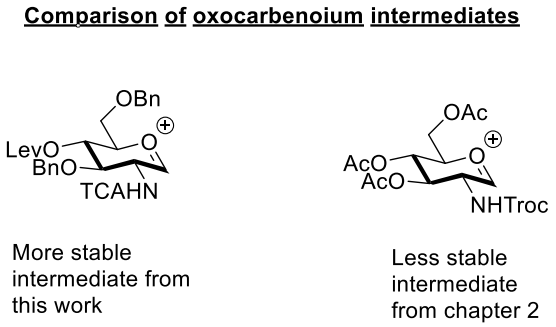


Figure 3.34 – Comparison of reactive donor intermediates

Whilst the isolated yield remains poor a sample that is ~95% pure was collected accounting for a further 20% of expected material. The identity of the inseparable impurity is difficult to determine due to the overlap of most of the peaks with the environments in the desired product. I had worries that the impurity may be the α glycoside resulting from a non-stereospecific reaction. This worry stemmed from differences in the degree of TCA participation in comparison to the Troc used in chapter 2. Examination of the ^{1}H and ^{13}C NMR spectra do not indicate the presence of an α anomeric H environment so this is unlikely to be the case. The impurity could instead stem from donor dimerisation following hydrolysis, as donor hydrolysis product was also isolated. Another less likely possibility is deprotection of the PMP group under acidic conditions and consequent formation of the 1,1-glycoside. If this was the case exploration of other glycosylation systems may prove beneficial due to the importance of the PMP and Nap protecting group pair in the proposed strategy. Future work could aim to explore mildly acidic Au(I) promoted glycosylation with alkyne donors (Fig. 3.35). The use of such homogenous gold catalysts has been documented on solid phase [59, 60] and has recently been applied to access oligosaccharides [61].

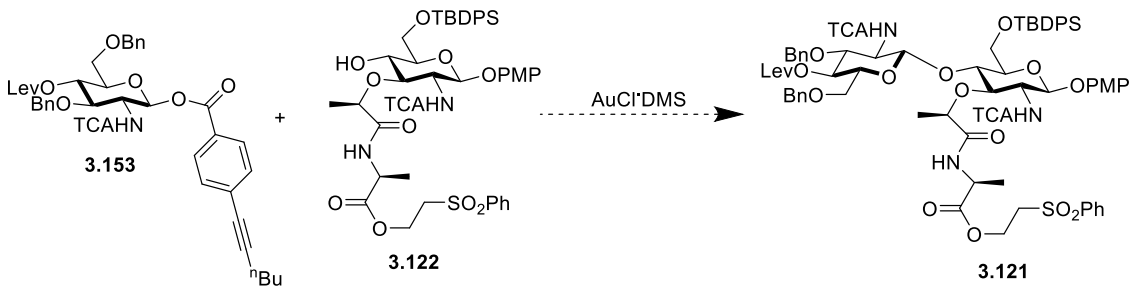


Figure 3.35 – Alternate milder glycosylation conditions for accessing desired disaccharides

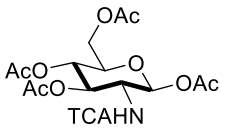
Conclusions and Future Directions

This chapter describes the syntheses of key building blocks for the modular assembly of crosslinked peptidoglycan fragments. In order to synthesise a required disaccharide intermediate **3.121**, novel MurNAc acceptor **3.122** was accessed in 5.3% yield over 7 linear steps, and novel GlcNAc donors **3.123** and **3.124** were accessed concisely from a known intermediate. Disaccharide **3.121** is of particular significance owing to the high degree of orthogonal protection allowing for selective elongation and peptide attachment. The synthesis of peptide building blocks with suitable crosslinking character was also investigated. A SOMOphilic amino acid was prepared for use, and methodology for universal access to alternate SOMOphilic amino acids was explored but proved unfruitful. Substantial progress was made towards accessing radical donor tripeptide with successful synthesis of precursor **3.117**, however, attempts at one pot deprotections and arylations were unsuccessful.

Future work should aim to progress the syntheses of disaccharide and peptide building blocks. Key steps in this will be the optimisation of glycosylation conditions, perhaps trialling milder systems, and investigation of stepwise deprotection and arylation of tripeptide **3.117** to yield a radical donor species for preliminary crosslinking studies. Successful realisation of these steps will provide building blocks amenable to the synthesis of peptidoglycan fragments that can be crosslinked by light. Design of fragments possessing this spatial and temporal control over substrate properties may allow for consequent control over biological immune activity and advance vaccine design.

Experimental

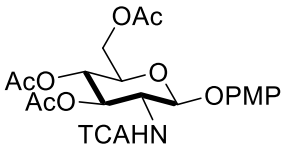
(2S,3R,4R,5S,6R)-6-(acetoxymethyl)-3-(2,2,2-trichloroacetamido)tetrahydro-2H-pyran-2,4,5-triyl triacetate [31]



3.80

(2S,3R,4R,5S,6R)-2,4,5-triacetoxy-6-(acetoxymethyl)tetrahydro-2H-pyran-3-aminium, (20 g, 51.8 mmol) was suspended in 100 mL dry DCM and 20.8 mL dry Pyridine under Ar. The suspension was cooled to 0 °C and Trichloroacetyl chloride (1.75 mL, 15.54 mmol) was added dropwise. The suspension rapidly became a yellow solution. The solution was stirred for 30 mins and warmed to ambient temperature. After 1 hr the reaction was diluted with 200 mL DCM and washed with 1 x 100 mL sat. $NaHCO_3$ sol. The aqueous layer was back extracted 2 x 100 mL DCM and the combined layers dried over anhydrous Na_2SO_4. The solution was concentrated *in vacuo*. Purification via flash column chromatography (SiO_2, gradient 85:15 pet. ether:EtOAc to 50:50 pet. ether:EtOAc) yielded **3.80** (24.11 g, 94%) as a white solid. ^{1}H NMR (400 MHz, $CDCl_3$) δ 7.00 (d, *J* = 9.4 Hz, 1H, N**H**TCA), 5.80 (d, *J* = 8.7 Hz, 1H, **H1**), 5.32 (dd, *J* = 10.8, 9.4 Hz, 1H, **H3**), 5.17 (t, *J* = 9.7 Hz, 1H, **H4**), 4.34 – 4.23 (m, 2H, **H2**, **H6**), 4.19 – 4.07 (m, 1H, **H6**), 3.87 (ddd, *J* = 10.0, 4.8, 2.2 Hz, 1H, **H5**), 2.11 (s, 3H), 2.10 (s, 3H, OAc-**H**), 2.07 (s, 3H, OAc-**H**), 2.05 (s, 3H, OAc-**H**). ^{13}C NMR (101 MHz, $CDCl_3$) δ 171.67, 170.74, 169.44, 162.45, 92.37, 92.02, 73.19, 72.07, 68.21, 61.89, 60.52, 54.42, 21.14, 20.81 (d, *J* = 2.5 Hz), 20.62 (d, *J* = 5.0 Hz), 14.28. $[\alpha]_D^{25}$ = +7.4 (0.27 g/100 mL, DCM). LRMS (ESI) Calcd for $C_{16}H_{20}Cl_3NNaO_{10}^+$ [M+Na] = 514.00 found 513.87.

(2R,3S,4R,5R,6S)-2-(acetoxymethyl)-6-(4-methoxyphenoxy)-5-(2,2,2-trichloroacetamido)tetrahydro-2H-pyran-3,4-diyl diacetate [62]



3.133

3.80 (12.06 g, 24.47 mmol) was dissolved in 75 mL dry DCM under Ar and added to a flame dried flask containing activated 3Å molecular sieves under Ar. *p*-methoxy phenol (6.07 g, 48.94 mmol) was added

and the solution cooled to 0 °C. TfOH (0.86 mL, 9.79 mmol) was added slowly, and the solution stirred for 30 mins. The reaction was warmed to ambient temperature and left to stir for 3 hrs. The reaction was diluted with 120 mL DCM and washed with 1x 60 mL sat. $NaHCO_3$ sol. The organic layer was dried over anhydrous Na_2SO_4 and concentrated *in vacuo*. Purification via flash column chromatography (SiO_2, gradient 90:10 pet. ether:EtOAc to 50:50 pet. ether:EtOAc) yielded **3.133** (10.71 g, 78%) as a white solid. ^{1}H NMR (400 MHz, $CDCl_3$) δ 6.97 (dd, *J* = 10.0, 7.8 Hz, 3H, N**H**TCA, PMP-Ar-**H**), 6.83 – 6.74 (m, 2H, PMP-Ar-**H**), 5.42 (dd, *J* = 10.7, 9.2 Hz, 1H, **H3**), 5.17 (t, *J* = 9.6 Hz, 1H, **H4**), 5.09 (d, *J* = 8.3 Hz, 1H, **H1**), 4.30 (dd, *J* = 12.3, 5.4 Hz, 1H, **H6**), 4.26 – 4.15 (m, 2H, **H2**, **H6**), 3.84 (ddd, *J* = 9.9, 5.4, 2.5 Hz, 1H, **H5**), 2.09 (s, 3H, OAc-**H**), 2.05 (s, 3H, OAc-**H**), 2.02 (s, 3H, OAc-**H**). ^{13}C NMR (101 MHz, $CDCl_3$) δ 171.02, 170.75, 169.45, 162.30, 156.08, 151.15, 119.21, 114.67, 100.57, 92.39, 89.68, 72.23, 71.57, 68.59, 62.24, 56.03, 55.75, 20.84, 20.67 (d, *J* = 3.5 Hz). $[\alpha]_D^{25}$ = -4.24 (0.37 g/100 mL, DCM)

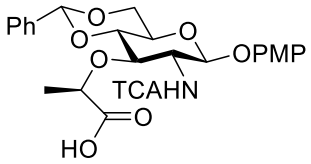
2,2,2-trichloro-N-((2R,4aR,6S,7R,8R,8aS)-8-hydroxy-6-(4-methoxyphenoxy)-2-phenylhexahydropyrano[3,2-d][1,3]dioxin-7-yl)acetamide [62]



3.134

3.133 (10.71 g, 19.2 mmol) was suspended in 75 mL dry MeOH under Ar. A solution of 25% NaOMe in MeOH (0.88 mL, 3.4 mmol) was added dropwise. The reaction was left to stir for 2 hrs with all solids dissolving after 10 mins. Amberlyst™ 15(H) resin was carefully added to bring the solution to pH_7. The resin was filtered, the filtrate concentrated *in vacuo* and dried on high vac. overnight. The resultant solid and CSA (1.12 g, 4.8 mmol) were dissolved in 100 mL dry MeCN under Ar. $PhCH(OMe)_2$ (14.41 mL, 96 mmol) was added and the reaction heated to 85 °C. After 10 mins of stirring the reaction was quenched with the addition of Et_3N and concentrated *in vacuo*. Purification via flash column chromatography (SiO_2, 98:2 DCM:MeOH) yielded **3.134** (4.54 g, 46%) as a white solid. ^{1}H NMR (400 MHz, DMSO) δ 9.01 – 8.94 (m, 1H, N**H**TCA), 7.52 – 7.43 (m, 2H, O_2CHPh-Ar-**H**), 7.43 – 7.34 (m, 3H, O_2CHPh-Ar-**H**), 6.99 – 6.91 (m, 2H, PMP-Ar-**H**), 6.90 – 6.81 (m, 2H, PMP-Ar-**H**), 5.66 (s, 1H, PhC**H**O_2), 5.63 – 5.59 (m, 1H, 3-O**H**), 5.21 – 5.11 (d, *J* = 8.1 Hz, 1H, **H1**), 4.27 (dd, *J* = 10.1, 4.9 Hz, 1H, **H5**), 3.88 (dq, *J* = 7.0, 3.4 Hz, 2H, **H2**, **H3**), 3.82 (t, *J* = 10.1 Hz, 1H, **H6**), 3.70 (s, 3H, PMP-Me-**H**), 3.59 (t, *J* = 9.0 Hz, 1H, **H4**), 3.49 (td, *J* = 9.7, 4.9 Hz, 1H, **H5**). ^{13}C NMR (101 MHz, DMSO) δ 161.72, 154.93, 151.15, 137.63, 128.90, 128.05, 118.29, 114.54, 100.69, 93.07, 81.01, 69.74, 67.68, 66.15, 58.04, 55.35. $[\alpha]_D^{25}$ = -23.15 (0.22 g/100 mL, Acetone) HRMS (ESI) Calc'd for $C_{22}H_{23}Cl_3NO_7^+$ [M+H] = 518.054 found 518.055

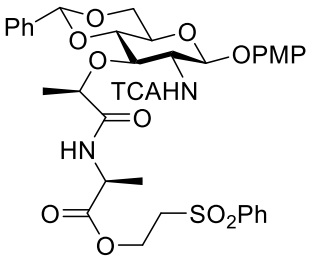
(R)-2-(((2R,4aR,6S,7R,8R,8aS)-6-(4-methoxyphenoxy)-2-phenyl-7-(2,2,2-trichloroacetamido)hexahydropyrano[3,2-d][1,3]dioxin-8-yl)oxy)propanoic acid



3.135

3.134 (2.95 g, 4.99 mmol) was dissolved in 45 mL 9:1 dry THF:DMF mix. A 60% dispersion of NaH in mineral oil (399 mg, 9.88 mmol) was added and the reaction stirred for 10 mins. The solution was cooled to 0 °C and (*2S*)- chloropropionic acid (1.73 mL, 19.96 mmol) was added dropwise. The solution was warmed to ambient temperature and left to stir for 15 mins. A second portion of NaH in mineral oil (998 mg, 24.95 mmol) was added and the reaction left to stir overnight. The reaction was quenched with dropwise addition of ice cold H_2O, and acidified to pH_3 by dropwise addition of 1.0M HCl. The solution was poured into 200 mL stirring ice water mix and the precipitate recovered by filtration. The solid was washed with 3 x 50 mL H_2O, 3 x 50 mL pet. ether, azetroped with toluene and dried on high vac. overnight to yield **3.135** (3.17 g, 94%) as a white solid. ^{1}H NMR (400 MHz, DMSO) δ 12.57 (bs, 1H, MurNAc-COO**H**), 7.41 (dddd, *J* = 11.8, 7.6, 5.6, 2.8 Hz, 5H, O_2CHPh-Ar-**H**), 6.98 – 6.91 (m, 2H, PMP-Ar-**H**), 6.90 – 6.81 (m, 2H, PMP-Ar-**H**), 5.74 (s, 1H, PhC**H**O_2), 5.19 (d, *J* = 8.1 Hz, 1H, **H1**), 4.33 – 4.23 (m, 2H, , MurNAc-$\mathbf{H_\alpha}$, **H6**), 4.08 – 3.98 (m, 1H, **H3**), 3.94 (dt, *J* = 10.1, 8.3 Hz, 1H, **H2**), 3.82 (q, *J* = 9.5 Hz, 2H, **H4**, **H6**), 3.70 (s, 3H, PMP-Me-**H**), 3.55 (td, *J* = 9.8, 5.0 Hz, 1H, **H5**), 1.27 (d, *J* = 6.8 Hz, 3H, MurNAc-Me-**H**). ^{13}C NMR (101 MHz, DMSO) δ 173.67, 161.57, 154.99, 151.06, 137.47, 128.81, 128.17, 125.79, 118.36, 114.54, 100.76, 100.07, 92.97, 80.95, 76.56, 74.75, 67.62, 65.64, 56.38, 55.35, 18.77. $[\alpha]_D^{25}$ = -8.80 (0.50 g/100 mL, Acetone). HRMS (ESI) Calc'd for $C_{25}H_{26}Cl_3NNaO_9^+$ [M+Na] = 612.057 found 612.054. IR (Transmittance) 3297, 2922, 2822, 1693, 1508, 1451, 1386, 1367, 1278, 1226, 1172, 1087, 1029, 1009, 967, 929, 875, 825, 760, 715 cm^{-1}

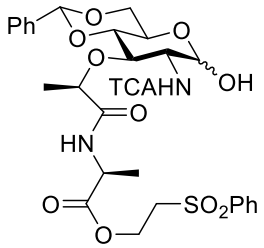
2-(phenylsulfonyl)ethyl ((R)-2-(((2R,4aR,6S,7R,8R,8aS)-6-(4-methoxyphenoxy)-2-phenyl-7-(2,2,2-trichloroacetamido)hexahydropyrano[3,2-d][1,3]dioxin-8-yl)oxy)propanoyl)-L-alaninate



3.136

3.135 (3.17 g, 5.35 mmol) and HATU (2.03 g, 5.35 mmol) were dissolved in 60 mL dry DMF under Ar and cooled to 0 °C. DIPEA (2.80 mL 16.05 mmol) was added slowly, and the solution left to stir for 10 mins. During this time a solution of (S)-1-oxo-1-(2-(phenylsulfonyl)ethoxy)propan-2-aminium chloride (6.96 mmol) in 40 mL dry DMF was prepared and added rapidly via syringe to the activated acid. The reaction was warmed to ambient temperature and left to stir for 1 hr. The reaction was concentrated *in vacuo* and the solid redissolved in 30 mL EtOAc. The solution was washed with 1 x 20 mL 1.0M HCl, the aqueous layer was back extracted with 1 x 20 mL EtOAc. The combined organic layers were washed with 1x 20 mL sat. $NaHCO_3$ sol., the aqueous layer was back extracted with 1 x 20 mL EtOAc. The combined organic layers were washed with 1 x 20 mL brine, dried over anhydrous Na_2SO_4 and concentrated *in vacuo*. Purification via flash column chromatography (SiO_2, 99:1 DCM:MeOH) yielded **3.136** (3.21 g, 72%) as a white solid. ^{1}H NMR (400 MHz, $CDCl_3$) δ 7.90 (dq, *J* = 8.3, 1.9 Hz, 3H, N**H**TCA, SO_2Ph-Ar-**H**), 7.70 – 7.61 (m, 1H, SO_2Ph-Ar-**H**), 7.61 – 7.50 (m, 2H, SO_2Ph-Ar-**H**), 7.50 – 7.40 (m, 2H, O_2CHPh-Ar-**H**), 7.39 – 7.30 (m, 3H, O_2CHPh-Ar-**H**), 6.94 (dd, *J* = 8.1, 2.4 Hz, 1H, Ala1-N**H**), 6.92 – 6.87 (m, 2H, PMP-Ar-**H**), 6.75 – 6.69 (m, 2H, PMP-Ar-**H**), 5.51 (s, 1H, PhC**H**O_2), 5.17 (d, *J* = 8.2 Hz, 1H, **H1**), 4.47 (qdd, *J* = 12.2, 6.6, 5.3 Hz, 2H, OC**H$_2$**), 4.39 – 4.31 (m, 1H, **H6**), 4.27 – 4.13 (m, 3H, MurNAc-**H$_\alpha$**, Ala1-**H$_\alpha$**, **H2**), 4.10 (dd, *J* = 10.1, 8.6 Hz, 1H, **H3**), 3.85 (t, *J* = 10.2 Hz, 1H, **H6**), 3.74 (d, *J* = 7.5 Hz, 4H, **H4**, PMP-Me-**H**), 3.59 (dtd, *J* = 19.3, 9.1, 4.4 Hz, 1H, **H5**), 3.50 – 3.34 (m, 2H, SC**H$_2$**), 1.40 (d, *J* = 6.7 Hz, 3H, MurNAc-Me-**H**), 1.32 (d, *J* = 7.2 Hz, 3H, Ala1-Me-**H**). ^{13}C NMR (101 MHz, $CDCl_3$) δ 172.48, 171.96, 163.09, 162.78, 155.82, 151.20, 139.13, 137.10, 134.34, 129.66, 129.18 (d, *J* = 9.1 Hz), 128.41, 128.15, 126.08, 118.92, 114.64, 101.44, 101.00, 92.68, 80.74, 78.11 (d, *J* = 16.4 Hz), 68.60, 66.53, 58.12 (d, *J* = 3.4 Hz), 55.69, 55.05, 48.24, 36.73, 31.68, 19.29, 17.38. $[\alpha]_D^{25}$ = -10.97 (0.31 g/100 mL, DCM) HRMS (ESI) Calc'd for $C_{36}H_{39}Cl_3N_2NaO_{12}S^+$ [M+Na] = 851.113 found 851.118. IR (Transmittance) 3308, 2981, 2882, 1760, 1696, 1658, 1536, 1509, 1462, 1447, 1389, 1372, 1344, 1309, 1297, 1170, 1142, 1085, 1027, 1003, 974, 824, 760, 747, 633, 594, 513 cm^{-1}

2-(phenylsulfonyl)ethyl ((R)-2-(((2R,4aR,7R,8R,8aS)-6-hydroxy-2-phenyl-7-(2,2,2-trichloroacetamido)hexahydropyrano[3,2-d][1,3]dioxin-8-yl)oxy)propanoyl)glycinate

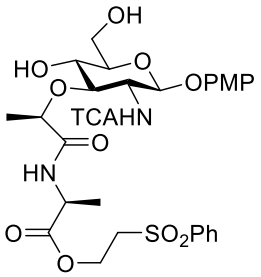


3.137

3.136 (10 mg, 0.012 mmol) was dissolved in 1 mL 9:1 MeCN:H_2O. CAN (19.7 mg, 0.036 mmol) was added, and the solution left to stir for 20 mins. The reaction was diluted with 10 mL DCM and extracted with 3 x 3 mL brine, dried over anhydrous Na_2SO_4, and concentrated *in vacuo*. Purification via flash column chromatography (SiO_2, gradient 100:0 DCM:MeOH to 98:2 DCM:MeOH) yielded **3.137** (7.9 mg, 91%). ^{1}H NMR (400 MHz, $CDCl_3$) δ 7.95 – 7.87 (m, 3H, Ar-**H**), 7.74 (d, *J* = 7.8 Hz, 1H, N**H**TCA), 7.70 –

7.64 (m, 1H, Ar-**H**), 7.62 – 7.52 (m, 3H, Ar-**H**), 7.46 (p, *J* = 3.9 Hz, 3H, Ar-**H**), 7.41 – 7.34 (m, 4H, Ar-**H**), 6.65 (d, *J* = 6.9 Hz, 1H, Ala1-N**H**), 5.58 (s, 1H, PhC**H**O_2), 5.46 (d, *J* = 3.6 Hz, 1H, **H1**), 4.59 – 4.33 (m, 2H, OC**H_2**), 4.29 (dd, *J* = 10.3, 4.8 Hz, 1H, **H6**), 4.25 – 4.04 (m, 4H, MurNAc-**H_α**, Ala1-**H_α**, **H2, H5**), 3.92 – 3.82 (m, 1H, **H3**), 3.82 – 3.67 (m, 2H, **H6**, **H4**), 3.55 – 3.37 (m, 2H, SC**H_2**), 1.38 (dd, *J* = 6.7, 5.5 Hz, 3H, MurNAc-Me-**H**), 1.31 (d, *J* = 7.2 Hz, 3H, Ala1-Me-**H**). ^{13}C NMR (101 MHz, $CDCl_3$) δ 172.43, 172.04, 134.15, 129.50, 128.33, 128.12, 125.98, 101.57, 91.77, 81.15, 77.85, 76.00, 63.22, 58.25, 55.67, 54.86, 48.04, 19.09, 17.17.

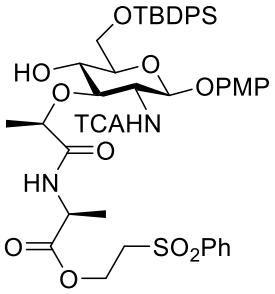
2-(phenylsulfonyl)ethyl ((R)-2-(((2R,3S,4R,5R,6S)-3-hydroxy-2-(hydroxymethyl)-6-(4-methoxyphenoxy)-5-(2,2,2-trichloroacetamido)tetrahydro-2H-pyran-4-yl)oxy)propanoyl)glycinate



3.138

3.136 (3.2 g, 3.85 mmol) and TsOH.H_2O (73 mg, 0.385 mmol) were suspended in 75 mL dry MeOH under Ar. The suspension was heated to 75 °C and stirred for 2 h. The reaction was concentrated in vacuo and purified via flash column chromatography (SiO_2, gradient 98:2 DCM:MeOH to 96:4 DCM:MeOH). **3.138** (908.9 mg, 32%) was obtained as a white solid. ^{1}H NMR (400 MHz, MeOD) δ 8.00 – 7.93 (m, 2H, SO_2Ph-Ar-**H**), 7.80 – 7.71 (m, 1H, SO_2Ph-Ar-**H**), 7.71 – 7.61 (m, 2H, SO_2Ph-Ar-**H**), 7.03 – 6.95 (m, 2H, PMP-Ar-**H**), 6.86 – 6.77 (m, 2H, PMP-Ar-**H**), 4.96 (d, *J* = 8.4 Hz, 1H, **H1**), 4.50 – 4.39 (m, 2H, OC**H_2**), 4.21 – 4.10 (m, 2H, MurNAc-**H_α**, **H2**), 4.06 (q, *J* = 7.3 Hz, 1H, Ala1-**H_α**), 3.94 (dd, *J* = 12.0, 2.3 Hz, 1H, **H6**), 3.75 (m, 1H, **H6**), 3.73 (s, 3H, PMP-Me-**H**), 3.67 – 3.55 (m, 4H, SC**H_2**, **H3**, **H4**), 3.46 (ddt, *J* = 9.6, 5.5, 2.5 Hz, 1H, **H5**), 1.42 (d, *J* = 6.7 Hz, 3H, MurNAc-Me-**H**), 1.27 (d, *J* = 7.3 Hz, 3H, Ala1-Me-**H**). ^{13}C NMR (101 MHz, MeOD) δ 173.73, 171.86, 163.01, 155.52, 151.73, 139.50, 133.92, 129.27, 127.89, 117.97, 114.14, 100.47, 92.87, 82.38, 78.00, 76.76, 68.80, 61.10, 58.25, 57.15, 54.68, 54.33, 17.78, 15.59. $[\alpha]_D^{25}$ = -12.00 (0.1 g/100 mL, DCM). HRMS (ESI) Calc'd for $C_{26}H_{36}Cl_3N_2O_{12}S^+$ [M+H] = 741.105 found 741.168. IR (Transmittance) 3310, 2981, 2885, 1695, 1656, 1533, 1507, 1448, 1338, 1215, 1142, 1082, 1028, 1009, 823, 758, 730, 689, 657 cm^{-1}

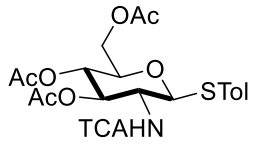
2-(phenylsulfonyl)ethyl ((R)-2-(((2R,3S,4R,5R,6S)-2-(((tert-butyldiphenylsilyl)oxy)methyl)-3-hydroxy-6-(4-methoxyphenoxy)-5-(2,2,2-trichloroacetamido)tetrahydro-2H-pyran-4-yl)oxy)propanoyl)glycinate



3.122

3.138 (908.9 mg, 1.23 mmol) and imidazole (249.9 mg, 3.67 mmol) were dissolved in 20 mL dry DCM under Ar. The solution was cooled to 0 °C and TBDPSCl (0.635 mL, 2.45 mmol) was added. The solution was left to stir for 1 h. The reaction was diluted with 20 mL DCM and washed with 1 x 12 mL 0.2M HCl, the aqueous layer was back extracted with 1 x 12 mL DCM. The combined organic layers were dried over anhydrous Na_2SO_4 and concentrated *in vacuo*. Purification via flash column chromatography (SiO_2, gradient 85:15 DCM:EtOAc to 75:25 DCM:EtOAc) yielded **3.122** as a white solid (871 mg, 72%). ^{1}H NMR (400 MHz, $CDCl_3$) δ 7.95 – 7.87 (m, 2H, SO_2Ph-Ar-**H**), 7.72 – 7.62 (m, 5H, SO_2Ph-Ar-**H**, TBDPS-Ar-**H**), 7.61 – 7.51 (m, 2H, SO_2Ph-Ar-**H**), 7.47 – 7.30 (m, 6H, TBDPS-Ar-**H**), 7.22 (d, *J* = 8.5 Hz, 1H, N**H**TCA), 7.00 – 6.89 (m, 3H, PMP-Ar-**H**, Ala1-N**H**), 6.76 – 6.67 (m, 2H, PMP-Ar-**H**), 5.02 (d, *J* = 8.2 Hz, 1H, **H1**), 4.56 – 4.39 (m, 2H, OC**H$_2$**), 4.32 (q, *J* = 7.2 Hz, 1H, Ala1-**H$_\alpha$**), 4.25 (q, *J* = 6.6 Hz, 1H, MurNAc- **H$_\alpha$**), 4.09 – 3.88 (m, 3H, **H2**, **H6**, **H6**), 3.87 – 3.74 (m, 2H, **H3**, **H4**), 3.73 (s, 3H, PMP-Me-**H**), 3.55 (dt, *J* = 9.2, 4.7 Hz, 1H, **H5**), 3.49 – 3.35 (m, 2H, SC**H$_2$**), 3.21 (bs, 1H, 4-O**H**), 1.45 (d, *J* = 6.7 Hz, 3H, MurNAc-Me-**H**), 1.35 (d, *J* = 7.2 Hz, 3H, Ala1-Me-**H**), 1.06 (s, 9H, TBDPS-^{t}Bu-**H**). ^{13}C NMR (101 MHz, $CDCl_3$) δ 172.41, 171.98, 162.55, 155.54, 151.32, 139.06, 135.62 (d, *J* = 8.0 Hz), 134.22, 132.91, 132.66, 129.89 (d, *J* = 2.6 Hz), 129.55, 128.05, 127.83, 118.66, 114.52, 100.02, 92.53, 80.67, 75.38, 71.45, 64.33, 58.10, 57.23, 55.62, 54.95, 48.01, 26.81, 19.23, 18.96, 17.34. $[\alpha]_D^{25}$ = -18.57 (0.14 g/100 mL, DCM). HRMS (ESI) Calc'd for $C_{45}H_{54}Cl_3N_2O_{12}SSi^+$ [M+H] = 979.222 found 979.220. IR (Transmittance) 3295, 2931, 2885, 1693, 1593, 1538, 1507, 1450, 1428, 1386, 1307, 1246, 1172, 1085, 1072, 824, 759, 747, 695 cm^{-1}

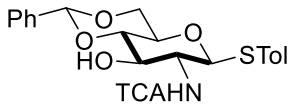
(2R,3S,4R,5R,6S)-2-(acetoxymethyl)-6-(p-tolylthio)-5-(2,2,2-trichloroacetamido)tetrahydro-2H-pyran-3,4-diyl diacetate [31]



3.139

3.80 (12.055 g, 24.47 mmol) and *p*-thiocresol (6.08 g, 48.94 mmol) were dissolved in 75 mL dry DCM under Ar and cooled to 0°C. $BF_3{\cdot}Et_2O$ (9.06 mL, 73.41 mmol) was added slowly and the solution turned dark red. The reaction was warmed to ambient temperature and left to stir for 1 hr. The solution was diluted with 100 mL DCM and washed with 100 mL sat. $NaHCO_3$ sol. The organic layer was dried over anhydrous Na_2SO_4 and concentrated *in vacuo*. Purification via flash column chromatography (SiO_2, gradient 85:15 toluene:EtOAc to 70:30 toluene:EtOAc) yielded **3.139** (9.44 g, 69%) as a white solid. ^{1}H NMR (400 MHz, $CDCl_3$) δ 7.44 – 7.37 (m, 2H, STol-Ar-**H**), 7.11 (dd, *J* = 7.4, 1.3 Hz, 2H, STol-Ar-**H**), 6.96 (d, *J* = 9.1 Hz, 1H, N**H**TCA), 5.33 (dd, *J* = 10.4, 9.4 Hz, 1H, **H3**), 5.05 (t, *J* = 9.7 Hz, 1H, **H4**), 4.77 (d, *J* = 10.3 Hz, 1H, **H1**), 4.27 – 4.14 (m, 2H, **H6**), 3.98 (td, *J* = 10.4, 9.2 Hz, 1H, **H2**), 3.74 (ddd, *J* = 10.1, 5.1, 2.6 Hz, 1H, **H5**), 2.34 (s, 3H, STol-Me-**H**), 2.09 (s, 3H, OAc-**H**), 2.00 (s, 3H, OAc-**H**), 1.93 (s, 3H, OAc-**H**). ^{13}C NMR (101 MHz, $CDCl_3$) δ 171.13, 170.72, 169.36, 161.74, 139.22, 134.19, 129.93, 127.65, 92.39, 86.68, 76.15, 73.28, 68.41, 62.40, 54.59, 21.34, 20.88, 20.69, 20.56. $[\alpha]_D^{25}$ = -16.36 (0.22 g/100 mL, DCM). LRMS (ESI) Calcd for $C_{21}H_{24}Cl_3NNaO_8S^+$ [M+Na] = 578.02 found 577.96.

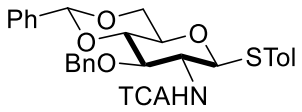
2,2,2-trichloro-N-((2R,4aR,6S,7R,8R,8aS)-8-hydroxy-2-phenyl-6-(p-tolylthio)hexahydropyrano[3,2-d][1,3]dioxin-7-yl)acetamide [31]



3.140

3.139 (9.44 g, 21.9 mmol) was suspended in 75 mL dry MeOH under Ar and vigorously stirred. A solution of 25% NaOMe in MeOH (0.975 mL, 4.38 mmol) was added slowly. The solution was left to stir for 30 mins, with all solids dissolving after 5 mins. The reaction was neutralised to pH_6 through addition of Amberlyst™ resin, filtered and the filtrate concentrated *in vacuo*. The resultant solid and CSA (1.27 g, 5.47 mmol) were dissolved in 100 mL dry MeCN under Ar. Benzaldehyde dimethyl acetal (16.4 mL, 109.5 mmol) was added and the reaction heated to 85 °C. After 1 h the reaction was neutralised with Et_3N and the solution concentrated *in vacuo*. Purification via flash column chromatography (SiO_2, gradient 99:1 DCM:MeCN to 90:10 DCM:MeCN) yielded **3.140** (5.70 g, 50%) as a white solid. ^{1}H NMR (400 MHz, $CDCl_3$) δ 7.57 – 7.29 (m, 7H, CHPh-Ar-**H** + STol-Ar-**H**), 7.19 – 7.11 (m, 2H, STol-Ar-**H**), 6.92 (d, *J* = 7.6 Hz, 1H, N**H**TCA), 5.53 (s, 1H, PhC**H**O_2), 5.10 (d, *J* = 10.4 Hz, 1H, **H1**), 4.38 (dd, *J* = 10.5, 4.8 Hz, 1H, **H6**), 4.27 (td, *J* = 9.4, 2.7 Hz, 1H, **H3**), 3.78 (dd, *J* = 10.5, 9.6 Hz, 1H, **H6**), 3.61 – 3.44 (m, 3H, **H2** + **H4** + **H5**), 2.88 (d, *J* = 3.1 Hz, 1H, 3-O**H**), 2.36 (s, 3H, STol-Me-**H**). ^{13}C NMR (101 MHz, $CDCl_3$) δ 162.09, 139.27, 136.97, 134.10, 130.13, 129.53, 128.53, 127.35, 126.40, 102.04, 92.53, 85.64, 81.44, 71.40, 70.55, 68.63, 57.61, 21.35, 2.04. $[\alpha]_D^{25}$ = -25.71 (0.14 g/100 mL, DCM). LRMS Calcd for $C_{22}H_{23}Cl_3NO_5S^+$ [M+H] = 518.04 found 517.87.

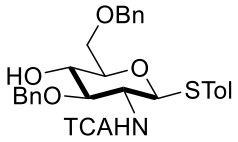
N-((2R,4aR,6S,7R,8R,8aS)-8-(benzyloxy)-2-phenyl-6-(p-tolylthio)hexahydropyrano[3,2-d][1,3]dioxin-7-yl)-2,2,2-trichloroacetamide [31]



3.141

3.140 (4.69 g, 9.03 mmol) was dissolved in 60 mL dry 90:10 THF:DMF mix under Ar. The solution was cooled to 0 °C and NaH (722.8 mg, 18.07 mmol) was added. The solution was left to stir for 5 mins before slow addition of BnBr (3.22 mL, 27.12 mmol). The solution was warmed to ambient temperature and left to stir for 10 mins, after which time additional NaH (722.8 mg, 18.07 mmol) was added. The reaction was left to stir for 1 hr before neutralisation with AcOH to pH_6 at 0 °C, followed by the addition of 200 mL H_2O. The precipitate was recovered by filtration and the solid washed with 3 x 50 mL H_2O, 3 x 50 mL pet. ether, azetroped with toluene and dried on high vac. overnight to yield **3.141** (4.92 g, 89%) as a white solid. ^{1}H NMR (400 MHz, $CDCl_3$) δ 7.53 – 7.44 (m, 2H, Ar-**H**), 7.39 (ddt, *J* = 7.7, 4.9, 2.4 Hz, 5H, Ar-**H**), 7.33 – 7.21 (m, 5H, Ar-**H**), 7.13 (d, *J* = 8.0 Hz, 2H, Ar-**H**), 6.85 (d, *J* = 7.8 Hz, 1H, N**H**TCA), 5.59 (s, 1H, PhC**H**O_2), 5.22 (d, *J* = 10.4 Hz, 1H, **H1**), 4.87 (d, *J* = 11.0 Hz, 1H, 3-OBn-C**H$_2$**), 4.66 (d, *J* = 11.0 Hz, 1H, 3-OBn-C**H$_2$**), 4.41 (dd, *J* = 10.5, 4.9 Hz, 1H, **H6**), 4.25 (dd, *J* = 9.8, 8.8 Hz, 1H, **H3**), 3.81 (t, *J* = 10.2 Hz, 1H, **H6**), 3.67 (t, *J* = 9.1 Hz, 1H, **H4**), 3.59 (td, *J* = 9.7, 4.9 Hz, 1H, **H5**), 3.47 (td, *J* = 10.1, 7.8 Hz, 1H, **H2**), 2.34 (s, 3H, STol-Me-**H**). ^{13}C NMR (101 MHz, $CDCl_3$) δ 161.65, 139.19, 137.72, 137.28, 134.14, 130.12, 129.24, 128.66, 128.50 (d, *J* = 6.2 Hz), 128.19, 127.41, 126.14, 101.42, 92.57, 85.34, 82.65, 77.32 (d, *J* = 7.9 Hz), 75.22, 70.68, 68.75, 57.10, 21.33. $[\alpha]_D^{25}$ = -28.44 (0.22 g/100 mL, Acetone). LRMS (ESI) Calcd for $C_{29}H_{29}Cl_3NO_5S^+$ [M+H] = 608.08 found 608.16

N-((2S,3R,4R,5S,6R)-4-(benzyloxy)-6-((benzyloxy)methyl)-5-hydroxy-2-(p-tolylthio)tetrahydro-2H-pyran-3-yl)-2,2,2-trichloroacetamide [31]

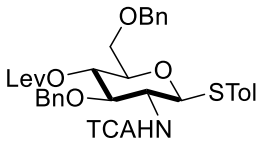


3.142

3.141 (5.81 g, 9.54 mmol) was suspended in 100 mL dry DCM under Ar and cooled to 0 °C. TES (22.7 mL, 143.1 mmol) was added followed by dropwise addition of TFA (3.65 mL, 47.7 mmol). The suspension was left to stir for 1 hr, after which additional TFA (3.65 mL, 47.7 mmol) was added dropwise. Following the second addition of TFA, the suspension immediately became a solution and 1 x 100 mL sat. $NaHCO_3$ sol. was slowly added. The organic layer was collected, dried over anhydrous Na_2SO_4, and concentrated *in vacuo*. Purification via flash column chromatography (SiO_2, gradient 99:1 DCM:MeOH to 97:3 DCM:MeOH) yielded **3.142** (2.34 g, 40%) as a white solid. ^{1}H NMR (400 MHz, $CDCl_3$)

δ 7.44 – 7.28 (m, 12H, Ar-**H**), 7.10 – 7.04 (m, 2H, Ar-**H**), 6.85 (d, *J* = 7.8 Hz, 1H, N**H**TCA), 5.11 (d, *J* = 10.3 Hz, 1H, **H1**), 4.81 – 4.68 (m, 2H, 3-OBn-C**H₂**), 4.65 – 4.53 (m, 2H, 6-OBn-C**H₂**), 3.99 (dd, *J* = 10.1, 8.5 Hz, 1H, **H3**), 3.83 (dd, *J* = 10.3, 4.8 Hz, 1H, **H6**), 3.77 (dd, *J* = 10.3, 4.7 Hz, 1H, **H6**), 3.69 (t, *J* = 9.0 Hz, 1H, **H4**), 3.57 (dt, *J* = 9.5, 4.7 Hz, 1H, **H5**), 3.44 (td, *J* = 10.2, 7.8 Hz, 1H, **H2**), 2.75 (bs, 1H, 4-O**H**), 2.32 (s, 3H, STol-Me-**H**). ^{13}C NMR (101 MHz, $CDCl_3$) δ 161.60, 138.84, 137.96, 137.81, 133.92, 129.99, 128.79, 128.65, 128.31, 128.24, 128.04, 127.90, 92.64, 84.87, 81.24, 78.08, 77.36, 75.24, 73.94, 73.46, 70.71, 56.71, 21.30. $[\alpha]_D^{25}$ = -23.33 (0.12 g/100 mL, DCM). LRMS (ESI) Calcd for $C_{29}H_{30}Cl_3NNaO_5S^+$ [M+Na] = 632.08 found 632.05

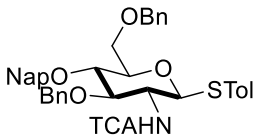
(2R,3S,4R,5R,6S)-4-(benzyloxy)-2-((benzyloxy)methyl)-6-(p-tolylthio)-5-(2,2,2-trichloroacetamido)tetrahydro-2H-pyran-3-yl 4-oxopentanoate



3.123

3.142 (600 mg, 0.98 mmol) was added to a stirred solution of levulinic acid (0.15 mL, 1.47 mmol), EDCI (281.8 mg, 1.47 mmol), and DMAP (47.6 mg, 0.39 mmol) in 10 mL dry DCM under Ar. The solution was stirred for 1 h after which time Et_3N (0.14 mL, 0.98 mmol) was added. The reaction was left to stir for 1 h after which time it was diluted with 15 mL DCM. The solution was washed with 1 x 15 mL 1.0 M HCl, 3 x 10 mL sat. $NaHCO_3$ sol., and 1 x 15 mL brine. The organic layer was dried over anhydrous Na_2SO_4 and concentrated *in vacuo*. Purification via flash column chromatography (SiO_2, gradient 100:0 DCM:acetone to 99:1 DCM:acetone) yielded **3.123** as a white solid (752.5 mg, quant.). ^{1}H NMR (400 MHz, $CDCl_3$) δ 7.45 – 7.40 (m, 2H, Ar-**H**), 7.34 (d, *J* = 4.3 Hz, 4H, Ar-**H**), 7.32 – 7.24 (m, 4H, Ar-**H**), 7.22 (dd, *J* = 8.0, 1.7 Hz, 2H, Ar-**H**), 7.04 (d, *J* = 8.0 Hz, 2H, Ar-**H)**, 6.91 (d, *J* = 7.5 Hz, 1H, N**H**TCA), 5.24 (d, *J* = 10.2 Hz, 1H, **H1**), 5.02 (dd, *J* = 9.9, 8.9 Hz, 1H, **H4**), 4.60 (s, 2H, 3-OBn-C**H₂**), 4.54 (s, 2H, 6-OBn-C**H₂**), 4.29 (dd, *J* = 10.0, 9.0 Hz, 1H, **H3**), 3.70 (ddd, *J* = 9.9, 5.5, 3.3 Hz, 1H, **H5**), 3.66 – 3.57 (m, 2H, **H6**), 3.40 (td, *J* = 10.1, 7.5 Hz, 1H, **H2**), 2.68 – 2.49 (m, 2H, Lev-C**H₂**), 2.46 – 2.34 (m, 2H, Lev-C**H₂**), 2.33 (s, 3H, Lev-Me-**H**), 2.12 (s, 3H, STol-Me-**H**). ^{13}C NMR (101 MHz, $CDCl_3$) δ 206.18, 171.69, 161.72, 138.91, 138.31, 137.67, 133.89, 130.06, 128.64, 128.46, 128.06 (d, *J* = 3.4 Hz), 127.93, 127.72, 92.50, 84.16, 78.79, 77.94, 74.86, 73.65, 71.90, 69.63, 57.29, 37.83, 29.87, 28.04, 21.30. $[\alpha]_D^{25}$ = -10.90 (0.11 g/100 mL, DCM). HRMS (ESI) Calc'd for $C_{34}H_{36}Cl_3NNaO_7S^+$ [M+Na] = 730.1171 found 730.1284. IR (Transmittance) 3656, 3306, 2980, 2890, 1689, 1533, 1455, 1381, 1308, 1182, 1068, 913, 826, 696, 645, 595, 480 cm^{-1}

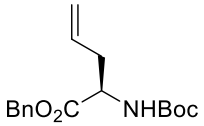
N-((2S,3R,4R,5S,6R)-4-(benzyloxy)-6-((benzyloxy)methyl)-5-(naphthalen-2-ylmethoxy)-2-(p-tolylthio)tetrahydro-2H-pyran-3-yl)-2,2,2-trichloroacetamide



3.124

3.142 (100 mg, 0.163 mmol) was dissolved in 2 mL dry 95:5 THF:DMF mix under Ar. The solution was cooled to 0 ^{o}C and NaH (13 mg, 0.326 mmol) was added. The solution was left to stir for 5 mins before the addition of NapBr (108.1 mg, 0.489 mmol). The solution was warmed to ambient temperature and stirred for 10 mins before the addition of NaH (13 mg, 0.326 mmol). The reaction was left to stir overnight, neutralised with AcOH at 0 ^{o}C and diluted with 10 mL H_2O. The suspension was extracted with 3 x 15 mL DCM and the combined organic layers washed with 1 x 15 mL brine, dried over anhydrous Na_2SO_4 and concentrated *in vacuo*. Purification via flash column chromatography (SiO_2, gradient 90:10 pet. ether:EtOAc to 80:20 pet. ether:EtOAc) yielded **3.124** as a white solid (84.8 mg, 69%). ^{1}H NMR (400 MHz, $CDCl_3$) δ 7.86 – 7.71 (m, 3H, Ar-**H**), 7.64 (d, *J* = 1.7 Hz, 1H, Ar-**H**), 7.52 – 7.41 (m, 4H, Ar-**H**), 7.39 – 7.19 (m, 11H, Ar-**H**), 7.06 (d, *J* = 7.9 Hz, 2H, Ar-**H**), 6.90 (d, *J* = 8.0 Hz, 1H, N**H**TCA), 5.09 (d, *J* = 10.0 Hz, 1H, **H1**), 4.92 (d, *J* = 11.2 Hz, 1H, Nap-C**H₂**), 4.85 – 4.73 (m, 2H, 3-OBn-C**H₂**), 4.70 (d, *J* = 10.7 Hz, 1H, Nap-C**H₂**), 4.63 (d, *J* = 11.9 Hz, 1H, 6-OBn-C**H₂**), 4.53 (d, *J* = 12.0 Hz, 1H, 6-OBn-C**H₂**), 4.13 (dd, *J* = 9.7, 8.3 Hz, 1H, **H3**), 3.88 – 3.77 (m, 2H, **H6**), 3.73 (dd, *J* = 9.4, 8.3 Hz, 1H, **H4**), 3.65 (ddd, *J* = 9.4, 3.8, 2.5 Hz, 1H, **H5**), 3.57 (td, *J* = 9.9, 8.0 Hz, 1H, **H2**), 2.32 (s, 3H, STol-Me-**H**). ^{13}C NMR (101 MHz, $CDCl_3$) δ 161.55, 138.73, 138.38, 137.77, 135.48, 133.94, 133.37, 133.12, 129.96, 128.66, 128.50, 128.33, 128.06 (d, *J* = 1.4 Hz), 127.98, 127.77 (t, *J* = 4.1 Hz), 126.64, 126.29, 126.13, 125.86, 92.67, 84.63, 81.62, 79.52, 78.45, 77.36, 75.56, 74.93, 73.60, 69.05, 56.94, 53.56, 29.84, 21.30. $[\alpha]_D^{25}$ = -10.00 (0.10 g/100 mL, DCM). HRMS (ESI) Calc'd for $C_{40}H_{38}Cl_3NNaO_5S^+$ [M+Na] = 772.1429 found 772.137. IR (Transmittance) 3285, 3055, 3030, 2862,1252, 1110, 1080, 1061, 1039, 1018, 992, 906, 884, 851, 814, 694, 619, 602, 560, 474, 428 cm^{-1}

benzyl (R)-2-((tert-butoxycarbonyl)amino)pent-4-enoate [63]

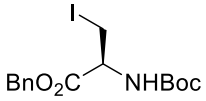


3.144

(R)-2-((tert-butoxycarbonyl)amino)pent-4-enoic acid (1.0 g, 4.97 mmol) and K_2CO_3 were suspended in 40 mL dry MeCN under Ar. Benzyl bromide (0.89 mL, 7.46 mmol) was added dropwise and the reaction left to stir overnight. The Reaction was diluted with 60 mL EtOAc and washed with 3 x 20 mL H_2O and

1 x 30 mL brine. The organic layer was dried over anhydrous Na_2SO_4 and concentrated *in vacuo*. Purification via flash column chromatography (SiO_2, gradient 100:0 pet. ether:EtOAc to 80:20 pet. ether:EtOAc) yielded **3.144** as a clear oil (1.33g, 88%). ^{1}H NMR (400 MHz, $CDCl_3$) δ 7.35 – 7.20 (m, 5H, Ar-**H**), 5.56 (ddt, *J* = 15.9, 11.2, 7.2 Hz, 1H, $\mathbf{H_\gamma}$), 5.16 – 4.90 (m, 5H, $\mathbf{H_\delta}$ + OC$\mathbf{H_2}$Ph + N**H**Boc), 4.33 (q, *J* = 6.6 Hz, 1H, $\mathbf{H_\alpha}$), 2.42 (dp, *J* = 20.9, 7.2 Hz, 2H, $\mathbf{H_\beta}$), 1.34 (s, 9H, Boc-^{t}Bu-**H**). ^{13}C NMR (101 MHz, $CDCl_3$) δ 172.07, 155.33, 137.93, 135.52, 132.32, 129.17, 128.94, 128.73, 128.52 (d, *J* = 8.6 Hz), 119.35, 80.06, 67.20, 53.11, 36.89, 33.69, 28.44. $[\alpha]_D^{25}$ = +8.78 (0.20 g/100 mL, DCM). LRMS (ESI) Calcd for $C_{12}H_{16}NO_2^+$ [M+H-Boc] = 206.12 found 206.19.

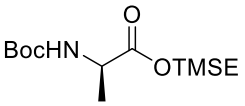
benzyl (S)-2-((tert-butoxycarbonyl)amino)-3-iodopropanoate [52]



3.147

BocHN-D-Ser-OBzl (1.00 g, 3.39 mmol), PPh_3 (1.06 g, 4.06 mmol) and Imidazole (276 mg, 4.06 mmol) were suspended in 20 mL dry DCM under Ar and the suspension cooled to 0 °C. Iodine (815 mg, 4.06 mmol) was added to the vigorously stirred suspension and the reaction warmed to ambient temperature. After stirring for 2 hrs the reaction was filtered and the filtrate washed with 1 x 20 mL sat. $Na_2S_2O_3$ sol., 1 x 20 mL H_2O and 1 x 20 mL brine. The organic layer was dried over anhydrous Na_2SO_4 and concentrated *in vacuo*. Purification via flash column chromatography (SiO_2, gradient 95:5 pet. ether:Et_2O to 75:25 pet. ether:Et_2O) yielded **3.147** as a white solid (1.13 g, 84%). ^{1}H NMR (400 MHz, $CDCl_3$) δ 7.38 (q, *J* = 2.2 Hz, 5H, Ar-**H**), 5.39 – 5.32 (m, 1H, N**H**Boc), 5.27 – 5.15 (m, 2H, OC$\mathbf{H_2}$Ph), 4.55 (dt, *J* = 7.9, 3.9 Hz, 1H, $\mathbf{H_\alpha}$), 3.58 (qd, *J* = 10.3, 3.9 Hz, 2H, $\mathbf{H_\beta}$), 1.45 (s, 9H, Boc-^{t}Bu-**H**). ^{13}C NMR (101 MHz, $CDCl_3$) δ 169.64, 155.00, 135.00, 128.77 (d, *J* = 7.3 Hz), 80.65, 68.12, 53.84, 28.42, 7.94. $[\alpha]_D^{25}$ = +5.00 (0.14 g/100 mL, DCM). HRMS (ESI) Calc'd for $C_{10}H_{13}INO_2^+$ [M+H-Boc] = 305.9986 found 305.9846.

2-(trimethylsilyl)ethyl (tert-butoxycarbonyl)-D-alaninate [64]

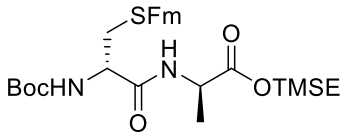


3.130

Boc-D-Ala-OH (5.0 g, 20.6 mmol) and HATU (9.89 g, 20.6 mmol) were dissolved in 50 mL dry DMF under Ar and cooled to 0 °C. DIPEA (9.06 mL, 52.0 mmol) was added slowly and the reaction left to stir for 10 mins. After this time, 2-trimethylsilyl ethanol (5.59 mL, 30.9 mmol) was added and the reaction

warmed to ambient temperature. The reaction was left to stir overnight before concentration *in vacuo*. The solid was redissolved in 50 mL EtOAc and washed with 1 x 50 mL 0.2M HCl and 1x 50 mL sat. $NaHCO_3$ sol.; both aqueous layers were back extracted with 1x 50 mL EtOAc. The combined organic layers were washed with brine, dried over anhydrous Na_2SO_4 and concentrated *in vacuo*. Purification via flash column chromatography (SiO_2, gradient 95:5 pet. ether:EtOAc to 90:10 pet. ether:EtOAc) yielded **3.130** as a clear oil (6.11 g, 81%). ^{1}H NMR (400 MHz, $CDCl_3$) δ 5.07 (s, 1H, Ala-N**H**), 4.33 – 4.17 (m, 3H, Ala-**H$_\alpha$** + TMSE-OC**H$_2$**), 1.46 (s, 9H, Boc-^{t}Bu-**H**), 1.39 (d, *J* = 7.2 Hz, 3H, Ala-**H$_\beta$**), 1.07 – 0.97 (m, 2H, TMSE-SiC**H$_2$**), 0.06 (s, 9H, TMS-Me-**H**). ^{13}C NMR (101 MHz, $CDCl_3$) δ 63.76, 28.44, 18.84, 17.42, -1.41. $[\alpha]_D^{25}$ = +10.70 (0.71 g/100 mL, DCM). LRMS (ESI) Calcd for $C_{13}H_{27}NNaO_4Si^+$ [M+Na] = 312.16 found 312.08

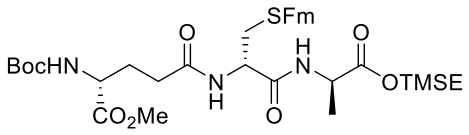
2-(trimethylsilyl)ethyl S-((9H-fluoren-9-yl)methyl)-N-(tert-butoxycarbonyl)-D-cysteinyl-D-alaninate



3.129

3.130 (434 mg, 1.5 mmol) was dissolved in 10 mL 20% TFA in dry DCM under Ar and left to stir at ambient temperature for 1 h. The reaction was then concentrated *in vacuo* and dried on high vac. for 1 h. During this time Boc-L-Cys-Fm-OH (400 mg, 1.0 mmol) and HATU (380 mg, 1.0 mmol) were dissolved in 6 mL dry DMF under Ar and cooled to 0 °C. DIPEA (0.26 mL, 1.5 mmol) was added slowly, and the reaction stirred for 10 mins. The deprotected amine was dissolved in 4 mL dry DMF under Ar and neutralised with DIPEA (0.52 mL, 3.0 mmol). This solution was added to the activated acid and the reaction left to stir overnight. The solution was concentrated *in vacuo*, the resultant solid redissolved in 20 mL EtOAc and washed with 1 x 10 mL 1.0M HCl and 1 x 10 mL sat. $NaHCO_3$ sol. The organic layer was washed with brine, dried over anhydrous Na_2SO_4, and concentrated *in vacuo*. Purification via flash column chromatography (SiO_2, gradient 95:5 pet. ether:EtOAc to 85:15 pet. ether:EtOAc) yielded **3.129** as a clear oil (405.3 mg, 71%). ^{1}H NMR (400 MHz, $CDCl_3$) δ 7.81 – 7.63 (m, 4H, Fm-Ar-**H**), 7.42 – 7.24 (m, 4H, Fm-Ar-**H**), 6.78 (d, *J* = 7.5 Hz, 1H, Ala-N**H**), 5.43 (d, *J* = 7.5 Hz, 1H, Cys-N**H**), 4.50 (p, *J* = 7.2 Hz, 1H, Ala-**H$_\alpha$**), 4.32 – 4.17 (m, 3H, Cys-H$_\alpha$ + TMSE-OC**H$_2$**), 4.15 (s, 1H, Fm-**H**), 3.31 – 3.21 (m, 1H, Fm-C**H$_2$**), 3.13 (dd, *J* = 12.9, 6.3 Hz, 1H, Fm-C**H$_2$**), 2.97 (dd, *J* = 14.0, 5.4 Hz, 1H, TMSE-SiC**H$_2$**), 2.80 (dd, *J* = 14.0, 7.0 Hz, 1H, TMSE-SiC**H$_2$**), 1.46 (s, 9H, Boc-^{t}Bu-**H**), 1.35 (d, *J* = 7.2 Hz, 3H, Ala-**H$_\beta$**), 1.06 – 0.95 (m, 2H, Cys-**H$_\beta$**), 0.05 (s, 9H, TMS-Me-**H**). ^{13}C NMR (101 MHz, $CDCl_3$) δ 172.67, 170.06, 145.89, 145.77, 141.18 (d, *J* = 5.3 Hz), 127.64 (d, *J* = 2.1 Hz), 127.12 (d, *J* = 7.6 Hz), 124.88 (d, *J* = 6.3 Hz), 119.93, 63.98, 48.39, 46.97, 36.51, 35.28, 28.36, 18.23, 17.37, -1.44. $[\alpha]_D^{25}$ = +18.33 (0.12 g/100 mL, DCM). HRMS (ESI) Calc'd for $C_{30}H_{43}N_2O_5SSi^+$ [M+H] = 571.2657 found 571.265. IR (Transmittance) 3307, 2954, 1713, 1657, 1509, 1450, 1391, 1366, 1249, 1219 ,1161, 1047, 911, 856, 836, 735 cm^{-1}

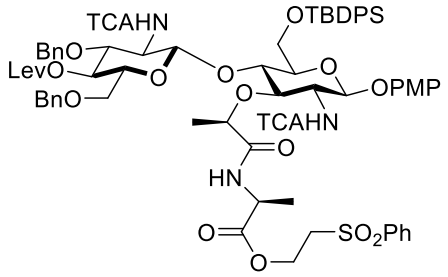
methyl N5-((S)-3-(((9H-fluoren-9-yl)methyl)thio)-1-oxo-1-(((R)-1-oxo-1-(2-(trimethylsilyl)ethoxy)propan-2-yl)amino)propan-2-yl)-N2-(tert-butoxycarbonyl)-L-glutaminate



3.117

3.129 (400 mg, 0.7 mmol) was dissolved in 10 mL 20% TFA in dry DCM under Ar and left to stir at ambient temperature for 1 h. The reaction was then concentrated *in vacuo* and dried on high vac. for 1 h. During this time Boc-D-Glu-OH-OMe (182.9 mg, 0.7 mmol) and HATU (266.2 mg, 0.7 mmol) were dissolved in 6 mL dry DMF under Ar and cooled to 0 °C. DIPEA (0.26 mL, 1.5 mmol) was added slowly, and the reaction stirred for 10 mins. The deprotected amine was dissolved in 4 mL dry DMF under Ar and neutralised with DIPEA (0.52 mL, 3.0 mmol). This solution was added to the activated acid and the reaction left to stir overnight. The solution was concentrated *in vacuo*, the resultant solid redissolved in 20 mL EtOAc and washed with 1 x 10 mL 1.0M HCl and 1 x 10 mL sat. $NaHCO_3$ sol. The organic layer was washed with brine, dried over anhydrous Na_2SO_4, and concentrated *in vacuo*. Purification via flash column chromatography (SiO_2, gradient 70:30 pet. ether:EtOAc to 50:50 pet. ether:EtOAc) yielded **3.117** as a clear oil (165 mg, 30%). ^{1}H NMR (400 MHz, $CDCl_3$) δ 7.75 – 7.63 (m, 4H, Fm-Ar-**H**), 7.43 – 7.27 (m, 4H, Fm-Ar-**H**), 7.03 (s, 1H, Cys-N**H**), 6.56 (s, 1H, Ala-N**H**), 5.33 (d, *J* = 9.3 Hz, 1H, Glu-N**H**), 4.49 (dh, *J* = 20.6, 6.5 Hz, 2H, Cys-$\mathbf{H_\alpha}$ + Ala-$\mathbf{H_\alpha}$), 4.29 (d, *J* = 10.4 Hz, 1H, Glu-$\mathbf{H_\alpha}$), 4.23 – 4.11 (m, 3H, TMSE-OC$\mathbf{H_2}$ + Fm-**H**), 3.73 (s, 3H, Glu-CO_2Me-**H**), 3.30 (dd, *J* = 13.1, 5.7 Hz, 1H, Fm-C$\mathbf{H_2}$), 3.23 – 3.13 (m, 1H, Fm-C$\mathbf{H_2}$), 3.05 – 2.96 (m, 1H, Cys-$\mathbf{H_\beta}$), 2.74 (dd, *J* = 14.0, 7.1 Hz, 1H, Cys-$\mathbf{H_\beta}$), 2.35 – 2.15 (m, 3H, Glu-$\mathbf{H_\beta}$ + Glu-$\mathbf{H_\gamma}$), 1.90 – 1.81 (m, 1H, Glu-$\mathbf{H_\beta}$), 1.42 (s, 9H, Boc-^{t}Bu-**H**), 1.32 (d, *J* = 7.2 Hz, 3H, Ala-Me-**H**), 1.04 – 0.91 (m, 2H, TMSE-SiC$\mathbf{H_2}$), 0.03 (s, 9H, TMS-Me-**H**). ^{13}C NMR (101 MHz, $CDCl_3$) δ 172.83, 172.55, 171.91, 155.78, 145.83 (d, *J* = 9.3 Hz), 141.31, 127.70 (d, *J* = 4.2 Hz), 127.20 (d, *J* = 8.0 Hz), 124.93, 119.96 (d, *J* = 1.4 Hz), 80.31, 63.85, 52.82, 52.55, 48.49, 46.96, 36.31, 34.90, 32.27, 28.77, 28.41, 17.77, 17.42, -1.42. $[\alpha]_D^{25}$ = +0.4 (0.5 g/100 mL, MeCN). HRMS (ESI) Calc'd for $C_{36}H_{52}N_3O_8SSi^+$ [M+H] = 714.3239 found 714.3394. IR (Transmittance) 3296, 2953, 1737, 1702, 1639, 1523, 1477, 1448, 1391, 1333, 1249, 1216, 1164, 1046, 910, 857, 837, 732, 641 cm^{-1}

(2R,3S,4R,5R,6S)-4-(benzyloxy)-2-((benzyloxy)methyl)-6-(((2R,3S,4R,5R,6S)-2-(((tert-butyldiphenylsilyl)oxy)methyl)-6-(4-methoxyphenoxy)-4-(((R)-1-oxo-1-(((S)-1-oxo-1-(2-(phenylsulfonyl)ethoxy)propan-2-yl)amino)propan-2-yl)oxy)-5-(2,2,2-trichloroacetamido)tetrahydro-2H-pyran-3-yl)oxy)-5-(2,2,2-trichloroacetamido)tetrahydro-2H-pyran-3-yl 4-oxopentanoate



3.121

Prior to the reaction 3 Å Molecular Sieves were activated at 350 °C overnight. These were added to a rigorously flame dried flask under Ar. To this flask was added **3.122** (150 mg, 0.153 mmol) and NIS (172.1 mg, 0.765 mmol) in 5 mL dry DCM. The solution was cooled to -20 °C and **3.123** (325 mg, 0.439 mmol) was added, followed by addition of TfOH (5.38 µl, 0.061 mmol). The solution was left to stir for 10 mins, after which time 5 mL sat. $NaHCO_3$ sol. was added. The aqueous layer was back extracted with 5 mL DCM and the combined layers washed with 5 mL sat. $Na_2S_2O_3$ sol., dried over anhydrous Na_2SO_4 and concentrated *in vacuo*. Purification via flash column chromatography (SiO_2, gradient 100:0 DCM:MeOH to 98:2 DCM:MeOH) yielded **3.121** (38.4 mg, 16%) as a white solid. ^{1}H NMR (400 MHz, $CDCl_3$) δ 7.88 – 7.82 (m, 2H, SO_2Ph-Ar-**H**), 7.79 – 7.69 (m, 3H, Ar-**H** + MurNAc-N**H**TCA), 7.68 – 7.56 (m, 3H, SO_2Ph-Ar-**H** + Ar-**H**), 7.56 – 7.45 (m, 2H, SO_2Ph-Ar-**H**), 7.44 – 7.22 (m, 21H, Ar-**H**), 6.98 – 6.91 (m, 2H, PMP-Ar-**H**), 6.89 – 6.82 (m, 1H, Ala-1-N**H**), 6.82 – 6.69 (m, 2H, PMP-Ar-**H**), 6.48 (d, *J* = 8.0 Hz, 1H, GlcNAc-N**H**TCA), 5.19 (dd, *J* = 9.8, 8.4 Hz, 1H, GlcNAc-**H4**), 4.82 (d, *J* = 7.6 Hz, 1H, MurNAc-**H1**), 4.72 (dd, *J* = 7.8, 2.0 Hz, 1H, GlcNAc-**H1**), 4.64 – 4.47 (m, 5H, MurNAc-**H$_\alpha$** + GlcNAc-3-OBn-C**H$_2$** + GlcNAc-6-OBn-C**H$_2$**), 4.42 – 4.29 (m, 3H, OC**H$_2$** + MurNAc-**H4**), 4.25 (q, *J* = 7.4 Hz, 1H, Ala-1-**H$_\alpha$**), 4.16 (dt, *J* = 9.4, 7.6 Hz, 1H, MurNAc-**H2**), 4.00 (dd, *J* = 11.6, 2.8 Hz, 1H, MurNAc-**H6**), 3.86 (dd, *J* = 9.5, 8.2 Hz, 1H, MurNAc-**H3**), 3.80 – 3.68 (m, 5H, MurNAc-**H6** + PMP-Me-**H** + GlcNAc-**H2**), 3.66 (dd, *J* = 10.8, 3.3 Hz, 1H, GlcNAc-**H6**), 3.57 (dd, *J* = 10.6, 4.3 Hz, 1H, GlcNAc-**H6**), 3.53 – 3.46 (m, 1H, GlcNAc-**H5**), 3.45 – 3.34 (m, 3H, MurNAc-**H5** + SC**H$_2$**), 2.68 – 2.56 (m, 2H, Lev-C**H$_2$**), 2.44 (td, *J* = 6.4, 2.6 Hz, 2H, Lev-C**H$_2$**), 2.14 (s, 3H, Lev-Me-**H**), 1.24 (dd, *J* = 12.0, 6.9 Hz, 6H, MurNAc-Me-**H** + Ala1-Me-**H**), 1.08 (s, 9H, TBDPS-^{t}Bu-**H**). ^{13}C NMR (101 MHz, $CDCl_3$) δ 206.34, 173.62, 172.08, 171.62, 162.93, 162.25, 155.60, 151.73, 139.23, 138.01, 137.51, 136.10, 135.82, 134.23, 133.91, 132.34, 130.08 (d, *J* = 8.6 Hz), 129.59, 128.71, 128.51, 128.23 – 127.99 (m), 127.86 (d, *J* = 4.0 Hz), 119.41, 114.50, 101.81, 99.04, 93.00, 92.33, 76.16, 75.84, 74.03, 73.76, 73.61, 71.64, 68.99, 62.00, 58.25, 57.58, 55.77, 55.06, 48.17, 37.81, 29.90, 29.70, 28.08, 27.03, 19.43, 18.72, 16.80. $[\alpha]_D^{25}$ = + 8.95 (0.38 g/100 mL, MeOH). HRMS (ESI) Calc'd for $C_{72}H_{81}Cl_6N_3NaO_{19}SSi^+$ [M+Na] = 1586.2949 found 1586.3678. IR (Transmittance) 3358, 2363, 1752, 1666, 1527, 1507, 1449, 1428, 1365, 1310, 1293, 1217, 1145, 1112, 1085, 1039, 964, 917, 823, 742, 702, 607, 589 cm^{-1}.

References

(1) Wolf, A. J.; Underhill, D. M. Peptidoglycan recognition by the innate immune system. *Nature Reviews Immunology* **2018**, *18* (4), 243-254.
(2) Fu, X.-P.; Yuan, Y.; Jha, A.; Levin, N.; Giltrap, A. M.; Ren, J.; Mamalis, D.; Mohammed, S.; Davis, B. G. Stereoretentive post-translational protein editing. *ACS Central Science* **2023**, *9* (3), 405-416.
(3) Ogawa, C.; Liu, Y.-J.; S Kobayashi, K. Muramyl dipeptide and its derivatives: peptide adjuvant in immunological disorders and cancer therapy. *Current Bioactive Compounds* **2011**, *7* (3), 180-197.
(4) Termin, A.; Schmidt, R. R. Glycosylimidates, 54. Synthesis of the GlcNAcβ (1→ 4) MurNAcβ (1→ 4) GlcNAcβ (1→ 4) MurNAc tetrasaccharide of bacterial peptidoglycan. *Liebigs Annalen der Chemie* **1992**, *1992* (5), 527-533.
(5) Enugala, R.; Carvalho, L. C.; Dias Pires, M. J.; Marques, M. M. B. Stereoselective Glycosylation of Glucosamine: The Role of the N-Protecting Group. *Chemistry–An Asian Journal* **2012**, *7* (11), 2482-2501.
(6) Inamura, S.; Fukase, K.; Kusumoto, S. Synthetic study of peptidoglycan partial structures. Synthesis of tetrasaccharide and octasaccharide fragments. *Tetrahedron Letters* **2001**, *42* (43), 7613-7616.
(7) Inamura, S.; Fujimoto, Y.; Kawasaki, A.; Shiokawa, Z.; Woelk, E.; Heine, H.; Lindner, B.; Inohara, N.; Kusumoto, S.; Fukase, K. Synthesis of peptidoglycan fragments and evaluation of their biological activity. *Organic & Biomolecular Chemistry* **2006**, *4* (2), 232-242.
(8) Enugala, R.; Pires, M. J.; Marques, M. M. B. Synthesis of the NAG–NAM disaccharide via a versatile intermediate. *Carbohydrate Research* **2014**, *384*, 112-118.
(9) Kusumoto, S.; Fukase, K.; Shiba, T. Key structures of bacterial peptidoglycan and lipopolysaccharide triggering the innate immune system of higher animals: chemical synthesis and functional studies. *Proceedings of the Japan Academy, Series B* **2010**, *86* (4), 322-337.
(10) Fujimoto, Y.; Inamura, S.; Kawasaki, A.; Shiokawa, Z.; Shimoyama, A.; Hashimoto, T.; Kusumoto, S.; Fukase, K. IEIIS Meeting minireview: chemical synthesis of peptidoglycan fragments for elucidation of the immunostimulating mechanism. *Journal of Endotoxin Research* **2007**, *13* (3), 189-196.
(11) Wang, N.; Huang, C. y.; Hasegawa, M.; Inohara, N.; Fujimoto, Y.; Fukase, K. Glycan sequence-dependent Nod2 activation investigated by using a chemically synthesized bacterial peptidoglycan fragment library. *ChemBioChem* **2013**, *14* (4), 482-488.
(12) Wang, N.; Hirata, A.; Nokihara, K.; Fukase, K.; Fujimoto, Y. Peptidoglycan microarray as a novel tool to explore protein–ligand recognition. *Peptide Science* **2016**, *106* (4), 422-429.
(13) Wang, N.; Hasegawa, H.; Huang, C. y.; Fukase, K.; Fujimoto, Y. Synthesis of Peptidoglycan Fragments from Enterococcus faecalis with Fmoc-Strategy for Glycan Elongation. *Chemistry–An Asian Journal* **2017**, *12* (1), 27-30.
(14) Zhang, Y.; Fechter, E. J.; Wang, T.-S. A.; Barrett, D.; Walker, S.; Kahne, D. E. Synthesis of heptaprenyl− Lipid IV to analyze peptidoglycan glycosyltransferases. *Journal of the American Chemical Society* **2007**, *129* (11), 3080-3081.
(15) Kahne, D.; Walker, S.; Cheng, Y.; Van Engen, D. Glycosylation of unreactive substrates. *Journal of the American Chemical Society* **1989**, *111* (17), 6881-6882.
(16) Shih, H.-W.; Chen, K.-T.; Cheng, T.-J. R.; Wong, C.-H.; Cheng, W.-C. A new synthetic approach toward bacterial transglycosylase substrates, Lipid II and Lipid IV. *Organic Letters* **2011**, *13* (17), 4600-4603.
(17) Lee, J.-C.; Greenberg, W. A.; Wong, C.-H. Programmable reactivity-based one-pot oligosaccharide synthesis. *Nature Protocols* **2006**, *1* (6), 3143-3152.
(18) Hesek, D.; Lee, M.; Morio, K.-i.; Mobashery, S. Synthesis of a fragment of bacterial cell wall. *The Journal of Organic Chemistry* **2004**, *69* (6), 2137-2146.
(19) Lee, M.; Hesek, D.; Lastochkin, E.; Dik, D. A.; Boggess, B.; Mobashery, S. Deciphering the nature of enzymatic modifications of bacterial cell walls. *ChemBioChem* **2017**, *18* (17), 1696-1702.

(20) Lee, M.; Hesek, D.; Shah, I. M.; Oliver, A. G.; Dworkin, J.; Mobashery, S. Synthetic peptidoglycan motifs for germination of bacterial spores. *Chembiochem: a European Journal of Chemical Biology* **2010**, *11* (18), 2525.
(21) Lee, M.; Hesek, D.; Dik, D. A.; Fishovitz, J.; Lastochkin, E.; Boggess, B.; Fisher, J. F.; Mobashery, S. From genome to proteome to elucidation of reactions for all eleven known lytic transglycosylases from Pseudomonas aeruginosa. *Angewandte Chemie International Edition* **2017**, *56* (10), 2735-2739.
(22) Ding, H.; Lyu, J.; Zhang, X.-L.; Xiao, X.; Liu, X.-W. Efficient and versatile formation of glycosidic bonds via catalytic strain-release glycosylation with glycosyl ortho− 2, 2-dimethoxycarbonylcyclopropylbenzoate donors. *Nature Communications* **2023**, *14* (1), 4010.
(23) Hackenberger, C. P.; O'Reill, M. K.; Imperiali, B. Improving glycopeptide synthesis: a convenient protocol for the preparation of β-glycosylamines and the synthesis of glycopeptides. *The Journal of Organic Chemistry* **2005**, *70* (9), 3574-3578.
(24) Carvalho, L. C.; Queda, F.; Almeida, C. V.; Filipe, S. R.; Marques, M. M. B. From a Natural Polymer to Relevant NAG-NAM Precursors. *Asian Journal of Organic Chemistry* **2018**, *7* (12), 2544-2551.
(25) Queda, F.; Covas, G.; Silva, T.; Santos, C. A.; Bronze, M. R.; Cañada, F. J.; Corvo, M. C.; Filipe, S. R.; Marques, M. M. B. A top-down chemo-enzymatic approach towards N-acetylglucosamine-N-acetylmuramic oligosaccharides: Chitosan as a reliable template. *Carbohydrate Polymers* **2019**, *224*, 115133.
(26) Chan, T. Y.; Chen, A.; Allanson, N.; Chen, R.; Liu, D.; Sofia, M. J. Solid phase synthesis of peptidoglycan monomers for the generation of a combinatorial library. *Tetrahedron Letters* **1996**, *37* (45), 8097-8100.
(27) Siriwardena, A.; Jørgensen, M. R.; Wolfert, M. A.; Vandenplas, M. L.; Moore, J. N.; Boons, G.-J. Synthesis and proinflammatory effects of peptidoglycan-derived neoglycopeptide polymers. *Journal of the American Chemical Society* **2001**, *123* (33), 8145-8146.
(28) Guan, R.; Roychowdhury, A.; Ember, B.; Kumar, S.; Boons, G.-J.; Mariuzza, R. A. Structural basis for peptidoglycan binding by peptidoglycan recognition proteins. *Proceedings of the National Academy of Sciences* **2004**, *101* (49), 17168-17173.
(29) Carvalho, L. R.; Corvo, M. C.; Enugala, R.; Marques, M. M. B.; Cabrita, E. J. Application of HR-MAS NMR in the solid-phase synthesis of a glycopeptide using Sieber amide resin. *Magnetic Resonance in Chemistry* **2010**, *48* (4), 323-330.
(30) Kadonaga, Y.; Wang, N.; Fujimoto, Y.; Fukase, K. Solid-phase synthesis of bacterial cell wall peptidoglycan fragments. *Chemistry Letters* **2014**, *43* (9), 1461-1463.
(31) Dallabernardina, P.; Benazzi, V.; Laman, J. D.; Seeberger, P. H.; Loeffler, F. F. Automated glycan assembly of peptidoglycan backbone fragments. *Organic & Biomolecular Chemistry* **2021**, *19* (45), 9829-9832.
(32) Plante, O. J.; Andrade, R. B.; Seeberger, P. H. Synthesis and use of glycosyl phosphates as glycosyl donors. *Organic Letters* **1999**, *1* (2), 211-214.
(33) Fujimoto, Y.; Konishi, Y.; Kubo, O.; Hasegawa, M.; Inohara, N.; Fukase, K. Synthesis of crosslinked peptidoglycan fragments for investigation of their immunobiological functions. *Tetrahedron Letters* **2009**, *50* (26), 3631-3634.
(34) Vollmer, W.; Blanot, D.; De Pedro, M. A. Peptidoglycan structure and architecture. *FEMS Microbiology Reviews* **2008**, *32* (2), 149-167.
(35) Lee, M.; Hesek, D.; Blázquez, B.; Lastochkin, E.; Boggess, B.; Fisher, J. F.; Mobashery, S. Catalytic spectrum of the penicillin-binding protein 4 of Pseudomonas aeruginosa, a nexus for the induction of β-lactam antibiotic resistance. *Journal of the American Chemical Society* **2015**, *137* (1), 190-200.
(36) Mashayekh, S.; Bersch, K. L.; Ramsey, J.; Harmon, T.; Prather, B.; Genova, L. A.; Grimes, C. L. Synthesis of bacterial-derived peptidoglycan cross-linked fragments. *The Journal of Organic Chemistry* **2020**, *85* (24), 16243-16253.
(37) Surdhar, P. S.; Armstrong, D. A. Reduction potentials and exchange reactions of thiyl radicals and disulfide anion radicals. *Journal of Physical Chemistry* **1987**, *91* (26), 6532-6537.

(38) Zhang, Z.; Magnusson, G. Conversion of p-methoxyphenyl glycosides into the corresponding glycosyl chlorides and bromides, and into thiophenyl glycosides. *Carbohydrate Research* **1996**, *295*, 41-55.
(39) Jurgens, A. R. Asymmetric synthesis of differentially protected meso-2, 6-diaminopimelic acid. *Tetrahedron Letters* **1992**, *33* (33), 4727-4730.
(40) Holcomb, R. C.; Schow, S.; Ayral-Kaloustian, S.; Powell, D. An asymmetric synthesis of differentially protected meso-2, 6-diaminopimelic acid. *Tetrahedron Letters* **1994**, *35* (38), 7005-7008.
(41) Gao, Y.; Lane-Bell, P.; Vederas, J. C. Stereoselective synthesis of meso-2, 6-diaminopimelic acid and its selectively protected derivatives. *The Journal of Organic Chemistry* **1998**, *63* (7), 2133-2143.
(42) Chowdhury, A. R.; Boons, G.-J. The synthesis of diaminopimelic acid containing peptidoglycan fragments using metathesis cross coupling. *Tetrahedron Letters* **2005**, *46* (10), 1675-1678.
(43) Cattaneo, V.; Oldrini, D.; Corrado, A.; Berti, F.; Adamo, R. Orthogonal cleavage of the 2-naphthylmethyl group in the presence of the p-methoxy phenyl-protected anomeric position and its use in carbohydrate synthesis. *Organic Chemistry Frontiers* **2016**, *3* (6), 753-758.
(44) Matsuzaki, Y.; Ito, Y.; Nakahara, Y.; Ogawa, T. Synthesis of branched poly-N-acetyl-lactosamine type pentaantennary pentacosasaccharide: Glycan part of a glycosyl ceramide from rabbit erythrocyte membrane. *Tetrahedron Letters* **1993**, *34* (6), 1061-1064.
(45) KIKUO, Y. Y. M. H. A. 2-[(ARYLOXYCARBONYL)AMINO]-3-KETOESTER AND ITS PRODUCTION, AND PRODUCTION OF 4-ALKOXYCARBONYL-2-OXAZOLINONE USING THE SAME. 2000.
(46) Yu, W.; Jin, Z. A New Strategy for the Stereoselective Introduction of Steroid Side Chain via α-Alkoxy Vinyl Cuprates: Total Synthesis of a Highly Potent Antitumor Natural Product OSW-11. *Journal of the American Chemical Society* **2001**, *123* (14), 3369-3370.
(47) Gritter, R. J.; Wallace, T. J. The manganese dioxide oxidation of allylic alcohols. *The Journal of Organic Chemistry* **1959**, *24* (8), 1051-1056.
(48) Laue, K. W.; Mück-Lichtenfeld, C.; Haufe, G. Enantioselective syntheses of 2-amino-4-fluoropent-4-enoic acids. Isosteres of asparagine. *Tetrahedron* **1999**, *55* (34), 10413-10424.
(49) Grigg, R.; McCaffrey, S.; Sridharan, V.; Fishwick, C. W.; Kilner, C.; Korn, S.; Bailey, K.; Blacker, J. Enantioselective synthesis of non-proteinogenic 2-arylallyl-α-amino acids via Pd/In catalytic cascades. *Tetrahedron* **2006**, *62* (52), 12159-12171.
(50) Heravi, M. M.; Hashemi, E.; Nazari, N. Negishi coupling: an easy progress for C–C bond construction in total synthesis. *Molecular Diversity* **2014**, *18*, 441-472.
(51) Brittain, W. D.; Cobb, S. L. Negishi cross-couplings in the synthesis of amino acids. *Organic & Biomolecular Chemistry* **2018**, *16* (1), 10-20.
(52) Koseki, Y.; Yamada, H.; Usuki, T. Efficient synthesis of benzyl 2-(S)-[(tert-butoxycarbonyl) amino]-ω-iodoalkanoates. *Tetrahedron: Asymmetry* **2011**, *22* (5), 580-586.
(53) Noverges Pedro, B.; Medio-Simón, M.; Jutand, A. Influence of the Ligand of palladium (0) complexes on the rate of the oxidative addition of aryl and activated alkyl bromides: Csp2− Br versus Csp3− Br reactivity and selectivity. *ChemCatChem* **2017**, *9* (12), 2136-2144.
(54) Hart, T. W.; Metcalfe, D. A.; Scheinmann, F. Total synthesis of (±)-prostagladin D 1: use of triethylsilyl protecting groups. *Journal of the Chemical Society, Chemical Communications* **1979**, (4), 156-157.
(55) Corey, E. J.; Gin, D. Y.; Kania, R. S. Enantioselective total synthesis of ecteinascidin 743. *Journal of the American Chemical Society* **1996**, *118* (38), 9202-9203.
(56) West, C. W.; Rich, D. H. Novel cyclic tripeptides and substituted aromatic amino acids via ruthenium-activated SNAr reactions. *Organic Letters* **1999**, *1* (11), 1819-1822.
(57) Ruiz-Gayo, M.; Albericio, F.; Pedroso, E.; Giralt, E. (S)-9-Fluorenylmethyl-L-cysteine, a useful HF-stable derivative for peptide synthesis. *Journal of the Chemical Society, Chemical Communications* **1986**, (20), 1501-1502.
(58) Jensen, H. H.; Pedersen, C. M.; Bols, M. Going to extremes:"super" armed glycosyl donors in glycosylation chemistry. *Chemistry–A European Journal* **2007**, *13* (27), 7576-7582.

(59) Přibylka, A.; Krchňák, V. Gold-Catalyzed Solid-Phase Synthesis of 3, 4-Dihydropyrazin-2 (1 H)-ones: Relevant Pharmacophores and Peptide Backbone Constraints. *ACS Combinatorial Science* **2017**, *19* (11), 681-686.
(60) La-Venia, A.; Medran, N. S.; Krchnak, V.; Testero, S. A. Synthesis of a small library of imidazolidin-2-ones using gold catalysis on solid phase. *ACS Combinatorial Science* **2016**, *18* (8), 482-489.
(61) Sutar, Y.; Vangala, M.; Hotha, S. Silver-assisted gold-catalyzed solid phase synthesis of linear and branched oligosaccharides. *Chemical Communications* **2022**, *58* (5), 641-644.
(62) Bélot, F.; Jacquinet, J.-C. Unexpected stereochemical outcome of activated 4, 6-O-benzylidene derivatives of the 2-deoxy-2-trichloroacetamido-D-galacto series in glycosylation reactions during the synthesis of a chondroitin 6-sulfate trisaccharide methyl glycoside. *Carbohydrate Research* **2000**, *325* (2), 93-106.
(63) Bremner, J. B.; Keller, P. A.; Pyne, S. G.; Boyle, T. P.; Brkic, Z.; David, D. M.; Robertson, M.; Somphol, K.; Baylis, D.; Coates, J. A. Synthesis and antibacterial studies of binaphthyl-based tripeptoids. Part 1. *Bioorganic & Medicinal Chemistry* **2010**, *18* (7), 2611-2620.
(64) Wingen, L. M.; Rausch, M.; Schneider, T.; Menche, D. Modular Total Synthesis of Farnesyl Analogues of Cell Wall Precursors Lipid I and II Containing the Staphylococcus aureus Pentaglycine Bridge Modification. *The Journal of Organic Chemistry* **2020**, *85* (15), 10206-10215.

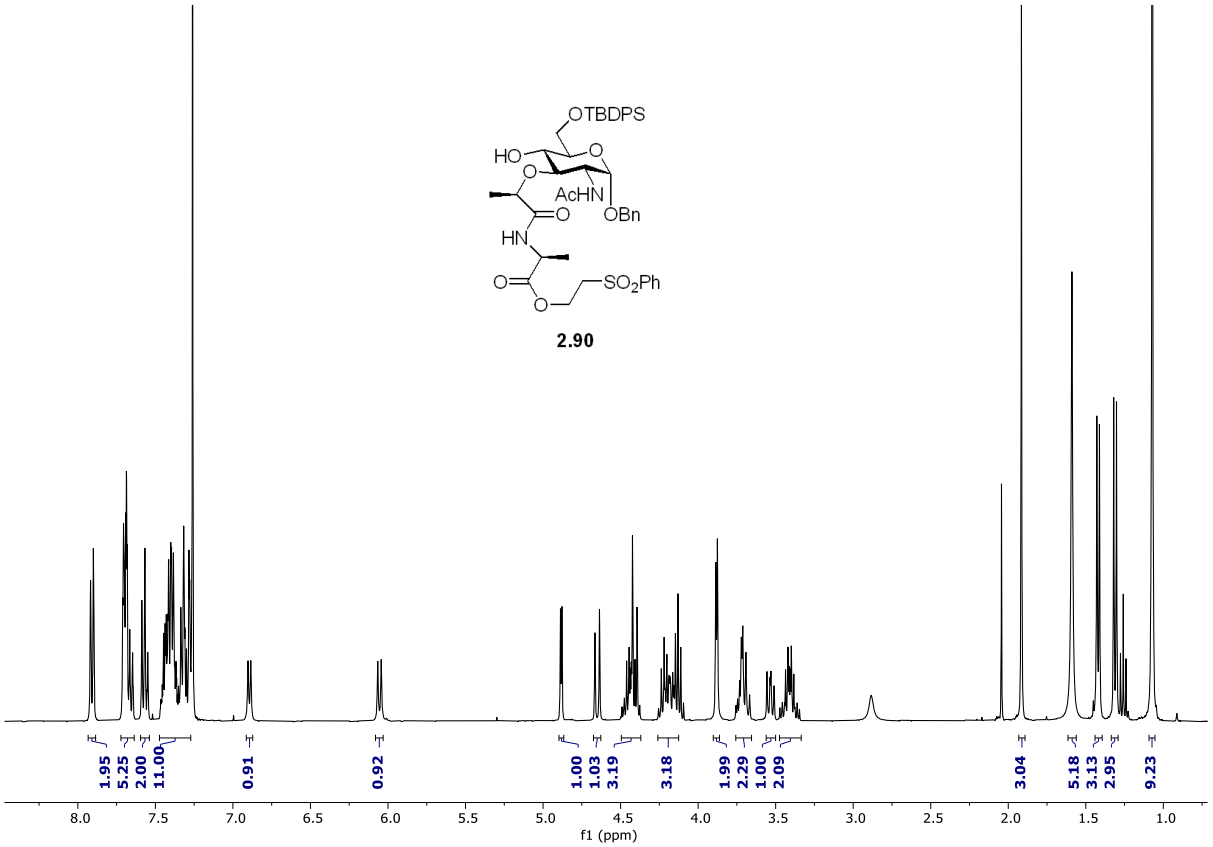
Thesis Conclusion

To conclude, the work in this thesis describes the synthesis of novel NAG-NAM fragments bearing high degrees of orthogonal protection, which in turn allows for unique functionalisations of interest to medicine. Chapter 2 describes the use of the TBDPS protecting group in the design of a novel MurNAc acceptor, and optimised methodology allowing its elaboration into an advanced disaccharide intermediate. Such an intermediate may be explored to design labelled Lipid II analogues for use in inhibitory assays of MurJ, an unexplored antibiotic target. Other applications of interest may also be concise access to newly described antibiotics, Anh-MurNAc-GlcNAc sugars or synthesis of a Lipid II radiotracer for PET imaging bacterial infection. Chapter 3 describes the use of the PMP group in the design of a novel MurNAc acceptor and the use of the Lev and Nap groups in the design of novel GlcNAc donors. Reaction of these monosaccharides allows for the creation of disaccharides bearing protection at the 4 OH non-reducing end orthogonal to one another, and when combined with appropriate radical donor and acceptor peptides may be crosslinked by light. This chemistry would allow for spatial and temporal control over peptidoglycan substrate properties and perhaps by extension immunostimulatory activity. This may advance vaccine design and help clinicians protect against microbial infection.

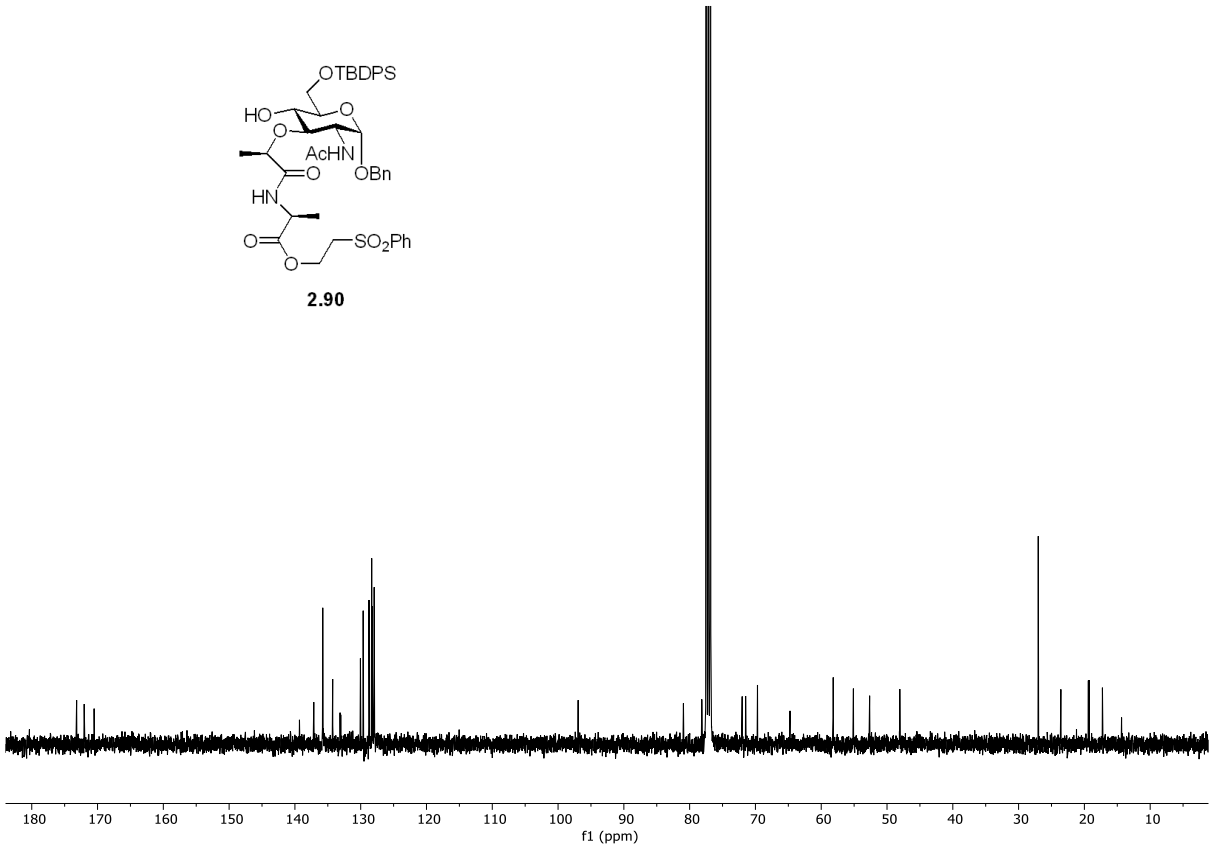
Future work will aim to progress these intermediates into the desired substrates and evaluate their utility in biology. Successful results will produce diverse means of antimicrobial medicine in the form of: novel antibiotics, improved vaccines and better diagnostics. Such advancements will be vital in the fight against the growing antimicrobial resistance problem.

Appendix: Exemplar NMR Spectra

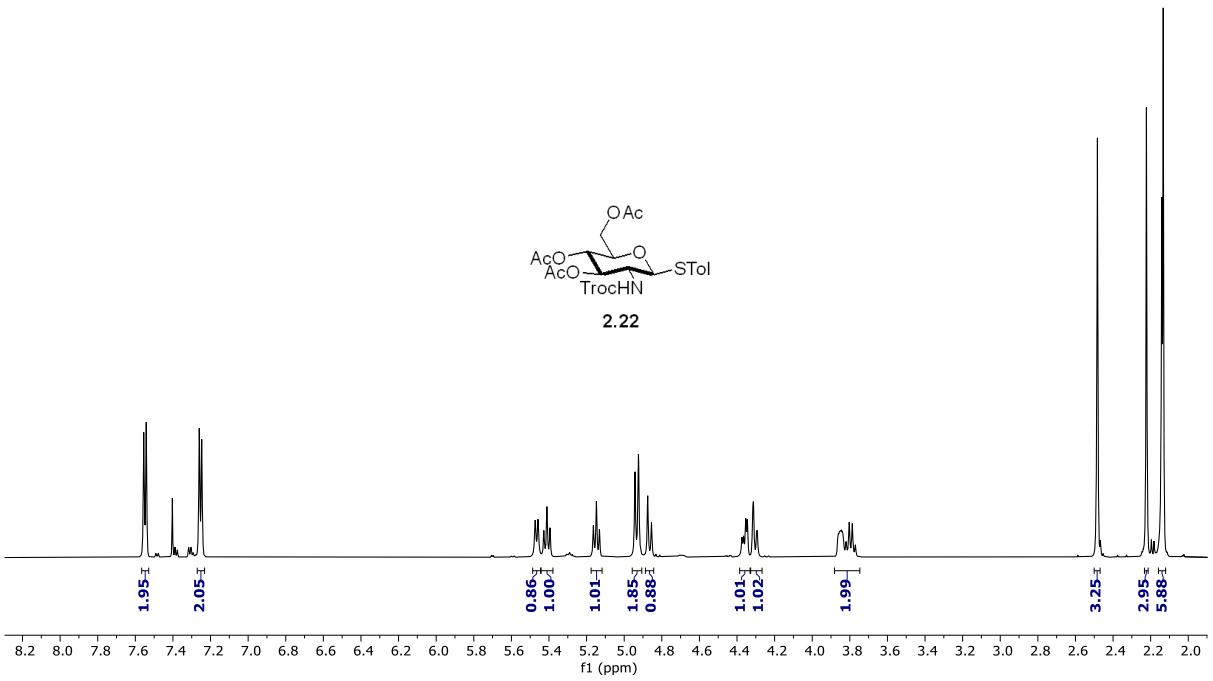
^{1}H NMR (400 MHz, $CDCl_3$) spectrum of compound **2.90**



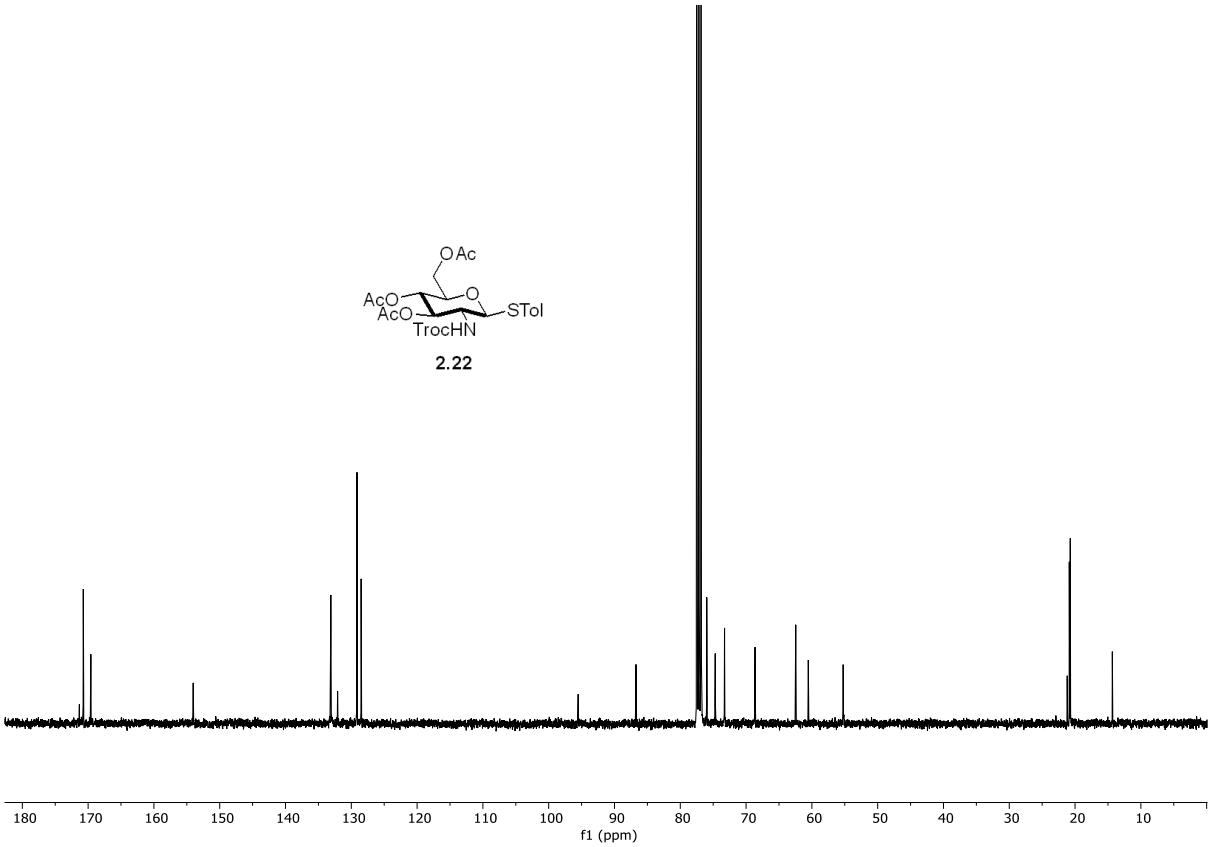
^{13}C NMR (101 MHz, $CDCl_3$) spectrum of compound **2.90**



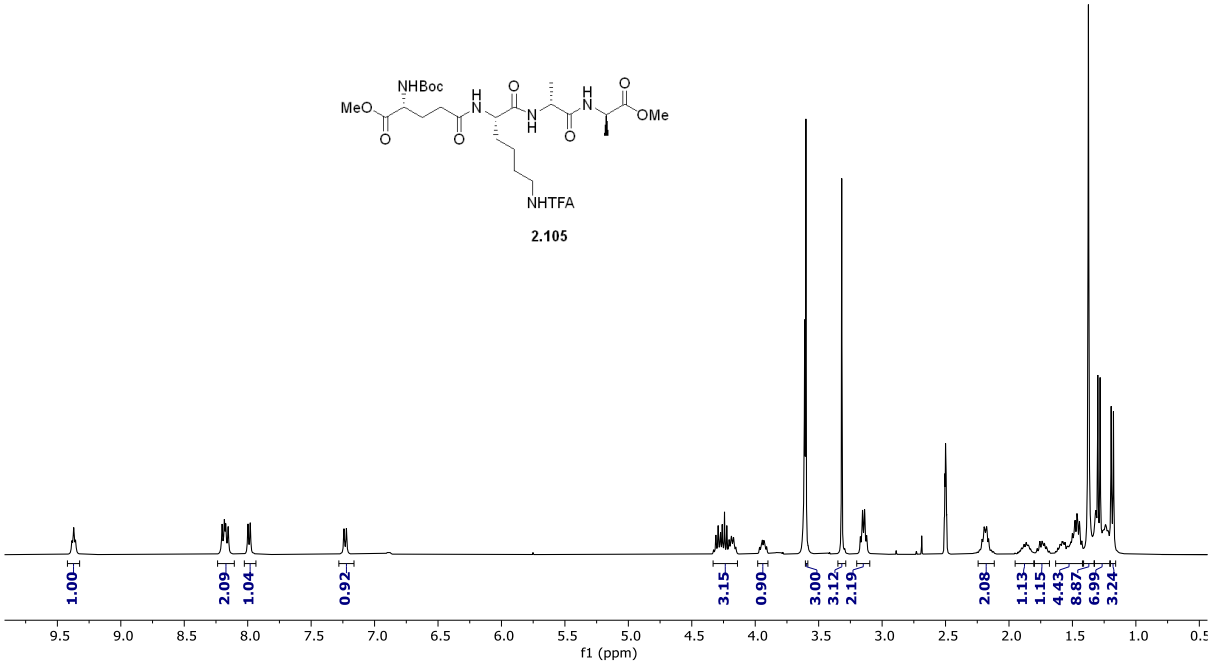
^{1}H NMR (601 MHz, $CDCl_3$) spectrum of compound **2.22**



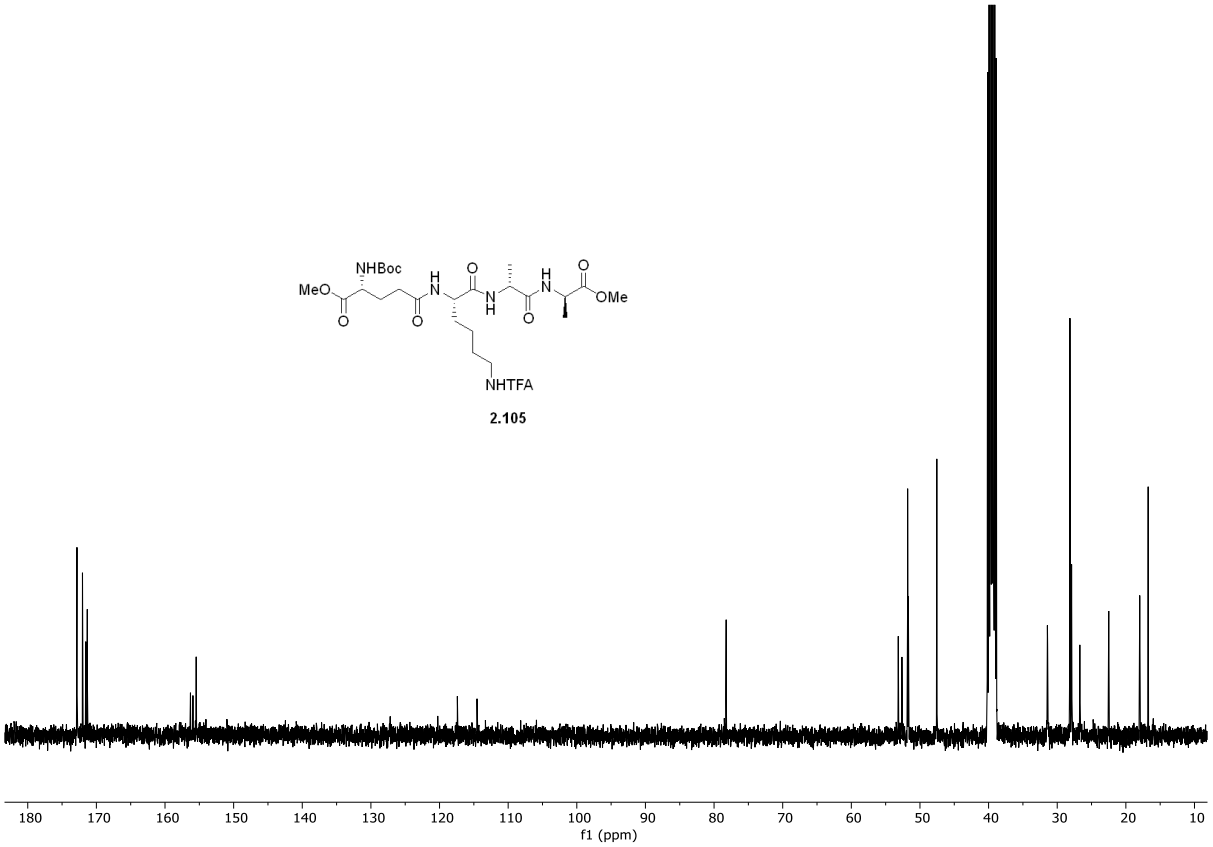
^{13}C NMR (151 MHz, $CDCl_3$) spectrum of compound **2.22**



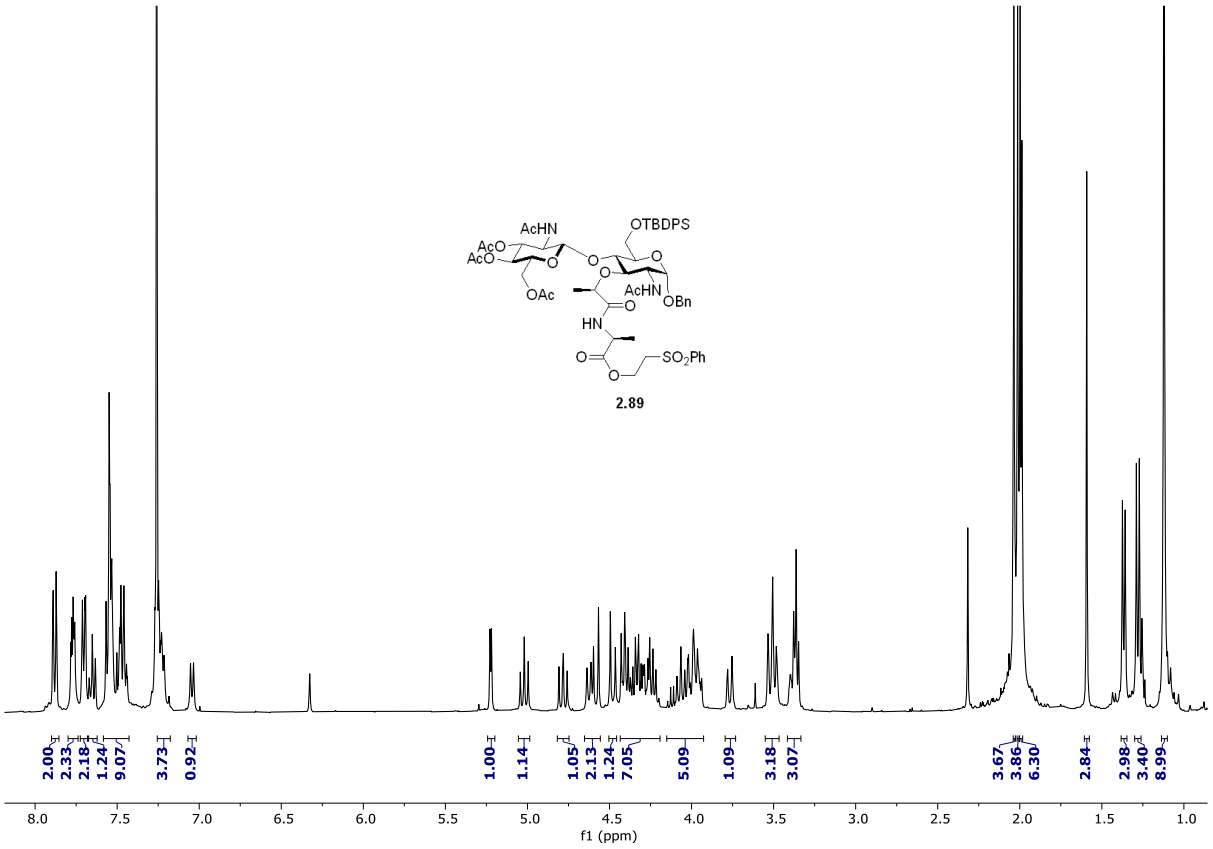
^{1}H NMR (400 MHz, DMSO) spectrum of compound **2.105**



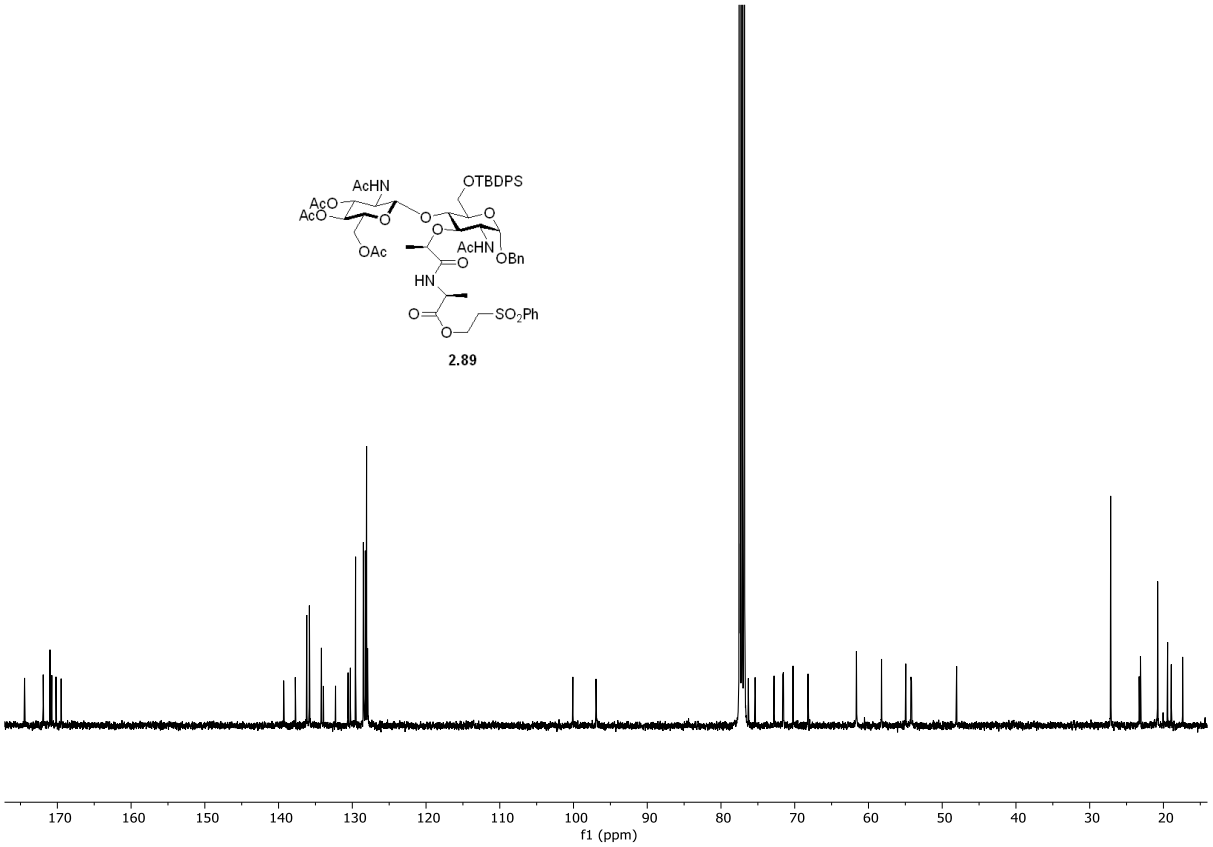
^{13}C NMR (101 MHz, $CDCl_3$) spectrum of compound **2.105**



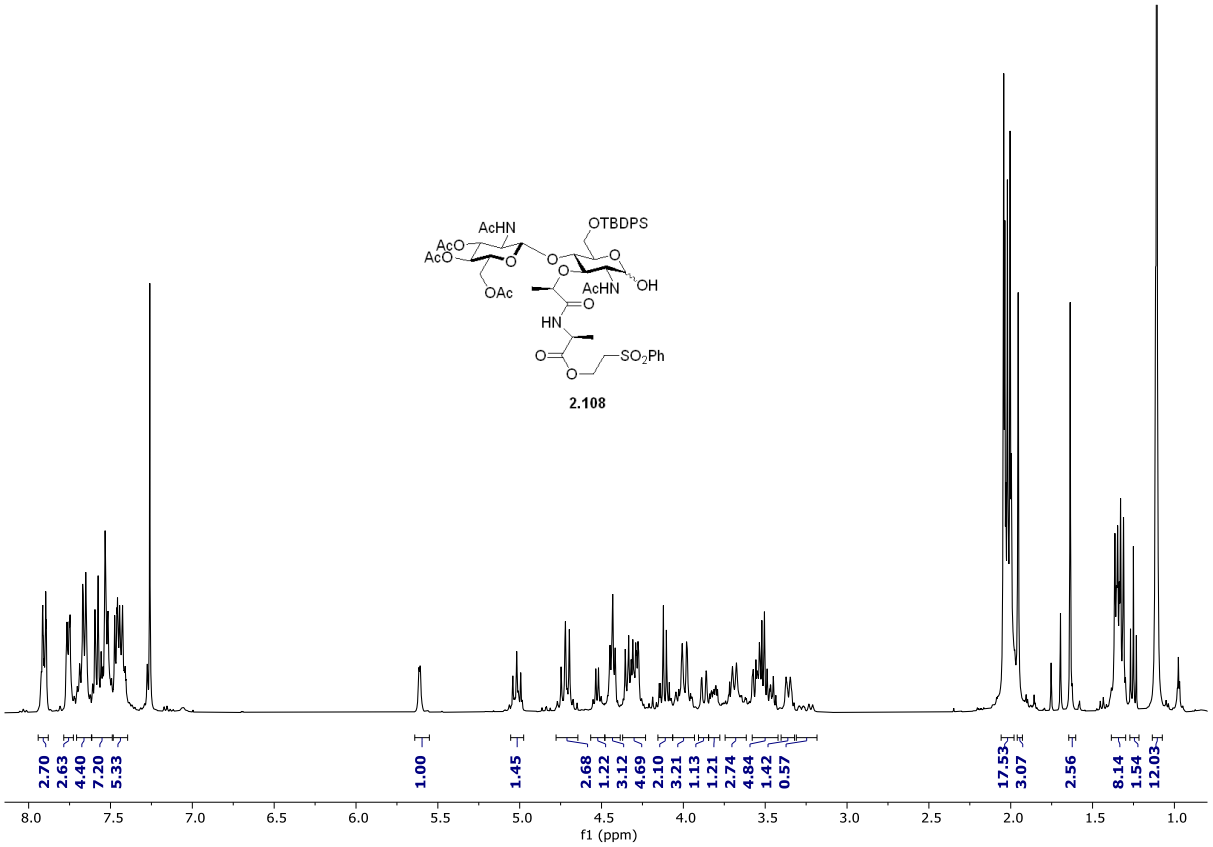
^{1}H NMR (601 MHz, $CDCl_3$) spectrum of compound **2.89**



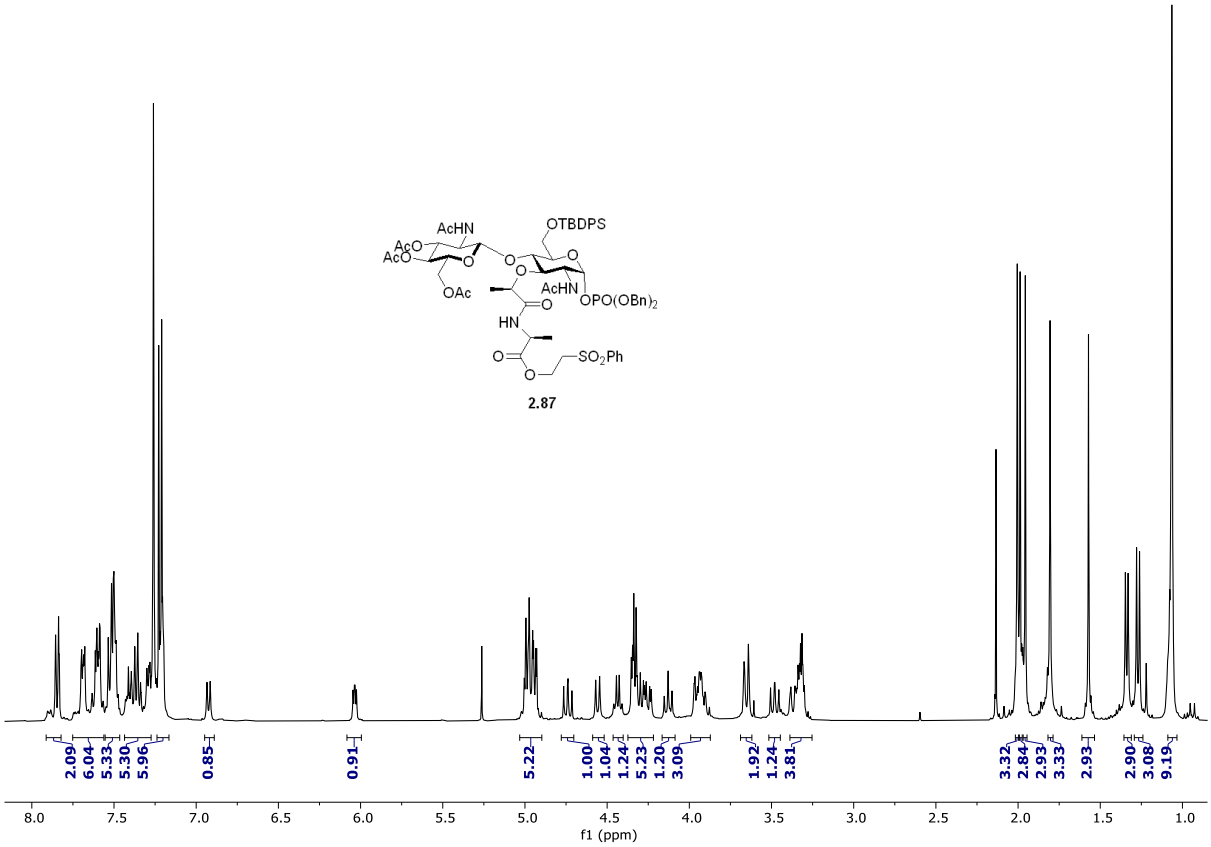
^{13}C NMR (151 MHz, $CDCl_3$) spectrum of compound **2.89**



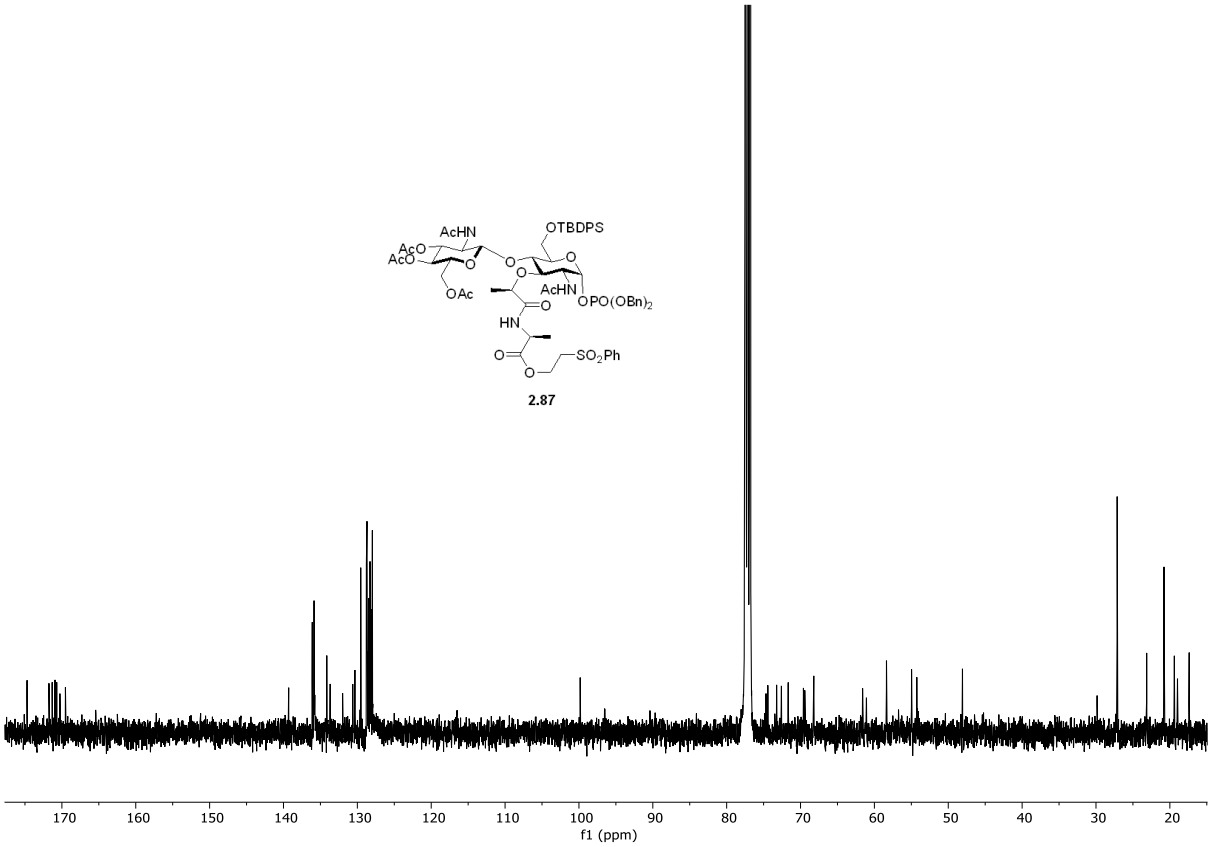
^{1}H NMR (400 MHz, $CDCl_3$) spectrum of compound **2.108**



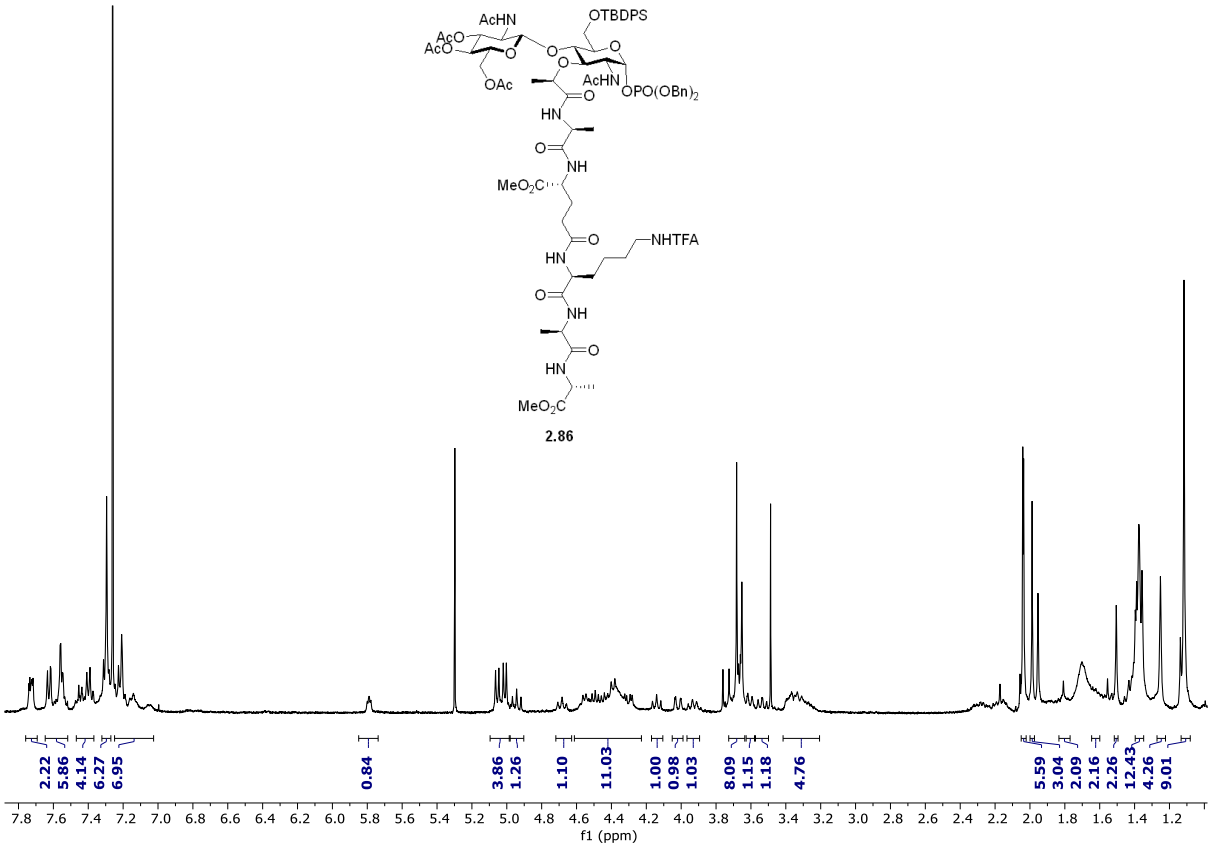
^{1}H NMR (400 MHz, $CDCl_3$) spectrum of compound **2.87**



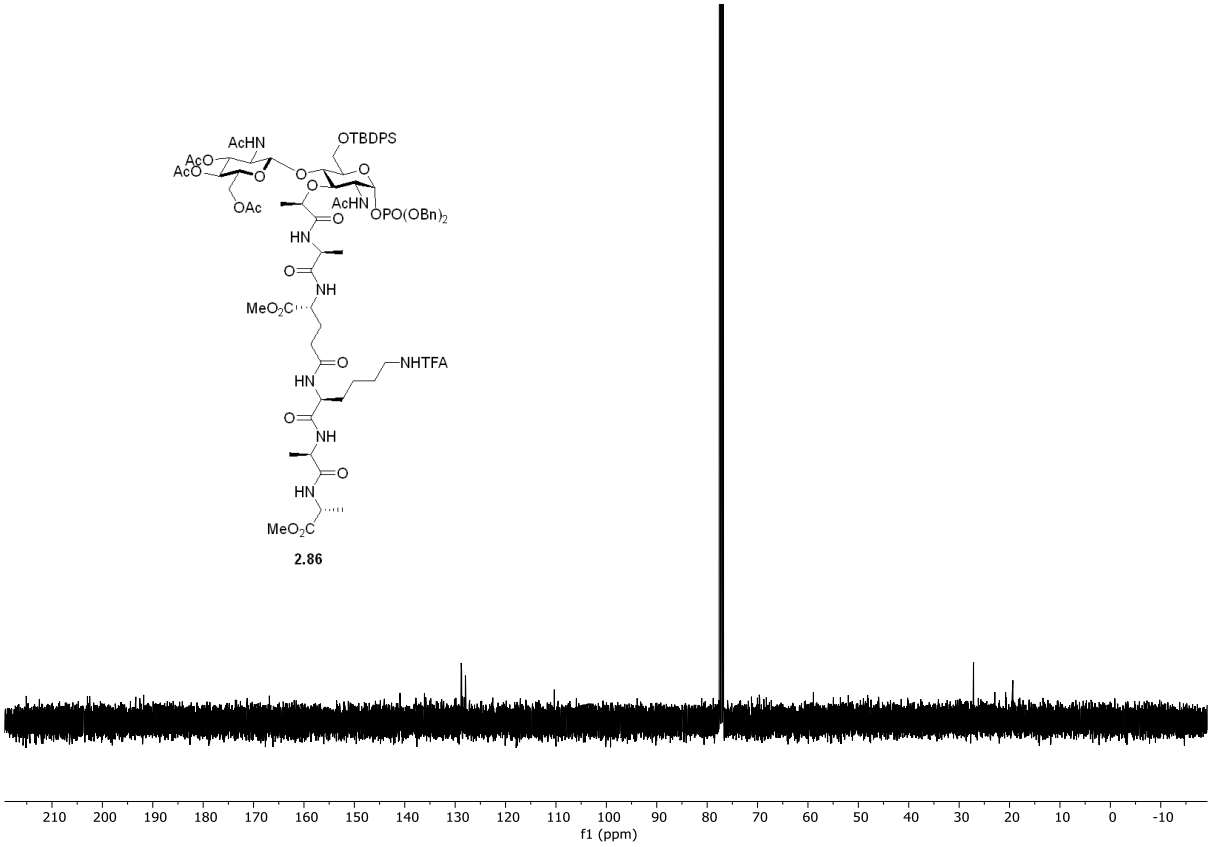
^{13}C NMR (101 MHz, $CDCl_3$) spectrum of compound **2.87**



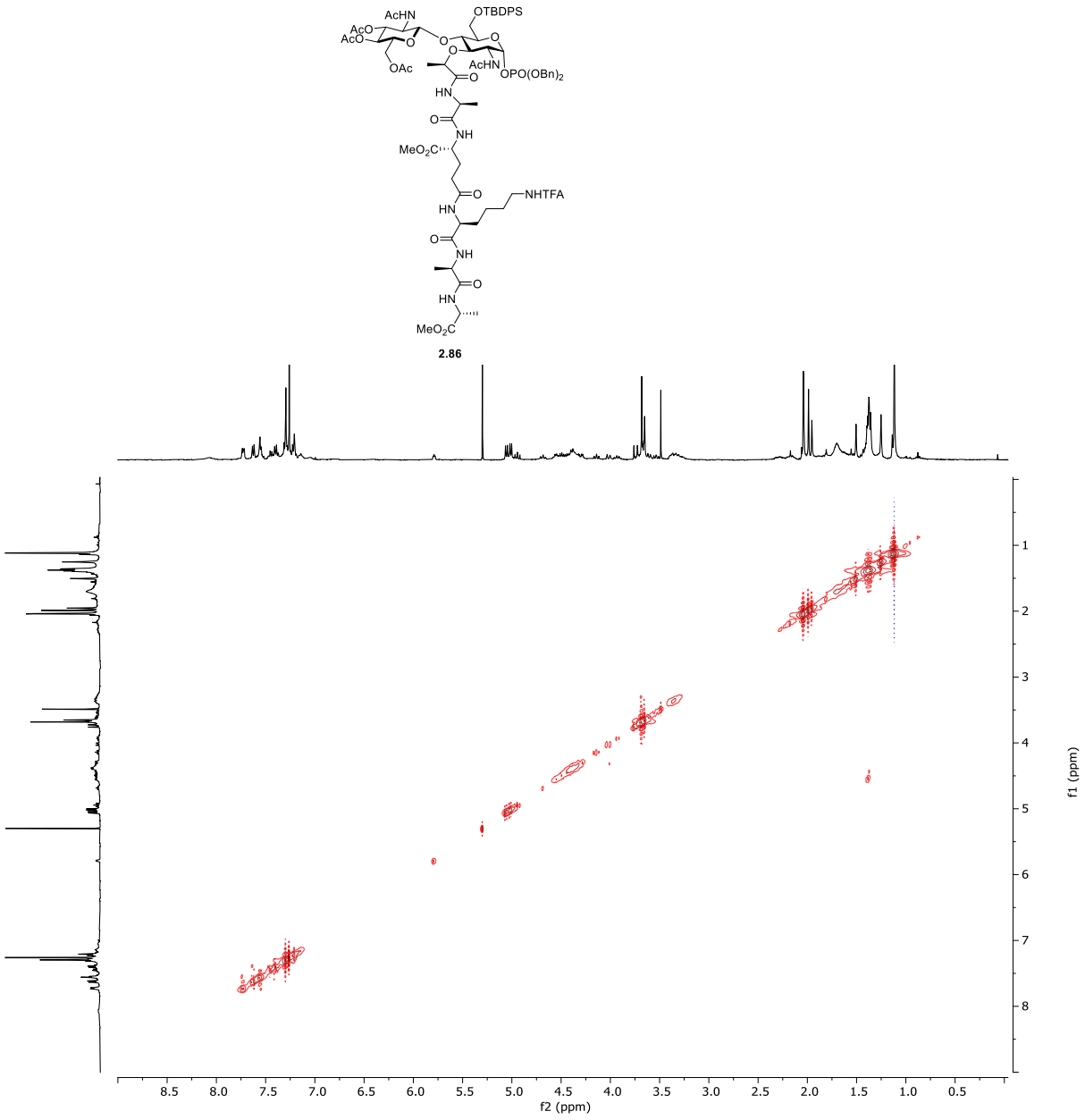
^{1}H NMR (601 MHz, $CDCl_3$) spectrum of compound **2.86**



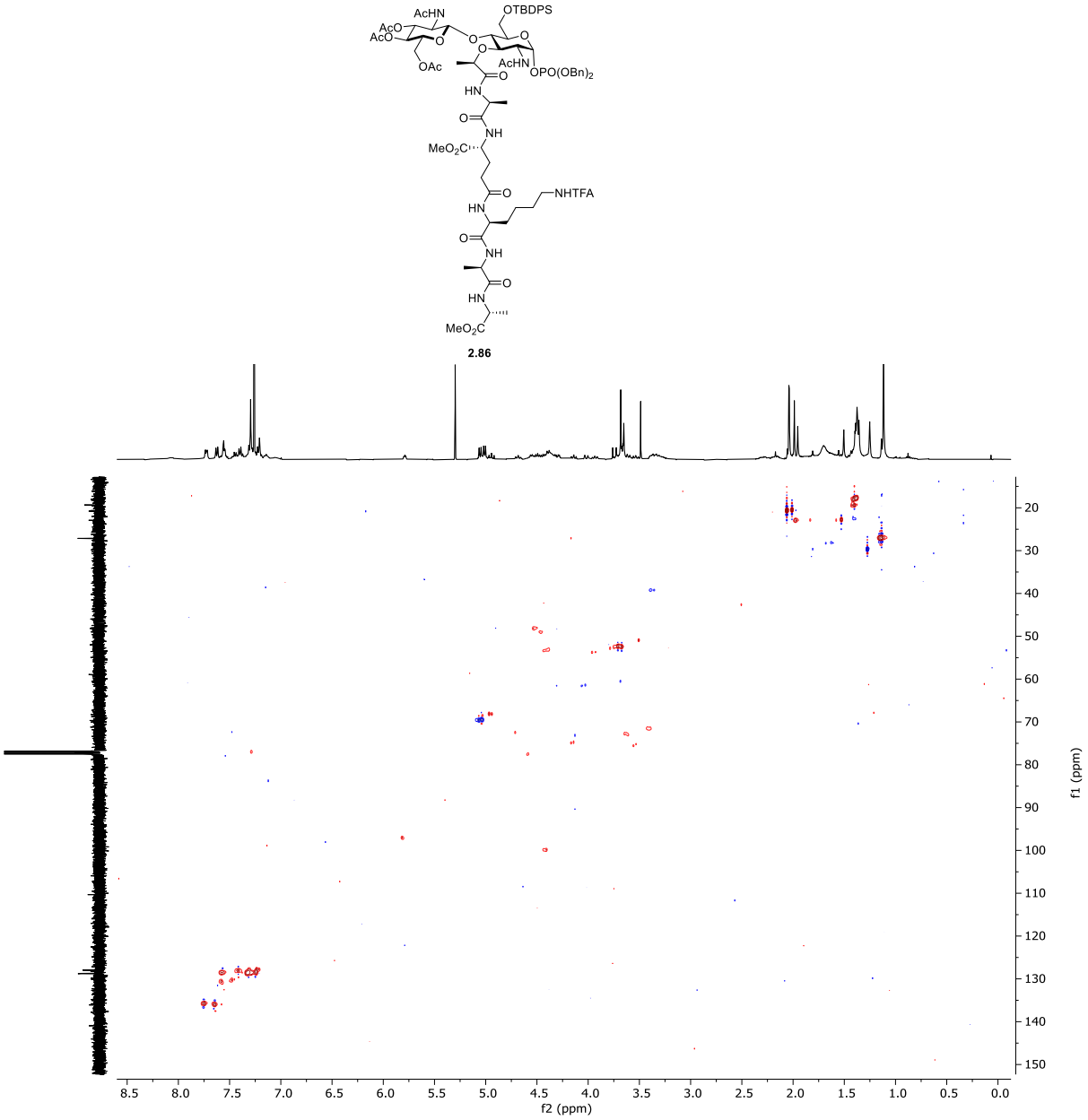
^{13}C NMR (151 MHz, $CDCl_3$) spectrum of compound **2.86**



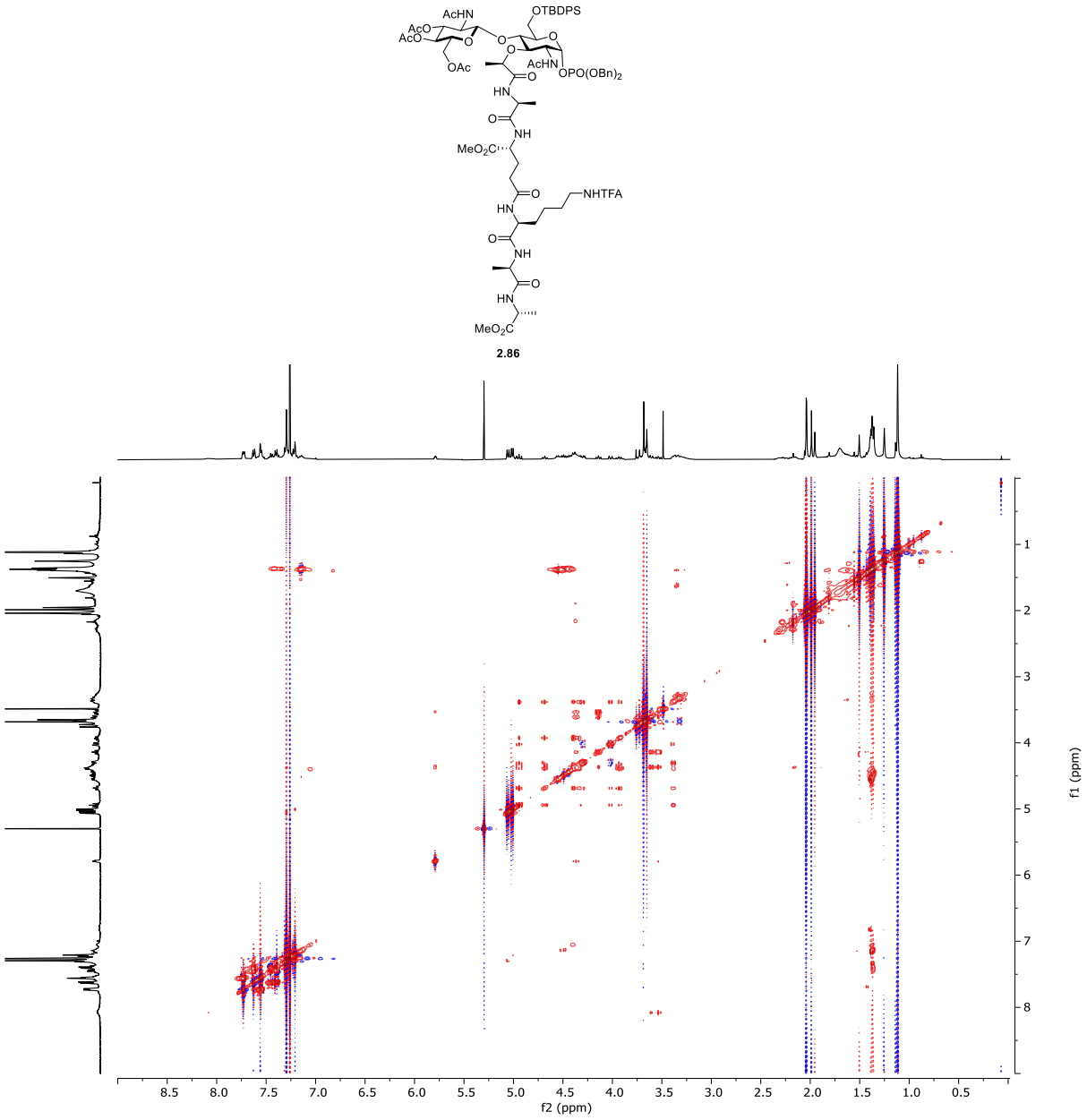
COSY (400 MHz, $CDCl_3$) spectrum of compound **2.86**



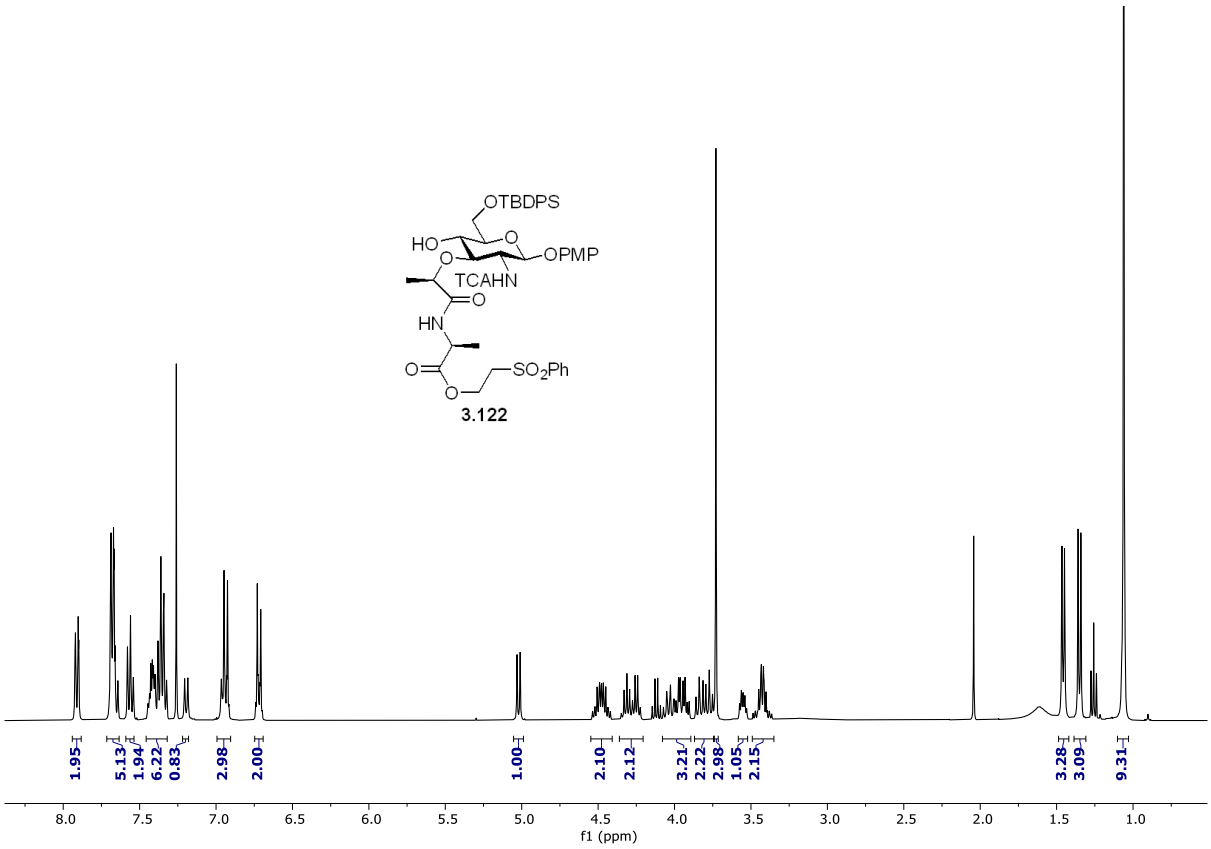
HSQC (400 MHz, $CDCl_3$) spectrum of compound **2.86**



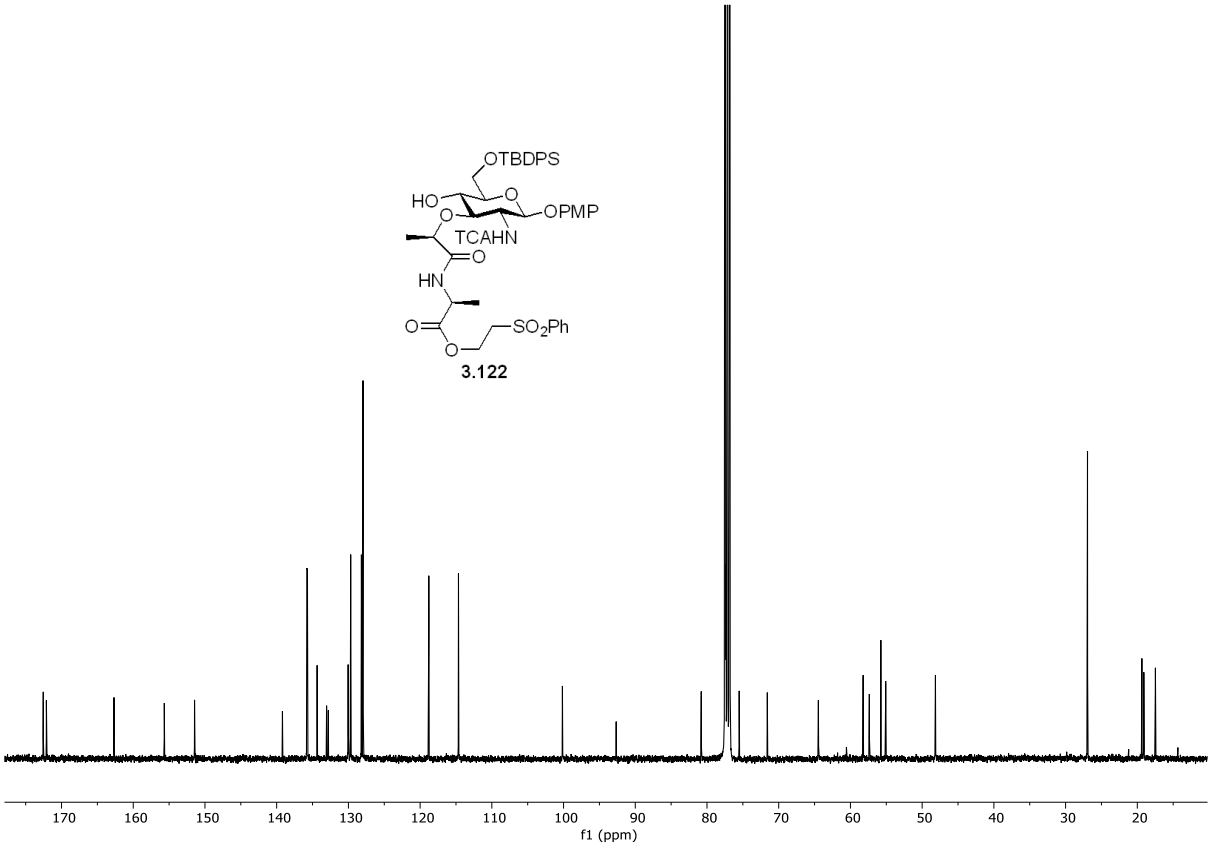
TOCSY (400 MHz, $CDCl_3$) spectrum of compound **2.86**



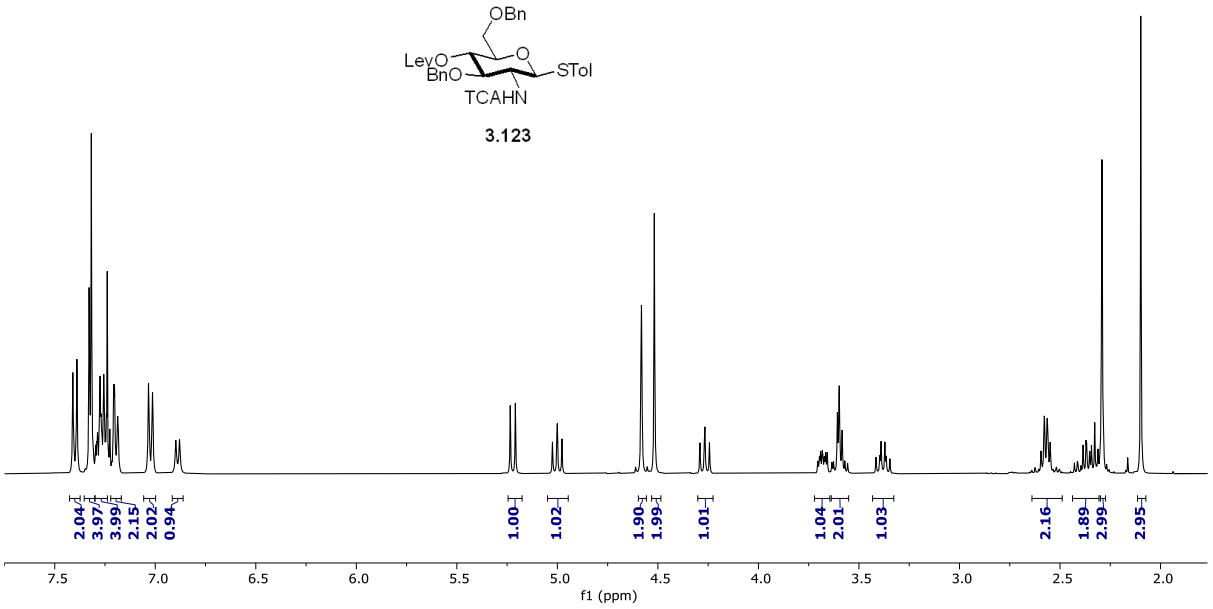
^{1}H NMR (400 MHz, $CDCl_3$) spectrum of compound **3.122**



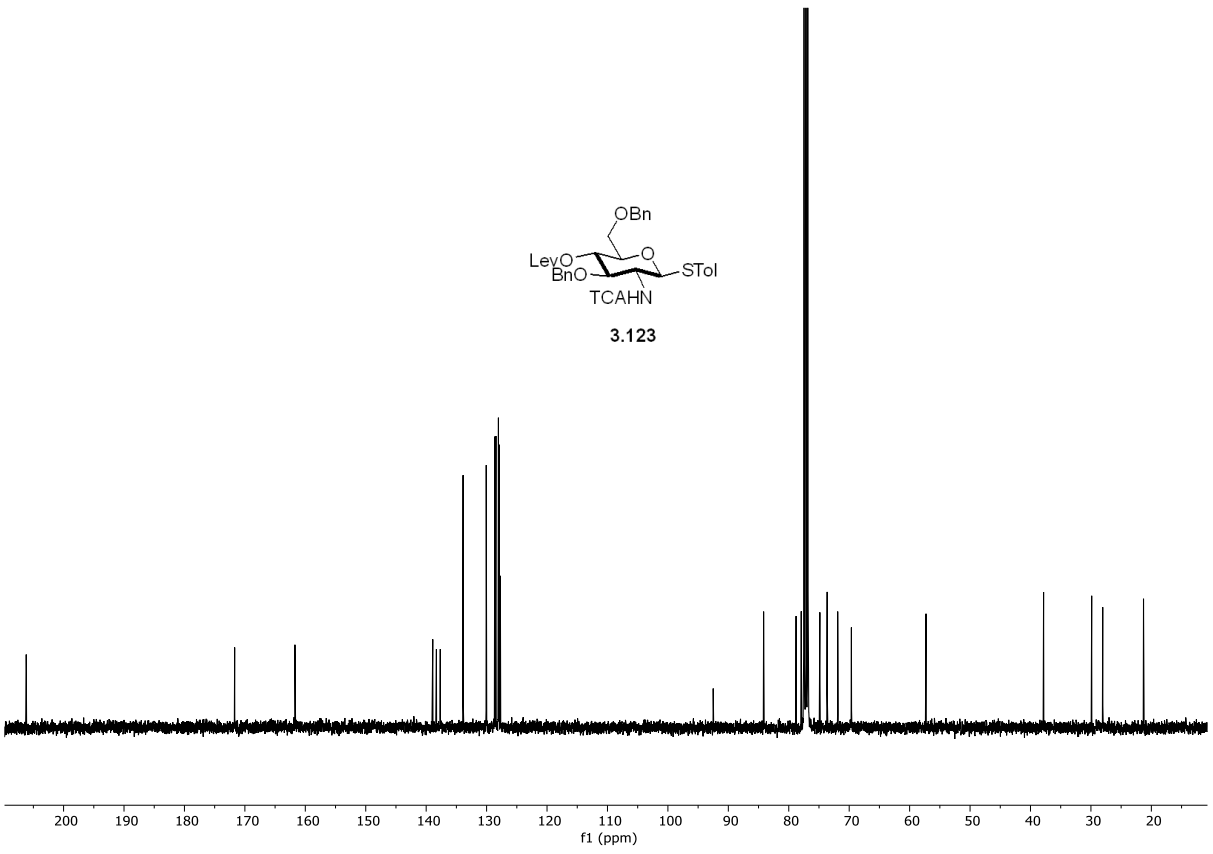
^{13}C NMR (101 MHz, $CDCl_3$) spectrum of compound **3.122**



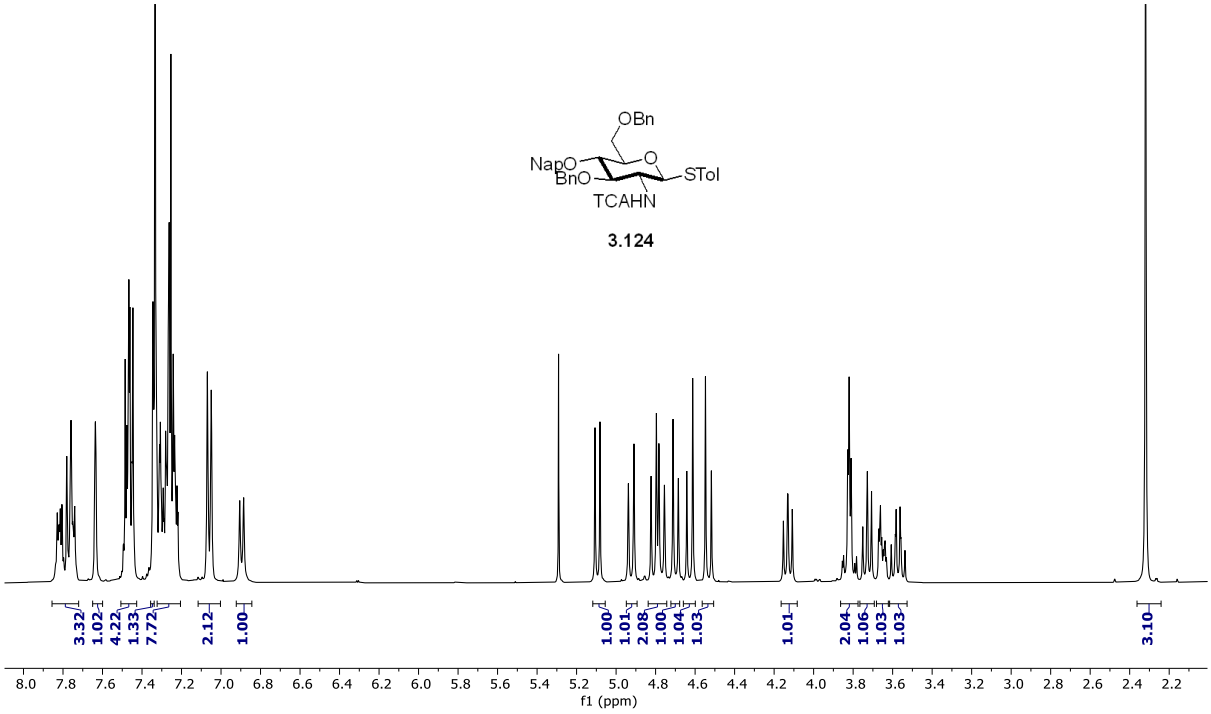
^{1}H NMR (400 MHz, $CDCl_3$) spectrum of compound **3.123**



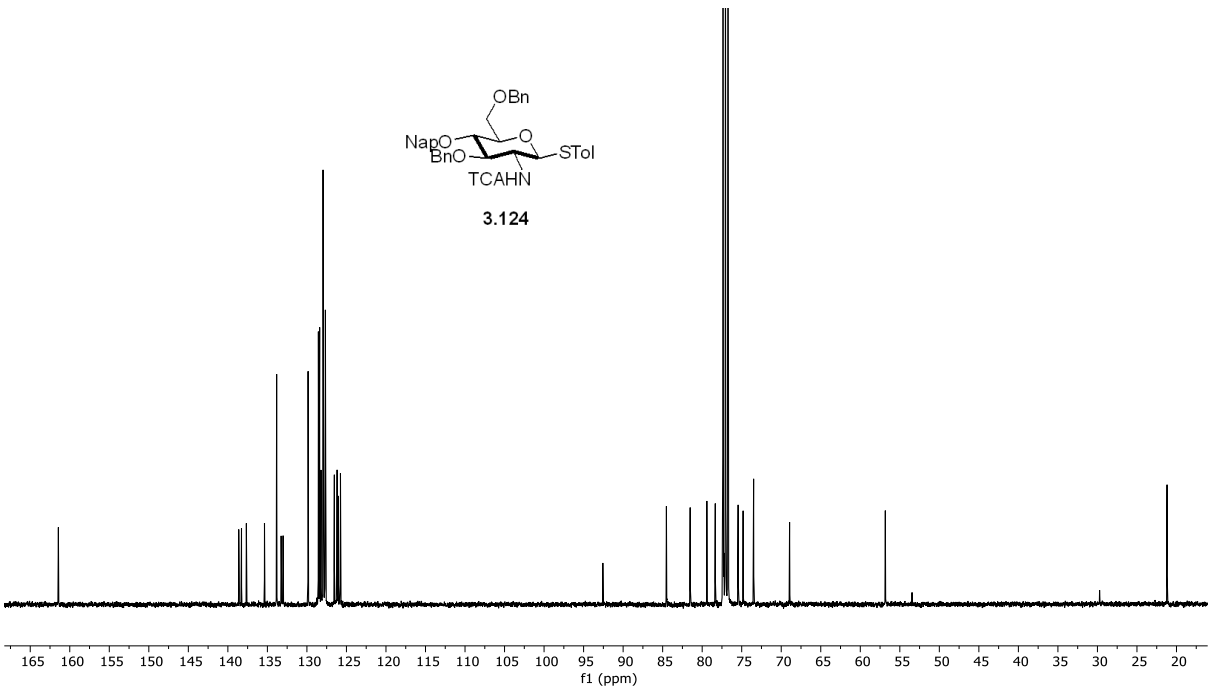
^{13}C NMR (101 MHz, $CDCl_3$) spectrum of compound **3.123**



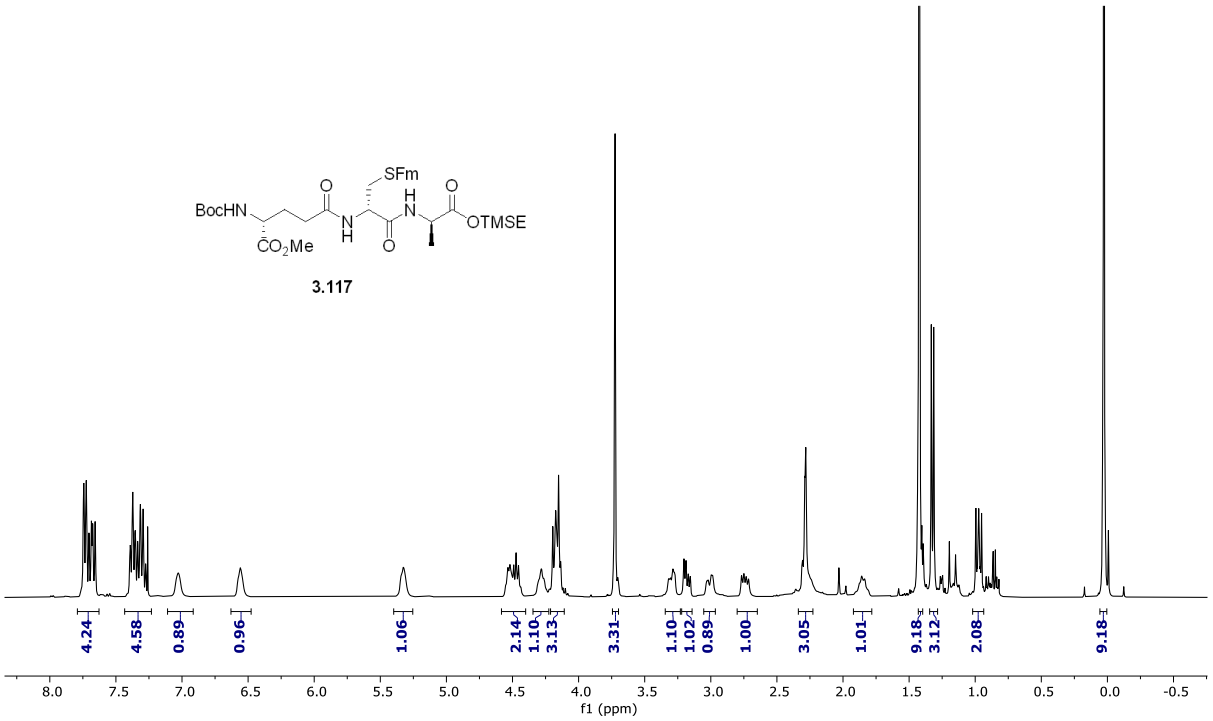
^{1}H NMR (400 MHz, $CDCl_3$) spectrum of compound **3.124**



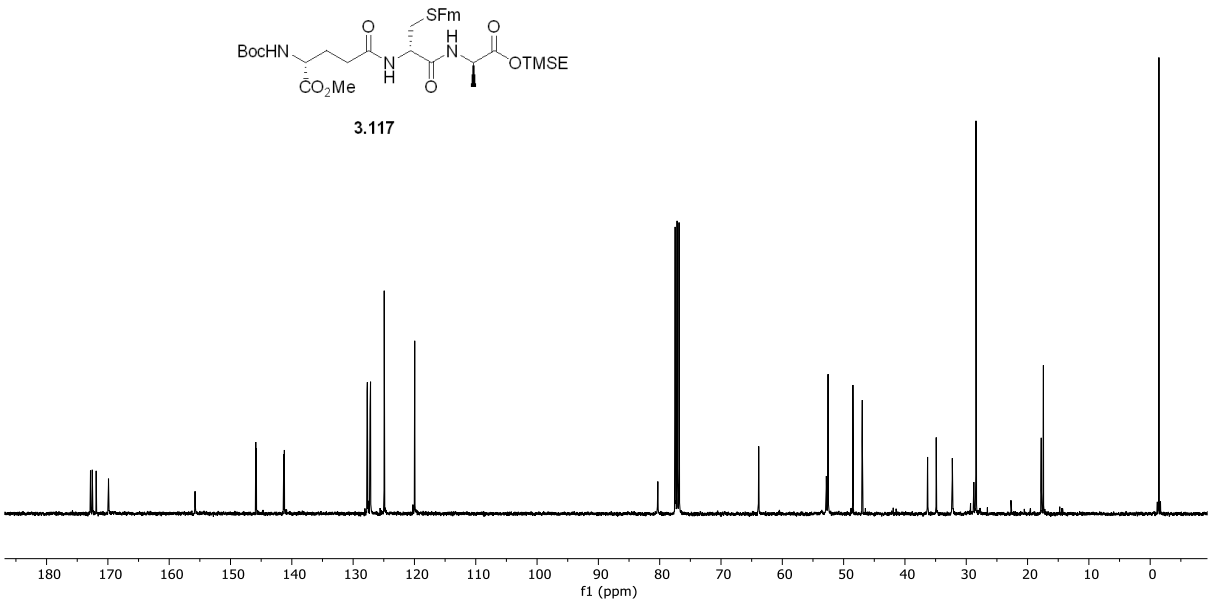
^{13}C NMR (101 MHz, $CDCl_3$) spectrum of compound **3.124**



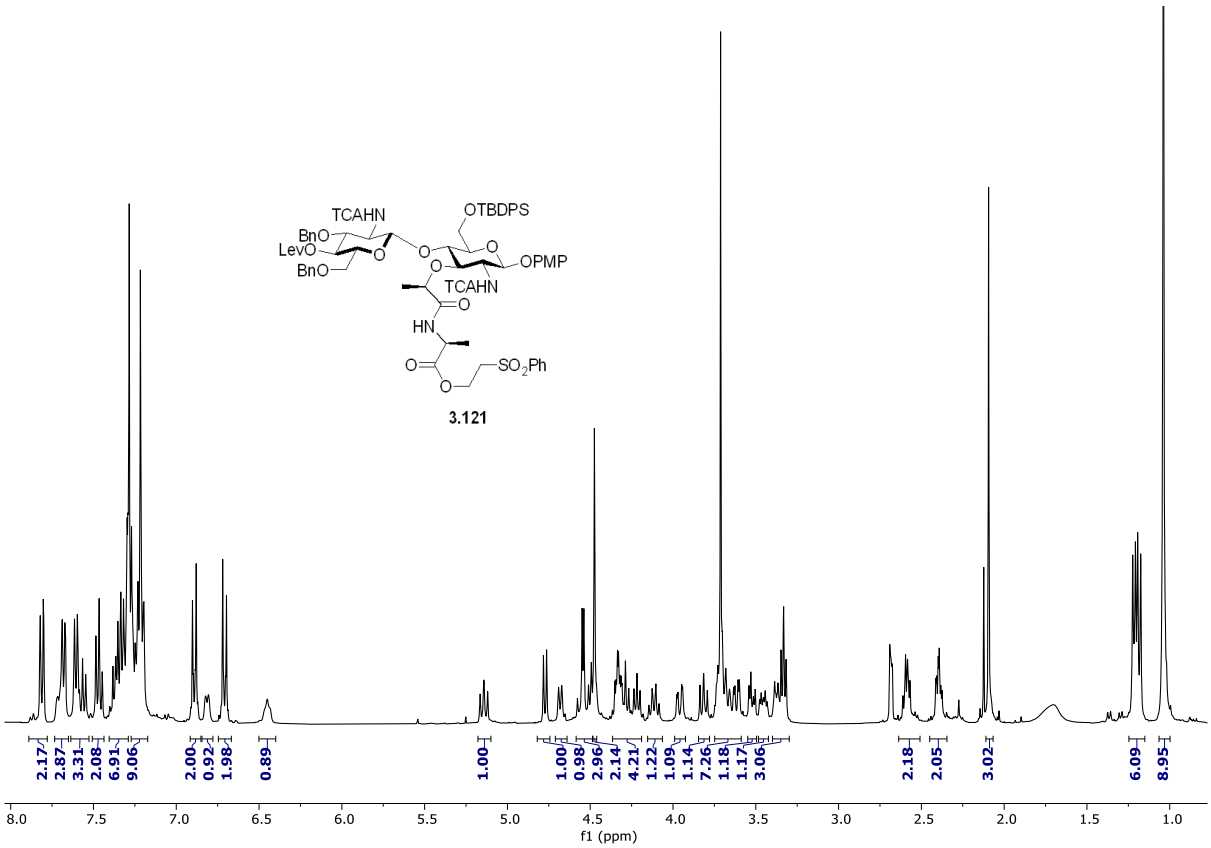
^{1}H NMR (400 MHz, $CDCl_3$) spectrum of compound **3.117**



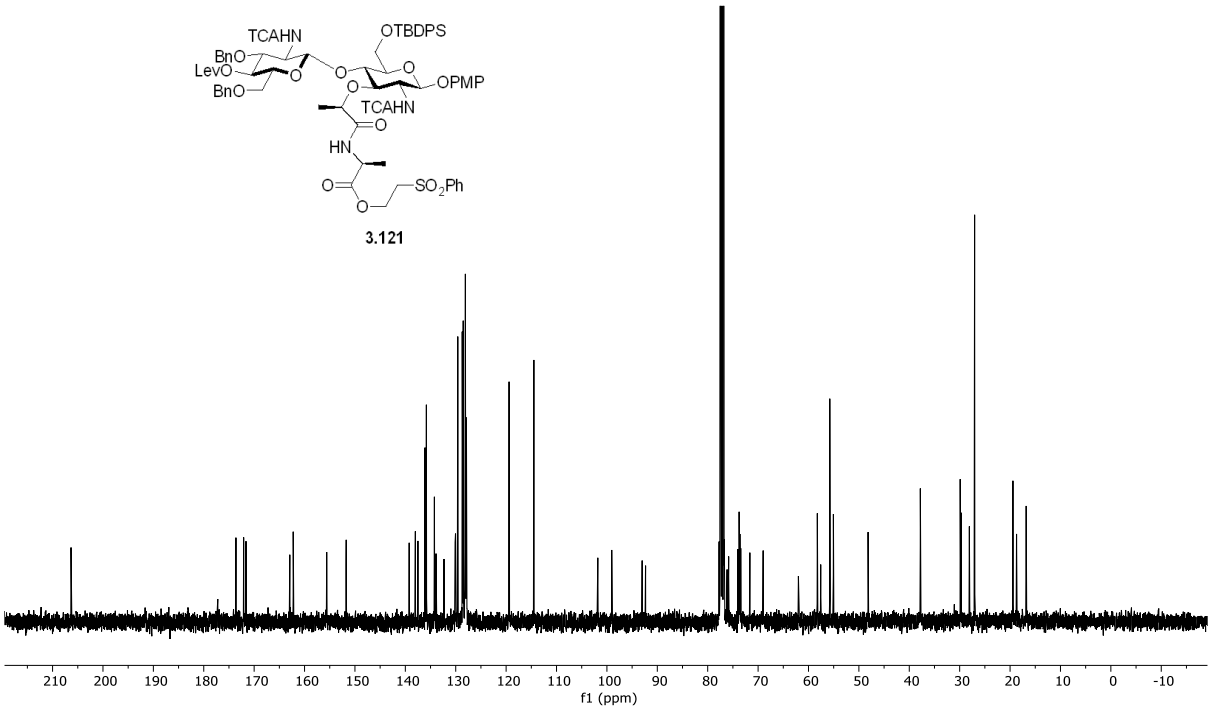
^{13}C NMR (101 MHz, $CDCl_3$) spectrum of compound **3.117**



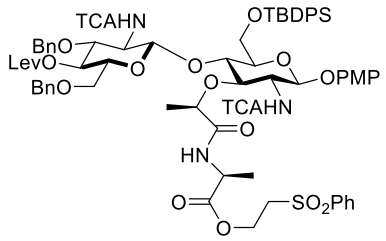
^{1}H NMR (400 MHz, $CDCl_3$) spectrum of compound **3.121**



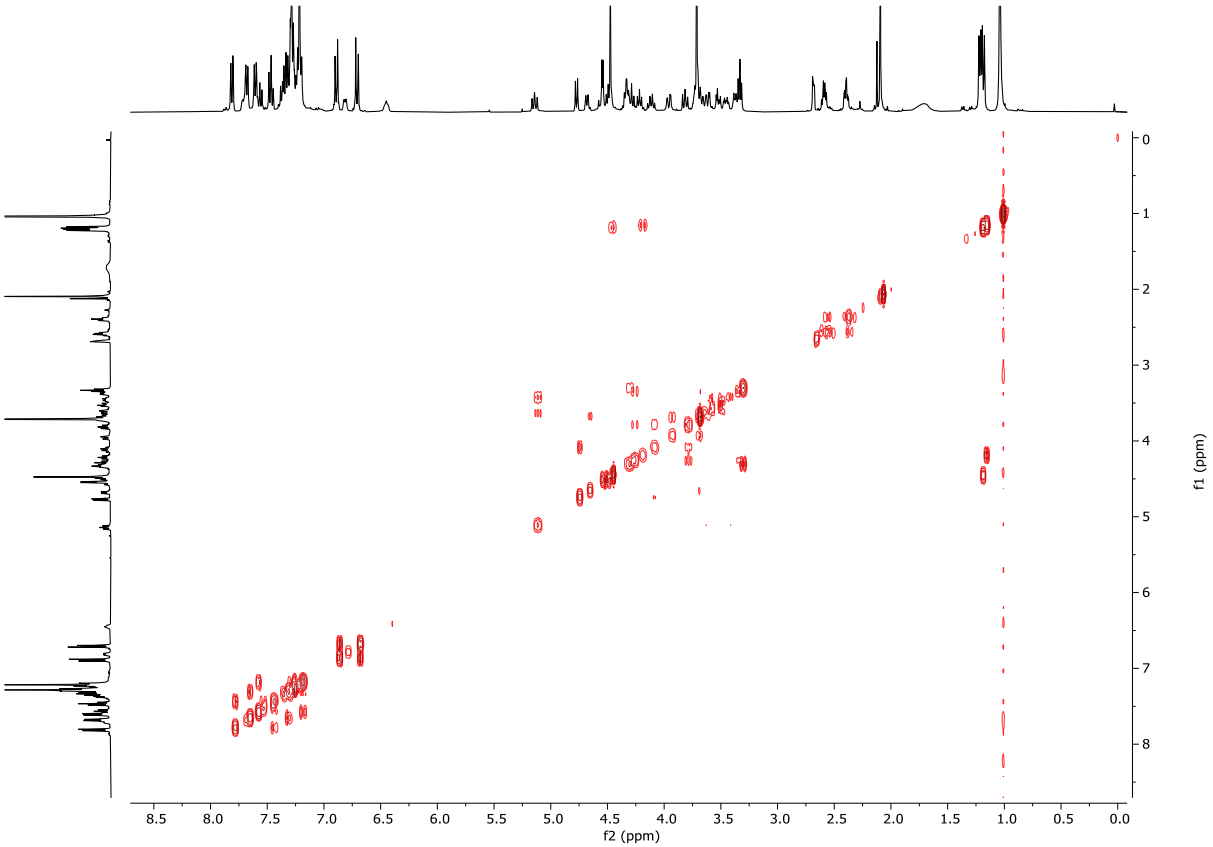
^{13}C NMR (101 MHz, $CDCl_3$) spectrum of compound **3.121**



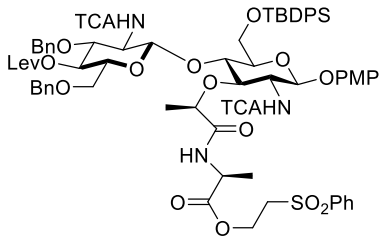
COSY (400 MHz, $CDCl_3$) spectrum of compound **3.121**



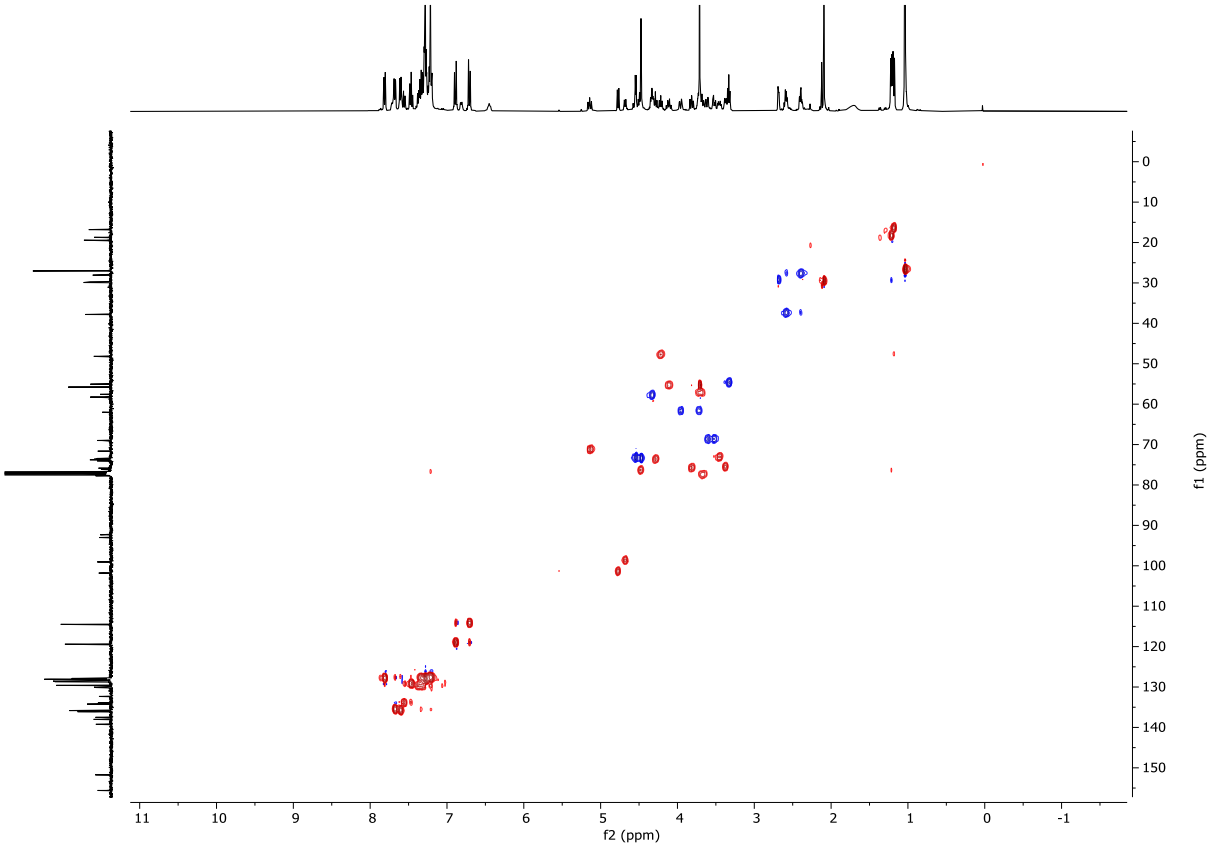
3.121



HSQC (400 MHz, $CDCl_3$) spectrum of compound **3.121**



3.121



TOCSY (400 MHz, $CDCl_3$) spectrum of compound **3.121**

